Technische Universität München
TUM School of Medicine and Health

Impact of *Helicobacter pylori* CagA on (canonical) Wnt/β-catenin Signaling

Martin Kullik

Vollständiger Abdruck der von der TUM School of Medicine and Health
der Technischen Universität München zur Erlangung eines

Doktors der Medizin (Dr. med.)

genehmigten Dissertation.

Vorsitz: Prof. Dr. Ernst J. Rummeny

Prüfende der Dissertation:

1. Prof. Dr. Markus Gerhard
2. Prof. Dr. Roland M. Schmid

Die Dissertation wurde am 16.08.2023 bei der Technischen Universität München eingereicht
und durch die TUM School of Medicine and Health am 06.06.2024 angenommen.

Impact of *Helicobacter pylori* CagA on (canonical) Wnt/β-catenin Signaling

To my family.

Contents

Abbreviations

AA	Amino Acids
ATCC	American Type Culture Collection
BFB	Bromophenol blue
bp	base pairs
cagA	Cytotoxin associated gene A (gene)
CagA	Cytotoxin associated gene A (protein)
*cag*PAI	Cytotoxin associated gene pathogenicity island (gene cluster)
CCLE	Cancer Cell Line Encyclopedia
CFU	Colony Forming Units
CIN	Numerical Chromosome Instability
CM	CagA Multimerization motif (types: **CM^{W}** = Western, **CM^{E}** = Eastern; motif also referred to as **CRPIA**: Conserved Repeat responsible for Phosphorylation-Independent Activity)
CMV	Cytomegalovirus
dcm	DNA cytosine methyltransferase
ddH_2O	double distilled water
dH_2O	distilled water
DENT	Bacterial culture supplement comprising vancomycin, trimethoprim, cefsulodin and amphotericin b
DGE	Differential Gene Expression
DMEM	Dulbecco's Modified Eagle Medium
DNA	Deoxyribonucleic acid
dNTPs	deoxy-Nucleoside Triphosphates
E. coli	*Escherichia coli*
EDTA	Ethylen-diamin-tetraacetic acid
EGFP	Enhanced green fluorescent protein
EGTA	Ethylene-glycol-tetraacetic Acid
EPIYA	glutamate-proline-isoleucine-tyrosine-alanine (CagA sequence motif)
Fc (region)	Fragment crystallizable (region)
FBS	Fetal Bovine Serum
GCSC	Gastric Cancer Stem Cells
H. pylori, HP	*Helicobacter pylori*
HKG	Housekeeping Genes
HRP	Horse radish peroxidase

IB	Immunoblot
IF	Immunofluorescence
IU	International Unit
kb	Kilo base pairs
kDa	Kilo Dalton
MOI	Multiplicity Of Infection
OD	Optical Density
o/n	over night
p.i.	post infectionem
PAA	Polyacrylamide
PAGE	Polyacrylamide Gel Electrophoresis
PBS	Phosphate buffered saline
PCR	Polymerase Chain Reaction
RLU	Relative Light Units
rpm	Revolutions per minute
RT	Room Temperature
SD	Standard Deviation
SDS	Sodium Dodecyl Sulfate
SV40	Simian vacuolating virus 40
T4SS	Type IV secretion System
TAE	Tris acetate EDTA
Taq	*Thermus aquaticus*
TBS	Tris buffered saline
TBS-T	Tris buffered saline 1% Tween 20
T_M	Melting temperature
TPM	Transcripts Per Million
Tris	Tris-(hydroxymethyl)-aminomethane
UV	ultraviolet
VacA	Vacuolating cytotoxin A
w/o	without
wt	Wild type

Nomenclature: Genes and proteins are denoted according to generally accepted rules and conventions. Human gene symbols are written entirely in UPPERCASE and *italicized* (HUGO Gene Nomenclature Committee, 2021). Bacterial gene symbols are written *italicized* (Demerec et al., 1966), hence "*cagA*" addresses the gene, whereas "CagA" addresses the protein.

Summary

Chronic infection with *Helicobacter pylori* implies a significantly increased risk for the development of gastric carcinoma, which is further elevated by *cag*PAI positive strains. The *cag*PAI encodes a type IV secretion system and the virulence factor CagA, which is translocated into gastric epithelial cells by the former. CagA's direct interaction with numerous proteins, in particular those involved in signal transduction, provides access to very fundamental host cell functions and is furthermore associated with carcinogenesis. CagA has therefore been identified as an independent risk factor for gastric carcinoma. Although previous studies do not provide a clear picture, there is much evidence that CagA may have an impact on cellular β-catenin turnover, where deregulation of the (canonical) Wnt/β-catenin pathway is considered a more significant driver of gastric carcinogenesis.

In the present work, while very early infection with CagA-competent *H. pylori* resulted in a transitory alteration of host cell morphology, in the medium term (≥ 24 h) CagA primarily caused a reduction in intrinsic (canonical) Wnt/β-catenin signal transduction activity in the nonpolarized host cell. This was inferred by both increases in phosphorylated β-catenin and the concomitant reduction in TCF/LEF-mediated transcriptional activity. By means of transfection and transduction experiments, it was shown that this inhibitory effect on the (canonical) Wnt/β-catenin signal transduction pathway was dose-dependent and could be attributed to C-terminal CagA (amino acids 201-1216). In this context, N-terminal CagA (amino acids 1-200) represented a functional antagonist insofar as it caused an increase in (canonical) Wnt/β-catenin signaling activity. As with wild type CagA (amino acids 1-1216), the C-terminal part showed a high affinity for the plasma membrane of the (non-polarized) host cell, in contrast to its N-terminal part, which was homogeneously distributed in the cytosol of functionally E-cadherin-deficient host cells.

These results are essentially subject to several limitations, which are mainly due to a partly low transfection efficiency, interference with the internal transfection and expression standard, and a considerable context dependency. A reasonably conclusive picture regarding the influence of CagA on (canonical) Wnt/β-catenin signal transduction emerges taking also into account the polarity of the host cell, its intrinsic (canonical) Wnt/β-catenin signal transduction activity, and the intracellular concentration of CagA.

Zusammenfassung:

Die chronische Infektion mit Helicobacter pylori *stellt ein signifikant erhöhtes Risiko für die Entwicklung eines Magenkarzinoms dar, was durch* cagPAI *positive Stämme noch zusätzlich gesteigert wird. Das* cagPAI *kodiert für ein Typ 4 Sekretionssystem und den Virulenzfaktor CagA, der darüber in die Epithelzellen des Magens transloziert wird. Dessen direkte Interaktion mit zahlreichen, insbesondere Signaltransduktions-Proteinen ermöglicht den Zugriff auf sehr grundlegende Funktionen der Wirtszelle und steht darüber hinaus mit der Karzinogenese im Zusammenhang. CagA wurde daher als unabhängiger Risikofaktor für das Magenkarzinom identifiziert. Wenngleich bisherige Untersuchungen kein eindeutiges Bild zeichnen, gibt es viele Belege dafür, dass CagA einen Einfluss auf den zellulären β-Catenin-Umsatz haben könnte, wobei hier die Deregulation des (kanonischen) Wnt/β-Catenin-Signalwegs als bedeutsamer Treiber der gastralen Karzinogenese erachtet wird.*

In der vorliegenden Arbeit hatte die sehr frühe Infektion mit CagA-kompetentem H. pylori *zwar eine transitorische Veränderung der Wirtszell-Morphologie zur Folge, mittelfristig (≥ 24 h) bewirkte CagA in erster Linie jedoch eine Reduktion der intrinsischen (kanonischen) Wnt/β-Catenin-Signaltransduktionsaktivität in der nicht polarisierten Wirtszelle. Darauf konnte sowohl durch Zunahme des phosphorylierten β-Catenins, als auch durch die damit einhergehende Reduktion der TCF/LEF vermittelten Transkriptionsaktivität geschlossen werden. Mittels Transfektions- und Transduktionsexperimenten konnte gezeigt werden, dass dieser hemmende Einfluss auf den (kanonischen) Wnt/β-Catenin-Signaltransduktionsweg dosisabhängig war und dem C-terminalen Teil von CagA zugeschrieben werden konnte (Aminosäuren 201-1216). In diesem Zusammenhang stellte der N-terminale Teil von CagA (Aminosäuren 1-200) einen funktionellen Gegenspieler dar, insofern als dass er eine Steigerung der (kanonischen) Wnt/β-Catenin-Signalaktivität bewirkte. Wie auch der CagA Wildtyp (Aminosäuren 1-1216), zeigte der C-terminale Teil eine hohe Affinität zur Plasmamembran der (nicht polarisierten) Wirtszelle, im Gegensatz zu dessen N-terminalem Teil, welcher sich homogen im Zytosol funktionell E-Cadherin defizienter Wirtszellen verteilte.*

Diese Ergebnisse unterliegen grundsätzlich einigen Einschränkungen, welche vornehmlich einer zum Teil geringen Transfektionseffizienz, der Interferenz mit dem internen Transfektions- und Expressionsstandard sowie einer beträchtlichen Kontext-Abhängigkeit geschuldet sind. Ein einigermaßen schlüssiges Bild hinsichtlich des Einflusses von CagA auf die (kanonische) Wnt/β-Catenin-Signaltransduktion ergibt sich lediglich unter Berücksichtigung der Polarität der Wirtszelle, deren intrinsischer (kanonischer) Wnt/β-Catenin-Signaltransduktionsaktivität sowie der intrazellulären Konzentration von CagA.

1 Introduction

1.1 *Helicobacter pylori* and its epidemiologic relevance

In 1984 Marshall and Warren isolated a hitherto unknown gram-negative helical shaped flagellated bacterium from gastric specimens of patients with gastritis and peptic ulcers: *Helicobacter pylori* (Marshall and Warren, 1984). In the following decades, *H. pylori* seropositivity was found to significantly increase the risk of developing gastric cancer (Parsonnet et al., 1991, Miehlke et al., 1997). Concerning this third most common cause of cancer-related deaths in the world (Graham, 2015), *H. pylori* was shown to be etiological in 89% of non-cardia gastric cancer cases worldwide in the year 2008 (Plummer et al., 2015). Whereas a decrease in infection prevalence in industrialized countries has become apparent, at least a 2-fold higher prevalence of *H. pylori* infection can be seen in countries with a high incidence of gastric cancer (Peleteiro et al., 2014). The prevalence of infections by *H. pylori* has been epidemiologically correlated to socioeconomic and educational status (Lim et al., 2013, den Hollander et al., 2013). Household crowding (Lim et al., 2013) or living in rural areas lead to a further predisposition (Bastos et al., 2013). Exact transmission routes are still unclear. In general, infection is mostly acquired in childhood and normally persists over the lifetime (Everhart, 2000). Adults in developed countries are exposed to a risk of acquiring an infection of less than 1% per year (Ernst and Gold, 2000).

H. pylori is a highly variable bacterium: Even within the very same individual, a remarkable genetic diversification has been observed between single bacteria, indicating considerable strain variation that is most likely acquired by continuous DNA exchange and recombination events (Israel et al., 2001, Kraft et al., 2006) following horizontal gene transfer (Tomb et al., 1997, Alm et al., 1999). These highly polymorphic gene loci entail a similarly high level of enzyme allelic variation (Go et al., 1996), which is assumed to facilitate survival in a less favorable milieu and a successful evasion of host immunity (Cooke et al., 2005). In addition, this may result in an increased risk of ulcers and the development of gastric malignancies (Gerhard et al., 1999). Multi-locus sequencing efforts by means of distinct *H. pylori* core genes has revealed that the global population comprises seven different subtypes that have evolved within the context of human subpopulations or ethnic subgroups (Falush et al., 2003, Wirth et al., 2004).

The World Health Organization (WHO) has classified *H. pylori* as a class I carcinogen (Logan, 1994). Chronic infection by *H. pylori* is accompanied by a significantly elevated risk of developing gastritis, severe gastric atrophy, intestinal metaplasia and, ultimately, gastric cancer (Covacci et al., 1999, Uemura et al., 2001, Peek and Blaser, 2002, Vogelmann and Amieva, 2007). In cases of gastric adenocarcinoma, the eradication of *H. pylori* was reported to at least delay the development of cancer in a prospective study with a mean follow-up period of 4.8 years (Uemura et al., 2001), which is in line with Fukase et al. (2008), who demonstrated that the eradication of *H. pylori* can significantly reduce the incidence of metachronous gastric carcinoma after endoscopic resection of early gastric cancer. However, since patients are initially largely asymptomatic, diagnosis occurs predominantly at advanced tumor stages. Although chemotherapy can improve the prognosis, conventional chemotherapeutic regimens only evince median survival rates of 7 to 9 months in cases of advanced disease at diagnosis (Wagner et al., 2010).

1.2 *H. pylori* virulence factors

To successfully and sustainably colonize the human stomach, *H. pylori* has developed various mechanisms (Salama et al., 2013). These are related to the presence of certain virulence factors, such as urease (see 1.2.1), vacuolating cytotoxin A (VacA; see 1.2.2) and the cytotoxin-associated gene pathogenicity island (*cag*PAI; see 1.2.3), which is encoding for a type IV secretion system (T4SS) and for the cytotoxin-associated protein A (CagA; see 1.2.4).

1.2.1 Urease

H. pylori utilizes urease to avoid the harmful acidic milieu of the gastric lumen by maintaining an advantageous microenvironment: Urease catalyzes the conversion of urea into carbon dioxide and ammonium ions, which elevates the pH to nearly neutral in close proximity to the bacteria. Since *H. pylori* experiences fluctuating pH conditions, the synthesis and activity of urease are tightly attuned to acidity level (Stingl and De Reuse, 2005). Furthermore, viscoelasticity of gastric epithelial mucins depends on pH and enables penetration by *H. pylori* in neutral conditions, whereas at a low pH the mucus forms a gel that effectively repels bacteria (Celli et al., 2009).

1.2.2 Vacuolating cytotoxin A (VacA)

Vacuolating cytotoxin A (VacA) is an important secreted virulence factor that can be internalized into gastric epithelial host cells and thus induce the accumulation of vacuole-like membranous vesicles in the cytoplasm (de Bernard et al., 1997). This is assumed to be achieved by the formation of VacA anion-selective channels in membranes facilitating the translocation of chloride ions and weak membrane-permeable bases into the lumen, thereby entailing osmotic swelling (Papini et al., 1994, Cover and Blanke, 2005). In addition, VacA has demonstrated its ability to directly disrupt mitochondrial functions, to stimulate apoptosis and to inhibit the proliferation of T-cells (Cover and Blanke, 2005). Interestingly, there is evidence that VacA plays an important role in partly antagonizing or controlling the effects of another major *H. pylori* virulence factor: CagA (see 1.2.4). By means of the EGFR- and Erk1/2-mediated signaling pathways, VacA and CagA reciprocally attenuate morphologic changes and the formation of vacuoles, respectively (Argent et al., 2008, Tegtmeyer et al., 2009).

1.2.3 Cytotoxin-associated gene pathogenicity island (*cag*PAI)

Strains equipped with *cag*PAI denote a significantly pronounced risk for *H. pylori*-caused diseases (Backert et al., 2004). This DNA segment of about 40 kb is integrated into the bacterial chromosome (Censini et al., 1996). It has been demonstrated that strains lacking the *cag*PAI are far less virulent (Covacci et al., 1999, Crabtree et al., 1999), but still capable of inflicting damage to the host cells (Toller et al., 2011). Among the 28 to 31 genes (Tomb et al., 1997, Odenbreit, 2000), *cag*PAI encodes for the cytotoxin-associated protein A (CagA; see 1.2.4) and a T4SS (Censini et al., 1996, Akopyants et al., 1998). CagA is the only known *cag*PAI-encoded virulence factor that is directly translocated into the cytosol of host gastric epithelial cells by T4SS (Segal et al., 1999, Odenbreit, 2000, Viala et al., 2004), which requires interaction with the host cell β1-integrine receptor localized at the outer cell membrane (Jiménez-Soto et al., 2009). Although there are many examples of bacterial T4SS (Backert and Meyer, 2006), no homologues to CagA are known among bacteria, as its origin seems to be a phage (Lehours et al., 2011, Kyrillos et al., 2016).

1.2.4 Cytotoxin-associated protein A (CagA)

Cytotoxin-associated protein A (CagA) is considered a promiscuous bacterial oncoprotein. Its oncogenic potential has been well demonstrated in a transgenic mouse model (Ohnishi et al., 2008) and it has been identified as an independent predictor for the development of advanced gastric lesions, such as intestinal metaplasia, dysplasia and gastric cancer (Pan et al., 2014). Depending on the particular *H. pylori* strain, *cag*PAI-encoded CagA is a 128 to 145 kDa protein (Covacci et al., 1993, Segal et al., 1999, Stein et al., 2002) that greatly impinges on various crucial pathways in the host cells. Most of its numerous host cellular binding partners are considered to be involved in vital cell functions and carcinogenesis. There are at least 25 identified eukaryotic direct binding partners of CagA known thus far, such as the Abl and Src family kinases, as well as Crk, Grb2, PI3K, Shp2, c-Met, E-cadherin, PAR1b or ZO-1 (Backert et al., 2010, Backert and Tegtmeyer, 2017).

CagA's tertiary structure comprises distinct domains (Hayashi et al., 2012, Kaplan-Türköz et al., 2012) harboring different functions (see Figure 1). It was demonstrated that the first 200 AA of amino-terminal CagA are capable of mediating the attachment of the protein to the inner layer of the host cell membrane of polarized MDCK cells, supposedly in order to bring other domains into close proximity with membrane-bound factors (Pelz et al., 2011). In addition, Tsang et al. (2010) described tandem WW domains (WW1 and WW2) in the N-terminal part of CagA (strain NTC 11637), which are characterized by two conserved tryptophanes (W), a high amount of polar AA and several prolines (P) at both termini, one of which is strictly invariant at the carboxy-terminal part, enabling a highly specific protein interaction with the proline-rich motif PPxY (i.e., PY motif) (Sudol et al., 1995) and can hence be considered Group I WW domains (Sudol and Hunter, 2000). Apart from three single AA substitutions in the middle part of WW2 (IFDKK instead of VFNKE), the abovementioned tandem WW domains conform with AA 120-152 and 204-236 of wt CagA from the (Western) *H. pylori* strain G27 (see Figure 2).

The middle domain (roughly AA 450-650) might interact directly with the plasma membrane of polarized MDCK cells since it harbors positively charged sections for membrane binding (Hayashi et al., 2012). The carboxy-terminal part of CagA (roughly AA 800-1200) comprises several multimerization motifs, i.e., highly conserved amino acid motifs (see Figure 2), and acts as an interface for manipulating host cellular processes.

At its glutamate-proline-isoleucine-tyrosine-alanine (EPIYA) sequence motifs, C-terminal CagA can be tyrosine-phosphorylated by the Abl and Src family of protein tyrosine kinases (Selbach et al., 2002, Stein et al., 2002, Hatakeyama, 2004, Tammer et al., 2007). Once phosphorylated, EPIYA motifs are considered to be scaffolds or hubs for interaction with different host proteins, including pro-oncogenic (Src homology region 2 domain-containing) tyrosine phosphatase Shp2, thus being aberrantly activated (Higashi et al., 2002b, Hatakeyama, 2004). This induces membrane accumulation and the activation of further host cellular Src homology 2 (SH2) domain-containing proteins, such as adapter proteins Crk or Grb2, thus altering different signaling cascades, like the activation of the PI3K/Akt pathway (Selbach et al., 2009) and a gp130-mediated switch from the JAK/STAT3 to the MAPK/Erk (K-ras) pathway (Bronte-Tinkew et al., 2009, Lee et al., 2010). The latter entails a characteristic morphological change that was termed the "hummingbird phenotype" due to the pronounced gastric epithelial cell elongation (Segal et al., 1999, Mimuro et al., 2002, Suzuki et al., 2005). It could be demonstrated that Shp2 is a *bona fide* oncogene that is altered or mutated in a number of cancers (Mohi and Neel, 2007) that might be particularly attributed to its Grb2/MAPK/Erk pathway activation (Hatakeyama, 2004). There are several

CagA variants regarding the number of EPIYA motifs (Covacci et al., 1993, Tummuru et al., 1993, Higashi et al., 2002a), and different types of EPIYA motifs can be further discriminated. The CagA proteins of Western *H. pylori* strains show variable numbers of types A, B and C (see Figures 1 and 2), whereas East Asian strains present type D rather than type C (Higashi et al., 2002a). The higher the count of EPIYA motifs, the more pronounced the SH2 binding and, accordingly, CagA proteins comprising more than one EPIYA motif favor host cell invasion into the extracellular matrix (Nagase et al., 2015).

However, phosphorylation of CagA is not imperative for the substantial encroachment on cell signaling: Through the interaction of the adapter protein Grb2 with the carboxy-terminal part of CagA, apart from its EPIYA motifs, transcriptional activity and cell scattering can likewise be effected via MAPK/Erk signaling (Hirata et al., 2002, Mimuro et al., 2002). This has been shown to increase interleukin-8 (IL-8) expression levels by the translocation of the nuclear factor-κB (NF-κB) p65 subunit into the nucleus in a c-Met-independent way (Brandt et al., 2005), which has been related to angiogenesis, tumorigenesis and metastasis (Waugh and Wilson, 2008, Song et al., 2010).

A further type of carboxy-terminal multimerization motif has been independently characterized by Ren et al. (2006), Suzuki et al. (2009) and Nesic et al. (2010), latterly referred to as CagA multimerization (CM) motif. These are located in the C-terminal reach of the EPIYA motifs (see Figure 1) and differentiated into Western (CM^W), Eastern (CM^E) and further subtypes, depending on the geographic variant of CagA (Ren et al., 2006). With regard to Suzuki et al. (2009) in particular, the amino acid sequence of the Western type reads as FPLKRHDKVDDLSKVG, which, except for the substitution of aspartate (D) by glycine (G) at position 10, corresponds to three sites at the carboxy-terminal part of wt CagA from (Western) *H. pylori* strain G27 (see Figure 2). The CM^W motifs can mediate the aberrant activation of phosphatidyl-inositol-3 kinase (PI3K) and Akt via activated tyrosine kinase c-Met (Suzuki et al., 2009). Here, CagA utilizes the gastric cancer stem cell marker CD44 (Takaishi et al., 2009) to form a complex with c-Met and the hepatocyte growth factor (HGF), which ultimately provokes proliferation (Bertaux-Skeirik et al., 2015, Wroblewski et al., 2015), most likely through NF-κB signaling (Suzuki et al., 2009). Further, it was concordantly found that the CM^W motif is capable of impeding the activity of the PAR1/MARK (partitioning defective/microtubule affinity regulating kinases) family of protein kinases by direct interaction with PAR1 (Saadat et al., 2007, Nesic et al., 2010), which Saadat et al. (2007) showed could cause disruption of the host cellular polarity very quickly (< 24 h) (Segal et al., 1999, Amieva et al., 2003, Bagnoli et al., 2005) through junctional and polarity defects in an EPIYA phosphorylation-independent way. The strength of this interaction is subject to CM polymorphisms such as its copy number or sequence composition (Nishikawa et al., 2016).

As the deregulation of (canonical) Wnt/β-catenin signaling (see 1.3) is a substantial driver of gastric carcinogenesis (Clements et al., 2002, Ooi et al., 2009, Nguyen et al., 2012), there is much evidence that CagA might also have an impact on β-catenin turnover, although observations at large do not provide a clear picture. The implication of CagA phosphorylation concerning the alteration of the (canonical) Wnt/β-catenin pathway is not concordant, and nor is its presumed ability to disrupt adherence junctions to increase the cytosolic β-catenin amount. According to El-Etr et al. (2004), CagA causes phosphorylation-dependent up-regulation of β-catenin expression and, consequently, transcription of its target genes, indicating its role in effecting (canonical) Wnt/β-catenin signaling by nuclear accumulation of β-catenin. Murata-Kamiya et al. (2007) demonstrated the formation of CagA/E-cadherin complexes in a CagA phosphorylation-independent way that are (mostly) lacking β-catenin.

At the same time, they observed a cytosolic and nuclear accumulation of β-catenin causing a differential β-catenin-dependent gene expression. In contrast, Suzuki et al. (2005) on the one hand related cytosolic accumulation of β-catenin to the disruption of adherence junctions in a predominantly CagA phosphorylation-dependent way. On the other hand, nuclear translocation of β-catenin in AGS cells seemed to be independent of disruption of adherence junctions, since functional E-cadherin was not mandatory for this and it could not be induced by the artificial disintegration of adherence junctions. Instead, Wnt/β-catenin signaling activation could be caused via CM^W-mediated c-Met/PI3K/Akt signaling in a phosphorylation-independent manner, in addition to NF-κB activation (Suzuki et al., 2009). An unprejudiced look at the immunofluorescence microscopy data of these investigations generally gives the impression of an unchanged intense membranous β-catenin load, irrespective of its cytosolic and nuclear accumulation. Notably, it could be shown, at least for colon cancer, that β-catenin and NF-κB signaling crosstalk at several levels, since β-catenin can directly bind to and thus inhibit NF-κB (Deng et al., 2002).

Map of wild type CagA

H. pylori strain G27

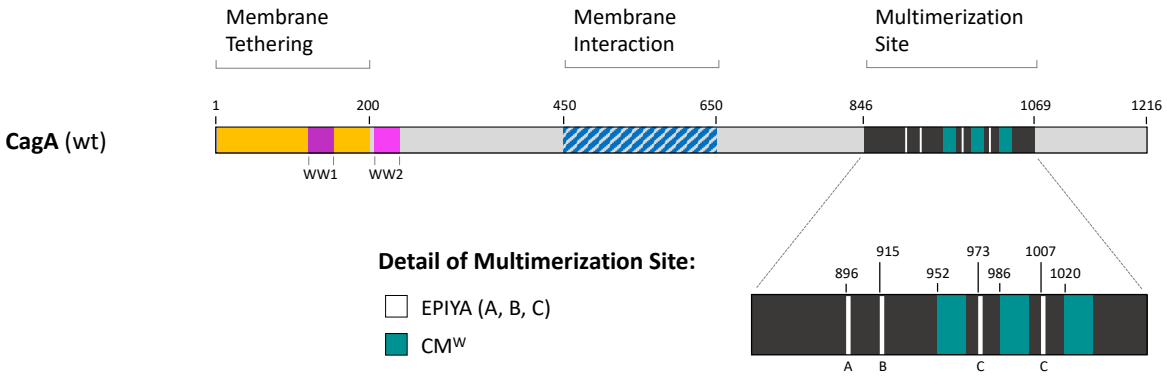

Figure 1: Map of wild type CagA.
Schematic representation of wt CagA (AA 1-1216) from *H. pylori* strain G27 (Odenbreit, 2000, Selbach et al., 2002, Stein et al., 2002, Bagnoli et al., 2005, Tammer et al., 2007, Tsang et al., 2010, Pelz et al., 2011, Hayashi et al., 2012); *orange section*: N-terminal part (AA 1-200) for membrane tethering; *pink sections*: WW1 (AA 120-152) and WW2 (AA 204-236) domains; *blue hatched section*: middle domain (roughly AA 450-650) for membrane interaction; *dark section*: multimerization site (AA 846-1069), depicted in detail in the enlargement; *white sections*: EPIYA motifs (type A, B or C); *teal sections*: CM^W motifs.

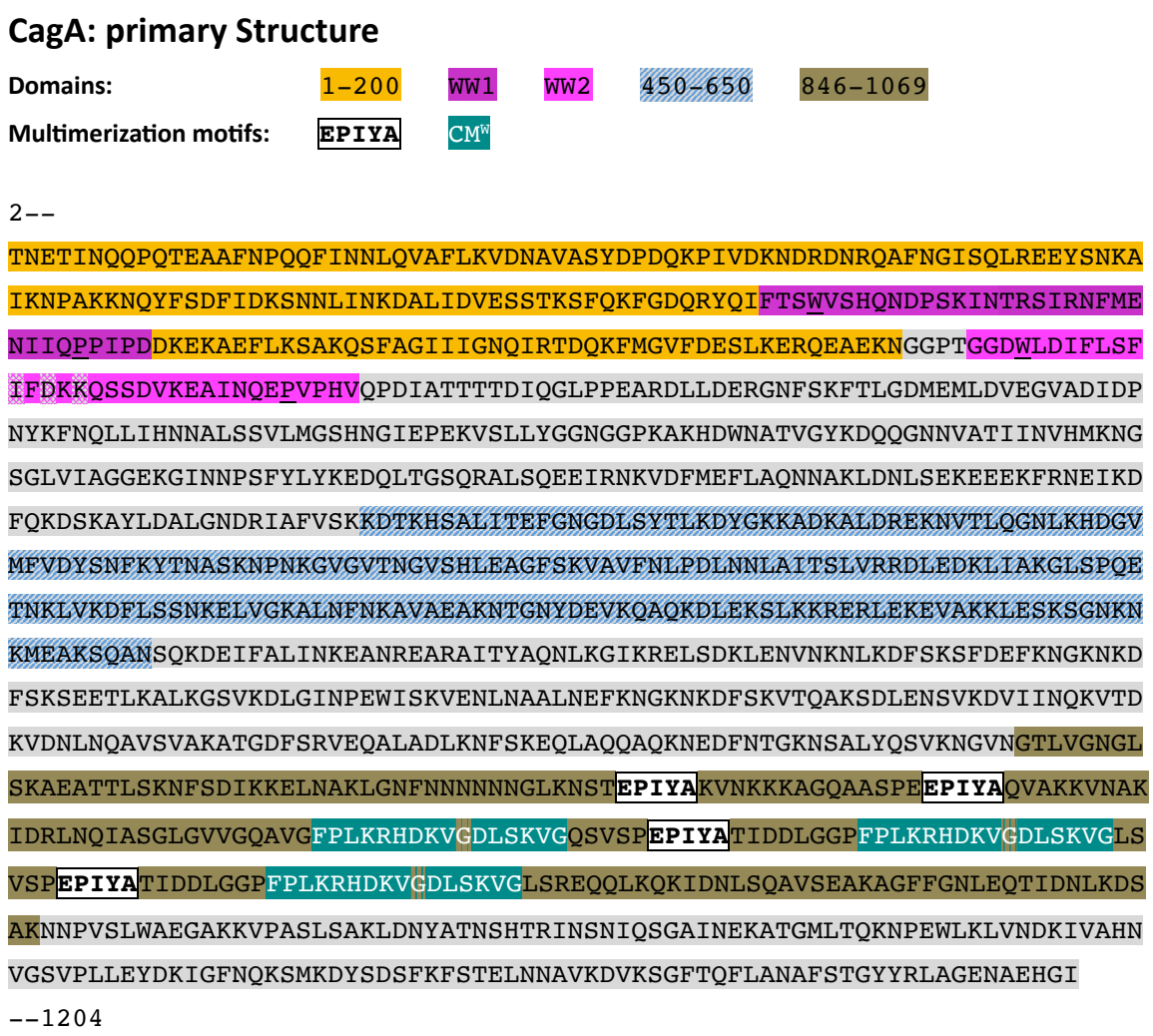

Figure 2: Sequence of wild type CagA.
Translation of wt *cagA* from *H. pylori* strain G27 into an amino acid sequence was performed in silico by NCBI BLASTX® after DNA sequencing of pTRE-tight-*GFP-cagA*-wt-*SBP* plasmid (kindly provided by Dr. Roger Vogelmann). Referring to Tsang et al. (2010), CagA features tandem WW domains (*pink*: the carboxy-terminal domain with three single AA substitutions in the middle part, IFDKK rather than VFNKE); according to Suzuki et al. (2009), G27 CagA (Western) features four EPIYA motifs (*bold/framed*: ABCC) and three distinct CM^W motifs (*teal*: with substitution of D by G at position 10); WW1 at AA 120, WW2 at AA 204; EPIYA motifs are located at AA 892, 911, 965 and 999; CM^W motifs are located at AA 944, 978, 1012.

1.3 Canonical Wnt/β-catenin signaling

The Wnt pathway is a markedly conserved means of regulating a variety of fundamental functions, such as cell proliferation, cell motility, tissue-specific single cell polarity, cell differentiation, apoptosis, definition of body axis as well as homeostasis of mature tissues (Logan and Nusse, 2004, Clevers, 2006, Willert and Nusse, 2012). Paradigms are changing towards a more integrated concept that considers Wnt signaling as a complex network processing intercellular and tissue-specific information (Kestler and Kühl, 2008, van Amerongen and Nusse, 2009, White et al., 2012). There are at least three characteristic routes known that can be induced by cell surface receptor binding of Wnt proteins. Regulation of the cytosolic β-catenin turnover is denoted by the canonical Wnt pathway (or rather the Wnt/β-catenin pathway) due to its outstanding role in controlling specific

processes in mature tissues (Clevers, 2006). Moreover, as this is presumably one target of CagA, it will be further addressed below. Mammalian genomes typically comprise 19 distinct Wnt genes that can be assigned to 12 subfamilies (Clevers, 2006, Willert and Nusse, 2012). Lipid modification of Wnt proteins is crucial for secretion into the extracellular space as well as accurate signaling properties (Willert et al., 2003).

1.3.1 Signal transduction and target genes

Once successfully secreted, Wnt proteins represent short-range signals affecting adjacent cells or those in close proximity by means of binding to a membrane-bound heterodimeric receptor complex (Sato et al., 2011). Whereas members of the frizzled protein family comprise seven transmembrane domains and each can interact with different Wnt proteins and *vice versa* (Bhanot et al., 1996), its vertebrate LDL receptor-related proteins 5 and 6 (LRP5/6) counterparts are single-pass transmembrane proteins that harbor distinct binding sites for several Wnt proteins (Pinson et al., 2000, Gong et al., 2010). In cases of inactive (canonical) Wnt/β-catenin signaling (see Figure 3, A), the unbound cytosolic axin acts as a scaffold and forms the so-called destruction complex (DC) by interaction with dishevelled (Dvl), CK1α/δ and GSK3α/β, together with the tumor suppressor proteins adenomatous polyposis coli (APC) and WTX (Hart et al., 1998, Ikeda et al., 1998, Liu et al., 2002, Major et al., 2007). This mediates phosphorylation and thus a rapid degradation of cytoplasmic β-catenin by the proteasome after ubiquitination due to recognition by βTrCP of the E3 ubiquitin ligase complex (Aberle et al., 1997, Major et al., 2007, Clevers and Nusse, 2012).

In terms of the activated (canonical) Wnt/β-catenin pathway (see Figure 3, B), shortly after Wnt has bound to the extracellular parts of the heterodimeric receptor, the LRP6 cytoplasmic domain is phosphorylated by serine-threonine kinases, either glycogen synthase kinase 3 β (GSK3β) or casein kinase 1 γ (CK1γ) (Zeng et al., 2005), which is a prerequisite for the cytosolic binding of axin to LRP6 (Tamai et al., 2004) that is promoted by dishevelled through its interaction with the frizzled cytoplasmic domain (Chen et al., 2003). Unlike other pathways, activated Wnt/β-catenin signaling does not recruit graded protein phosphorylation, but implies a distinct means of inducing signal transduction: The binding of axin to the receptor complex entails the disintegration of the DC and, consequently, the cessation of β-catenin ubiquitination (Bhanot et al., 1996, Pinson et al., 2000), causing its accumulation in the cytosol which, ultimately, facilitates the translocation of unphosphorylated β-catenin to the nucleus (Behrens et al., 1996, Molenaar et al., 1996). In the nucleus, β-catenin transiently converts DNA-bound T-cell factor or lymphoid enhancer binding factor (TCF/LEF) family members into transcriptional activators (Molenaar et al., 1996, Behrens et al., 1996) by superseding the Groucho corepressor (Daniels and Weis, 2005). There is some evidence that active (canonical) Wnt/β-catenin signaling is independent of the absolute amount of unphosphorylated β-catenin in the nucleus, and is rather based on its relative change (Goentoro and Kirschner, 2009), which refers to the ratio of the β-catenin amounts prior to and after alteration of the (canonical) Wnt/β-catenin pathway. Notably, even though β-catenin is located in substantial amounts at the cell membrane, due to its relevance for the attachment of the cytoskeleton to the plasma membrane by means of interaction with E-cadherin at adherence junctions (Peifer et al., 1992), a physiological interconnection between these two properties of β-catenin is not assumed (Clevers and Nusse, 2012).

Considering these multiple β-catenin/TCF/LEF target genes (Vlad et al., 2008, Nusse, 2016), the histologic character of each particular cell determines its unique expression pattern

(Logan and Nusse, 2004). Several factors and regulators of the (canonical) Wnt/β-catenin pathway are controlled by β-catenin/TCF/LEF itself. Wnt signaling is negatively regulated by its induction of axin and inhibition of frizzled or LRP6 (Logan and Nusse, 2004, Khan et al., 2007) and it is augmented by increased *TCF* and *LEF* gene expressions (Arce et al., 2006). Considering that the Wnt pathway plays an elementary role in development and cell homeostasis, it is not surprising that proto-oncogenes like *CCND1* (Shtutman et al., 1999, Tetsu and McCormick, 1999), encoding for Cyclin D1 protein, and *MYC* (He et al., 1998), encoding for c-Myc, are likewise among the target genes. Moreover, the expressions of matrix metalloproteinase 7 (*MMP7*), extracellular matrix proteolysis and motility promoting uPAR as well as activator protein 1 (AP-1), influence many fundamental cellular processes and are controlled by β-catenin/TCF/LEF (Brabletz et al., 1999, Mann et al., 1999).

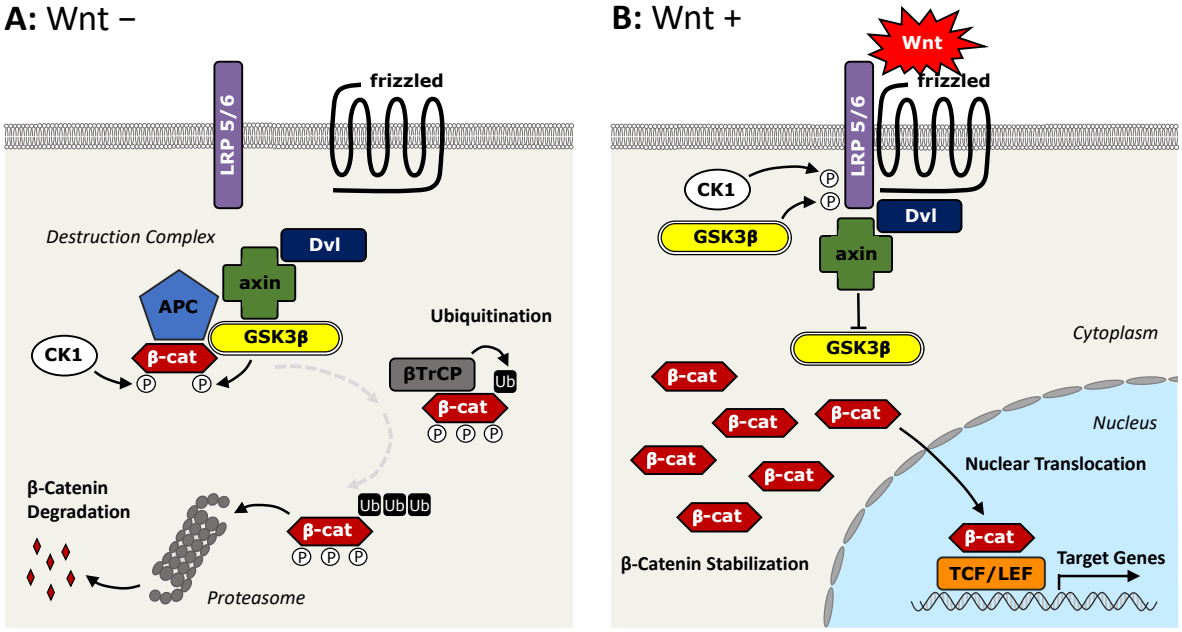

Figure 3: Canonical Wnt/β-catenin pathway.
LRP5/6: LDL receptor-related proteins 5 and 6; *Dvl*: dishevelled; *APC*: adenomatous polyposis coli protein; *GSK3β*: glycogen synthase kinase 3 β; *CK1*: casein kinase 1; *β-cat*: β-catenin; *βTrCP*: β-transducin repeat-containing protein; *Ub*: ubiquitin; *P*: phosphate group; *TCF/LEF*: T-cell factor or lymphoid enhancer binding factor. [**A**] Low cytosolic β-catenin levels in the absence of Wnt: remote LRP5/5 and frizzled receptor proteins; axin evokes assembly of multiprotein destruction complex (with its core components APC, GSK3β, CK1, βTrCP and β-catenin) to phosphorylate cytosolic β-catenin; subsequent ubiquitination and proteasomic degradation of phosphorylated β-catenin. [**B**] Elevated cytosolic and nuclear β-catenin levels through extracellular binding of Wnt to heterodimeric receptor: CK1 and GSK3β phosphorylate dimerized frizzled/LRP5/6 receptor; attaching of axin and Dvl; receptor-bound axin inhibits GSK3β and thus phosphorylation and degradation of cytosolic β-catenin; nuclear translocation of β-catenin and target gene expression by means of TCF/LEF.

1.3.2 CagA Wnt-dependent dysregulation: Pivotal for gastric tumorigenesis

Correa (1988) presented a human model of gastric carcinogenesis that conceives the tumorigenesis of intestinal-type gastric adenocarcinoma as a multistage process. In this model, chronic superficial gastritis develops into chronic atrophic gastritis, intestinal metaplasia, followed by dysplasia and, ultimately, gastric adenocarcinoma. In more than 70% of patients diagnosed with gastric cancer, several kinds of signaling pathways were dysregulated. These were proliferation or stem cell-related pathways and are associated with

various cell cycle regulators (e.g., c-Myc, E2F, p21), NF-κB signaling and Wnt/β-catenin signaling (Ooi et al., 2009). As mentioned above (see 1.3), Wnt/β-catenin signaling is a highly conserved means of controlling fundamental cellular and tissue-specific processes in multicellular animal organisms (Logan and Nusse, 2004, Clevers, 2006, Clevers and Nusse, 2012) and greatly crosstalks with other important routes of signal transduction (Hendriks and Reichmann, 2002, Katoh, 2007, Takebe et al., 2011, Borggrefe et al., 2016). Remarkably, 30-50% of gastric cancers show the activation of Wnt signaling (Clements et al., 2002, Ooi et al., 2009). The outstanding significance of the Wnt pathway in gastric malignancy is reflected in the finding that homeostasis of gastric cancer stem cells (GCSC) depends on it. Cycling of CD44 positive GCSC can be triggered by PGE2 or Wnt (Araki et al., 2003, Castellone et al., 2005, Ishimoto et al., 2010). Nguyen et al. (2012) found a strong correlation between tumorigenesis and progression through the maintenance of GCSC on the one hand and the aberrant activation of Wnt/β-catenin on the other. In addition, as intestinal-type gastric carcinomas present with a more invasive phenotype according to elevated nuclear β-catenin levels (Miyazawa et al., 2000), the (canonical) Wnt/β-catenin pathway seems to have a strong impact on epithelial-mesenchymal transition (EMT) and thus metastasis (Talbot et al., 2012).

As Wnt/β-catenin signaling is increasingly gaining significance concerning tumorigenesis of gastric cancer, somatic mutations of Wnt signaling pathway proteins are found in gastric cancer cells. Next-generation sequencing and genotyping confirmed *CTNNB1* and *APC* as driver genes, although with varying prevalence (Holbrook et al., 2011, Wang et al., 2011, Lee et al., 2012b, Nagarajan et al., 2012, Zang et al., 2012, Fassan et al., 2014). In addition to mutations of the TCF/LEF family (Duval et al., 1999, Kim et al., 2009), mutations of the *CTNNB1* gene, encoding the β-catenin protein, show an enhanced Wnt signaling activator function. Mutations in *CTNNB1* predominantly occur at exon 3, encoding for the GSK3β phosphorylation consensus region of β-catenin, thus making it resistant to the DC and causing its constitutive activation (Park et al., 1999, Woo et al., 2001, Clements et al., 2002, Ebert et al., 2002). Mutations of *APC* can be found in more advanced tumor stages with a frequency similar to that of *CTNNB1* (Rhyu et al., 1994, Ogasawara et al., 2006, Fang et al., 2012), thus emphasizing its relevance regarding tumor progression. Further, the loss of the Wnt repressor function in gastric cancer has been shown for mutations in *DKK1* (Aguilera et al., 2006), *AXIN1* (Kim et al., 2009) or *RUNX3* (Ito et al., 2011), which are inhibitors of the (canonical) Wnt/β-catenin pathway.

1.4 Objectives

Dysregulation of (canonical) Wnt/β-catenin signaling is a substantial driving force of gastric tumorigenesis. Notably, *H. pylori* was demonstrated to alter TCF/LEF transcriptional activity and hence appears to be some kind of catalyzer of gastric cancer. This effect is mainly attributed to its virulence factor CagA (see 1.2.4), which alters the (canonical) Wnt/β-catenin signaling activity level and could be correlated with premalignant conditions. However, the exact mechanisms of how CagA affects (canonical) Wnt/β-catenin signaling and the involvement of distinct CagA domains are not understood. Therefore, the main aim of this work is to decipher CagA's impact on (canonical) Wnt/β-catenin signaling.

To address this, the following specific objectives were defined:

Impact of CagA on (canonical) Wnt/β-catenin signaling:

- Does CagA induce changes in TCF/LEF transcriptional activity?
- Does CagA exert influence on the host cells in a dose-dependent manner?

Relevance of CagA domains:

- To what extent are the amino- and carboxy-terminal domains involved in the effects on (canonical) Wnt/β-catenin signaling activity?

Spatial distribution in the host cell:

- Do the amino- and carboxy-terminal domains show differential subcellular localization once CagA is translocated into the host cell?

2 Materials & Methods

2.1 Laboratory equipment

2.1.1 Instruments and devices

Instrument	Manufacturer
Advanced fluorescence and ECL imager	Intas Science Imaging Instruments, Göttingen (Germany)
Biofuge fresco (Heraeus)	Thermo Fisher Scientific, Waltham, MA (USA)
C1000 Touch thermal cycler	Bio Rad Laboratories, Hercules, CA (USA)
Forma Series II water jacket CO_2-incubator	Thermo Fisher Scientific, Waltham, MA (USA)
Gel Doc™ XR^+ documentation system	Bio Rad Laboratories, Hercules, CA (USA)
Hera cell 240 CO_2-incubator (Heraeus)	Thermo Fisher Scientific, Waltham, MA (USA)
Hera freeze basic (Heraeus)	Thermo Fisher Scientific, Waltham, MA (USA)
Hera safe KS18 safety cabinet (Heraeus)	Thermo Fisher Scientific, Waltham, MA (USA)
Leica SP5, confocal microscope	Leica, Wetzlar (Germany)
Mega fuge 2.0 RS (Heraeus)	Thermo Fisher Scientific, Waltham, MA (USA)
Mini-Sub Cell GT electrophoresis chamber	Bio Rad Laboratories, Hercules, CA (USA)
NanoDrop ND 1000 spectrometer	Thermo Fisher Scientific, Waltham, MA (USA)
Nikon Eclipse TS 100 + Nikon Digital Sight DS-L3	Nikon, Tokio (Japan)
Novex® XCell SureLock™ mini-cell	Life Technologies, Carlsbad, CA (USA)
Orion microplate luminometer	Berthold, Bad Wildbad (Germany)
Power Pac HC	Bio Rad Laboratories, Hercules, CA (USA)
Trans Blot SD Semidry, transfer cell	Bio Rad Laboratories, Hercules, CA (USA)

Table 1: Laboratory equipment

2.1.2 Consumables

Consumables	Manufacturer
Blotting paper (Whatman)	GE Healthcare, Little Chalfont (UK)
Cover slips	Menzel, Braunschweig (Germany)
Cryotubes (Nalgene)	Thermo Fisher Scientific, Waltham, MA (USA)
Filter 0,45 µm	Sartorius, Göttingen (Germany)
Microcentrifuge tubes (0.5 ml, 1.5 ml, 2.0 ml)	VWR international, Radnor, PA (USA)
Microscope slides, superfrost plus	Menzel, Braunschweig (Germany)
Multiwell tissue culture plates (6-, 12-, 24-well) (Falcon)	BD Labware, Franklin Lake, NJ (USA)
Novex® gel cassettes	Life Technologies, Carlsbad, CA (USA)
Novex® gel combs	Life Technologies, Carlsbad, CA (USA)
Parafilm® "M"	Pechiney Plastics Packaging, Boscobel, WI (USA)
Pipette tips	VWR international, Radnor, PA (USA)
Protran® nitrocellulose transfer membrane (Whatman)	GE Healthcare, Little Chalfont (UK)
Serologic pipettes (2 ml, 5 ml, 10 ml, 25 ml)	Greiner Bio-one, Kremsmünster (Austria)
TipOne® graduated filter tips	Starlab, Hamburg (Germany)
Tissue culture dishes (100 × 20 mm; Dia × H) (Falcon)	BD Labware, Franklin Lake, NJ (USA)
Tissue culture flasks (25 cm^2, 75 cm^2, 185 cm^2)	VWR international, Radnor, PA (USA)
Tubes, polypropylen (15 ml, 50 ml)	Greiner Bio-one, Kremsmünster (Austria)

Table 2: Consumables

2.1.3 Software

Software	Manufacturer
ChemoStar recording software	Intas Science Imaging Instruments, Göttingen (Germany)
CLC Workbench	Quiagen, Venlo (Netherlands)
GraphPad Prisme	GraphPad Software, La Jolla, CA (USA)
IMAGEJ software	Wayne Rasband, NIH, Bethesda, MD (USA)
Microsoft Excel	Microsoft Corporation, Redmond, WA (USA)
Molecular Imager Gel Doc XR^+ System	Bio Rad Laboratories, Hercules, CA (USA)
Photoshop CS	Adobe Systems, Mountain View, CA (USA)

Table 3: Software

2.2 Reagents

2.2.1 Cell culture reagents

Reagent	Manufacturer
Dulbecco's modified Eagle medium (D-MEM; 1x; +4.5 g/l D-glucose, +L-glutamine), liquid	Gibco, Carlsbad, CA (USA)
Fetal bovine serum (FBS), liquid	Sigma-Aldrich, St Louis, MO (USA)
L-glutamine (200 mM)	Gibco, Carlsbad, CA (USA)
Lipofectamine® 2000 reagent, liquid	Life Technologies, Carlsbad, CA (USA)
Lithium Chloride, powder	Merck, Darmstadt (Germany)
Opti-MEM® I reduced-serum medium (1x), liquid	Gibco, Carlsbad, CA (USA)
Penicillin-streptomycin (10,000 U/ml)	Gibco, Carlsbad, CA (USA)
Puromycin, powder	Merck, Darmstadt (Germany)
RPMI 1640 medium (1x; + L-glutamine), liquid	Gibco, Carlsbad, CA (USA)
Trypsin, 0.25% (1x), phenol red, liquid	Gibco, Carlsbad, CA (USA)

Table 4: Cell culture reagents

2.2.2 Microbiology, molecular biology and biochemistry reagents

Reagent	Manufacturer
2-[4-(2-hydroxyethyl)piperazin-1-yl]ethanesulfonic acid (HEPES)	Sigma-Aldrich, St Louis, MO (USA)
Acetic acid	Merck, Darmstadt (Germany)
Acetone	Merck, Darmstadt (Germany)
Acrylamide (Bis 19:1, 40%)	Ambion, Carlsbad, CA (USA)
Agar-Agar	Roth, Karlsruhe (Germany)
Ammonium persulfate (APS)	Roth, Karlsruhe (Germany)
Ampicillin sodium salt	Sigma-Aldrich, St Louis, MO (USA)
Beef serum albumin (BSA), albumin fraction V (pH 7.0)	AppliChem, Darmstadt (Germany)
BHI medium	Sigma-Aldrich, St Louis, MO (USA)
Brucella broth	Oxoid Limited, Basingstoke (UK)
Bromophenol blue	Bio Rad Laboratories, Munich (Germany)
Clarity™ Western ECL substrate, immunodetection reagent	Bio Rad Laboratories, Hercules, CA (USA)
Columbia blood agar	Oxoid Limited, Basingstoke (UK)

Defibrinated horse blood	Oxoid Limited, Basingstoke (UK)
Disodium hydrophosphate (Na_2HPO_4)	Merck, Darmstadt (Germany)
Dithiothreitol (DTT)	Roth, Karlsruhe (Germany)
Ethanol, absolute	AppliChem, Darmstadt (Germany)
Ethylene-diamine-tetraacetic acid (EDTA)	AppliChem, Darmstadt (Germany)
Ethylene-glycol-tetraacetic acid (EGTA)	Roth, Karlsruhe (Germany)
Glucose	Thermo Fisher Scientific, Waltham, MA (USA)
Glycerol	AppliChem, Darmstadt (Germany)
Glycin	Roth, Karlsruhe (Germany)
Glycylglycine (GlyGly)	AppliChem, Darmstadt (Germany)
GoTaq® DNA polymerase	Promega, Madison, WI (USA)
Helicobacter pylori selective supplement (DENT supplement)	Oxoid Limited, Basingstoke (UK)
Herculase® II fusion DNA polymerase	Agilent Technologies, Santa Clara, CA (USA)
Hydrochloric acid (HCl)	Merck, Darmstadt (Germany)
Isopropyl alcohol	AppliChem, Darmstadt (Germany)
Kanamycin sulfate	Sigma-Aldrich, St Louis, MO (USA)
Lithium chloride (LiCl)	Merck, Darmstadt (Germany)
Lysogeny broth agar (LB, Luria/Miller)	Roth, Karlsruhe (Germany)
Lysogeny broth medium (LB, Luria/Miller)	Roth, Karlsruhe (Germany)
Magnesium sulfate	Roth, Karlsruhe (Germany)
Methanol, absolute	Merck, Darmstadt (Germany)
Milk powder, blotting grade	Roth, Karlsruhe (Germany)
Monopotassium phosphate (KH_2PO_4)	Merck, Darmstadt (Germany)
Phosphate buffered saline (PBS)	Roth, Karlsruhe (Germany)
Ponceau S	Sigma-Aldrich, St Louis, MO (USA)
Potassium chloride (KCl)	Merck, Darmstadt (Germany)
Potassium nitrate (KNO_3)	Merck, Darmstadt (Germany)
Precision Plus Protein™ all blue standard	Bio Rad Laboratories, Hercules, CA (USA)
Precision Plus Protein™ dual color standard	Bio Rad Laboratories, Hercules, CA (USA)
Restore Western BGA, stripping buffer	Thermo Fisher Scientific, Waltham, MA (USA)
Roti®-Safe GelStain	Roth, Karlsruhe (Germany)
Saponin	Sigma-Aldrich, St Louis, MO (USA)
Sodium chloride (NaCl)	Roth, Karlsruhe (Germany)
Sodium dodecyl sulfate (SDS)	Roth, Karlsruhe (Germany)
Sodium hydroxide (NaOH)	AppliChem, Darmstadt (Germany)

Tetramethylethylenediamine (TEMED, ultra pure)	Life Technologies, Carlsbad, CA (USA)
Tris	Roth, Karlsruhe (Germany)
Triton® X-100 (Octoxynol-9)	AppliChem, Darmstadt (Germany)
Tryptone	AppliChem, Darmstadt (Germany)
Tween® 20 (Polyoxyethylene sorbitan monolaurate)	AppliChem, Darmstadt (Germany)
Vectashield® HardSet™ mounting medium with DAPI	Vector Lab, Burlingame, CA (USA)
WC agar	Oxoid Limited, Basingstoke (UK)
Yeast extract	Sigma-Aldrich, Buchs (Switzerland)
β-Mercaptoethanol	Sigma-Aldrich, St Louis, MO (USA)

Table 5: Molecular biology and biochemistry reagents

2.2.3 Cloning materials

Item	Manufacturer
Agarose, low EED	Sigma-Aldrich, St Louis, MO (USA)
BamHI, BglII, BspHI, DpnI, EcoRI, EcoRV, MluI, NcoI, NheI, PstI, PvuII, SalI, SmaI, SpeI, SphI (Restriction enzymes)	Promega, Madison, WI (USA)
Bench Top 1kb DNA ladder	Promega, Madison, WI (USA)
pCignal™ Lenti Renilla Control	Quiagen, Venlo (Netherlands)
pCignal™ Lenti TCF/LEF Reporter	Quiagen, Venlo (Netherlands)
Gel loading dye (6x)	Roth, Karlsruhe (Germany)
Gibson Assembly® cloning kit	NEB, Ipswich, MA (USA)
One Shot® MAX Efficiency™ DH10B™ T1 phage resistant cells	Life Technologies, Carlsbad, CA (USA)
One Shot® OmniMax™ 2 $T1^R$	Life Technologies, Carlsbad, CA (USA)
Platinum® *Taq* DNA polymerase high fidelity	Life Technologies, Carlsbad, CA (USA)
Subcloning Efficiency™ DH5α™ competent cells	Life Technologies, Carlsbad, CA (USA)
sureENTRY™ Transduction Reagent	Quiagen, Venlo (Netherlands)
T4 DNA Ligase	NEB, Ipswich, MA (USA)
TOPO® TA Cloning® kit	Life Technologies, Carlsbad, CA (USA)

Table 6: Cloning materials

2.2.4 Plasmids

Plasmid	Originator/Distributor/Manufacturer
pcDNA3.1	Thermo Fisher Scientific, Waltham, MA (USA)
pcDNA4/TO	Thermo Fisher Scientific, Waltham, MA (USA)
pCignal™ Lenti Renilla Control (luc)	Quiagen, Hilden, Germany
pCignal™ Lenti TCF/LEF Reporter (luc)	Quiagen, Hilden, Germany
pCMV-dR8.91	Kindly provided by Prof. D. Trono, Lausanne, Switzerland
pEGFP-C1	Clontech Laboratories, Mountain View, CA (USA)
pEGFP-N1	Clontech Laboratories, Mountain View, CA (USA)
pFOPflash	Kindly provided by Prof. H. Clevers, Utrecht, Netherlands (Korinek et al., 1997)
pLenti CMV Puro DEST	Addgene, Cambridge, MA (USA)
pMD2.G	Kindly provided by Prof. D. Trono, Lausanne, Switzerland
pRL CMV (*Renilla* luciferase)	Promega, Madison, WI (USA)
pTOPflash	Kindly provided by Prof. H. Clevers, Utrecht, Netherlands (Korinek et al., 1997)

Table 7: Plasmids used (for cloning, transfection, transduction, stuffer, etc.)

2.2.5 Kits

If not stated otherwise, those commercial kits were used according to the manufacturer's protocol.

Kit	Manufacturer
DNeasy® Blood&Tissue kit	Quiagen, Venlo (Netherlands)
Dual-Luciferase® reporter assay system	Promega, Madison, WI (USA)
Pure Yield™ plasmid midi prep system	Promega, Madison, WI (USA)
Pure Yield™ plasmid mini prep system	Promega, Madison, WI (USA)
Wizard® SV gel and PCR clean-up system	Promega, Madison, WI (USA)

Table 8: Preparation kits utilized

Buffers and solutions

Buffer	Composition
Fixation solution (for IF)	Methanol/Acetone 1:1 (-20 °C)
Lysis buffer (TOP/FOP assay)	25 mM GlyGly
	4 mM EGTA (pH 8.0)
	15 mM $MgSO_4$
	1% Triton X-100
	[optional: 1 mM DTT]
PBS buffer (phosphate buffered saline, 10x)	1.37 M NaCl
	27 mM KCl
	100 mM Na_2HPO_4
	18 mM KH_2PO_4
	pH 7.4 (HCl)
Permeabilization and blocking buffer (for IF)	PBS (1x)
	3% (w/v) BSA
	1% (w/v) Saponin
	0.5% Triton X-100
SDS lysis buffer (1x)	2% w/v SDS
	62.5 mM TRIS pH 6.8
	10% Glycerol
	0.01% Bromophenol blue
	50mM DTT (added instantly before use)
SDS running buffer (10x)	0.1% (w/v) SDS
	25 mM Tris (pH 6.8)
	200 mM Glycine
SDS sample buffer (4x)	0.8% (w/v) SDS
	160 mM Tris (pH 6.8)
	30% Glycerol
	0.01% (w/v) Bromophenol blue
Semi dry transfer buffer	48 mM Tris ultra
	39 mM Glycine
	0.0379% SDS (10%)
	20% MeOH
TAE buffer (1x)	40 mM Tris
	20 mM Acetic acid

	1 mM EDTA (pH 8.0)
TBS buffer (10x)	500 mM Tris
	1.5 M NaCl
	pH 7.5 (HCl)
TBS-T buffer (1x)	1/10 TBS (10x) buffer diluted in ddH_2O
	0.1% Tween 20
Washing buffer 1 (for IF)	PBS (1x)
	3% (w/v) BSA
	1% (w/v) Saponin
Washing buffer 2 (for IF)	PBS (1x)
	1% (w/v) Saponin

Table 9: Prepared buffers and solutions

2.2.6 Antibodies

Antibody	Dilution	Manufacturer
Alexa Fluor 488 goat anti-mouse	IF 1:300	Molecular Probes, Invitrogen, OR (USA)
Alexa Fluor 594 chicken anti-rabbit	IF 1:300	Molecular Probes, Invitrogen, OR (USA)
Anti-goat IgG, HRP conjugate	IB 1:2500	Promega, Madison, WI (USA)
Anti-mouse IgG, HRP conjugate	IB 1:2500	Promega, Madison, WI (USA)
Anti-rabbit IgG, HRP conjugate	IB 1:2500	Promega, Madison, WI (USA)
Hoechst 33342	IF 1:10000	Hoechst, Frankfurt (Germany)
Mouse anti-β-actin	IF 1:1000	Sigma-Aldrich, St Louis, MO (USA)
Mouse anti-β-catenin	IB 1:2000	BD Transduction Laboratories, Franklin Lake, NJ (USA)
	IF 1:500	
Rabbit anti-$CagA_{1\text{-}877}$	IB 1:5000	Against CagA AA 1-877 (recombinant GST fusion protein expressed in *E. coli*)
	IF 1:200	
Rabbit anti-FLAG	IB 1:2500	Sigma-Aldrich, St Louis, MO (USA)
	IF 1:200	
Rabbit anti-nonP-β-catenin	IB 1:1000	Cell Signaling, Boston, MA (US)
Rabbit anti-P-β-catenin	IB 1:1000	Cell Signaling, Boston, MA (US)

Table 10: Antibodies used (IB: Western blotting, IF: Immunofluorescence staining)

2.2.7 Media and agarose plates

Medium	Composition	Comment
Luria-Bertani (LB) agar plates	0.5% (w/v) NaCl 0.5% (w/v) Yeast extract 1.0% (w/v) Tryptone 1.5% (w/v) Agar-Agar pH 7.4 (NaOH)	After autoclaving, medium was cooled down to approximately 55 °C, corresponding antibiotic was added and medium was transferred to culture plates, once having reached RT plates were stored at -4 °C
Luria-Bertani (LB) medium	1.0% (w/v) NaCl 0.5% (w/v) Yeast extract 1.0% (w/v) Tryptone pH 7.4 (NaOH)	After autoclaving, medium was cooled down to approximately 55 °C, corresponding antibiotic was added, once having reached RT medium was stored at -4 °C
Super optimal broth (SOB medium)	10 mM NaCl 2.5 mM KCl 0.5% (w/v) Yeast extract 2.0% (w/v) Tryptone pH 7.4 (NaOH) 20 mM $MgSO_4$	Preparation and $MgSO_4$ may be autoclaved the same time, but separately, afterwards merging of both
Super optimal broth with catabolite repression (SOC medium)	SOB medium 20 mM Glucose solution (20%)	After cooling of SOB medium to less than 50 °C, filter-sterilized glucose solution was added
WC DENT horse blood agar plates	500 ml ddH_2O 43 g/l WC agar 0.8 g/l KNO_3 DENT supplement* 35 ml (defibrinated) horse blood 10% [optional: 100 µg/ml kanamycin]	WC agar and KNO_3 were dissolved in deionized water and autoclaved (2 min), thereafter cooling down medium to 50 °C and subjoining dent supplement* and defibrinated horse blood, solution was immediately dispensed in petri dishes, stored at 4 °C *** comprising: 5 mg Vancomycin; 2.5 mg Trimethoprim; 2.5 mg Cefsulodin; 2.5 mg Amphotericin B**

Table 11: Media and agarose plates

2.3 Cell lines and bacterial strains

2.3.1 Eukaryotic cells

Cell line	Origin	Specification
AGS	*Homo sapiens* ♀ stomach, gastric adenocarcinoma (primary)	Hyperdiploid (modal chromosome number 49, 60% of cells), persistently infected with parainfluenza virus type 5 (PIV5) (ATCC, CRL-1739); **mutations:** activation of Wnt/β-catenin signaling through mutation at *CTNNB1* (Caca et al., 1999, Asciutti et al., 2011); frameshift causing dysfunctional E-cadherin (*CDH1*) expression (Caca et al., 1999, Oliveira et al., 2009); deleterious mutations at *LGR5*, *KRAS* and *TAB2* (5.1.1.2.1); **Wnt/β-catenin signaling activity:** strong (= 0.68, by comparison to NCI-N87 (= 1) (see 5.1.2.3);
MKN45 *alias:* *MKN-45*	*Homo sapiens* ♀ stomach, gastric adenocarcinoma (metastasis)	Hypertriploid (8% polyploidy); poorly differentiated; impaired stabilization of wt p53 through deletion at *CDKN2A* (Iida et al., 2000); **mutations:** 4-AA deletion at E-cadherin key Ca^{2+}-binding motif presumably effecting reduced cell-cell-adhesion (Oda et al., 1994); deleterious mutations at *WNT5B* and *FZD7* (see 5.1.1.2.2); **Wnt/β-catenin signaling activity:** weak (= 0.06), by comparison to NCI-N87 (= 1) (see 5.1.2.3);
23132 *alias:* *23132-87* *23132/87*	*Homo sapiens* ♂ stomach, gastric adenocarcinoma (primary)	Aneuploid (chromosomal numbers varying: 30-109); **mutations:** microsatellite instability, causing various frameshifts (*AXIN1*, *AXIN2*, *FZD6*, *NLK*, *RNF43*, *WNT1*); pathologic mutation at *CDH1* affecting cadherin domain (Klijn et al., 2015); deleterious mutations at *CSNK1E*, *DKK1*, *DKK2*, *DVL2*, *FZD5*, *FZD8*, *LRP6* and *TCF3* (see 5.1.1.2.3); **Wnt/β-catenin signaling activity:** subordinate (= 0.08), by comparison to NCI-N87 (= 1) (see 5.1.2.3);
293T *alias:* *HEK 293T*	*Homo sapiens* ♀ fetal kidney, (presumably) immature neurons from adrenal precursor structure (Shaw et al., 2002, Lin et al., 2014)	Hypertriploid (modal chromosome number 64, 30% of cells) (ATCC, CRL-1573); potentially tumorigenic (Stepanenko and Dmitrenko, 2015); Human Embryonic Kidney (HEK) 293 cells are transduced by sheared adenovirus type 5 (AD5) (Graham et al., 1977) causing deregulation of pRB/p53 pathways (Stepanenko et al., 2013) thus interfering with cell cycle control and counteracting apoptosis (Berk, 2005); 293T derivate with additionally compromised genome integrity through overexpression of SV40 LTag therefore inhibiting p53 (DuBridge et al., 1987, Lin et al., 2014); **mutations:** deleterious mutations at *LGR4*, *TP53* and *ZNRF3* (see 5.1.1.3); **Wnt/β-catenin signaling activity:** intact (Liu et al., 2007, Upadhyay et al., 2008);

Table 12: Immortalized cell lines

2.3.2 Prokaryotic cells

H. pylori strain	Origin	Specification
G27	Isolated from endoscopy biopsy specimens (Covacci et al., 1993)	Human pathogen, single circular chromosome (1,652,983 bp), contains one plasmid of 10,032 bp encoding 11 genes, single plasticity region (between ORFs 927 and 985) containing many *H. pylori*-specific genes (Baltrus et al., 2009)
G27 ΔCagA	*H. pylori* strain G27	CagA deficient isogenic strain generated by allelic exchange through natural transformation
PMSS1	Clinical isolate capable of infecting mice, premouse strain (Lee et al., 1997)	Human pathogen, CagA and VacA positive (Lee et al., 1997)
PMSS1 ΔCagA	*H. pylori* strain PMSS1	CagA deficient isogenic strain generated by allelic exchange through natural transformation

Table 13: *Helicobacter pylori* strains

2.4 Cloning of the *cagA* gene and its constructs

In addition to the full-length wild type (wt) *cagA* gene, truncated versions (so-called "constructs") have also been created that can likewise be introduced into eukaryotic host cells by transfection or transduction. These are all derived from a pTRE-tight-*GFP-cagA*-wt-*SBP* plasmid kindly provided by Dr. Roger Vogelmann and originally constructed from wt *cagA* of *H. pylori* strain G27 (Covacci et al., 1993). In general, wt *cagA* and its constructs were defined and amplified by PCR using primers that attached additional sequences (such as FLAG-tag, the Kozak sequence or just linker-DNA). All constructs were verified by sequencing.

Basically, this should generate or provide three different variants of the CagA protein: In addition to wt CagA also an amino-terminal ("NT") as well as a carboxy-terminal variant ("CT") of this protein (see Figure 4). The latter are also collectively referred to as "constructs" or "truncated versions" in the following.

- **wt *cagA* ⟶ wt CagA**
  Full length CagA protein comprising amino acids 1-1216 (i.e., *cagA* bp 1-3648)
- ***cagA*-NT$_{AA1-200}$ ⟶ CagA-NT$_{AA1-200}$**
  The amino-terminal domain of CagA, comprising amino acids 1-200 (i.e., *cagA* bp 1-600)
- ***cagA*-CT$_{AA201-1216}$ ⟶ CagA-CT$_{AA201-1216}$**
  The middle and carboxy-terminal domains of CagA, harboring the EPIYA and CM^{W} multimerization motifs and comprising amino acids 201-1216 (i.e., *cagA* bp 601-3648)

Map of the CagA protein and its constructs

H. pylori strain G27

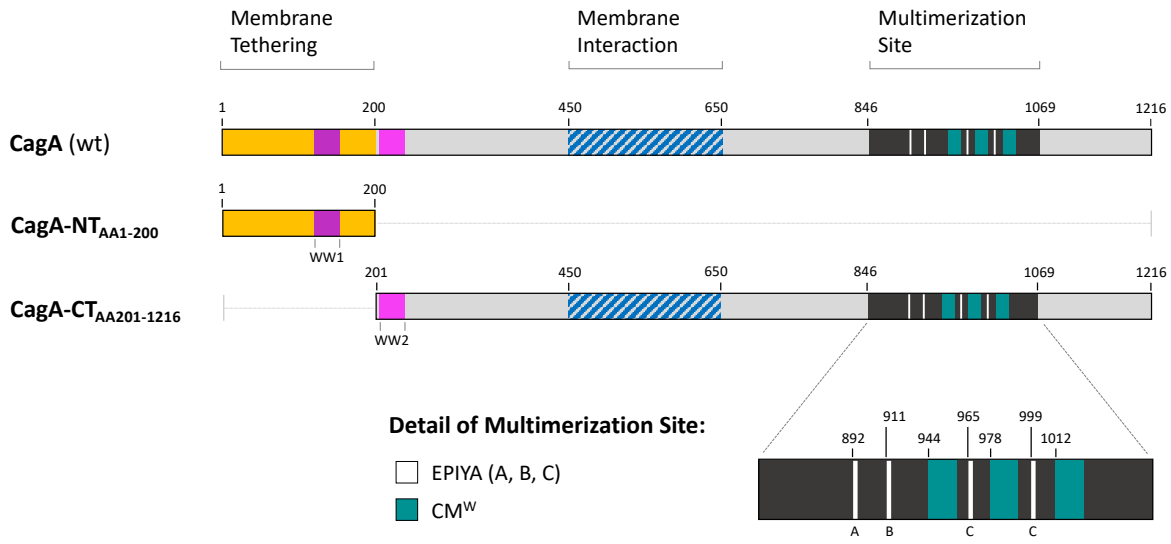

Figure 4: Map of CagA protein and its constructs.
Schematic representation of *H. pylori* strain G27 wild type CagA (AA 1-1216) and its constructs (CagA-NT$_{AA1-200}$ and CagA-CT$_{AA201-1216}$); *orange section*: N-terminal part (AA 1-200) for membrane tethering; *pink sections*: WW1 (AA 121-153) and WW2 (AA 205-237) domain, respectively; *blue hatched section*: middle domain (roughly AA 450-650) for membrane interaction; *dark section*: multimerization site (AA 846-1069), depicted in detail in the enlargement; *white sections*: EPIYA motifs (type A, B or C), *teal sections*: CM^{W} motifs.

2.4.1 pEGFP-*cagA* (wt or constructs)

Since successfully transfected eukaryotic cells can be easily detected by green fluorescence through expression of the *EGFP* gene (Chalfie et al., 1994, Cormack et al., 1996), the pEGFP cloning vector system was used. It basically comprises two variants with different localization of the multi cloning site with respect to the *EGFP* gene, allowing for production of fusion proteins in which the insert is either located at the carboxy-terminal (pEGFP-C$_{1-3}$) or at the amino-terminal (pEGFP-N$_{1-3}$) part of the *EGFP* gene. In transfection experiments only pEGFP-C1-*cagA* constructs have been utilized (see 3.2.2). The CMV promoter ensures that construct genes are strongly expressed and the SV40 poly A sequence, located downstream of the multi cloning site, stabilizes the mRNA following transcription. To add specific restriction sites, cloning into the pEGFP vector system was done in a two-step approach, which comprised TOPO® TA cloning (see 2.4.1.1) followed by conventional cloning (see 2.4.1.2).

2.4.1.1 TOPO® TA cloning (step 1)

In contrast to conventional molecular cloning (see 2.4.1.2), the TOPO® TA cloning technique allows for subcloning without the use of restriction enzymes. The rationale is based on two principles: (i) the ability of the complementary single overhanging 3'-adenin (A) and 3'-thymidine (T) residues of two different DNA fragments to spontaneously hybridize and (ii) the fact that vaccinia virus topoisomerase I provides a phosphor-tyrosyl bond between itself and a terminal DNA fragment (in this context, at the overhanging 3'-thymidine of the vector). This bond can then be targeted by the non-overhanging 5'-hydroxyl group of the second DNA fragment (i.e., the insert) once hybridization has been completed, resulting in ligation of the two fragments. The probability is even increased if the primers used for amplification of the

particular insert contain guanine residues close to the 5'-end. In addition to the possibility of adding distinct restriction sites by suitable primers, the single 3'-adenin overhangs are attached to the insert by using a *Taq* DNA polymerase for its amplification (due to its non-template-dependent terminal transferase activity). In these experiments, the TOPO® TA cloning kit was used, which provides an already linearized plasmid vector (pCR™4-TOPO®) with single 3'-thymidine overhangs. The latter belong to the 5'-CCCTT parts where vaccinia virus topoisomerase I has already bound and cleaved the (former) phosphodiester backbone just behind. Whereas the native topoisomerase only mediates the covalent rejoining of the backbone after relaxation of the DNA molecule, the provided topoisomerase remains covalently bound to the linearized vector waiting for its own liberation. Once the complementary 3'-adenosin of the insert hybridizes with the single overhanging 3'-thymidine of the vector, the phosphodiester backbones are covalently connected while releasing the topoisomerase. According to the manufacturer's protocol, the whole procedure was done at RT within 30 minutes.

In order to preserve the different *cagA* constructs and to be capable of DNA sequencing, TOPO® TA cloning was utilized as the first step of transferring them to the desired expression vector system (pEGFP-C1, pEGFP-N1). First, wt *cagA* and its constructs (*cagA*-$NT_{AA1-200}$, *cagA*-$CT_{AA201-1216}$) were defined and amplified by PCR using primers that attached a PstI-cleavage site to the 5'-end and a SmaI-cleavage site to the 3'-end (see 5.2.1). In this case, Platinum® *Taq* DNA polymerase was used and a pTRE-tight-*GFP-cagA*-wt-*SBP* plasmid, kindly provided by Dr. Roger Vogelmann, served as template. Thereafter, TOPO® TA cloning was performed following the manufacturer's instructions. Finally, constructs were transformed into competent *E. coli* (DH5α™) and cultivated overnight (o/n). After evaluating the pCR4 TOPO *cagA* constructs by sequencing, further cloning steps were conducted via conventional cloning by means of restriction enzyme digestion and ligation (see 2.5.3 and 2.4.1.2).

2.4.1.2 Conventional molecular cloning (step 2)

H. pylori wt *cagA* and its constructs were inserted into the pEGFP-C1 vector to express them in different immortalized cell lines. The template wt *cagA* and its constructs were generated by TOPO® TA cloning (see 2.4.1.1). Conventional molecular cloning is based on (i) specific restriction enzyme cleavage followed by (ii) the correct recombination of the intended vector system and the insert, i.e., the gene of interest. In the first step, both the vector and the insert are digested by at least one distinct restriction enzyme, whereas the insert has to be cut twice. It is more convenient to use two different restriction enzymes for cutting both in order to make sure there is only one possible orientation the insert can be successfully introduced into the vector. If the preferential restriction enzymes do not show identical or compatible working conditions, two consecutive steps are applied. This was the case with the cloning of wt *cagA* and its constructs into the pEGFP-C1 vector system, as SmaI and PstI were applied, which have different optimal work temperatures (25 °C vs. 37 °C). After cleavage of the DNA, the fragments were run over agarose gels to verify and separate the desired gene or vector backbone. The bands were cut out and purified using commercial kits (see 2.2.5). Subsequently, the fragments were combined in a 2:1 to 3:1 molar ratio of insert and vector (50 ng) and ligated by the T4 ligase at 14 °C o/n, using a thermal cycler to ensure a constant temperature. DH10B™ competent *E. coli* was used to obtain high transformation yields. The bacterial suspension was spread and incubated on agarose plates (containing the required antibiotic) and lastly individual colonies were propagated and screened for the desired DNA construct by restriction enzyme digestion (see 2.5.3).

2.4.2 pcDNA4/TO-*cagA* (wt or constructs): Isothermal assembly

In 2009 Daniel Gibson and colleagues developed a very powerful method that allows several different DNA fragments to be combined in an isothermal reaction to form new constructs regardless of their length (Gibson et al., 2009, Gibson, 2011). Compared to conventional cloning strategies using restriction endonucleases and ligases, it holds several advantages. This so-called Gibson assembly (i) is less laborious since it comprises fewer work steps and thus is less time consuming, it (ii) circumvents restriction digestion, it is possible to (iii) synthesize the entire backbone vector by PCR, furthermore, (iv) no restriction scars are generated, and (v) multiple DNA fragments can be joined simultaneously in a single-tube reaction.

The underlying principle is to generate adjacent fragments with identical (redundant) sequences at the ends. With appropriate primers, each fragment can be extended by the terminal sequence of the intended neighboring fragment by means of PCR. Thereby the 5'-end of the primer should be identical to the terminal 30 bp (3'-end) of the drafted adjacent fragment (i.e., complementary to the 5'-end of its complementary strand). The 3'-end of the primer should anneal to the terminal part (i.e., the 3'-end of the complementary strand) of the other fragment (i.e., the template of the PCR). To verify size and yield of the obtained PCR products, they can be run over an agarose gel and subsequently gel purified, if necessary. To perform the assembly reaction, fragments should be put together in equimolar concentrations. In the first step, a T5 exonuclease cuts back the 5'-ends, generating single strain 3'-DNA overhangs that can subsequently anneal to each other by forming hydrogen bonds. Afterwards, a DNA polymerase replenishes the gaps between assembled DNA fragments by means of the complementary DNA strand. Finally, the fragments are covalently linked by a DNA ligase creating a new contiguous DNA construct of immaculately joined fragments. The DNA construct is then transformed into competent bacteria (see 2.6.2), propagated o/n (see 2.6.1), extracted and purified (see 2.5.1) and finally screened via restriction digestion (see 2.5.3). To definitely verify the newly created DNA construct, at least the crucial parts, such as intersection areas between the particular fragments, were sequenced.
This method was utilized to insert wt *cagA* and its constructs into the pcDNA4/TO vector backbone. To introduce a FLAG-tag (Hopp et al., 1988) (in order to be capable of easily detecting the wt CagA protein and its constructs by anti-FLAG-antibodies), primers were partly equipped with a FLAG-sequence (DNA: GATTATAAAGATGATGATGATAAG ⟶ protein: DYKDDDDK) plus a short linker sequence (DNA: CGTAGTCGTAGT or GCCTCGGCCTCG ⟶ protein: ASAS) to circumvent steric hindrance by the CagA protein (see 5.2.2). Thus, each construct was created in three versions: one without FLAG-tag or linker sequence, one with N-terminal FLAG-tag and one with C-terminal FLAG-tag. Furthermore, to make sure *cagA* was highly expressed in eukaryotic cells, the N-terminal parts of wt *cagA* and its constructs were upgraded by a Kozak (Kozak, 1987) consensus sequence (DNA: GCCACCATGG). Ultimately, the primers comprised two parts: one consisting of approximately 20 bp for the correct annealing with wt *cagA*, its constructs or the vector backbone, respectively, the other of roughly 30 bp either consisting of FLAG-tag plus linker sequence (plus Kozak sequence, where required) or just vector or sequence (plus Kozak sequence, where required), respectively, depending on the particular ending and the intended localization of the FLAG-tag. Conditioning and amplification of the DNA fragments was done by means of the Herculase® II fusion DNA polymerase according to the manufacturer's protocol. Table 14 describes the optimized approach, Table 15 shows the implemented PCR protocol. Since

some primer combinations appeared to be quite complex in that showing diverging annealing temperatures, cycling was done with distinct temperature gradients. For fragment lengths shorter than 1 kb, only 2% DMSO was used.

Reagent/Item	Volume
Herculase buffer (5x)	5.0 µl
dNTPs	0.25 µl
DNA template (15 ng)	5.0 µl
forward primer (100 nM)	0.625 µl
reverse primer (100 nM)	0.625 µl
DMSO (2-4%)	0.5-1.0 µl
ddH_2O	ad 25 µl
Herculase® II DNA polymerase	0.25 µl
Total volume	25 µl

Table 14: Conditioning and amplification of DNA fragments for isothermal assembly via PCR, thermocycling approach

Repetition	Temperature	Duration
1x	95 °C	2’
30x	95 °C	20”
	50-70 °C (gradient)	20”
	72 °C	30”
1x	72 °C	3’
	12 °C	∞

Table 15: Conditioning and amplification of DNA fragments for isothermal assembly via PCR, thermocycling protocol

Analytical agarose gel electrophoresis (see 2.5.4) of merely 1 µl per PCR product solution provided sufficient information in terms of successful amplification, yield, purity and optimal annealing temperature. To eliminate unmodified templates, PCR products were digested by DpnI, to eliminate PCR primers the solution was subsequently column purified by the Wizard® SV gel and PCR clean-up system kit.

The recombination reaction was performed in a total volume of 10 µl in a thermocycler at a constant temperature of 50 °C for one hour, and the volume of PCR product used did not exceed 5 µl, since a total of 5 µl of Gibson Assembly® master mix, containing all necessary enzymes, was required. The total amount of DNA used was between 0.001 and 0.25 pmol (total mass: 25 to 50 ng). The insert and the vector were applied at a molar ratio of 3:1. The Gibson Assembly product was transformed into competent *E. coli* and the bacterial suspension was then spread on LB-agar plates containing the appropriate antibiotic (see 2.6.1). For verification of reliable expression of cloned wt *cagA* or its construct see 2.8.3.

2.4.3 Lentivirus suitable *cagA* constructs: Gateway® recombinational cloning

Gateway cloning is a high throughput means of transferring virtually any kind of DNA sequence into a suitable expression vector. It involves at least two successive recombination reactions (first BP, then LR), each of which completely dispenses with restriction enzymes and ligations in the sense of conventional cloning strategies and, moreover, reliably preserves the reading frame. (Hartley et al., 2000, Katzen, 2007). It is therefore a very forward, fast and easy technique, which proves to be very convenient, particularly for the transfer of large constructs. In this project, Gateway® recombinational cloning was applied to generate wt *cagA* or its constructs that can be easily transduced into eukaryotic cells via a lentiviral shuttle (Salmon and Trono, 2001). Both recombination reactions are derived from lambda bacteriophage's (lysogenic) recombination capability, at which recombinations take place between (pairwise) specific sequences of two different DNA fragments or vectors (i.e., BP: attB1/attB2 vs. attP1/attP2, then LR: attL1/attL2 vs. attR1/attR2), respectively, resulting in circular structures.

The first reaction (BP) introduces the desired DNA fragment into a so-called donor vector, resulting in a so-called entry clone that is a prerequisite for the second reaction (LR). Therefore, the DNA fragment has to be equipped with flanking attB1 and attB2 recombination sites. This was done by PCR with Herculase® II fusion DNA polymerase after suitable primers have been designed according to the manufacturer's protocol (see 5.2.3). Since the plasmid that is hosting the template (pEGFP-N1-*cagA*) and the donor vector (pDONR™221) both carry kanamycin resistance cassettes, the PCR product had to be treated by DpnI in order to cleave the originating vector and facilitate the selection of the generated constructs. To monitor quality and yield, 2 µl of DpnI-digested PCR product was subjected to agarose gel electrophoresis (see 2.5.4). Other than recommended by the protocol, purification of PCR products was performed directly by means of the Wizard® SV Gel and PCR clean-up system. As mentioned above, the BP-recombination reaction between the linearized attB PCR product (i.e., the DNA construct) and the donor vector simply creates the entry clone carrying the desired DNA sequence, which is then flanked by attL recombination sequences. To this end, the attB PCR product and donor vector had to be merged in equimolar amounts of 50 fmol and a total volume of 10 µl. The reaction was performed according to the protocol by accurately applying the provided reagents. Thereafter, DH5α™ chemically competent *E. coli* was transformed immediately (see 2.6.2) and finally spread on prewarmed LB-agar plates containing 100 µg/ml of kanamycin for positive selection of clones. The donor vectors that have not undergone recombination inhibit growth of competent bacteria since they still possess the ccdB gene, which is located at the very section (embraced by the attP recombination sequences) that should have been replaced by BP-reaction, hence enabling a negative selection upon transformation. Prior to verifying successful cloning by DNA sequencing, constructs were screened by restriction enzyme digestion (see 2.5.3). Correct pDONR™221 wt *cagA* or its constructs were stored in glycerol stocks (see 2.6.1).

The second reaction (LR) finally transfers the desired DNA construct to a target vector by a simple recombination reaction. This was done according to the manufacturer's protocol, but at halved volumes and amounts. For the recombination reaction, both the particular entry clones (i.e., pDONR™ 221 *cagA* constructs) and the destination vector, which was pLenti CMV Puro DEST, were utilized in amounts of 150 µg plus the volumes of LR Clonase™ mix (2 µl) and TE buffer (pH 8; 6 µl). The total reaction volume of 10 µl was briefly vortexed

twice and thereafter incubated for 16.5 h at constantly 25 °C. Replenished by 1 µl of Proteinase K solution the formulation was finally incubated again at 37 °C for 10 minutes. Thereafter, One Shot® OmniMax™ 2 T1R competent cells were transformed (see 2.6.2) and spread on prewarmed LB-agar plates containing 35-50 µg/ml of ampicillin for positive selection. Negative selection was again achieved by positive clones lacking the ccdB genes (and competent bacteria lacking the ccdA gene). In order to check for positive pLenti CMV Puro *cagA* (wt or constructs), small aliquots of bacterial suspension underwent colony PCR (see 2.5.6) prior to generating glycerol stocks and further working steps.

2.5 Molecular biological techniques

2.5.1 DNA extraction and purification

The isolation of plasmid DNA from suspensions of transformed bacteria (see 2.6.2) comprises several steps. Whereas chromosomal DNA and proteins are denatured at alkaline conditions, plasmid DNA remains stable. Consecutive neutralization causes precipitation of the former while the relatively small bacterial DNA plasmids stay in solution. Thereafter, silica membrane columns are used for plasmid extraction and purification. Prior to washing column bound DNA, purity and suitability for further biologic usage, such as transfection of eukaryotic cells, is ensured by removing endotoxins from the column bound plasmids. Depending on the amount of bacterial suspension, the isolation of plasmid DNA from o/n cultivation was done either with the Pure Yield™ plasmid mini prep system (3 ml) or the Pure Yield™ plasmid midi prep system (100 ml), according to the manufacturer's protocol. The elution of the purified DNA plasmids was done with 50 µl or 500 µl, respectively, of nuclease free ddH_2O prewarmed at 50 °C. If not meant for immediate usage, plasmid solutions were short time stored at -4 °C or permanently stored at -80 °C.

2.5.2 Photospectrometric analysis of DNA

By means of photospectrometric analysis, the concentration and purity of nucleic acid solutions can be evaluated. Here the optical density, as defined by specific absorption patterns at distinct wavelengths of ultraviolet light, is measured. UV light of 260 nm wavelength is absorbed directly proportional to the concentration of nucleic acids. This correlation is described by the Beer-Lambert law, which allows calculation of the quantity of unknown nucleic acid samples due to absorbance at 260 nm (A_{260}) by choosing the appropriate conversion factor. Since proteins absorb UV light at 280 nm wavelength, possible contaminations can be estimated by the A_{260}/A_{280} relationship: Pure DNA will show an A_{260}/A_{280} of about 1.8. Quantitative and qualitative analysis of DNA probes were conducted via NanoDrop ND 1000 spectrometer.

2.5.3 Restriction enzyme cleavage

The selective hydrolysis of plasmids or DNA fragments by restriction endonucleases was done for analytical or processing purposes. In order to process DNA or to verify that a cloning strategy achieved successful insertion of the required DNA sequence into the vector system, the plasmid or construct was specifically cleaved at at least two different sites by one or two distinct restriction enzymes, simultaneously or sequentially. The fragments were separated by agarose gel electrophoresis (see 2.5.4) and analyzed by UV light. If necessary, DNA bands were carefully excised from the gel and purified using the Wizard® SV Gel and PCR Clean-Up

system, according to the manufacturer's protocol. The cloning strategies required, in part, a specific treatment of the DNA constructs to be processed, such as degradation of original vector DNA with DpnI after PCR amplification or linearization of intermediates prior to further working steps. The restriction enzymes were purchased at Promega and each was used with the recommended and provided buffer solution according to manufacturer's instructions. Usually, DNA was digested at 37 °C for one hour following optional heat inactivation at 65 °C for 15 minutes. The calculations were normally based on a total volume of 20 µl. The optimized protocol is shown in Table 16.

Reagent/Item	Volume
DNA	200 ng
Restriction enzyme (10 U/µl)	0,5 µl
Buffer (10x)	2 µl
ddH_2O	ad 20 µl
Total volume	20 µl

Table 16: Standard protocol for restriction enzyme cleavage

2.5.4 Agarose gel electrophoresis

The separation of mixtures of different DNA fragments can easily be done by agarose gel electrophoresis. While setting in the cast, agarose forms three-dimensional structures with more or less defined pores whose sizes depend on the agarose concentration. The main factor for DNA migration in an electric field is the size of the DNA molecule. In the electric field, the negatively charged phosphate backbone is pulled towards the anode. Smaller molecules can much easier pass the agarose pores and therefore migrate faster. The velocity of double stranded DNA is inversely proportional to the logarithm to the base 10 of the number of base pairs. In addition, the movement of circular DNA is depending on its conformation, as supercoiled plasmids are more compact and can therefore migrate faster than relaxed forms, resulting in several mostly distinct bands whose sizes are sometimes not correctly represented by standard DNA size markers.

To prepare gels, agarose was diluted in 1x TAE buffer (see Table 9) in a concentration of 0.5 to 2.0% (w/v) according to the length of the fragments to separate. For complete dissolution, the gel formulation was carefully heated by means of a microwave oven to approximately 85 °C. After cooling down, Roti®-Safe DNA stain was added at a concentration of 4 µl per 100 ml liquid agarose gel. Once polymerized, the comb, providing wells for the samples, was removed, the gel transferred to the electrophoresis chamber and entirely submerged in 1x TAE buffer. Prior to pipetting the prepared DNA samples into the wells, they were mixed with sample buffer (containing BFB) by 20% (v/v). Finally, the lid was put on the chamber, a voltage of 70 V was applied, and DNA fragments were separated for 60 to 90 minutes according to their length and agarose concentration. The visualization and documentation of the separated DNA bands was done with the Gel Doc™ XR^+ documentation system by means of UV light (302 nm) and a computer-assisted photo-documentation system (see 2.1).

2.5.5 Polymerase chain reaction

By means of polymerase chain reaction, even single copies of a distinct DNA region of up to 10 kb can be specifically amplified by several orders of magnitude through utilizing appropriate primers. An editing of DNA sequences is possible as well. In principle, a PCR is a matched algorithm with different temperature regimens that enables specific biochemical processes. In the first step, the temperature is risen to 95 °C in order to entirely separate the double-stranded DNA template by disrupting the hydrogen bonds between complementary bases (denaturation). After 20 to 30 seconds, the temperature is reduced to about 50 °C depending on the optimal annealing temperature of the primer pair (which is approximately 5 °C below their T_M). Primers are short single stranded DNA sequences complementary to both three prime ends of the separated sense and anti-sense strands of the target DNA. Upon binding to the templates, stable hydrogen bonds are formed between the complementary DNA bases. After the annealing step, the temperature is increased to the optimal working temperature of the applied heat stable DNA polymerase, which is 72 °C in case of the *Taq* DNA polymerase. If dNTPs are present, the polymerase starts to add them in complementary fashion to the templates in 5'-3' direction (elongation/extension), starting with the free 3'-hydroxyl group of the attached primer, creating a new complementary strand. The elongation time depends on the length of the template: At optimal conditions the DNA polymerase is capable of adding up to 1000 residues per minute. The particular sequence of working steps is repeated around 30 times, with the amount of the target increasing exponentially as the newly synthesized strands themselves become templates. This whole process is preceded by an initialization step at 95 °C for 2 to 5 minutes, during which the DNA polymerase is heat activated. To make sure that any remaining single-stranded DNA is entirely complemented after the last cycle, a final elongation step of additional 5 to 15 minutes is added. Finally, to prevent degradation of the PCR product until it is retrieved from the device, a final hold at 4 to 12 °C is set for infinite time. Table 17 exemplifies the standard PCR protocol used for cloning *H. pylori cagA* (wt or constructs) into pEGFP vectors.

Repetition	Temperature	Duration
1x	95 °C	5'
30x	95 °C	30"
	60 °C	45"
	72 °C	30" (1'/kb)
1x	72 °C	10'
	4 °C	∞

Table 17: Standard PCR protocol

2.5.6 Colony PCR

Colony PCR is a fast and simple way to specifically screen colonies of transformed bacteria for distinct DNA sequences. This technique was applied in several approaches to circumvent rather laborious screening for correct clones by DNA purification and restriction digestion. Individual colonies of bacteria, which were transformed the previous day by plasmids

comprising the putative new DNA constructs and grown on LB agar plates o/n, were picked by sterile filter tips and resuspended in 3 ml of double distilled water. Thereafter, they were incubated for at least one hour at 37 °C at an ambient air containing 5% CO_2 under permanent agitation at 220 rpm. At last, 10 µl of bacterial suspension were supplemented with 12.5 µl of GoTaq polymerase and 1 µM of appropriate forward and reverse primers to a total volume of 25 µl. The amplification of the target sequences was done in a thermocycler according to Table 18.

To verify that cloning was successful, 10 µl per PCR product was run over an agarose gel. If so, the corresponding bacterial colonies were propagated o/n and the DNA was extracted the following day and sequenced.

Repetition	Temperature	Duration
1x	95 °C	5’
30x	95 °C	30”
	60 °C	45”
	72 °C	30” (1’/kb)
1x	72 °C	5’
	4 °C	∞

Table 18: Colony PCR protocol

2.6 Microbiological techniques

In order to minimize the risk of contaminating experiments, heat-stable equipment and solutions were consequently autoclaved at 121 °C and 2 bar for at least 20 minutes prior to usage. Heat sensitive media and solutions were sterilized by filters with appropriate pore size to remove bacteria or viruses (200 nm or 20 nm, respectively).

2.6.1 Culture and storage conditions of *E. coli*

Competent *E. coli* strains (DH5α™, DH10B™) were cultivated o/n at 37 °C and 5% CO_2, either on LB-agar plates or in LB-medium shaking at 220 rpm, both containing the appropriate antibiotic.

From bacteria that had been successfully transformed and propagated o/n on LB-agar plates (see 2.6.2), individual colonies were transferred separately by sterile pipette tips to 3 ml of fresh LB-medium containing the appropriate antibiotic. If not meant to be used for screening by colony PCR (see 2.5.6), transformed and suspended bacteria were thus again o/n cultivated in 100 ml of fresh LB-medium containing the appropriate antibiotic to obtain a dense bacterial suspension. Storage of bacteria was done by means of so-called glycerol stocks that were prepared as follows: LB-medium suspensions of o/n bacterial cultures were transferred into cryotubes containing 30% (v/v) Glycerol, vortexed very briefly but thoroughly and then immediately shock frozen in liquid nitrogen and finally stored at -80 °C.

In the case of bacteria from deep-frozen glycerol stocks, a tiny heap of still frozen bacterial suspension was carefully transferred by an inoculation loop to 100 ml of fresh LB-medium containing the appropriate antibiotic and cultivated o/n.

2.6.2 Transformation of chemically competent bacteria (*E. coli*)

Deep-frozen vials containing suspensions of competent bacteria were placed directly on ice to thaw to freezing point. The DNA solutions were precooled in the same manner, and the volume used for transformation was no more than one-tenth the volume of the competent bacteria. Both were carefully merged (i.e., 4 µl DNA-solution vs. 50 µl cell suspension), strictly avoiding pipetting up and down during mixing. After 30 minutes of incubation on ice, bacteria were heat-shocked for 30 seconds at 42 °C (water bath) and again put on ice for two further minutes. Afterwards, competent cells were mixed with 950 µl of SOC-medium and incubated at 37 °C and 250 rpm for at least one hour. Then bacteria were spun down at 5000 rpm for 3 minutes and resuspended in 300 µl of fresh LB-medium. Finally, 1:1 and 1:10 suspensions were spread onto prewarmed LB-agar plates (37 °C) containing the appropriate selection antibiotic and incubated o/n at a constant temperature of 37 °C and ambient air containing 5% CO_2.

2.6.3 Culture and storage conditions of *H. pylori*

For each experiment, frozen *H. pylori* strains were freshly taken from a -80 °C stock, immediately resuspended in 500 µl of prewarmed (37 °C) *Brucella* DENT medium supplemented with 10% FBS and consecutively spread onto freshly prepared and prewarmed (37 °C) WC DENT horse blood agar plates, or those containing extra kanamycin, as in case of ΔCagA *H. pylori* strains. After the bacterial suspension was allowed to dry on the plates for about half an hour, they were turned upside down and incubated at 37 °C under microaerophilic conditions (5% O_2, 5% CO_2) for two days.

Bacteria were subcultured by carefully harvesting with an inoculation loop and thoroughly resuspending in 500 µl of prewarmed (37 °C) *Brucella* DENT medium supplemented with 10% FBS. After microscopically verifying high numbers of the motile spiral form of *H. pylori*, thereof 100 µl were again spread onto prewarmed (37 °C) WC DENT horse blood agar plates containing additional kanamycin, where required, and grown for two further days in the incubator.

2.6.4 *H. pylori* stocks

Bacteria were harvested from WC DENT agar plates by cautiously scraping the surface with a sterile bacterial spreader and resuspended in 1000 µl of prewarmed (37 °C) *Brucella* broth, supplemented with 20% FBS and 20% glycerol. Aliquots of 100 µl were snap frozen in liquid nitrogen.

2.7 Cell culture

Cell lines were grown in DMEM supplemented with D-Glucose (4.5 g/l), L-Glutamine (2 mM), penicillin and streptomycin (100 U/ml each), and 10% FBS. When cells were not to be used for other purposes, they were routinely cultured in 75 cm^2-tissue culture flasks, incubated at 37 °C and 5% CO_2 atmosphere. The splitting of the cultured cells was done at a confluence of roughly 80-90%. To this end, culture medium was completely removed, cells were carefully

rinsed once with 1x PBS and 1 ml of 0.25% trypsin solution was added. To block up trypsinization, normal culture medium supplemented with 10% FBS was added after 2-5 minutes of incubation. The cell suspension was thoroughly resuspended and transferred into 15 ml-tubes. After centrifugation at 1200 rpm for 4 minutes, cells were resuspended in fresh culture medium and approximately one-sixth to one-eighth of the volume of the suspensions was transferred to new culture flasks (of the same size) and sufficiently provided with fresh medium.

For the selection and propagation of stable cell lines (see 2.7.3), the culture medium was directly supplemented with puromycin solution according to the tolerated concentration of the respective cell line (i.e., AGS and 23132: 0.75 µg/ml, MKN45: 1.0 µg/ml).

2.7.1 Cell counting

The Neubauer hemocytometer is a useful instrument to determine the number of cells. It consists of a transparent block of glass that, together with an appropriate cover slip, confines a counting chamber that can be examined by a light microscope. In order to exclude dead cells, cell suspensions were 1:10 diluted in trypan blue, which cannot pass intact cell membranes, and 10 µl of the diluted cell suspensions were added to the counting chamber. Cell concentrations are obtained by relating averaged live cell numbers of the four corner squares (each consisting of 16 smaller squares) to the volume (0.1 mm × 1 mm^2 = 0.1 µl).

2.7.2 Transfection

2.7.2.1 Performing transfection of eukaryotic cells

24 h prior to transfection, cells were seeded in the designated plates at the appropriate concentration and volume (see Table 19). Basically, the transfection formulation for each approach was subdivided for the preparation of the lipofection agent (Lipofectamine® 2000) and the DNA solution. After mixing, the solutions were incubated at room temperature for 30 minutes in order to effectively form the liposomes that entrap the plasmids. Finally, the transfection solution was added directly to the culture medium. In general, cells were incubated for 24 h (unless otherwise noted).

Prior to cell lysis, cells were rinsed once with 1x PBS after of the culture medium was removed. Lysis was done according to the setup of the experiment: 24 well plates were lysed with 100 µl of lysis buffer, 12 and 6 well plates with 500 or 1000 µl, respectively. After brief incubation at RT, lysates were vigorously resuspended. Samples that were not processed immediately were stored at -20 °C.

	Luciferase assay	Immunofluorescence	Western blot
Well plate size	24 well	12 well	6 well
Cell concentration	1×10^5 cells/well	1.5×10^5 cells/well	5×10^5 cells/well
Volume medium	500 µl/well	1000 µl/well	2000 µl/well
Volume transfection formulation	100 µl/well	200 µl/well	500 µl/well
Lipofectamine® 2000	0.625* µl/well	2.5 µl/well	3.125 µl/well
DNA	500* ng/well	1000 ng/well	2500 ng/well

Table 19: Conditions and prerequisites for transfections.
* In case of transfection and pTOPflash/pFOPflash reporter assay of 293T cells (see 3.2.2) a total amount of 1.75 µl/well Lipofectamine® 2000 and 350 ng/well DNA were used.

2.7.2.2 Optimization of the transfection protocol

In order to optimize the efficiency of the transfection protocol, a two dimensional approach was derived from the luciferase assay, as described in Table 19 (see 2.7.2.1). For this, the total amount of DNA (200, 350, 500 and 650 ng/well) and the relative amount of Lipofectamine® 2000 (µl per µg of DNA) allocated per well (24 well plate) were varied. Therefore, in addition to the obligatory 6.25 ng/well of *Renilla* luciferase plasmid (pRL CMV; see 2.2.4 & 2.10), the empty pcDNA3.1 vector was utilized to adjust the amount of DNA (see 2.2.4). After incubation at 37 °C and 5% CO_2 atmosphere for 24 h, 293T cells were lysed and subjected to luciferase assay. The experiment was performed in duplicates. As depicted in Figure 5, the highest luminescence could be obtained at a total of 350 ng/well and a Lipofectamine ratio of 1:5 [µg/µl].

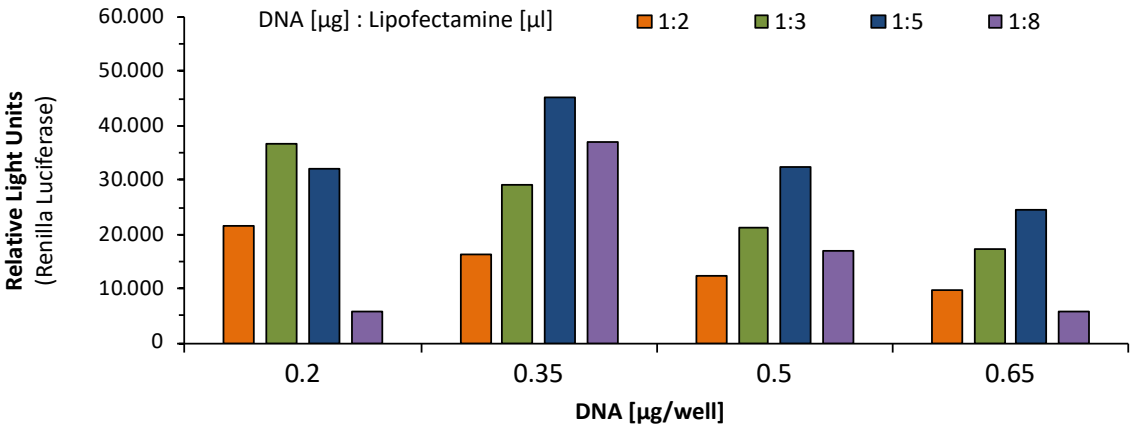

Figure 5: Optimization of the transfection conditions.
Transfection of 293T cells with different amounts of DNA and lipofectamine: Normalization to obligatory *Renilla* luciferase encoding plasmid (pRL CMV; see 2.2.4; 6.25 ng/well), pcDNA3.1 plasmid was utilized to adjust DNA amounts applied per well; cells were incubated for 24 h and thereafter lysed and immediately deep-frozen for later analysis; transfection efficiency is shown as mean (N = 2) of relative light units (RLU) according to *Renilla* luciferase activity (see 2.10).

2.7.3 Transduction: Generation of stable cell lines

Lentivirus was used to stably integrate specific DNA sequences into mammalian cell lines with a very high efficiency (Salmon and Trono, 2001). Stable cell lines have been generated by lentiviral transduction employing two different protocols: Cells with an inducible TCF/LEF reporter (i.e., firefly luciferase) and/or constitutively expressing *Renilla* luciferase were generated using commercial kits (pCignal™), whereas stable expression of *cagA* (wt or constructs) in eukaryotic cells was achieved by cloning and transduction through second-generation packaging (Zufferey et al., 1997).

2.7.3.1 Transduction by pCignal™ Lenti reporter assay

Inducible TCF/LEF reporter (i.e., firefly luciferase) cell lines or those constitutively expressing *Renilla* luciferase or those with both were generated using pCignal™ Lenti TCF/LEF Reporter (luc) or pCignal™ Lenti Renilla Control (luc), respectively (see 2.2.4). Cells were seeded at a density of 5×10^5 cells per well in a 12 well plate containing a total volume of 1000 µl (Medium: DMEM supplemented with D-Glucose, L-Glutamine, penicillin and streptomycin as well as 10% FBS; see 2.7). Incubation was done at 37 °C and 5% CO_2 atmosphere. The medium was removed after 24 h of incubation and 450 µl of DMEM containing 10% FBS but not supplemented with antibiotics, 50 µl of lentiviral constructs, and 0.4 µl of positively charged sureENTRY™ transduction reagent were added. After 20 h of incubation with lentiviral constructs, the medium was exchanged for DMEM/FBS supplemented with penicillin and streptomycin. To select successfully transfected clones, selection antibiotic (puromycin) was added (MKN45 cells: 1 µg/ml; 23132 and AGS cells: 0.75 µg/ml). Viability was verified by inspecting the cells under a light microscope. Transduced cell lines were cultured for an additional 5 days in selection medium before experimental use.

2.7.3.2 Transduction by lentivirus second-generation packaging

According to the second-generation lentiviral packaging system (Zufferey et al., 1997), the envelope vector pM2.G and packing vector pCMV-dR8.91 (both kindly provided by Professor Didier Trono; see 2.2.4) were used to transfer *cagA* (wt or constructs) into immortalized cell lines. In a first step, *cagA* (wt or constructs) had been Gateway cloned into the lentiviral destination vector pLenti CMV Puro DEST (see 2.4.3) (Campeau et al., 2009).

2.7.3.2.1 Generation of viral particles and $CaCl_2$-mediated transfection

Lentiviral particles were generated by means of $CaCl_2$-mediated transfection of 293 cells with pLenti CMV Puro *cagA* (wt or constructs) (see 2.4.3) according to a protocol adapted from laboratory of virology and genetics of Professor Didier Trono, Lausanne, Switzerland. Cells were seeded in 100 × 20 mm tissue culture dishes at a concentration of 4×10^6 cells per plate. 1 ml of 0.25 M $CaCl_2$ solution was supplemented with pMD2.G, pCMV-dR8.91 and pLenti CMV Puro *cagA* (wt or construct; 20 µg each) to produce the required components for a potential lentivirus (being capable of transducing *cagA* or its constructs into mammalian cell lines). While carefully blowing bubbles into this preparation with a serologic 2 ml pipette, 1 ml of 2x HEPES was added dropwise. After 20 minutes of incubation at RT, 1 ml of the solution was dropwise distributed directly to the medium of the 293 cells prepared the former day. 24 h after $CaCl_2$ transfection, the cell culture medium was replaced by fresh one, and after another 30 h, the supernatant containing the functional lentivirus particles was harvested, centrifuged at 2000 rpm for 8 min at 4 °C and filtered (pore size 0.45 µm). The filtrate was immediately either used for transduction or stored at -80 °C.

2.7.3.2.2 Transduction by *cagA* (wt or constructs) lentivirus particles

Cell lines with an inducible firefly luciferase and a constitutively expressed *Renilla* luciferase (see 2.7.3.1; AGS, MKN45 and 23132 cells) were seeded the day before at a concentration of 5×10^5 cells per well to a 6 well plate, according to a protocol of Eric Campeau (Campeau, 2016). For transduction, cells were trypsinized, centrifuged (300 g, 5 min, RT) and resuspended in fresh prewarmed medium containing 25%, 50% or 75% of lentivirus filtrate. After 48 h of incubation, medium was replaced by fresh one supplemented with puromycin, in the case of MKN45 cells at a concentration of 1.0 µg/ml, in the case of 23132 and AGS cells at a concentration of 0.75 µg/ml. The medium was exchanged every 48 h and cell viability was verified using light microscopy. No cell swelling or detachment could be observed for any of the cell lines used. 5 days after transduction and after sufficient growth in selection medium, the cell lines were again trypsinized, centrifuged and distributed in fresh 24 well plates (125,000 cells/well; 500 µl/well; n = 2). The cells were cultivated at appropriate concentrations of puromycin for another 24 h at humidified ambient air with 5% CO_2 and 37 °C and lastly lysed and treated as described in 2.7. It should be noted that two different internal controls have been utilized in these experiments, cell culture medium either containing puromycin at the appropriate concentration or just plain cell culture medium.

2.7.4 Lithium chloride-induced Wnt/ß-catenin signaling activation

LiCl is an inhibitor of GSK3β-kinase and therefore an activator of (canonical) Wnt/β-catenin signaling as the β-catenin destruction complex is impaired (Stambolic et al., 1996, Hedgepeth et al., 1997). Within the context of cell culture experiments, LiCl provides a suitable means of increasing the (canonica)l Wnt/β-catenin signaling level. 24 h after the transfection procedure, the appropriate volume of a sterile LiCl stock solution was directly added to the cell culture medium in the wells (24 well plate) at different molar concentrations (50 and 100 mM). Cells were incubated for additional 24 h and lysed (see 2.7) to analyze Wnt signaling activity by means of the pTOPflash/pFOPflash reporter assay (see 2.10).

2.7.5 Infection: Co-culture with *H. pylori*

4×10^4 cells per well were seeded in 24 well plates to achieve 50-60% confluency at the time of infection. To synchronize cells, cell culture medium was replaced by fresh medium not supplemented by FBS and cells were o/n cultivated. Prior to infection, medium was exchanged again by medium containing FBS but no antibiotics. At the day of the infection, the cells were counted to determine the quantity of bacteria to be added. The cells were infected at MOI 20. To calculate the number of bacteria, the number of cells was multiplied by the MOI:

$$N_{bacteria} = N_{cells} \times MOI \qquad [CFU]$$

Bacteria, grown on agar plates, were harvested and thoroughly resuspended in 1 ml of *Brucella* medium supplemented with DENT and 10% FBS. From a 1:10 dilution the OD (at 600 nm) was measured in order to calculate the bacteria concentration by means of the conversion factor (2×10^8 CFU/ml), which has beforehand been empirically deduced from a growth curve and is representing the amount of bacteria causing an optical density of 1 (Blanchard and Nedrud, 2012):

$$C_{bacteria} \approx OD_{600\,nm} \times 2 \times 10^8 \times 10 \qquad [CFU/ml]$$

The volume of bacteria suspension required per well could thus be calculated, whereas a total volume of 1000 µl was to be administered per well:

$$V_{bacteria} = N_{bacteria} / C_{bacteria} \times 10^3 \qquad [µl]$$

The co-cultures were incubated in separate biosafety level 2 (BSL-2) incubators and the experiment was finally terminated by adding lysis buffer (see Table 9) in order to quantify protein levels or the activity level of Wnt signaling, respectively.

2.8 Western blotting

2.8.1 Sodium dodecyl sulfate polyacrylamide gel electrophoresis

Sodium dodecyl sulfate (SDS) is an anionic detergent that linearizes polypeptide chains and imparts an evenly distributed negative charge according to their overall length (i.e., charge per unit mass). To overcome tertiary and quaternary structures, disulfide linkages need to be treated by reducing agents such as DTT while heating up to near boiling. Thus protein mixtures can be separated according to their size by means of a homogeneous electric field: the larger the polypeptide chain, the more delayed the passage through the pores in the gel. Acrylamide gels are used for SDS gel electrophoresis. Their pore size depends on the amount of acrylamide being cross-linked by bisacrylamide in a polymerization reaction. This is induced by ammonium persulfate and TEMED, which provide free radicals and stabilize the reaction. The definition of the pore size is crucial for the size spectrum of efficiently separated proteins.

After cells have been lysed according to 2.7, cell lysates were transferred to microcentrifuge tubes and boiled at 95 °C for 15 minutes. The separating gels were prepared according to the pore size required (see Table 20). Since the molecular weight of β-catenin is about 92 kDa, a 12% (m/v) polyacrylamide gel was suitable for separation. This was also applicable to β-actin (about 42 kDa), whereas wt CagA has a molecular weight of about 145 kDa, which required gels at lower percentages for sufficient separation. To obtain both separation of β-actin and wt CagA on a single membrane, gels with a polyacrylamide gradient were produced, ranging from 6% (m/w) at the top (cathode) to 15% (m/w) at the bottom (anode).

	Stacking gel	Separating gels		
	-	6%	12%	15%
TRIS 0.5 M pH 6.5 0.4% SDS	0.5 ml	-	-	-
TRIS 1.5 M pH 8.8 0.4% SDS	-	1.5 ml	1.5 ml	1.5 ml
10% APS	10 µl	30 µl	30 µl	30 µl
TEMED	2 µl	6 µl	6 µl	6 µl
40% Acrylamide	0.2 ml	0.9 ml	1.8 ml	2.25 ml
dH_2O	1.288 ml	3.564 ml	2.664 ml	2.214 ml
Total volume	2 ml	6 ml	6 ml	6 ml

Table 20: Western blot acrylamide gel composition.

Gels were cast in vertically oriented Novex® gel cassettes, thereby leaving enough spacing to the upper edge to cast the stacking gel later on. They were finally covered by isopropyl alcohol to avoid bubbles while completely setting for approximately half an hour. Subsequently, the stacking gel (see Table 20) was cast on top after entirely removing isopropyl alcohol coverage. The comb was carefully placed into the stacking gel, strictly avoiding trapping of air bubbles, and again the gel was allowed to fully set for half an hour. The gel cassette containing the polymerized acrylamide gel was then mounted into the appropriate Novex® XCell SureLock™ chamber that was hereafter filled with 1x SDS running buffer. After removing the comb, making sure no air bubbles were left behind and wells were correctly formed, cell lysates were slowly pipetted into the latter, also taking account of an appropriate marker (Precision Plus Protein™). Finally, the chamber was closed and connected to the power supply. In order to properly run the proteins through the stacking gel part, the voltage was set to 120 V for the first 20 minutes. Hereafter it was raised to 150 V and the gel was run until the protein front reached the lower end of the separating gel.

2.8.2 Semi dry blotting & blocking

Transferring the separated proteins from the acrylamide gel to a nitrocellulose membrane was done by the semi dry method. The gel cassette was removed from the chamber and carefully opened keeping the gel on one of the halves. Before transferring it to the preincubated nitrocellulose membrane in the transfer cell, the stacking gel part and the protruding notch in the lower part of the gel (cathode site of the gel) were truncated. To avoid drying-out, the gel was immediately covered with preincubated filter membranes. After the membrane-gel-filter pile was soaked with 1x semi dry buffer (see Table 9) the chamber was closed. With a constant current of 2 mA/cm^2 the proteins were blotted into the nitrocellulose membrane for 100 minutes.

Ponceau S dye was used to verify that proteins were successfully transferred to the nitrocellulose membrane prior to further working steps. If indicating a sufficient protein loading, the membrane was repeatedly rinsed with 1x TBS-T buffer (see Table 9) until the red stain was entirely removed. The membrane was subsequently blocked for 1 h by 1x TBS-T 5% non-fat milk at RT in order to prevent further non-specific binding of proteins to the membrane and thus reducing background noise. Thereafter it was briefly rinsed in 1x TBS-T.

2.8.2.1 Incubation with primary antibody

The primary antibodies were diluted in 1x TBS-T supplemented with 5% BSA according to Table 10 (see 2.2.6). The membranes were transferred to appropriate plastic boxes or 50 ml polypropylene tubes maintaining the side formerly in contact with the agarose gel top face. In most cases, the membranes were split to be able to investigate blotted cell lysates with different antibodies in the same working step. After sufficiently covering the membranes with primary antibody solution, the boxes were sealed with Parafilm® or, respectively, the tubes just closed by lids (to make sure the membrane could not run dry). Then, the membranes were incubated o/n at 4 °C, being gently agitated or, in case of tubes, steadily rolled. The next day, the antibody solution was removed and the membranes were rinsed five times with 1x TBS-T buffer for at least 10 minutes each time in order to entirely eliminate primary antibodies that were not specifically bound.

2.8.2.2 Incubation with secondary antibody

Each secondary antibody used within the scope of these experiments was coupled with a horseradish phosphatase that mediates a chemiluminescent reaction by cleaving an appropriate substrate. The secondary antibodies were used in a dilution of 1:2500 in 1x TBS-T 5% non-fat milk and added abundantly to the particular membranes. Since the membranes were incubated for only 1 h at RT under gentle agitation no covering was required. Thereafter the secondary antibodies were removed by rinsing the membranes at least three times with 1x TBS-T prior to detection.

2.8.2.3 Chemiluminescence detection

Detection of stained protein bands was done according to the manufacturer's protocol of Clarity™ Western ECL substrate, which is a suitable substrate for the horseradish phosphatase that was linked to the secondary antibodies. The membranes were incubated for approximately 5 minutes at RT while protected from light and wrapped in plastic foil afterwards. Chemiluminescence was detected by a fluorescence imager (see 2.1.1).

2.8.3 Expression of *cagA* (wt or constructs) in eukaryotic cells

To make sure that plasmidic wt *cagA* or its constructs (see 2.4.2) could be reliably expressed in the host cells, 293T cells were transiently transfected and amounts of correctly expressed proteins were quantified by immunoblotting. After 36 h of incubation following transfection, distinct bands of correct molecular weight could be detected, verifying successful transfection and expression of most types of wt CagA or its constructs (see Figure 6). CagA-$NT_{AA1-200}$ constructs were expressed, although the carboxy-terminal tagged variant (CagA-$NT_{AA1-200}$-FLAG) appeared to be far less pronounced. CagA-$CT_{AA201-1216}$ constructs were expressed as well, although their bands appeared very faint, by way of comparison. The bands of wt CagA turned out something more distinct than those of CagA-$CT_{AA201-1216}$ constructs. Interestingly, lanes of both non-tagged and amino-terminal FLAG-tagged types of wt CagA and CagA-$CT_{AA201-1216}$, presented further bands. Whereas CagA-$CT_{AA201-1216}$ w/o showed an additional band at roughly 90 kDa, wt CagA w/o and wt CagA N-FLAG showed an additional band at roughly 80 kDa and 65 kDa, respectively, which might have been the very same.

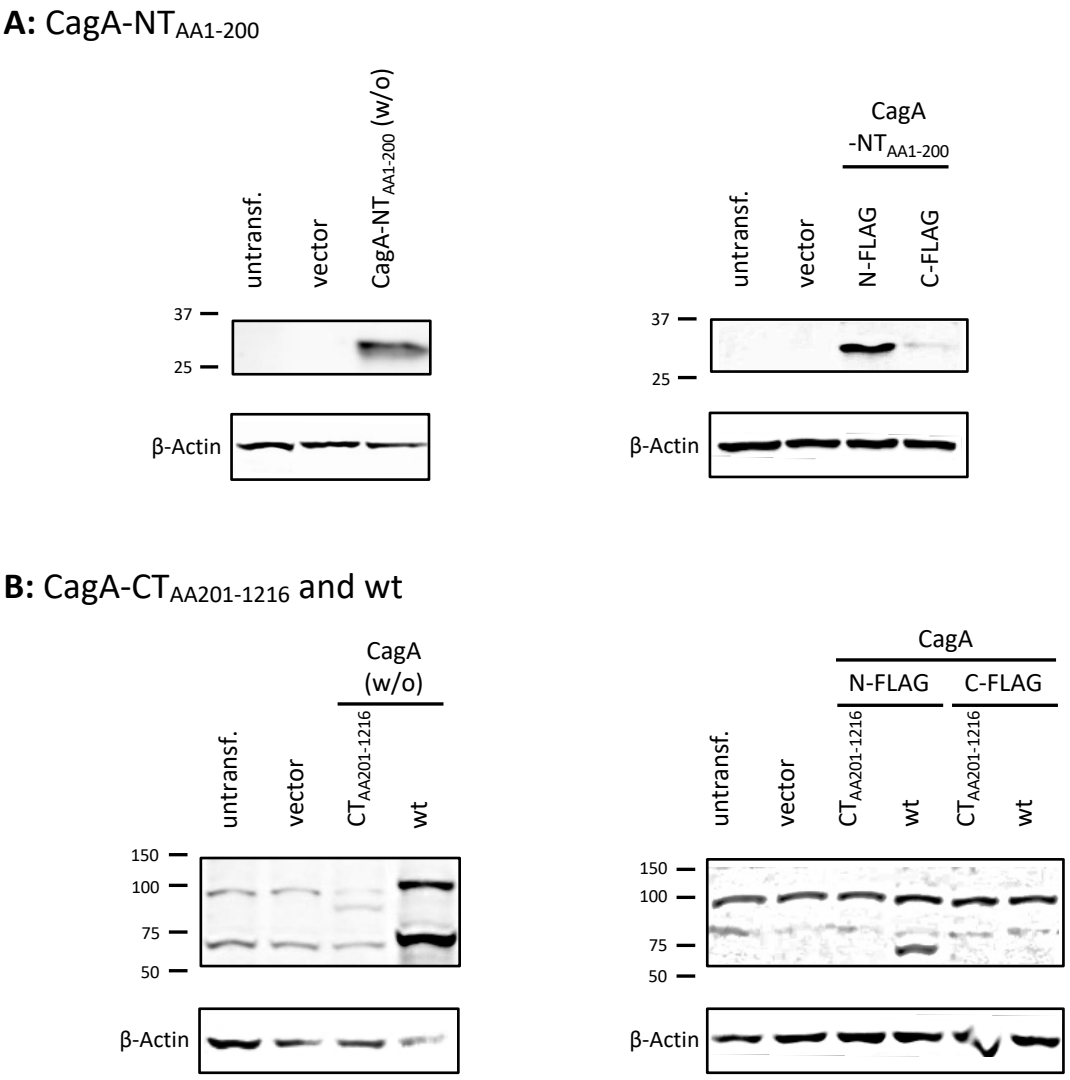

Figure 6: Expression of wt *cagA* and its constructs subsequent transient transfection.
Cell lysates of 293T cells 36 h subsequent transfection by plasmidic *cagA* (wt or constructs) were immunoblotted with antibodies specific for either FLAG (amino or carboxy-terminal tagged constructs) or $CagA_{1-877}$ (w/o = without tagging); [**A**] CagA-$NT_{AA1-200}$ (w/o, N-terminal FLAG or C-terminal FLAG); [**B**] CagA-$CT_{AA201-1216}$ or wt (w/o, N-terminal FLAG or C-terminal FLAG); loading control was provided by β-actin; left side: molecular weight markers positions [kDa]; CagA-$NT_{AA1-200}$ constructs (~23 kDa) are clearly expressed; CagA-$CT_{AA201-1216}$ (~113 kDa) and wt CagA (~135 kDa) show rather marginal amounts; additional bands can be found with CagA-$CT_{AA201-1216}$ w/o (~90 kDa), wt CagA w/o (~80 kDa) and wt CagA N-FLAG (~65 kDa).

2.9 Immunofluorescence staining

Immunofluorescence staining is a powerful means of visualizing distinct cellular structures in the context of entire cells, especially if combined with confocal laser scanning microscopy. Similar to staining of a western blot membrane, primary antibodies are used that specifically attach to distinct cellular peptide structures or epitopes, labeling them for the secondary antibodies. While the former are produced in organisms exposed to certain foreign proteins, the latter are solely species-specific and linked to a specific fluorophore that can be excited by a distinct wavelength and thus gives a very detailed spatial resolution. In contrast to conventional light microscopy, a confocal laser scanning microscope does a punctual readout by using point illumination while disregarding light beams not parallel to the optically

conjugate plane by means of a pinhole. By scanning over a regular raster, 2D or 3D imaging is possible, allowing optical sectioning.

Before seeding cells in (conventional) 12 well plates, they were lined with sterile glass cover slips. To prevent confluency, only 1.5 × 10^5 cells were applied per well. The next day, cells were transfected with the desired plasmid using Lipofectamine® 2000 (per well: 1000 ng DNA, 2.5 µl Lipofectamine®; see Table 19). As a control, 1000 ng of empty pcDNA4/TO were used. 24 h following transfection culture medium was removed, cells were carefully rinsed once with 1x PBS and subsequently covered by ice cold 1:1 acetone/methanol fixative for 15 minutes. Hereafter, fixed cells were rinsed thrice with 1x PBS and transferred to opaque plastic chambers lined up with Parafilm® and providing sufficient humidity by means of wet strips of paper towel. Since orientation of the cover slips remained the same, 200 µl of permeabilization and blocking buffer (see Table 9) could be applied for 15 minutes at RT in order to precondition cells for the next step. The primary antibody was diluted in washing buffer 1 according to Table 10 (see Table 9 and 2.2.6, respectively). Independently from plasmidic *cagA* (wt or construct) transfected, mouse anti-β-catenin antibody was applied to stain the cytoskeleton (β-actin). Untagged wt CagA or its constructs were stained by rabbit anti-$CagA_{1\text{-}877}$ antibody, in the case of FLAG-tagged constructs, rabbit anti-FLAG-antibody was used instead. After providing each glass platelet with 50 µl of the respective antibody solution, cells were incubated o/n at 4 °C in their humidified chamber protected from light. The following day, secondary antibodies and Hoechst 33342, a specific fluorophore and blue DNA stain, were diluted in washing buffer 1 according to Table 10 (see Table 9 and 2.2.6, respectively). Here Alexa Fluor 488 goat anti-mouse antibody was used to ultimately stain the cytoskeleton (β-actin) and Alexa Fluor 594 chicken anti-rabbit antibody to finally stain CagA (wt or constructs). Cover slides were rinsed thrice with washing buffer 1 and afterwards incubated with the secondary antibody dilution as well as the fluorophore for at least 1 h at RT, again protected from light in the opaque chamber with sufficient humidity. Slides were rinsed thrice with washing buffer 2 (see Table 9) and finally transferred upside down to microscope slides already provided with a small droplet of Vectashield® HardSet™ mounting medium. In order to circumvent fluorescence intensity decrease, confocal laser scanning microscopy was performed within 3 days and the slides were stored at -20 °C until then.

2.10 pTOPflash/pFOPflash reporter system

By linking a particular promoter region to the coding sequence for an unrelated reporter gene, alterations in the expression level of certain pathways can be examined, such as the (canonical) Wnt/β-catenin pathway by means of the pTOPflash/pFOPflash reporter assay system (Van de Wetering et al., 1996, Korinek et al., 1997). This comprises two distinct plasmids, both containing the coding sequence for firefly (*Photinus pyralis*) luciferase and a c-Fos minimal promoter. Whereas pTOPflash comes with three copies of TCF/LEF binding sites (CCTTTGATC) upstream of the promoter, activating firefly luciferase transcription upon β-catenin binding, pFOPflash contains only mutated copies of TCF/LEF and therefore serves as a negative control, representing the leakiness of this promoter. Firefly luciferase is synthesized depending on the amount of β-catenin stabilized. By adding a defined amount of a suitable substrate of firefly luciferase to cell lysates, the actual activity level of (canonical) Wnt/β-catenin signaling is represented by the amount of luminescence generated, which can easily be read by means of a luminometer (see below). Beside the readout from pFOPflash transfected cells, another internal control representing the transfection efficiency or the extent of successfully treated cells is necessary. Hence, a constitutively expressed luciferase

from sea pansy (*Renilla reniformis*), encoded by a further plasmid, is co-transfected and its activity can be readout the same way. Since the luciferases are of different evolutionary origin and therefore have distinct structures and substrates, they can be investigated sequentially in the same sample if activity of the first one is being quenched while simultaneously adding the substrate for the second one.

Transfections were performed according to 2.7.2, in each case, cells were seeded in 24 well plates. Experiments were done in duplicates and in two separate plates, one for pTOPflash and another for pFOPflash plasmids. The total amount of DNA per well was 500 ng in the case of the experiments presented under 3.2.1 or 350 ng in the case of the experiments presented under 3.2.2. These were allocated to 100 ng of either pTOPflash or pFOPflash plasmids, 6.25 ng of the *Renilla* luciferase encoding plasmid (pRL CMV; see 2.2.4) and different amounts of *cagA* (wt or constructs; 20, 100 or more nano grams, as stated at the respective results). Empty vectors (pcDNA4/TO or pEGFP, respectively) were used to adjust the amount of DNA in each well and as negative controls. 24 h after transfection, cells were rinsed once with 1x PBS. Lysis was done with 100 µl of lysis buffer per well (24 well plate; see Table 9) and 15 min of agitation at a rocking table (50 rpm). If lysed probes were meant to be analyzed by western blotting, 10 µl of cell lysates were boiled in 4x SDS sample buffer (see Table 9). Samples that were not processed immediately were stored at -20 °C.

20 µl of the lysate were transferred to an appropriate white colored round-bottom 96 well plate for automatic readout by a Orion Microplate luminometer. Therefore, the Dual-Luciferase® reporter assay system was used according to the manufacturer's protocol.

3 Results

3.1 Infection of eukaryotic cells with *H. pylori*

3.1.1 *H. pylori* and particularly CagA attenuate TCF/LEF transcriptional activity level

AGS, MKN45 and 23132 cell lines, stably transduced with (the genes of) both an inducible TCF/LEF reporter (i.e., firefly luciferase) and a constitutively expressed *Renilla* luciferase (see 2.7.3.1), were infected (MOI 20; N = 2) with CagA-proficient wt *H. pylori* or an isogenic mutant strain (ΔCagA). After adding the bacteria to the cells, transcriptional activity was analyzed every two hours and its progression over time from 4 to 24 h p.i. is depicted in Figure 7.

As described in 5.1.2, the utilized cell lines show different intrinsic Wnt/β-catenin signaling activity levels. AGS cells show the strongest intrinsic Wnt/β-catenin signaling activity (roughly 10-times higher than MKN45 and 23132 cells, see 5.1.2.3 and Figure 24) and in general showed the most distinct reactions among all gastric cancer cell lines in respect to CagA (see Figure 8, A). Since cell lines differed considerably (by several powers of ten) concerning *Renilla* and firefly luciferase raw value ranges (*Renilla*: 23132 > AGS ≫ MKN45), the relative firefly luciferase values (as simple quotient from both) were incomparable. To obtain an estimation of dimensions, entire MKN45 and 23132 cell records (i.e., all *Renilla* and firefly luciferase raw values) were adjusted/offset to the mean (N = 48) *Renilla* luciferase raw values of the entire AGS cell record (i.e., adjusting/offsetting of cell lines' putative different general expression levels). In addition, adjusted/offset raw values were also normalized to mean *Renilla* luciferase values of uninfected AGS cells 4 h p.i. (control). For comparability, the corresponding relative TCF/LEF expression values were also normalized to the relative TCF/LEF values from uninfected AGS cells 4 h p.i.

Concerning the underlying adjusted/offset and normalized absolute *Renilla* luciferase intensities, no relevant variation could be seen in respect of uninfected controls, at least for AGS and MKN45 cells (see Figure 7, A to B, lower small graphs, right lateral, grey lines). Cells subjected to infection by both, wt *H. pylori* or its CagA-deficient isogenic mutant strain, showed generally elevated *Renilla* luciferase readouts compared to uninfected controls (see Figure 7, A to C, lower small graphs, right lateral, dark and light green lines). In infected MKN45 and 23132 cells, there is a (further) decrease in *Renilla* luciferase activity due to CagA (i.e., wt *H. pylori*). 23132 cells evinced a decline in all adjusted/offset and normalized absolute *Renilla* luciferase values over the course of 24 h. These are transiently highest in infected cells at 10 to 12 h p.i. (see Figure 7, C, lower small graphs, right lateral).

The corresponding adjusted/offset and normalized absolute firefly luciferase levels evinced an increasing trend over the 24 h of infection, which likewise applied to uninfected control cells (see Figure 7, A to C, upper small graphs, right lateral). AGS cells showed the most distinct response, which is quite meager in case of MKN45 and 23132 cells and roughly conforms with the intrinsic Wnt/β-catenin signaling activity level (slope of adjusted/offset normalized firefly value in uninfected AGS cells approx. 4 times higher than in MKN and 23132 cells; compare Figure 24). For AGS cells, adjusted/offset and normalized absolute firefly luciferase levels of the uninfected control partly surpassed those of infected cells,

while the lowest values were obtained for those infected by CagA-proficient wt *H. pylori* (see Figure 7, A, upper small graph, right lateral, dark green line). Findings were different for MKN45 and 23132 cells, where infection with wt *H. pylori* implied slightly higher absolute firefly luciferase values compared to uninfected controls (see Figure 7, B and C, upper small graphs, right lateral). Irrespective of cell line, at the interval 4-12 h p.i., wt *H. pylori* strain PMSS1 caused a small peak in adjusted/offset and normalized firefly luciferase values.

A general comparison of the normalized relative TCF/LEF transcriptional activity of the CagA-deficient isogenic mutant strain with wt *H. pylori*-infected cells revealed that CagA causes its increment over 24 h of infection (irrespective of cell line; see Figure 7, A to C, large graphs). Since infection as such provoked an increase in the *Renilla* luciferase expression in gastric cancer-derived cells lines, the evaluation should focus mostly on infected cells.

In summary, CagA proficiency entailed a reduction in the absolute and relative TCF/LEF transcriptional activity level, particularly concerning AGS cells. According to their higher intrinsic Wnt/β-catenin signaling activity, these showed a strong response, whereas MKN45 and 23132 cells behaved rather inertly.

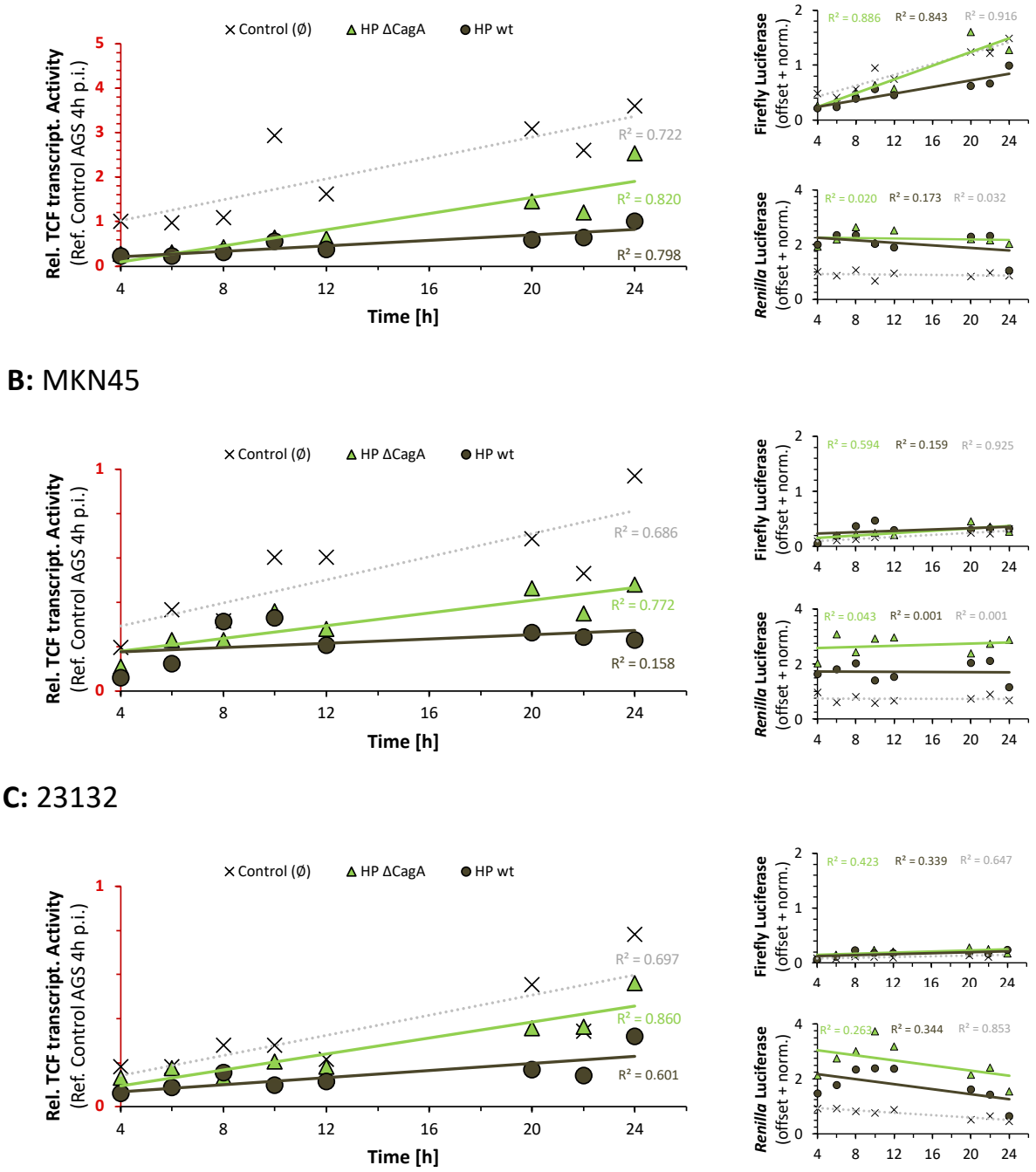

Figure 7: Time progression of TCF/LEF transcriptional activity due to infection by *H. pylori* strains.
[**A**] AGS, [**B**] MKN45 and [**C**] 23132 cell lines (stably transduced with inducible TCF/LEF-controlled firefly luciferase and constitutively expressed *Renilla* luciferase) were co-cultured with *H. pylori* strain PMSS1 (wt) or its CagA-deficient isogenic mutant PMSS1 ΔCagA (MOI 20) for at least 24 h; *grey:* uninfected controls; *light green:* isogenic mutant strain (ΔCagA); *dark green:* wt *H. pylori*; graphs on the left show relative TCF/LEF transcriptional activity uniformly normalized to relative TCF/LEF from uninfected AGS cells 4 h p.i. (note different scaling!) is shown as mean (N = 2); small graphs on the right illustrate adjusted (to mean *Renilla* from entire AGS series) and normalized (to *Renilla* from uninfected AGS cells 4 h p.i.) firefly and *Renilla* luciferase intensities (mean, N = 2).

3.1.2 Wild type *H. pylori* initially induces transient morphological changes

To determine whether CagA-proficient wt *H. pylori* or its isogenic mutant strain (ΔCagA) were able to induce hummingbird morphological changes in host cells and to be able to correlate these changes with the effects observed on TCF/LEF transcriptional activity level (see 3.1.1), the phenotype of the cells was repeatedly microscopically monitored for 24 h. Pictures were taken every two hours after infection.

Although AGS, MKN45 and 23132 cell lines all originate from gastric adenocarcinomas, the latter do not change their phenotype at all, while the former transiently presents the hummingbird phenotype if infected with the CagA-proficient wt strain (see Figure 8, A and C). This morphological alteration was also observed in MKN45 cells (see Figure 8, B), but again only when infected with CagA-proficient wt *H. pylori*. The first changes in cell morphology were recognized 4 h p.i., while after 12 h these changes were clearly less marked in the observed cultures of AGS and MKN45 cells and disappeared 20 h p.i.

In short, CagA can induce a transient change in host cell morphology in the very early infection (4-12 h p.i.).

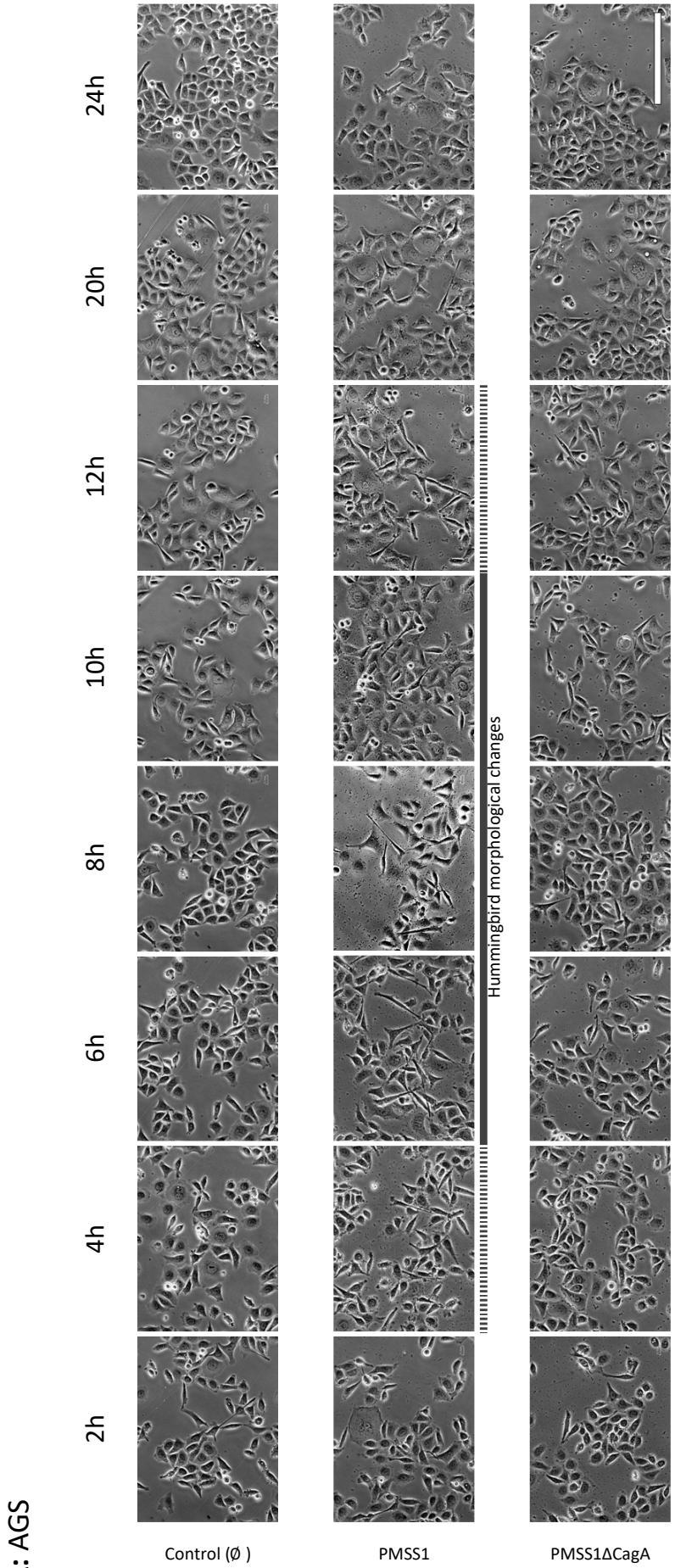
A: AGS
2h
4h
6h
8h
10h
12h
20h
24h
Hummingbird morphological changes
Control (Ø)
PMSS1
PMSS1ΔCagA

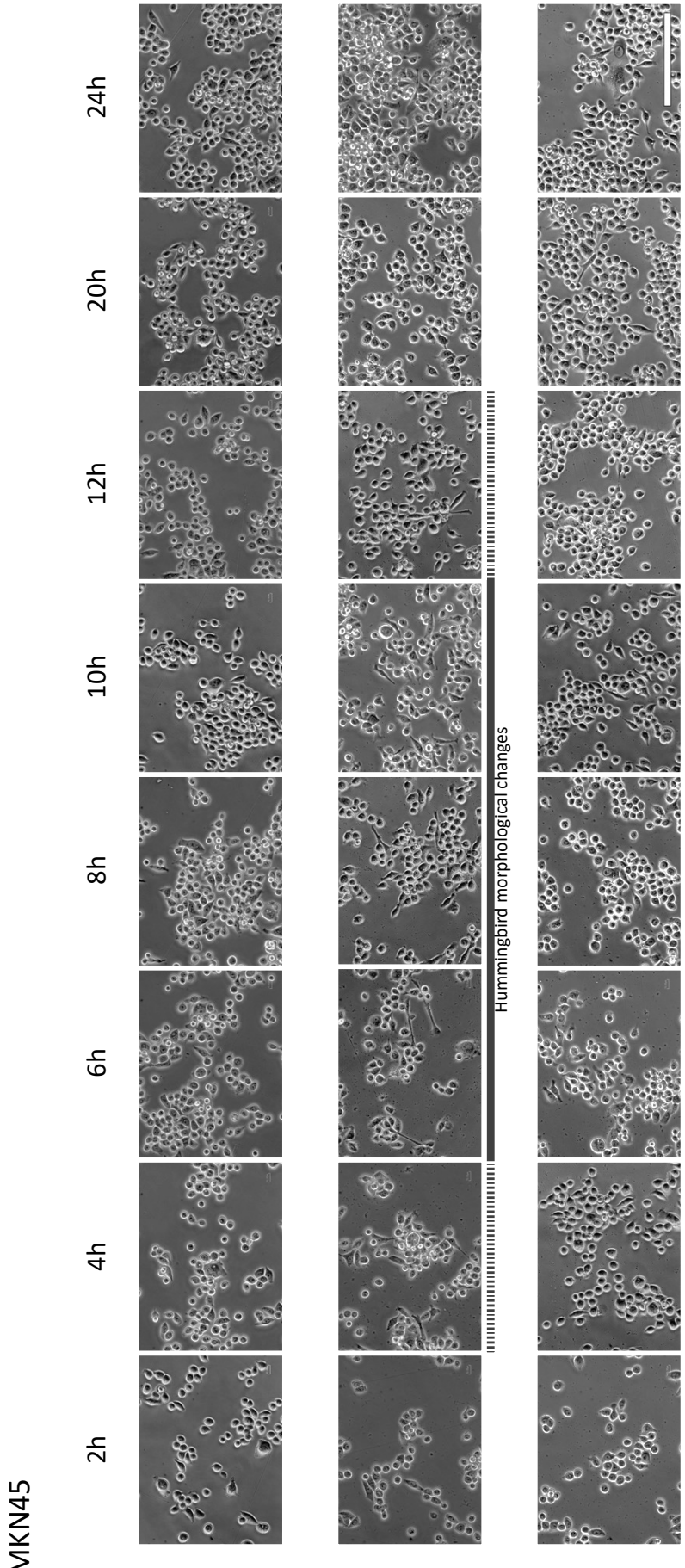
B: MKN45
2h
4h
6h
8h
10h
12h
20h
24h
Hummingbird morphological changes
Control (Ø)
PMSS1
PMSS1ΔCagA

C: 23132

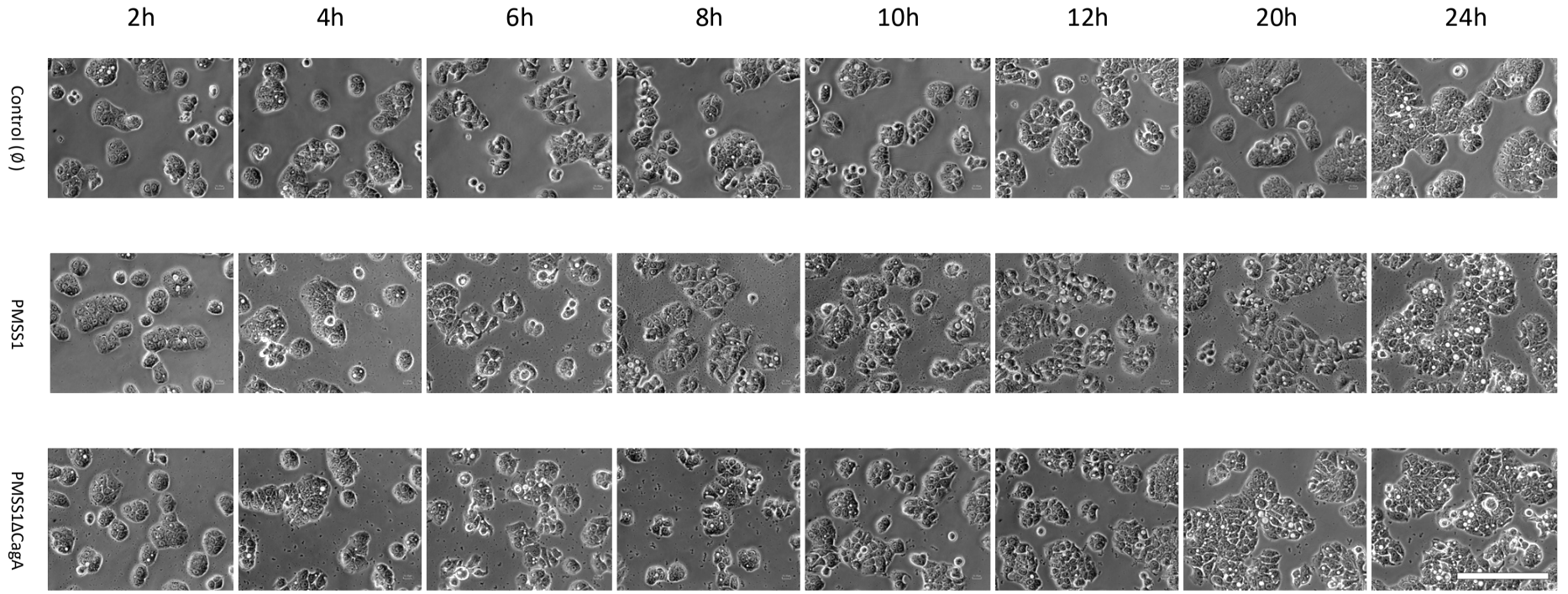

Figure 8: Cell phenotype alterations through co-culture with *H. pylori*.
[**A**] AGS, [**B**] MKN45 and [**C**] 23132 cells (stably transduced by TCF/LEF-controlled firefly luciferase and constitutively expressed *Renilla* luciferase) were co-cultured by either *H. pylori* wild type strain PMSS1 or its CagA deficient isogenic mutant (PMSS1 ΔCagA) for 24 h; microscopic pictures were routinely taken from mostly corresponding spots in the culture dishes; white scale bar (see PMSS1 ΔCagA, 24 h): 100 µm; the hummingbird phenotype of AGS and MKN45 cells can be clearly recognized between 4 h and at least 12 h after culture medium was supplemented with wild type PMSS1 strain; no alterations of host cell phenotype if bacteria are incapable of transferring CagA.

3.1.3 Alteration of ß-catenin amounts owing to CagA

To assess the levels of phosphorylated and unphosphorylated β-catenin in the context of *H. pylori*-altered (canonical) Wnt/β-catenin signaling activity, the very same samples were utilized as in 3.1.1. (i.e., AGS, MKN45 and 23132 cells vs. wt *H. pylori* or its isogenic ΔCagA mutant strain). Note that protein load is very limited since experiments were performed in a 24-well plate setting (see 2.7.5).

Figure 9 shows the amounts of CagA detected by anti-$CagA_{1-877}$ antibodies after 12 and 24 h of infecting different cultured cell lines with the wt *H. pylori* PMSS1 or PMSS1 ΔCagA strain, in terms of a co-culture. At 12 h following infection with the wt strain (PMSS1), the roughly 125 to 145 kDa protein CagA (Covacci et al., 1993, Segal et al., 1999, Stein et al., 2002) could be reliably detected from lysates of infected AGS, MKN45 and 23132 cell lines (which were stably transduced with an inducible TCF/LEF-controlled firefly luciferase and a constitutively expressed *Renilla* luciferase). There was no CagA detectable in cases of infection with the CagA isogenic mutant strain (PMSS1 ΔCagA) in conformity with the controls. Although amounts were far less pronounced after 24 h, wt CagA was still detectable.

Concerning the impact on β-catenin amounts, cell lines were considered separately, as in 3.1.1 regarding the evaluation of the TCF/LEF time progression. In AGS cells, particularly after 24 h of infection by wt *H. pylori*, the amounts of phosphorylated β-catenin increased at the expense of unphosphorylated β-catenin, while total β-catenin amounts were unaffected (see Figure 10, A and B, first column). The opposite was observed during infection by an isogenic mutant strain, which instead shows a reduction in phosphorylated β-catenin to even below the level of uninfected controls.

In contrast, MKN45 cells show a reduction in phosphorylated β-catenin in favor of unphosphorylated β-catenin in light of stable amounts of total β-catenin through wt *H. pylori*, predominantly at 24 h p.i. (see Figure 10, A and B, second column). Accordingly, the isogenic mutant strain indicates comparably higher amounts of phosphorylated β-catenin, which, other than for AGS cells, tends to surpass those of uninfected controls.

The interpretation of the behavior of 23132 cells with respect to infection and/or CagA is more intricate and is also aggravated because of the (inadvertent) elution of the right part of the non-P-β-catenin plot at 24 h p.i. (see Figure 10, B, third column, lowest line, right-hand plot). Whereas at 12 h p.i., the infection *per se* (i.e., both wt and isogenic mutant strain) causes an increment in unphosphorylated β-catenin at the expense of phosphorylated β-catenin (see Figure 10, A, third column), the opposite can cautiously be deduced at 24 h p.i., where values drop even below uninfected controls 24 h p.i. (see Figure 10, B, third column). Both correspond to the behavior of all adjusted/offset and normalized absolute *Renilla* luciferase values over the course of 24 h in Figure 7 C (lower small graphs, right lateral).

In conclusion, depending on the intrinsic Wnt/β-catenin signaling activity level of the cell lines used, CagA causes either an increment in phosphorylated β-catenin (high Wnt: AGS cells) or a decrement in phosphorylated β-catenin (low Wnt: MKN45 and 23132 cells).

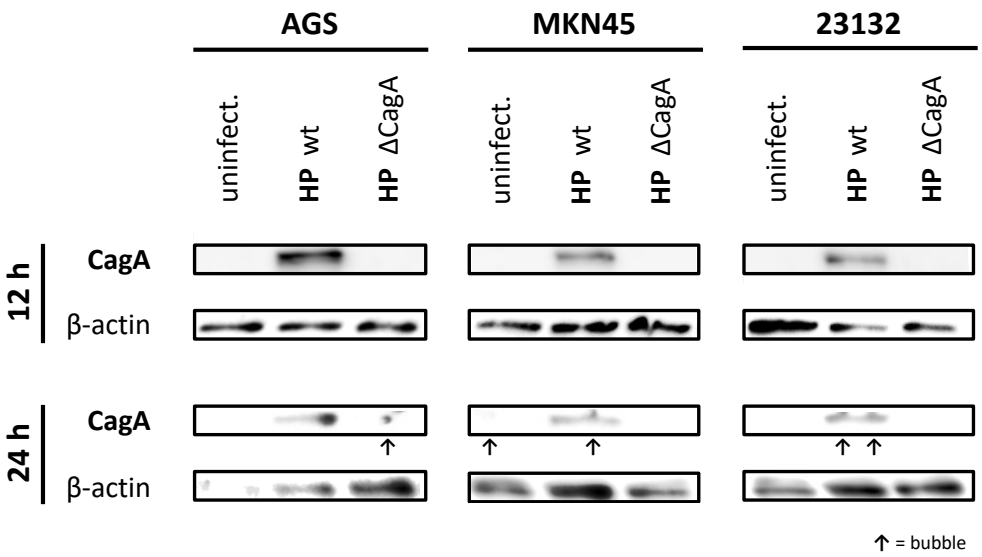

Figure 9: Amounts of wt CagA due to infection by *H. pylori* PMSS1.
Different cell lines (AGS, MKN45 and 23132; each stably transduced by inducible TCF/LEF-controlled firefly luciferase and constitutively expressed *Renilla* luciferase, see 3.1.1 and 2.7.3) were co-cultured (MOI 20) with either wt *H. pylori* strain PMSS1 or its isogenic mutant strain PMSS1 ΔCagA for 12 or 24 h, respectively; cell lysates were immunoblotted with antibodies specific for $CagA_{1\text{-}877}$; loading control was provided by β-actin; infection with wildtype strain, but not with its isogenic ΔCagA mutant strain, yielded a distinct CagA band at roughly 135 kDa; small arrows up (↑) indicate impairment of WB developing due to air bubbles.

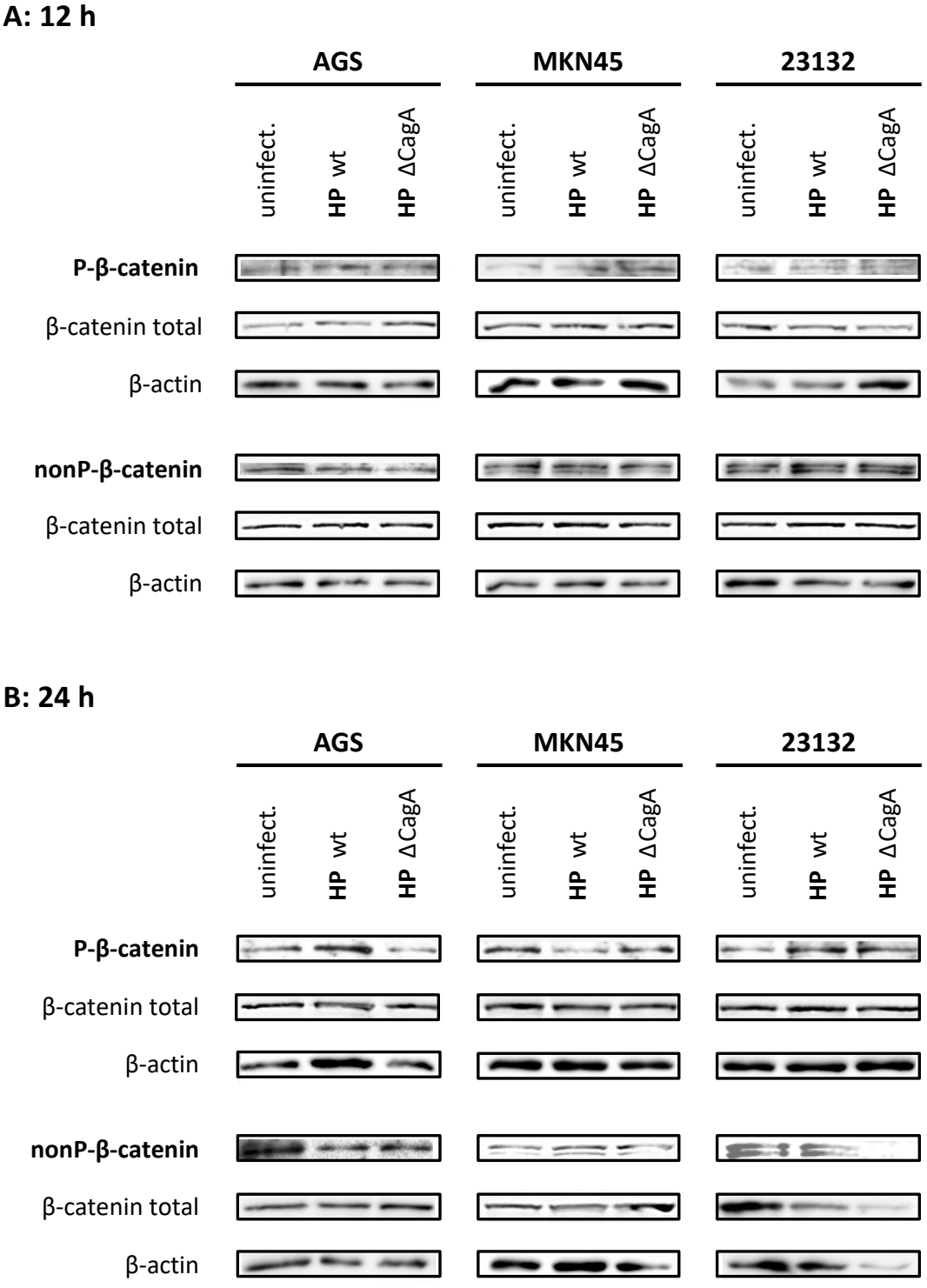

Figure 10: Amounts of total, phosphorylated and unphosphorylated β-catenin due to infection by CagA-proficient HP wt strain or its isogenic mutant.
Different cell lines (AGS, MKN45, 23132; each stably transduced by inducible TCF/LEF-controlled firefly luciferase and constitutively expressed *Renilla* luciferase, see 3.1.1 and 2.7.3) were co-cultured (MOI 20) with either wt *H. pylori* strain PMSS1 or its isogenic mutant strain PMSS1 ΔCagA for [**A**] 12 and [**B**] 24 h, respectively; first, cell lysates were immunoblotted with antibodies specific for β-catenin (total) and, following stripping, again immunoblotted with antibodies specific for either phosphorylated β-catenin (P-β-catenin) or unphosphorylated β-catenin (nonP-β-catenin); loading control was provided by β-actin; in the case of AGS cells, the increment in phosphorylated β-catenin was at the expense of unphosphorylated β-catenin, whereas the inverse of this behavior was observed in the case of MKN45 and apparently inconclusive behavior in the case of 23132 cells.

3.2 *H. pylori* CagA and its domains in context of (canonical) Wnt/ß-catenin signaling

From 3.1.1 it can be concluded that wt CagA proficiency caused an alteration of relative (and absolute) TCF/LEF transcriptional activity of the host cells upon infection (see Figure 7, A to C, large graphs, left lateral). From 4-12 h p.i., a transient increment of (relative and absolute) TCF/LEF transcriptional activity could be observed regarding infection by *H. pylori per se* (see Figure 7, A to C, upper small graphs, right lateral), which coincided with the transient occurrence of the hummingbird phenotype (see Figure 8, A and B, second and third rows).

With respect to wt CagA, an increment of phosphorylated β-catenin at the expense of unphosphorylated β-catenin could be deduced for AGS cells, which was the opposite in the case of MKN45 cells (see Figure 10, A and B, first and second columns) and indicates that this was context-dependent.

To verify these findings of CagA's impact on the (canonical) Wnt/β-catenin pathway, wt *cagA* was overexpressed in host cells while monitoring TCF/LEF activity levels by means of the pTOPflash/pFOPflash reporter assay (see 2.10). In addition, as CagA's impact on the host cells was demonstrated to be domain-specific (Bagnoli et al., 2005, Pelz et al., 2011, Hayashi et al., 2012), truncated *cagA* constructs (see 2.4) were likewise applied.

3.2.1 CagA alters Wnt signaling activity

3.2.1.1 Transfection of different cell lines with *H. pylori* wt *cagA* or its constructs

Eukaryotic cell lines (AGS, MKN45 or 23132), previously stably transduced with an inducible TCF/LEF-controlled pTOPflash reporter gene, were transiently transfected with wt *cagA* or its constructs (i.e., *cagA*-$NT_{AA1-200}$ or *cagA*-$CT_{AA201-1216}$) and a constitutively expressed *Renilla* luciferase (coinstantaneously). For verification that artificially introduced *cagA* (wt or constructs) were expressed in eucaryotic cells, see 2.8.3. Figures 11, 12 and 13 (large graphs) illustrate alterations in the relative TCF/LEF transcriptional activity level. As described below, this relative transcriptional behavior needs to be considered with reservation, even more since uniformly adjusting firefly luciferase raw data to mean *Renilla* luciferase readouts, as was done in 3.1.1, was rather unrewarding.

Initially, and independently of cell lines, transient transfection with low DNA amounts of wt *cagA* or its constructs yielded an increment of relative TCF/LEF transcriptional activity after 24 h compared to controls, represented by blank pcDNA4/TO plasmids (see Figures 11, 12 and 13, A to C, large graphs, left lateral, 20 ng/well *cagA* DNA). Further, *cagA*-$CT_{AA201-1216}$ (i.e., CagA-$CT_{AA201-1216}$ protein) featured a behavior almost similar to that of wt *cagA*, which was mostly opposite to that of *cagA*-$NT_{AA1-200}$ (i.e., CagA-$NT_{AA1-200}$ protein). Regardless of cell line, it was notable that C-terminal FLAG-tagged *cagA*-$NT_{AA1-200}$, on the one hand, and all *cagA*-$CT_{AA201-1216}$ and wt *cagA* variants, on the other, showed a contrasting behavior regarding DNA up-titration (see Figures 11, 12 and 13, C, large graphs, left lateral, orange bars). While in all cell lines the amount of transfected *cagA*-$NT_{AA1-200}$-FLAG and the relative TCF/LEF transcriptional activity were proportional (i.e., through increasing the load of construct-encoding plasmid, higher relative TCF/LEF transcriptional values were obtained), with a maximum activation of 8-fold in AGS cells (MKN45: 6-fold; 23132: 3-fold), the opposite was observed in the case of *cagA*-$CT_{AA201-1216}$ and wt *cagA* (i.e., a maximum elevated relative

TCF/LEF transcriptional activity level at lowest DNA amounts). Moreover, with regard to AGS cells, at high amounts, *cagA*-$CT_{AA201-1216}$ and wt *cagA* reduced the relative TCF/LEF transcriptional activity level even below the baseline value, indicating its relative inhibition. Similar observations were made using MKN45 cells subjected to transfection with the carboxy-terminal FLAG-tagged *cagA*-$CT_{AA201-1216}$ and wt *cagA*. The 23132 cells displayed a rather indolent behavior. Concretely, during up-titration, relative TCF/LEF transcriptional activity levels in AGS cells, transfected with *cagA*-$CT_{AA201-1216}$ or wt *cagA* (all variants in each case), decreased from an initial 2-4-fold (20 ng/well DNA) to 0.7-fold at higher amounts (500 ng/well DNA). Accordingly, MKN45 cells yielded a reduction in relative TCF/LEF transcriptional activity from an initial 5-2.5-fold to 1.5-fold and 23132 cells from an initial 2.5-fold to 1.5-fold. For all cell lines, the *cagA*-$NT_{AA1-200}$ (w/o) construct showed a slightly inversely proportional declining increased relative TCF/LEF transcriptional activity by up-titration (AGS: 3- to 2-fold; MKN45: 5- to 4-fold; 23132: 2- to 1.5-fold). The impact of amino-terminal FLAG-tagged *cagA*-$NT_{AA1-200}$ on TCF/LEF transcriptional activity in part corresponded to that of *cagA*-$CT_{AA201-1216}$ or wt *cagA*.

It is worth noting that when looking at underlying normalized absolute firefly and *Renilla* luciferase readouts (see Figures 11, 12 and 13, small graphs, right-hand side) compared to the controls, a considerable decline in the net *Renilla* luciferase intensity by a factor of approximately 0.2 to 0.4 could be found, if even minute amounts of wt *cagA* or its constructs (20 ng/well DNA) were expressed in these unpolarized gastric adenocarcinoma-derived cell lines. This was in contrast to the highest amounts of *cagA*-$CT_{AA201-1216}$ and wt *cagA*, where *Renilla* luciferase intensities in particular transcended the control levels. Firefly luciferase intensities did not show such a clear trend for this and were, by tendency, slightly reduced related to the control values. As described above with respect to relative TCF/LEF transcriptional activity, C-terminal FLAG-tagged *cagA*-$NT_{AA1-200}$ in particular displayed an opposing behavior: Whereas absolute normalized *Renilla* luciferase intensity showed a dose-dependent inverse proportional behavior, the corresponding normalized absolute firefly luciferase intensity recovered and in part exceeded the control level while up-titrating. As absolute firefly luciferase activity was basically referred to *Renilla* luciferase activity, this explained the relative inhibition or activation of TCF/LEF transcriptional activities in cases of *cagA*-$CT_{AA201-1216}$ and wt *cagA* or *cagA*-$NT_{AA1-200}$, respectively.

In summary, although validity was affected by a reduction of *Renilla* luciferase expression through even minute amounts of pcDNA4/TO plasmid-encoded CagA, this experiment at least supports the conclusion that CagA's impact on host cellular gene expression is dose-dependent and that CagA-$CT_{AA201-1216}$ acts similarly to wt CagA, in contrast to CagA-$NT_{AA1-200}$.

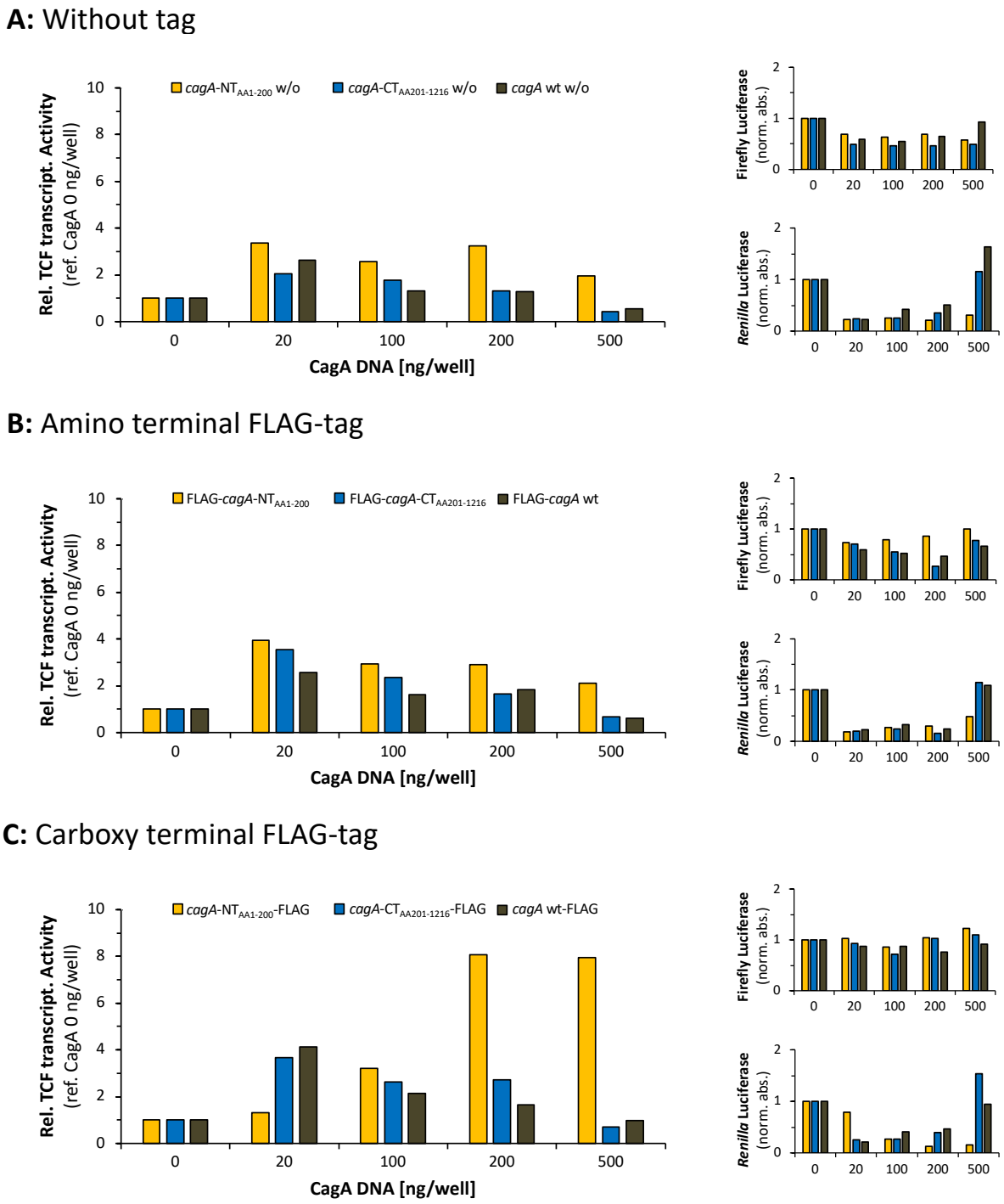

Figure 11: Transient expression of wt *cagA* and its construct DNA in AGS cells.
Altered Wnt signaling levels in terms of TCF/LEF transcriptional activity through increasing amounts of *cagA*-NT$_{AA1-200}$, *cagA*-CT$_{AA201-1216}$ and wt *cagA* (pcDNA4/TO-encoded; amino- or carboxy-terminal FLAG, tagged or without tag = w/o, respectively) transfected to AGS cells (see 2.7.2) shown as mean (N = 2) of intensity of firefly bioluminescence divided by the corresponding internal standard (*Renilla* luciferase, see 2.10) and finally in reference to a control (cells transfected by blank pcDNA4/TO); right side: small graphs illustrate respective normalized absolute firefly and *Renilla* luciferase intensities; lysis of cell cultures after 24 h of incubation; [**A**] without tag; [**B**] amino-terminal FLAG-tag; [**C**] carboxy-terminal FLAG-tag; *orange*: *cagA*-NT$_{AA1-200}$; *blue*: *cagA*-CT$_{AA201-1216}$; *olive*: wt *cagA*; basically, *cagA* and both constructs were capable of increasing levels of (canonical) Wnt/β-catenin signaling; intriguingly, increasing amounts of all amino-terminal FLAG-tagged constructs and all versions of the large constructs (*cagA*-CT$_{AA201-1216}$ and wt *cagA*), respectively, caused a reduction in TCF/LEF transcription activity relating to an initial maximum, even partly below control levels (*cagA*-CT$_{AA201-1216}$ and wt *cagA*); titration of *cagA*-NT$_{AA1-200}$-FLAG effected a kind of a proportional increment of Wnt signaling activity and in the case of non-tagged *cagA*-NT$_{AA1-200}$, besides generally activating TCF/LEF expression levels, no clear trend could be perceived.

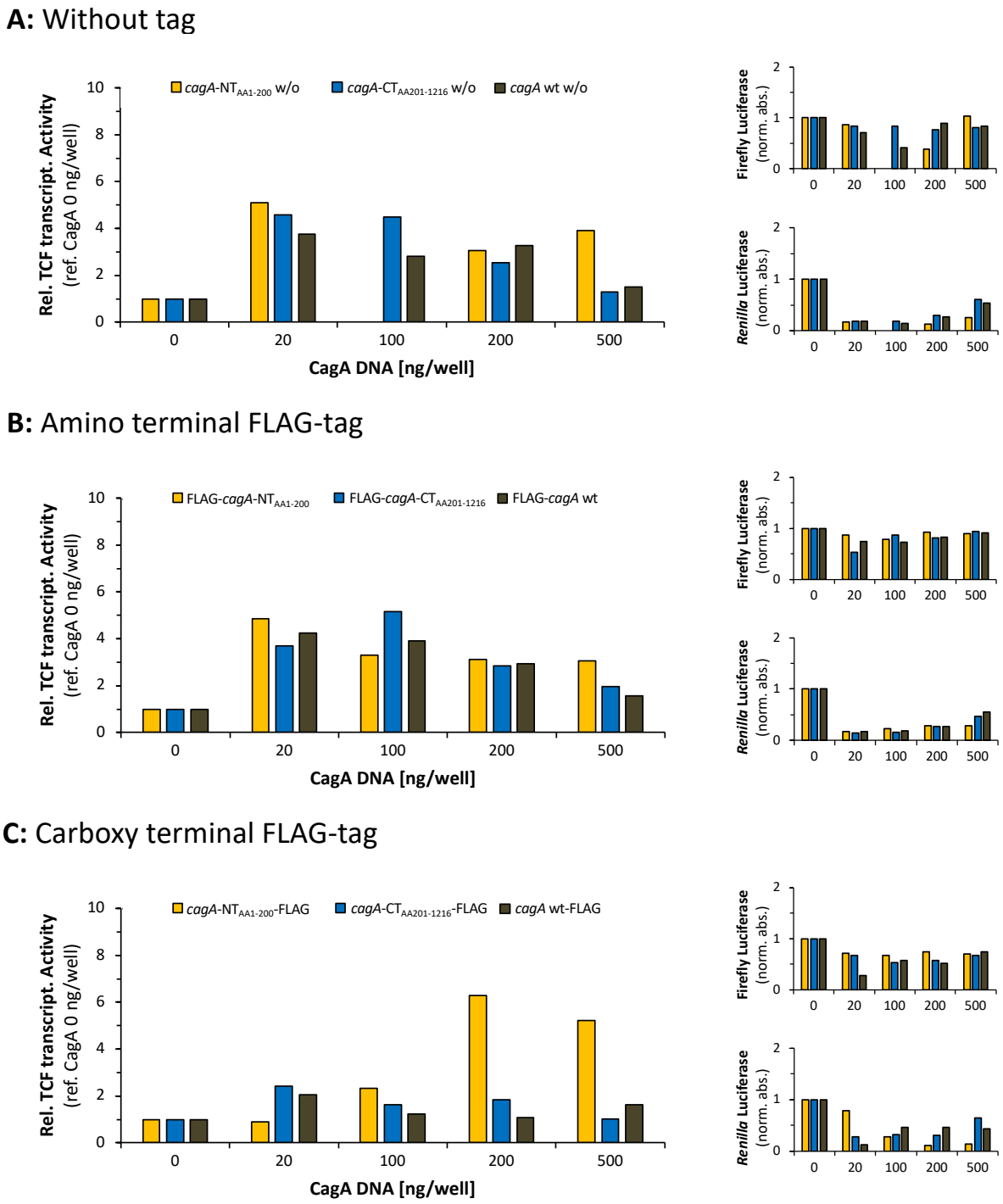

Figure 12: Transient expression of wt *cagA* and its construct DNA in MKN45 cells.
Altered Wnt signaling levels in terms of TCF/LEF transcriptional activity through increasing amounts of *cagA*-NT$_{AA1-200}$, *cagA*-CT$_{AA201-1216}$ and wt *cagA* (pcDNA4/TO encoded; amino- or carboxy-terminal FLAG, tagged or without tag = w/o, respectively) plasmids transfected to MKN45 cells (see 2.7.2) is shown as mean (N = 2) of intensity of firefly bioluminescence divided by corresponding internal standard (*Renilla* luciferase, see 2.10) and referred to control (cells transfected by blank pcDNA4/TO); right side: small graphs illustrate respective normalized absolute firefly and *Renilla* luciferase intensities; lysis of cell cultures after 24 h of incubation; [**A**] without tag; [**B**] amino-terminal FLAG-tag; [**C**] carboxy-terminal FLAG-tag; *orange*: *cagA*-NT$_{AA1-200}$; *blue*: *cagA*-CT$_{AA201-1216}$; *olive*: wt *cagA*; basically, *cagA* and both constructs were capable of increasing levels of (canonical) Wnt/β-catenin signaling; intriguingly, increasing amounts of all amino-terminal FLAG-tagged constructs and all versions of the large constructs (*cagA*-CT$_{AA201-1216}$ and wt *cagA*), respectively, caused a reduction in TCF/LEF transcription activity relating to an initial maximum, even partly below control levels (*cagA*-NT$_{AA201-1216}$ and wt *cagA*); titration of *cagA*-NT$_{AA1-200}$-FLAG effected a kind of a proportional increment of Wnt signaling activity and in the case of non-tagged *cagA*-NT$_{AA1-200}$, besides generally activating TCF/LEF expression level, no clear trend could be perceived.

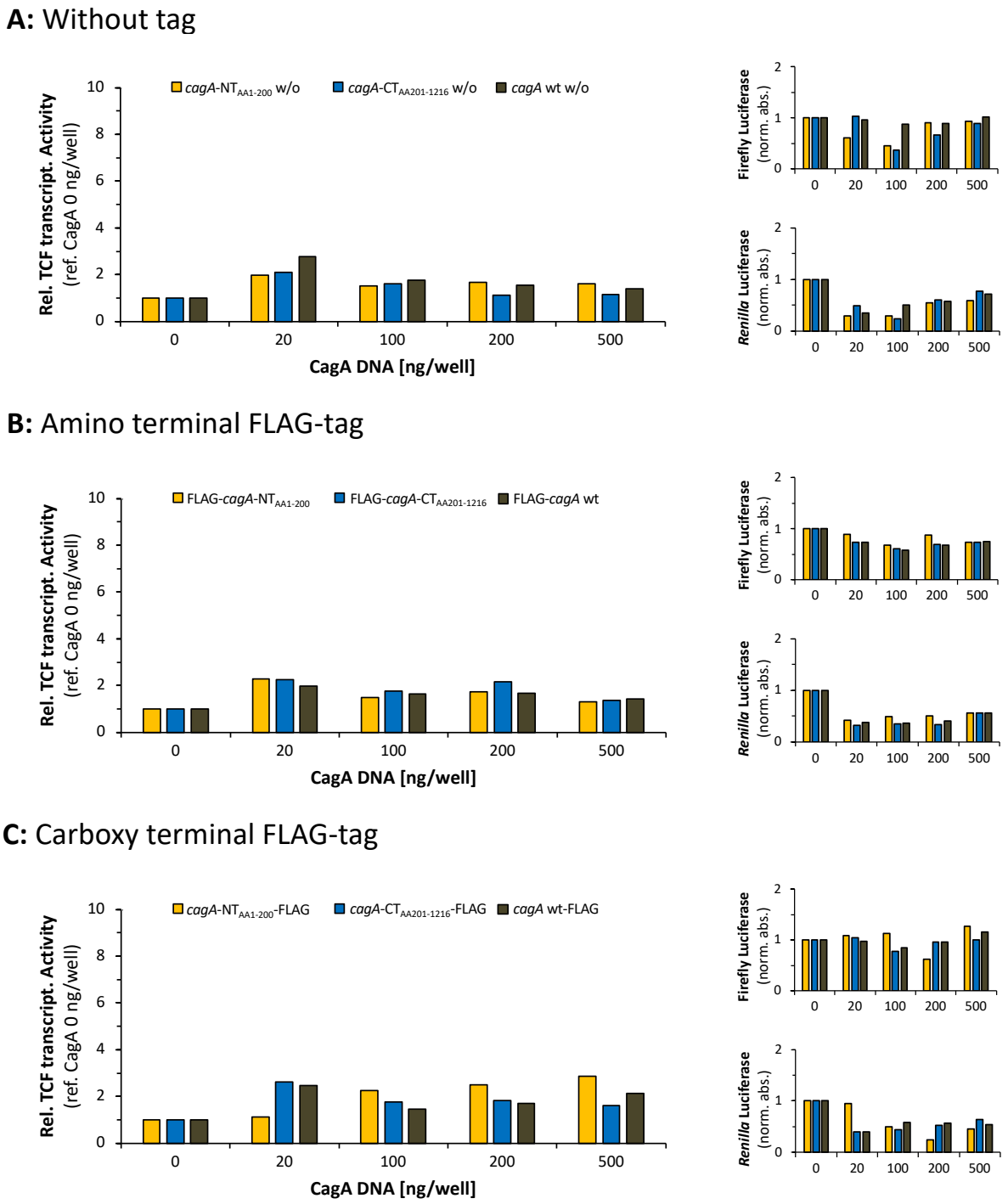

Figure 13: Transient expression of wt *cagA* and its construct DNA in 23132 cells.
Altered Wnt signaling levels in terms of TCF/LEF transcriptional activity through increasing amounts of *cagA*-NT$_{AA1-200}$, *cagA*-CT$_{AA201-1216}$ and wt *cagA* (pcDNA4/TO-encoded; amino- or carboxy-terminal FLAG, tagged or without tag = w/o, respectively) plasmids transfected to 23132 cells (see 2.7.2) is shown as mean (N = 2) of intensity of firefly bioluminescence divided by corresponding internal standard (*Renilla* luciferase, see 2.10) and referred to control (cells transfected by blank pcDNA4/TO); right side: small graphs illustrate respective normalized absolute firefly and *Renilla* luciferase intensities; lysis of cell cultures after 24 h of incubation; [**A**] without tag; [**B**] amino-terminal FLAG-tag; [**C**] carboxy-terminal FLAG-tag; *orange*: *cagA*-NT$_{AA1-200}$; *blue*: *cagA*-CT$_{AA201-1216}$; *olive*: wt *cagA*; basically, *cagA* and both constructs were capable of increasing levels of (canonical) Wnt/β-catenin signaling; intriguingly, increasing amounts of all amino-terminal FLAG-tagged constructs and all versions of the large constructs (*cagA*-CT$_{AA201-1216}$ and wt *cagA*), respectively, caused a reduction in TCF/LEF transcription activity relating to an initial maximum; titration of *cagA*-NT$_{AA1-200}$-FLAG effected a kind of proportional increment of Wnt signaling activity and in the case of non-tagged *cagA*-NT$_{AA1-200}$, besides generally activating TCF/LEF expression level, no clear trend could be perceived.

3.2.1.2 Transduction of different cell lines with *cagA* (wt or constructs)

As transduction provides a very powerful means of successfully transferring and expressing even large nucleic acids in host cells, it was utilized as a further attempt to study the (canonical) Wnt/β-catenin signaling activity level in the context of wt *cagA* or its constructs (see 2.7.3.2.2). Moreover, since this approach is largely different, systematic errors resulting from transfection could possibly, at least in part, be circumvented. Experiments were performed with AGS, MKN45 and 23132 cell lines that had been previously stably transduced with both an inducible TCF/LEF reporter (i.e., firefly luciferase) and a constitutively expressed *Renilla* luciferase (see 2.7.3.1). Figure 14 shows that wt *cagA* and its deletion constructs exhibited similar trends to those already observed in the previous titration experiments transfecting pcDNA4/TO-*cagA* (see 3.2.1.1), although the MKN45 cells displayed an entirely inverse behavior in this case (which however corresponds to findings in 3.1.3). A similar procedure was followed as in 3.1.1 in order to make firefly luciferase raw data comparable and obtain an estimation of firefly luciferase amounts with respect to the underlying *Renilla* luciferase readouts: The entire AGS, MKN45 and 23132 cell records (i.e., all *Renilla* and firefly luciferase raw values) were (i) adjusted to the mean (N = 2) *Renilla* luciferase raw values of untransfected but puromycin-treated AGS cells (i.e., adjusting/offsetting of cell lines' putative different general expression levels) and (ii) also normalized to it. Relative TCF/LEF values of the entire record were likewise referred to the mean (N = 2) relative TCF/LEF values of non-transduced but puromycin-treated AGS cells.

Again, the comparatively strongest response was observed in the AGS cells. Although the corresponding normalized relative TCF/LEF transcriptional activity levels were far lower in the case of 23132 cells, increasing amounts of *cagA*-$NT_{AA1-200}$-containing lentiviral supernatants caused a proportionally increasing relative TCF/LEF transcriptional activity level (see Figure 14, A and C, large graphs, left lateral, orange bars). Whereas in the case of AGS cells 25% of *cagA*-$NT_{AA1-200}$-containing lentiviral supernatant reduced the relative TCF/LEF transcriptional activity level by 0.6-fold with respect to the control, and 75% of the lentiviral supernatant caused an increase of 1.2-fold, in the case of 23132 cells even 25% of *cagA*-$NT_{AA1-200}$-containing lentiviral supernatant sufficed to increase relative TCF/LEF transcriptional activity level by 1.7-fold and 75% increased the relative TCF/LEF transcriptional activity level by 3.3-fold. Here, both *cagA*-$CT_{AA201-1216}$ and wt *cagA* indicated an opposing trend that could be seen in AGS cells showing the highest increment of normalized relative TCF/LEF transcriptional activity level with 25% of the lentiviral supernatant (see Figure 14, A, large graphs, left lateral, blue and olive bars; *cagA*-$CT_{AA201-1216}$: 2.0-fold, wt *cagA*: 1.8-fold), which decreased to even below base level with 75% of the lentiviral supernatant (*cagA*-$CT_{AA201-1216}$: 0.7-fold, wt *cagA*: 1.1-fold). Likewise, in the case of 23132 cells, 25% of the *cagA*-$CT_{AA201-1216}$- or wt *cagA*-containing lentiviral supernatant increased relative TCF/LEF transcriptional activity levels to 3.7- and 3.5-fold, respectively (see Figure 14, C, large graphs, left lateral, blue and olive bars). The lowest values were obtained with 75% of *cagA*-$CT_{AA201-1216}$- or wt *cagA*-containing lentiviral supernatant (*cagA*-$CT_{AA201-1216}$: 1.6-fold, wt *cagA*: 1.7-fold).

As already mentioned, MKN45 cells displayed a totally contrary behavior in this context (see Figure 14, B). Beginning with *cagA*-$NT_{AA1-200}$, 25% of lentiviral supernatant resulted in a 1.3-fold increase in normalized relative TCF/LEF transcriptional activity levels, whereas 75% of lentiviral supernatant decreased this by 0.6-fold. In contrast, referring to the control, *cagA*-$CT_{AA201-1216}$ and wt *cagA* caused a considerable reduction in relative TCF/LEF transcriptional activity levels at small amounts (25% of lentiviral supernatant;

cagA-$CT_{AA201-1216}$: 0.6-fold, wt *cagA*: 0.5-fold) and induced its enhancement at high amounts (75% of lentiviral supernatant; *cagA*-$CT_{AA201-1216}$: 1.1-fold, wt *cagA*: 1.6-fold).

The corresponding underlying adjusted/offset and normalized absolute firefly and *Renilla* luciferase readouts (see Figure 14, small graphs, right-hand side) in the case of AGS and 23132 cells showed that, unlike firefly luciferase activity, *Renilla* luciferase activity did not substantially correspond to increasing amounts of *cagA* lentiviral supernatant. In contrast, titration of MKN45 cells with increasing amounts of *cagA* and its deletion constructs altered the absolute *Renilla* luciferase activity (i.e., the adjusted/offset and normalized absolute *Renilla* luciferase readouts) in that *cagA*-$NT_{AA1-200}$ caused an increase and wt *cagA* an incremental reduction in adjusted/offset normalized absolute *Renilla* luciferase activity, yet invariably still above the control level. Nevertheless, looking at the absolute firefly luciferase activity of *cagA*-CTAA201-1216 and wt *cagA* in MKN45 cells, their dose-dependent increase is evident. This is consistent with the findings in 3.1.3, where infection by CagA proficient *H. pylori* in MKN45 cells causes a decrease in phosphorylated β-catenin, leading to activation of (canonical) Wnt/β-catenin signaling.

In conclusion, stably transduced *cagA* affects (canonical) Wnt/β-catenin signaling activity, and depends on the applied amounts, the *cagA* domains expressed and the host cellular context. CagA-$NT_{AA1-200}$ and CagA-$CT_{AA201-1216}$ (i.e., N- and C-terminal CagA) are functional opponents that can both decrease or increase Wnt/β-catenin signaling activity in a dose-dependent manner: At low amounts, the N-terminal part causes inhibition while the C-terminal part promotes activation. This is entirely reciprocal at medium to higher doses and is most evident in AGS cells. However, in MKN45 cells, with restriction, a completely opposite behavior is shown.

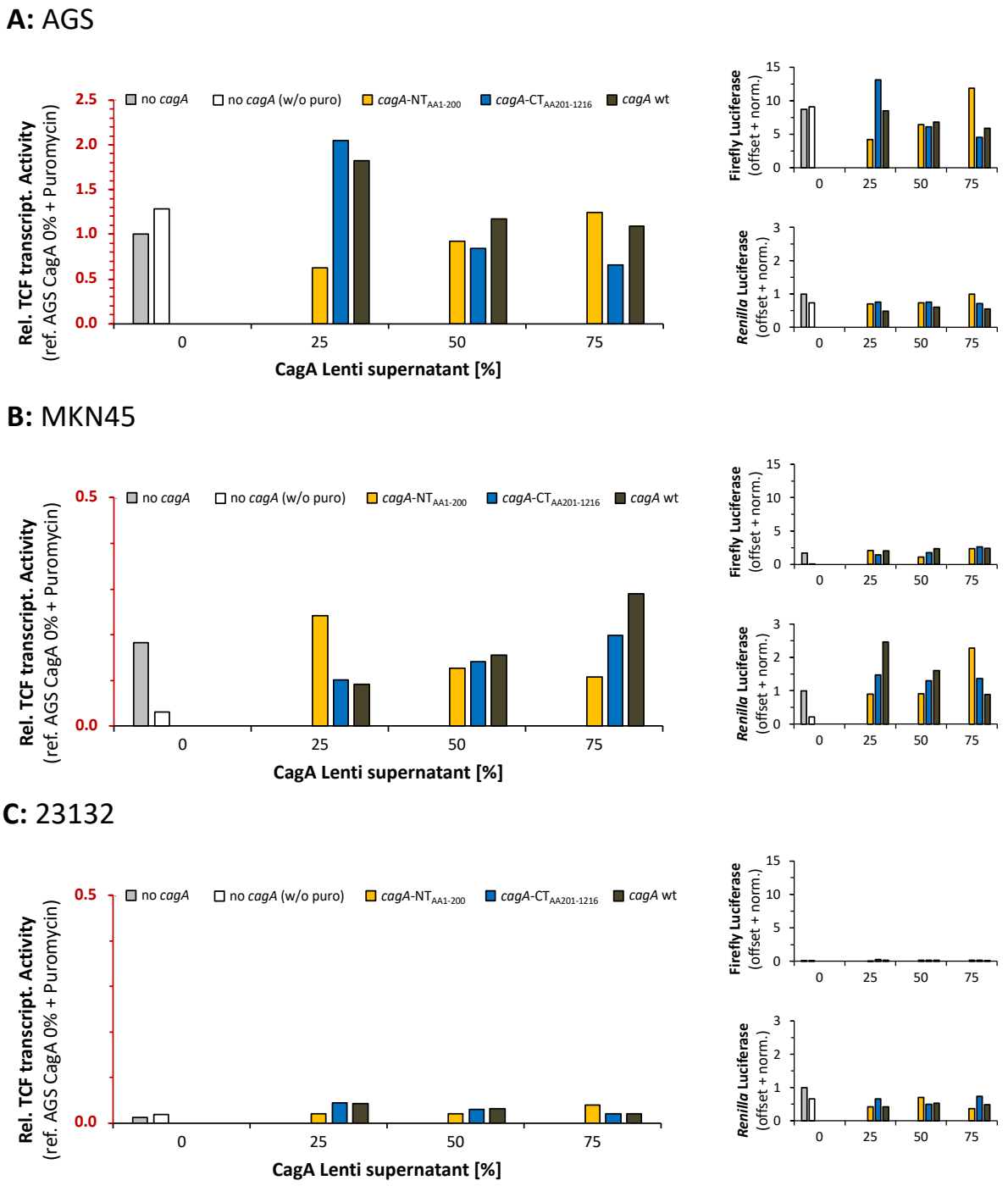

Figure 14: Stable expression of wt *cagA* and its constructs in different cell lines.
Lentiviral transduction of [**A**] AGS, [**B**] MKN45 and [**C**] 23132 cell lines by wt *cagA* and its constructs at different amounts (i.e., ratio of lentiviral supernatant applied; cells previously transduced by inducible TCF/LEF reporter and constitutively expressing *Renilla* luciferase); left side: altered (canonical) Wnt/β-catenin signaling by means of relative TCF/LEF transcriptional activity shown as mean (N = 2) firefly bioluminescence divided by corresponding internal standard (*Renilla*, see 2.7.3) and uniformly referred to AGS cell control (no lentiviral particles, medium containing puromycin, note different scaling!); right side: small graphs illustrate respective adjusted/offset and normalized absolute firefly and *Renilla* luciferase intensities (both adjusted to mean *Renilla* luciferase of non-transduced but puromycin-treated AGS cells); lysis after 24 h of incubation in cell culture medium comprising 25, 50 or 75% (v/v) of *cagA*-NT$_{AA1-200}$, *cagA*-CT$_{AA201-1216}$ or wt *cagA* lentiviral supernatant; *grey:* culture medium containing puromycin; *white:* plain culture medium (w/o puromycin); *orange:* *cagA*-NT$_{AA1-200}$; *blue:* *cagA*-CT$_{AA201-1216}$; *olive:* wt *cagA*; titration of *cagA* (wt or constructs) evokes opposite behavior of (i) AGS and 23132 and (ii) MKN45 cells: In (i) AGS and 23132 cells, increasing amounts of *cagA*-CT$_{AA201-1216}$ and wt *cagA* initially increase relative TCF/LEF transcriptional activity levels and subsequently gradually reduce it to roughly base level or below (AGS cells) and impact of *cagA*-NT$_{AA1-200}$ on Wnt signaling activity is kind of proportional; in (ii) MKN45 cells, *cagA*-NT$_{AA1-200}$ is capable of increasing relative TCF/LEF transcriptional activity level by factor 1.3 at lower amounts and higher concentrations attenuate it even below base level, whereas *cagA*-CT$_{AA201-1216}$ and wt *cagA* displays inverse behavior.

3.2.2 Carboxy terminal CagA inhibits (canonical) Wnt/ß-catenin signaling in dose-dependent manner

To gain a more comprehensive insight into the impact of CagA on host cellular (canonical) Wnt/β-catenin signaling activity, 293T cells were given preference to gastric adenocarcinoma-derived cell lines. The 293T cells feature a markedly high transfection capability and have an intact (canonical) Wnt/β-catenin pathway that can easily be induced (Liu et al., 2007, Upadhyay et al., 2008), allowing the adjustment of different levels of (canonical) Wnt/β-catenin signaling activity through graded LiCl induction (see 2.7.4). A higher extent of control could be obtained by conducting parallel transfections of host cells with pTOPflash or pFOPflash reporter plasmids (plus a constitutively expressed *Renilla* luciferase in each case), in contrast to the abovementioned experiments where cell lines stably transduced with an inducible TCF/LEF reporter (i.e., firefly luciferase) were used. Transfections were conducted according to the optimized transfection approach (DNA 350 ng/well, Lipofectamine ratio 1:5 [µg/µl]; see 2.7.2.2). Since the localization of the FLAG-tag on CagA-$NT_{AA1-200}$ constructs had an effect on the response of (canonical) Wnt/β-catenin signaling (see 3.2.1.1), these were not applied here. Instead, the pEGFP-C1 vector system was utilized, meaning that wt CagA and its constructs were linked to an EGFP protein at their N-terminal end, whereas the expression of this fusion protein is regulated by a CMV promoter (see 2.4.1). Relative TCF/LEF transcriptional activities were referred to controls (transfection by blank vector; N = 6). To assess the dimensions of the responses with respect to underlying *Renilla* luciferase raw values, which are (directly) affected by LiCl, entire records (i.e., all *Renilla* and firefly luciferase raw values) were (i) adjusted to the mean (N = 12) *Renilla* luciferase raw values of the entire record at 0 mM LiCl (i.e., adjusting/offsetting of the cell lines' putative different general expression levels) and also (ii) normalized to it.

Figures 15 and 16 depict the results of these experiments. The higher the Wnt/β-catenin activity level, the more pronounced are the cells' responses to CagA or its constructs. On the left side of Figure 15 (large graphs), cellular response in terms of normalized relative TCF/LEF transcriptional activity level to the titration of different amounts of wt *cagA* or its constructs at distinct (canonical) Wnt/β-catenin signaling activity levels is shown, with the corresponding bars of the pTOPflash and pFOPflash readout values directly adjoining (pTOPflash: left; pFOPflash: right). It should be noted that the corresponding pFOPflash values turned out to be so low that they are hardly visible above the abscissa. Figure 16 shows the very same data in a comparative manner, disregarding the corresponding pFOPflash values to emphasize the differences between wt *cagA* and its constructs.

With respect to cells cultivated in an LiCl-free medium, the induction of the normalized relative TCF/LEF transcriptional activity of vector control-transfected cells could be achieved by means of 50 mM (factor 1.65) and 100 mM LiCl (factor 6-7) (see Figures 15 and 16, large graphs, left-hand set of bars). In contrast to the previous transfection experiments (see 3.2.1), wt *cagA* and its constructs did not increase the relative TCF/LEF transcriptional activity level, neither at low amounts nor at higher amounts, as these invariably show values lower than the corresponding controls. Regarding *cagA*-$NT_{AA1-200}$ (see Figure 15, A, and Figure 16, A to C, large graphs, orange bars, respectively), at each specifically adjusted (canonical) Wnt/β-catenin signaling activity level (i.e., LiCl 0, 50 or 100 mM), a slight decline, if any alteration, in normalized relative TCF/LEF transcriptional activity level could be observed with increasing amounts transfected. However, *cagA*-$CT_{AA201-1216}$ (see Figure 15, B, and Figure 16, A to C, large graphs, blue bars, respectively) and wt *cagA* (see Figure 15, C, and Figure 16, A to C, large graphs, olive bars, respectively) showed a consistent negative trend with

increasing amounts. This even held true for cells with uninduced (canonical) Wnt/β-catenin signaling activity levels (i.e., LiCl 0 mM; see Figure 16, A, large graph). Here, 20 ng/well of plasmidic *cagA* sufficed to reduce normalized relative TCF/LEF transcriptional activity levels by 0.82-fold (*cagA*-$CT_{AA201-1216}$) and 0.7-fold (wt *cagA*), respectively. At high (canonical) Wnt/β-catenin signaling activity levels (i.e., LiCl 100 mM; see Figure 16, C, large graph), *cagA*-$CT_{AA201-1216}$ reduced normalized relative TCF/LEF transcriptional activity level by 0.8-fold (20 ng/well) and 0.57-fold (100 ng/well), compared to the base level, which was even more pronounced in cells transfected by wt *cagA*. Here, normalized relative TCF/LEF transcriptional activity levels were reduced by 0.67-fold (20 ng/well) and 0.39-fold (100 ng/well), respectively. In both cases, a further reduction in normalized relative TCF/LEF transcriptional activity levels was obtained by transfection with higher amounts of plasmidic *cagA* (240 ng/well), which could hardly be recognized by *cagA*-$NT_{AA1-200}$.

The relation of corresponding adjusted/offset and normalized absolute firefly and *Renilla* luciferase values is shown in the small graphs on the right side of Figures 15 and 16. With increasing amounts of *cagA* DNA (*cagA*-$CT_{AA201-1216}$ and wt *cagA*), firefly luciferase values (TOPflash) revealed a steadily decreasing trend (Figure 15, B and C, and Figure 16, A to C, small upper graphs, right side, blue and olive bars), where *Renilla* luciferase values of *cagA*-$CT_{AA201-1216}$ showed an almost negligible increasing trend (Figure 15, B, and Figure 16, A to C, small lower graphs, right side, blue bars), while those of wt *cagA* showed a steadily increasing trend, most evident in cases of the highest DNA amounts (Figure 15, C, and Figure 16, A to C, small lower graphs, right side, olive bars). The situation with *cagA*-$NT_{AA1-200}$ was different: Except for its highest amounts, no decline in adjusted/offset and normalized firefly luciferase activity could be seen, whereas *Renilla* luciferase activity showed a steadily decreasing trend (see Figure 16, A to C, small lower graph, right side, orange bars).

In conclusion, similar to wt CagA, CagA's carboxy-terminal domain (CagA-$CT_{AA201-1216}$) clearly had a negative impact on (canonical) Wnt/β-catenin signaling in a dose-dependent manner that was more pronounced the higher the cellular (canonical) Wnt/β-catenin signaling activity level.

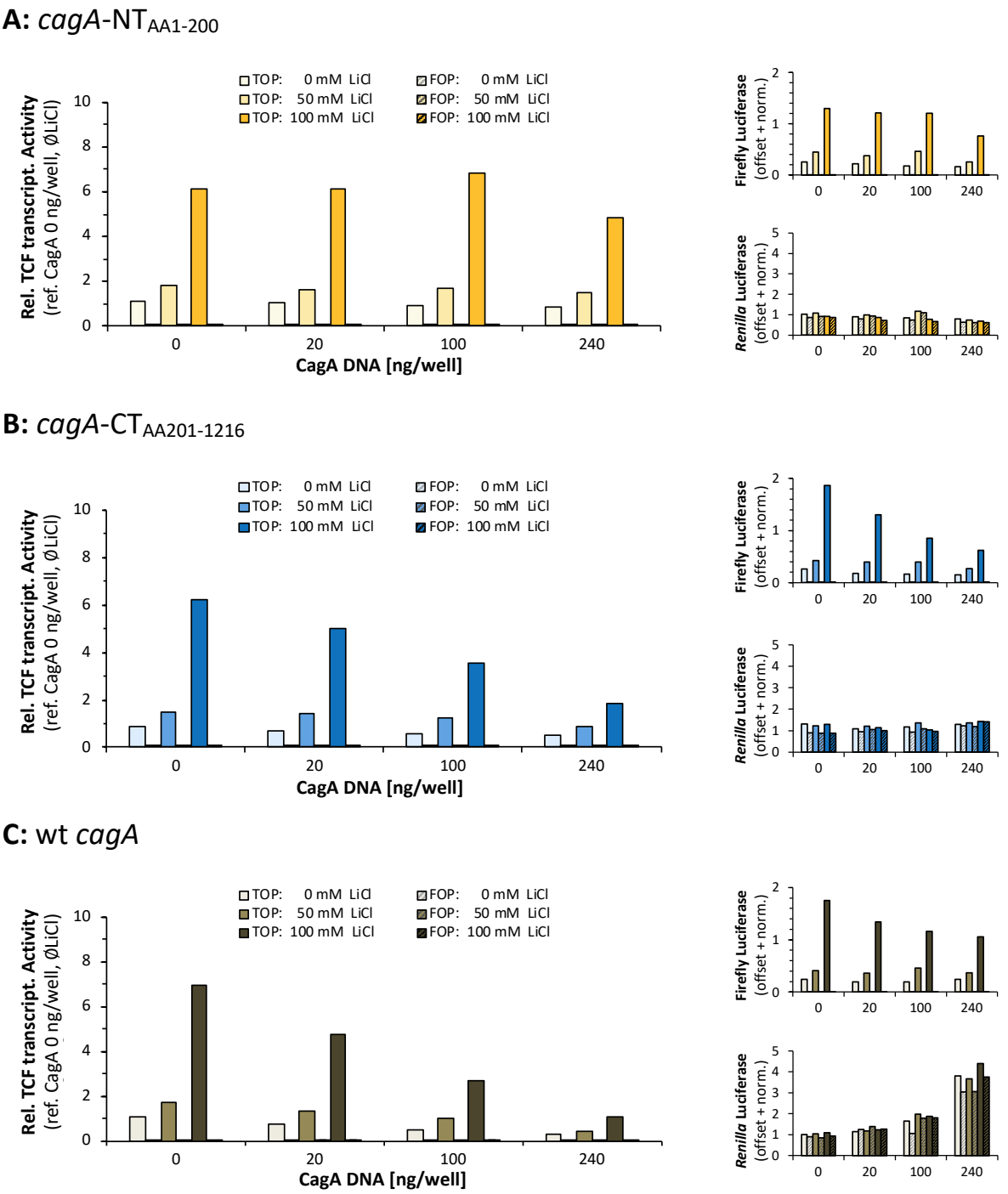

Figure 15: Titration of wt *cagA* or its constructs at varying (canonical) Wnt/β-catenin signaling activity levels. Altered Wnt signaling activity levels through increasing transfected amounts of *cagA*-$NT_{AA1-200}$ (*orange*), *cagA*-$CT_{AA201-1216}$ (*blue*) and wt *cagA* (*olive*) (pEGFP-C1) at different molar concentrations of LiCl (0, 50 and 100 mM) in 293T cells by means of TCF/LEF transcriptional activity are shown as mean (N = 2) of intensity of firefly luciferase bioluminescence related to corresponding internal transfection standard (see 2.10) and referred to the control (cells transfected by blank pEGFP-C1, no LiCl added, N = 6); *right side:* small graphs illustrate respective adjusted/offset and normalized absolute firefly and *Renilla* luciferase intensities; lysis of cell cultures after 48 h of incubation (see 2.7.2.1); *pale:* LiCl 0 mM (pTOPflash), *pale/hatched:* LiCl 0 mM (pFOPflash), *medium:* LiCl 50 mM (pTOPflash), *medium/hatched:* LiCl 50 mM (pFOPflash), *dark:* LiCl 100 mM (pTOPflash), *dark/hatched:* LiCl 100 mM (pFOPflash); note that corresponding pFOPflash values (always on the right) almost merge with the abscissa; [**A**] *cagA*-$NT_{AA1-200}$; [**B**] *cagA*-$CT_{AA201-1216}$; [**C**] wt *cagA*; distinct (canonical) Wnt/β-catenin activity levels are obtained according to the particular amounts of LiCl provided; increasing amounts of *cagA*-$NT_{AA1-200}$ do not appreciably affect TCF/LEF transcriptional activity, irrespective of its underlying activity level; increasing amounts of *cagA*-$CT_{AA201-1216}$ or wt *cagA* inversely proportionally reduce the TCF/LEF transcriptional activity level in each case.

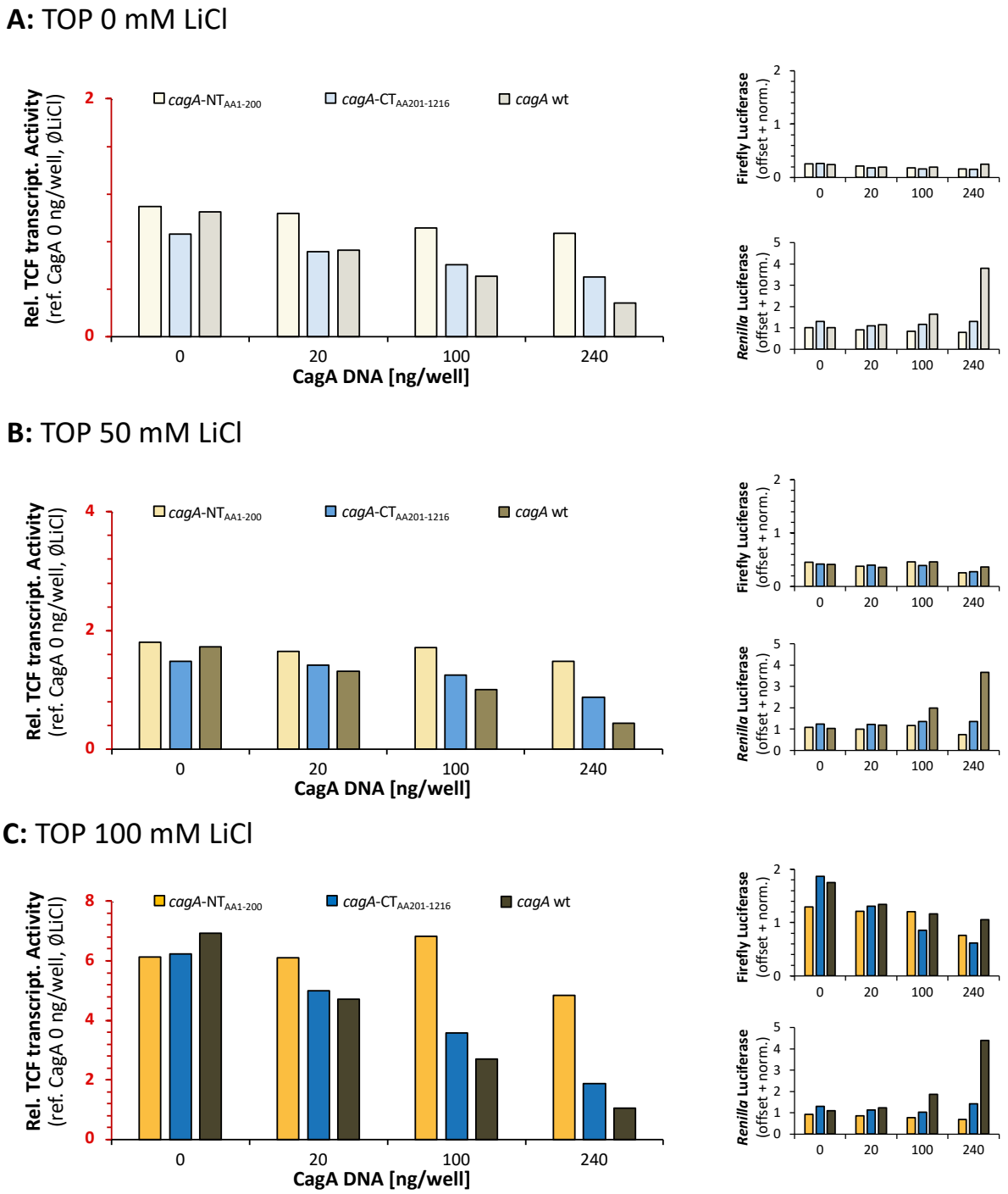

Figure 16: Titration of wt *cagA* and its constructs at varying (canonical) Wnt/β-catenin signaling activity levels (pTOPflash, competitive).
Altered Wnt signaling activity levels through increasing transfected amounts of *cagA*-NT$_{AA1-200}$ (*orange: pale/medium/dark*), *cagA*-CT$_{AA201-1216}$ (*blue: pale/medium/dark*) and wt *cagA* (*olive: pale/medium/dark*) (pEGFP-C1-encoded) in 293T cells by means of TCF/LEF transcriptional activity (pTOPflash solely) are competitively shown as mean (N = 2) of intensity of firefly luciferase bioluminescence related to corresponding internal transfection standard (see 2.10) and referred to the control (cells transfected by blank pEGFP-C1, no LiCl added, N = 6) at different molar concentrations of LiCl (0, 50 and 100 mM, note different scaling!); *right side:* small graphs illustrate respective adjusted/offset and normalized absolute firefly and *Renilla* luciferase intensities; lysis of cell cultures after 48 h of incubation (see 2.7.2.1); [**A**] LiCl 0 mM (*pale*); [**B**] LiCl 50 mM (*medium*); [**C**] LiCl 100 mM (*dark*); distinct (canonical) Wnt/β-catenin activity levels are obtained according to the particular amounts of LiCl provided; increasing amounts of *cagA*-NT$_{AA1-200}$ do not appreciably affect TCF/LEF transcriptional activity, irrespective of its underlying activity level; increasing amounts of *cagA*-NT$_{AA201-1216}$ or wt *cagA* inversely proportionally reduce the TCF/LEF transcriptional activity level in each case.

3.3 Intracellular localization of CagA and its constructs

To address the role of CagA domains on its localization in the host cell, pcDNA4/TO wt *cagA* and its deletion constructs (*cagA*-$NT_{AA1-200}$, *cagA*-$CT_{AA201-1216}$, see 2.4) were transfected in AGS and MKN45 cells. Procedures were performed as described in 2.9 and Table 19, because previous experiments indicated that cells need to be transfected with higher amounts of wt *cagA* or its constructs to allow for detection via immunofluorescence imaging.

In Figures 17, 18, 19 and 20, the cytoskeleton (β-actin) displays cyan green, wt CagA and its constructs display red and the nucleus displays blue due to the actual excitation maxima of the secondary antibodies or the (conjugated) florescent dyes. Note that both the anti-$CagA_{1-877}$ and the anti-FLAG-antibody showed background staining in the nuclear region of controls. It becomes obvious that CagA-$NT_{AA1-200}$ constructs (second row in each case) distribute homogeneously throughout the cytoplasm and in a less pronounced way throughout the nucleoplasm, thus sparing the plasma membrane and nuclear membrane plus its affiliated cell organelles (see Figures 17, 18, 19 and 20, second row). Since in AGS cells the β-actin filaments permeate the cytoplasm to a considerable extent, cytoskeletal cyan green and red gleaming CagA-$NT_{AA1-200}$ in part superimpose and the cytoplasm appears bright red/tangerine (see Figures 17 and 18, second row, merge column). As the staining of the MKN45 cells cytoskeleton (i.e., β-actin filaments) is primarily restricted to the plasma membrane region, hardly any superimposition can be recognized (see Figures 19 and 20, second row, merge column). In contrast, CagA-$CT_{AA201-1216}$ and wt CagA almost spare the nucleus, irrespective of FLAG-tagging or cell line used. They predominantly accumulate at the plasma membrane and localization in the cytosol is very subordinate (see Figures 17, 18, 19 and 20, third and fourth row). Here, the co-localization of CagA and the cytoskeleton again display the plasma membrane region as partly bright red/tangerine, which can be seen in MKN45 cells in particular.

In summary, CagA-$NT_{AA1-200}$ does not show localization at the plasma membrane and, contrary to CagA-$CT_{AA201-1216}$ and wt CagA, is also distributed in the cytosol and the nucleosol. Since both CagA-$CT_{AA201-1216}$ and wt CagA show a similar intracellular distribution pattern, its carboxy-terminal AA 201-1216 seem capable of predominantly tethering the whole wt CagA molecule to the plasma membrane.

AGS + CagA (w/o tag)

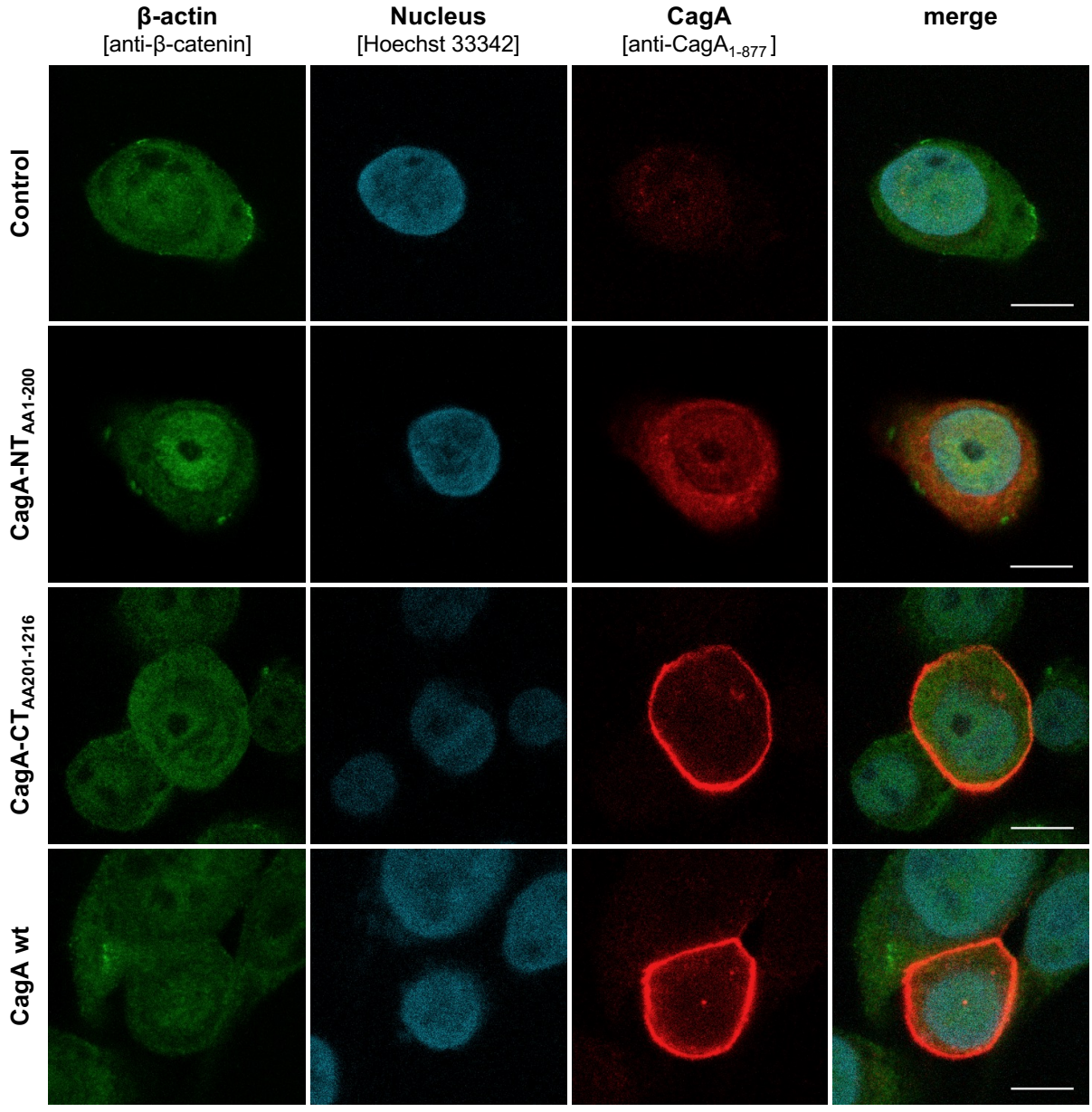

Figure 17: Spatial intracellular distribution of wt CagA and its constructs (without tag) in AGS cells. Transient transfection of AGS cells by means of pcDNA4/TO *cagA* (wt or constructs; 24 h); confocal laser scanning microscopy: x-y planes; white scale bar: 10 µm; controls: transfection with blank pcDNA4/TO; *cyan green:* β-actin (mouse anti-β-catenin); *blue:* nucleus (Hoechst 33342); *red:* wt CagA or its constructs (rabbit anti-$CagA_{1-877}$); bright red/tangerine cytoplasm since CagA-$NT_{AA1-200}$ homogeneously distributes to the cytoplasm, sparing both plasma membrane and nuclear membrane; superimposition of CagA-$CT_{AA201-1216}$ or wt CagA at the plasma membrane (bright red/tangerine).

AGS + FLAG-CagA

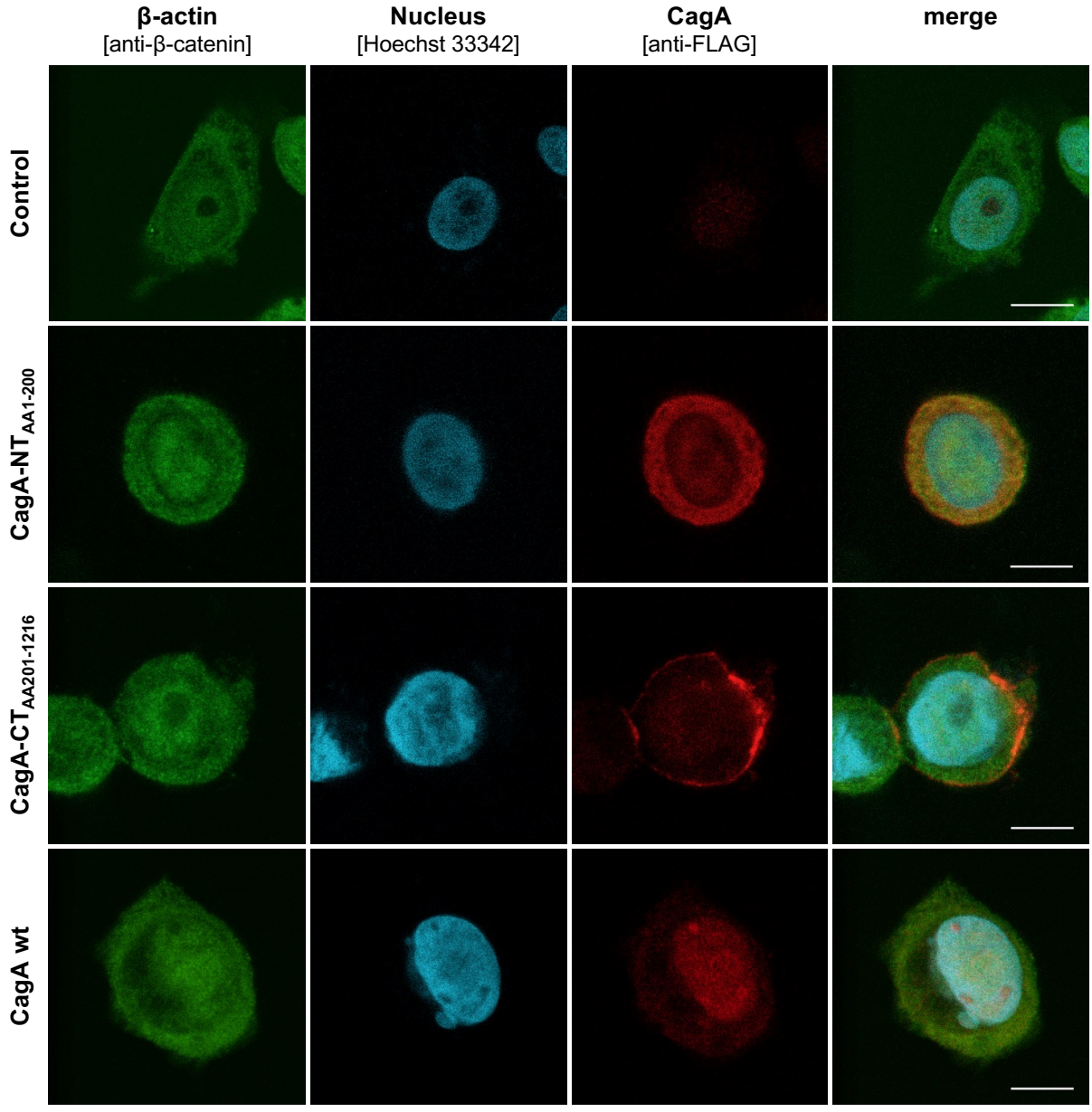

Figure 18: Spatial intracellular distribution of N-terminal FLAG-tagged wt CagA and its constructs in AGS cells. Transient transfection of AGS cells by means of pcDNA4/TO *cagA* (wt or constructs; 24 h); confocal laser scanning microscopy: x-y planes; white scale bar: 10 µm; controls: transfection with blank pcDNA4/TO; *cyan green:* β-actin (mouse anti-β-catenin); *blue:* nucleus (Hoechst 33342); *red:* wt CagA or its constructs (rabbit anti-FLAG); bright red/tangerine cytoplasm since CagA-$NT_{AA1-200}$ homogeneously distributes to the cytoplasm, sparing both plasma membrane and nuclear membrane; superimposition of CagA-$CT_{AA201-1216}$ or wt CagA at the plasma membrane (bright red/tangerine).

MKN45 + CagA (w/o tag)

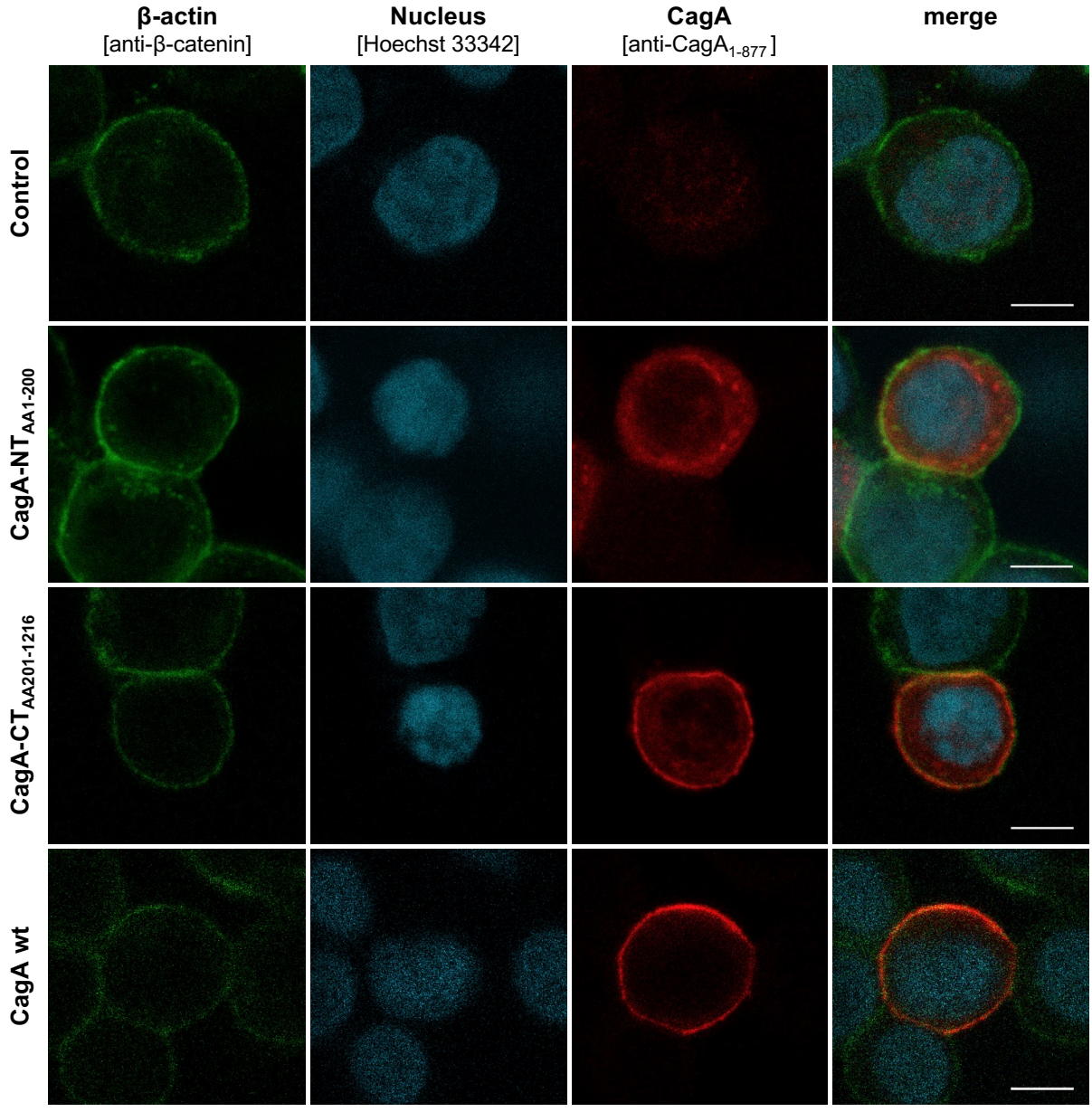

Figure 19: Spatial intracellular distribution of wt CagA and its constructs (without tag) in MKN45 cells. Transient transfection of MKN45 cells by means of pcDNA4/TO *cagA* (wt or constructs; 24 h); confocal laser scanning microscopy: x-y planes; white scale bar: 10 µm; controls: transfection with blank pcDNA4/TO; *cyan green:* β-actin (mouse anti-β-catenin); *blue:* nucleus (Hoechst 33342); *red:* wt CagA or its constructs (rabbit anti-$CagA_{1-877}$); CagA-$NT_{AA1-200}$ homogeneously distributes to the cytoplasm, sparing both plasma membrane and nuclear membrane; bright red/tangerine plasma membrane through superimposition of CagA-$CT_{AA201-1216}$ or wt CagA, respectively (since β-actin is predominantly localized at the plasma membrane).

MKN45 + FLAG-CagA

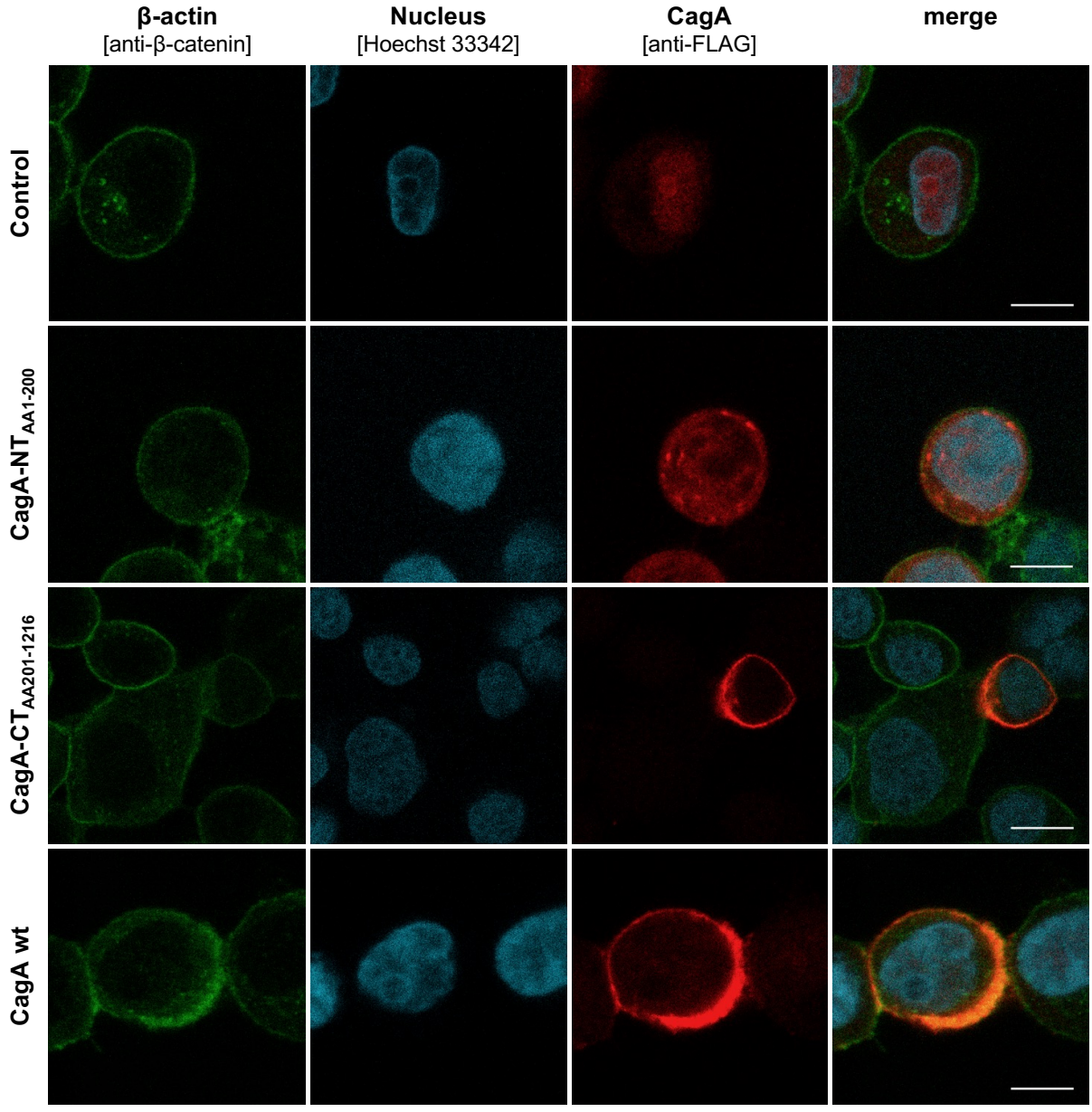

Figure 20: Spatial intracellular distribution of N-terminal FLAG-tagged wt CagA and its constructs in MKN45 cells.
Transient transfection of MKN45 cells by means of pcDNA4/TO *cagA* (wt or constructs; 24 h); confocal laser scanning microscopy: x-y planes; white scale bar: 10 µm; controls: transfection with blank pcDNA4/TO; *cyan green:* β-actin (mouse anti-β-catenin); *blue:* nucleus (Hoechst 33342); *red:* wt CagA or its constructs (rabbit anti-FLAG); CagA-$NT_{AA1-200}$ homogeneously distributes to the cytoplasm, sparing both plasma membrane and nuclear membrane; bright red/tangerine plasma membrane through superimposition of CagA-$CT_{AA201-1216}$ or wt CagA, respectively (since β-actin is predominantly localized at the plasma membrane).

4 Discussion

A growing body of evidence proposes *H. pylori* CagA's impact on (canonical) Wnt/β-catenin signaling, the deregulation of which has been demonstrated to be involved in the development of gastric adenocarcinoma (see 1.1). Bagnoli et al. (2005) found (for MDCK cells) that wild type CagA is capable of disrupting host cell polarity and inducing morphological changes, which resemble epithelial-mesenchymal transition (EMT). In this context, the amino-terminal two-thirds of CagA show affinity for the apicolateral cell-cell junctions, whereas the carboxy-terminal domain, harboring the multimerization motifs (see 1.2.4), can induce cell elongation and pseudopodia. Based on this, Pelz et al. (2011) observed (in MDCK and NCI-N87 cells) that C-terminal CagA, similar to wt CagA, positively regulates (canonical) Wnt/β-catenin signaling activity, whereas CagA's N-terminal AA 1-200 promote cell-cell adhesion and exhibit an antagonistic role concerning morphological changes, which was attributed to the inhibition of (canonical) Wnt/β-catenin signaling activity. This project, therefore, involved a more comprehensive examination of these findings, mainly of the impact on (canonical) Wnt/β-catenin signaling activity, hypothesizing amino-terminal CagA having an inhibitory effect that (partly) counteracts the activating effect of the C-terminal part. Accordingly, wild type CagA as well as its N- and C-terminal constructs (i.e., CagA-$NT_{AA1-200}$ or CagA-$CT_{AA201-1216}$; see 2.4) were examined regarding their influence on (canonical) Wnt/β-catenin signaling activity in a dose-dependent manner, which was furthermore related to the particular spatial allocation in host cells. For this purpose, gastric cancer cell lines should be exposed to (i) wt CagA by infection with wt *H. pylori* strains or to (ii) plasmid-encoded *cagA* or its deletion mutants through transfection or transduction while observing their (canonical) Wnt/β-catenin signaling activity (i.e., TCF/LEF transcriptional activity) by use of a pTOPflash/pFOPflash luciferase reporter system and, in addition, by confocal immunofluorescence microscopy.

4.1 Observations and implications

The impact of CagA on the (canonical) Wnt/β-catenin pathway was investigated using different approaches. In accordance with their higher intrinsic (canonical) Wnt/β-catenin signaling activity level (see 5.1.2.3), AGS cells basically showed the most distinct effects among the gastric adenocarcinoma cell lines. In contrast, 23132 cells exerted the most inert behavior, which can presumably be attributed to the various deleterious mutations of (canonical) Wnt/β-catenin signaling components (see 5.1.1.2.3).

Contrary to the underlying hypothesis and the general opinion (El-Etr et al., 2004, Franco et al., 2005, Murata-Kamiya et al., 2007, Kurashima et al., 2008, Suzuki et al., 2009), wt CagA and its C-terminal part were first of all found to inhibit (canonical) Wnt/β-catenin signaling activity, which puts the focus on potential technical inconsistencies and limitations. Although transfection (and transduction) of cultured (cancer) cells appears to be unfavorable in several aspects (see 4.2), it is a well-established technique and widely used regarding CagA research and thus considered an appropriate means of comparing the various approaches. As transfection experiments with *cagA*-$NT_{AA1-200}$ yield high amounts of (truncated) CagA protein (see 2.8.3), the cloning strategy and transfection protocol applied in this work were efficient.

Concerning cell culture, the inhibition of (canonical) Wnt/β-catenin signaling activity in principle allows different scenarios to be considered. However, it should be pointed out that this has a decisive influence on cell division. Since β-catenin is directly regulating the expression of c-Myc (He et al., 1998) and cyclin D1 (Tetsu and McCormick, 1999, Herbst et al., 2014), which triggers G1-phase progression (Shtutman et al., 1999, Tetsu and McCormick, 1999), and, moreover, since axin, GSK3β, APC and β-catenin are involved in organizing mitosis (Niehrs and Acebron, 2012), the latter playing a leading role in coordinating centrosome function (Hadjihannas et al., 2010, Mbom et al., 2013), it was demonstrated by Stolz et al. (2015) that unimpaired (canonical) Wnt/β-catenin signaling allows for the proper course of mitosis by means of microtubule assembly and chromosome segregation. If experimental conditions of CagA exposure were to cause a general inhibition of cell division of a cell culture, corresponding *Renilla* luciferase readouts would be basically reduced related to the controls at the time of lysis – but this could not be observed in general (see 4.1.1.1 and 3.2.2 in particular). On further reflection, an inhibition of (canonical) Wnt/β-catenin signaling (due to methodical reasons) affecting only part of the cells (i.e., those efficiently exposed to wt *cagA* or its constructs DNA) would not be readily apparent, but, on the contrary, would rather promote the selection of those with unaffected or increased (canonical) Wnt/β-catenin signaling activity, with the consequence that net (canonical) Wnt/β-catenin signaling activity of the cell culture would be equal to controls' or even increased. Thus, it can be assumed that inhibition of the (canonical) Wnt/β-catenin signaling activity under the premise of relatively stable corresponding *Renilla* luciferase expression may indeed be a valid observation.

In short, inhibition of (canonical) Wnt/β-catenin signaling in the context of these experiments need not be fundamentally aberrant. Since infection of gastric adenocarcinoma cell lines with wt *H. pylori* can in fact cause an attenuation of the transcriptional activity at the TCF/LEF consensus site while promoting phosphorylation of β-catenin (see 3.1.1), the observation of reduced TCF/LEF transcriptional activity cannot simply be ascribed to inadequate experimental conception and implementation.

4.1.1 CagA's impact on transcriptional activity

4.1.1.1 Impact on CMV promoter-driven *Renilla* luciferase expression

A considerable issue in this work was the interference with CMV promoter-driven constitutive expression of *Renilla* luciferase, which was utilized as an internal transfection and expression control in the pTOPflash/pFOPflash reporter assays (see 2.10). In preliminary experiments, when transfecting N87, MDCK, COS and 293 cells with different vectors (i.e., pTETon, pEGFP), even blank vectors or plain induction with doxycycline affected its expression level compared to controls. This was further complicated through the expression of *cagA* (wt or constructs). To overcome these constraints – in terms of a straightforward, strong and constitutive expression of *cagA,* avoiding the need for its induction or EGFP labeling (but also having the possibility of introducing sequences, like Kozak, and circumventing classical restriction digestion) – advanced cloning strategies were applied, also with regard to the capability of transduction of *cagA* (see 2.4). However, there was only moderate success.

Attention should at first be directed to *Renilla* luciferase readouts in Figures 11, 12 and 13 (lower small graphs, right lateral). Despite the highly cautious handling of cultivated cell lines and adhering most carefully to the transfection protocol, the *Renilla* values of controls (blank

pcDNA4/TO plasmids) and those of (transiently) *cagA*-expressing cells are not comparable and imply that CagA interferes with the constitutive expression of *Renilla* luciferase (similar to previous experiments).

Hauser et al. (1995) demonstrated that the viral promoter-driven expression of foreign genes depends on ras and (the gene products of) other oncogenes, such as receptor tyrosine kinases, serine/threonine kinases or GTP-binding proteins. Accordingly, Behre et al. (1999) showed that the CMV promoter-driven expression of the *Renilla* luciferase gene is increased by 4-fold owing to ras activity. Although experiments in this work also evinced reverse trends by reducing *Renilla* luciferase expression, this does not preclude this being directly attributed to CagA: Independent of labeling with the FLAG-tag, *cagA*-$CT_{AA201-1216}$ and wt *cagA* show a regressive inhibition of *Renilla* expression under up-titration (see Figures 11, 12 and 13, lower small graphs, right lateral, blue and olive bars) and even cause its activation at very high doses (500 ng/well DNA) relative to the controls. This possibly suggests the interaction of carboxy-terminal multimerization motifs with MAPK/Erk, i.e., the K-ras pathway (see 1.2.4). Unlabeled and amino-terminal FLAG-tagged *cagA*-$NT_{AA1-200}$ do not seem to affect *Renilla* luciferase expression at higher amounts (see Figures 11, 12 and 13, A and B, lower small graphs, right lateral, orange bars). Likewise, at low amounts of transfection (20 ng/well DNA) and related to controls, *Renilla* luciferase expression is hardly affected by carboxy-terminal FLAG-tagged *cagA*-$NT_{AA1-200}$ in all gastric cancer cell lines. However, increasing amounts show a reduction of *Renilla* luciferase activity (i.e., its decreased expression) in a dose-dependent manner, indicating the FLAG-tag might influence distinct host cellular processes (see Figures 11, 12 and 13, C, lower small graphs, right lateral, orange bars). It needs to be pointed out that the CagA region around AA 200 harbors tandem WW domains (see 1.2.4 and Figure 4), according to which CagA-$NT_{AA1-200}$ has a single WW domain at its C-terminal end. Thus, assuming that the interaction by means of WW domains has an influence here, the observations concerning CagA-$NT_{AA1-200}$-FLAG suggest that the amino-terminal WW domain (AA 120-152) might be affected by the C-terminal FLAG-tag. Concerning LiCl-treated (polarized) 293T cells (see 3.2.2), wt *cagA* and its constructs do not seem to affect *Renilla* luciferase expression at lower amounts (20 ng/well DNA). However, except for *cagA*-$CT_{AA201-1216}$, the situation is different at higher amounts (240 ng/well DNA): Whereas wt *cagA* causes an increment, *cagA*-$NT_{AA1-200}$ could rather cause a slight decrement of *Renilla* luciferase expression (see Figures 15 and 16, lower small graphs, right lateral). Taken together, this implies that N-terminal CagA, probably by means of its WW domain(s), has access to the same processes as the C-terminal multimerization motifs, which conversely affect *Renilla* luciferase expression in a dose-dependent manner.

In addition to transient *cagA*-expression, CMV promoter-driven constitutive expression of *Renilla* luciferase is promoted by *H. pylori* infection itself, independent of its ability to transfer wt CagA to host cells, i.e., independent of CagA (see Figure 7, A to C, lower small graph, right lateral). This emphasizes that infection *per se* has a considerable influence on host cellular signaling networks (see 4.2.2). At least in AGS and MKN45 cells infected with wt *H. pylori* or its CagA-deficient isogenic mutant strain, *Renilla* luciferase expression levels are stable throughout the observation period and therefore comparable.

4.1.1.2 Implications for relative TCF/LEF transcriptional activity

At transfection experiments, due to the interference with CMV promoter-driven expression of *Renilla* luciferase (see 4.1.1.1), the relevance of the relative TCF/LEF transcriptional activity is limited as this represents firefly luciferase activity with respect to the underlying *Renilla*

luciferase activity. In principle, observations at very high amounts (≥ 240 ng/well DNA) of *cagA* or its constructs should be interpreted with care, if not disregarded. Moreover, since the *Renilla* luciferase expression levels of the lowest *cagA* amounts already differ considerably from those of the controls, particularly concerning transfected gastric cancer cell lines (see 3.2.1.1), a qualitative comparison of the two lowest *cagA* amounts (i.e., 20 vs. 100 ng/well) should be given preference over the general comparison with the blank vector. The following can therefore be concluded from relative TCF/LEF transcriptional activity: wt CagA dose-dependently affects the (canonical) Wnt/beta-catenin pathway, which might be its activation at very low doses (see 3.2.1.2) but its inhibition at medium to higher doses. This also pertains to CagA-$CT_{AA201-1216}$ and behaves in the opposite way with regard to CagA-$NT_{AA1-200}$. With increasing levels of host cellular (canonical) Wnt/β-catenin signaling activity, this impact becomes even more pronounced (see 3.2.2).

Firefly luciferase readouts from infected gastric cancer cell lines indicate that CagA impairs (canonical) Wnt/β-catenin signaling activity. This is reflected by a reduction in relative TCF/LEF transcriptional activity levels, independent of cellular context (see 3.1.1). In the case of AGS cells that feature strong intrinsic (canonical) Wnt/β-catenin signaling activity (see 5.1.2.3), CagA entails a reduction of normalized TCF/LEF transcriptional activity, even below the levels of uninfected cells, contrary to (canonical) Wnt/β-catenin signaling in rather inert MKN45 and 23132 cells, where at best the infection-related (i.e., the CagA deficient isogenic mutant strain effected) increment of normalized TCF/LEF transcriptional activity is slightly reduced by CagA (see Figure 7, A to C, upper small graph, right lateral). Corresponding western blots from AGS cells, particularly at 24 h p.i., substantiate these findings, as phosphorylated β-catenin increases at the expense of unphosphorylated β-catenin (see Figure 10), which conforms with a reduction in (canonical) Wnt/β-catenin signaling activity since β-catenin is being directed to destruction. Western blots from MKN45 and 23132 cells in this regard are rather inconclusive, which might be due to their considerably lower intrinsic (canonical) Wnt/β-catenin signaling activity level (see 5.1.2.3) and the fact that infection *per se* with *H. pylori* causes mild activation of normalized TCF/LEF transcriptional activity compared to uninfected controls. Thus, in the infection experiments, a comparison of relative TCF/LEF transcriptional activity should generally be limited to the infected cells (primarily AGS und MKN45), which means that the impact of wt *H. pylori* on (canonical) Wnt/β-catenin signaling is reasonable only in relation to its CagA-deficient isogenic mutant strain. From this, it can be concluded that infection with CagA-proficient *H. pylori* causes inhibition of the (canonical) Wnt/β-catenin pathway (during the observation period of 24 h).

4.1.1.3 Aberrant behavior of transduced MKN45 cells

The transduction of gastric cancer cell lines with *cagA* (or its constructs; see 3.2.1.2) should overcome the putative effects of transfection on *Renilla* luciferase expression. In contrast to transduced AGS and 23132 cells, for which the expression of wt *cagA* or its constructs shows no clear trend, and at best a slight reduction in *Renilla* luciferase expression (see Figure 14, A and C, lower small graphs, right lateral), transduced MKN45 cells display an increase in *Renilla* luciferase expression (see Figure 14, B, lower small graph, right lateral). Curiously, in the case of *cagA*-$NT_{AA1-200}$, this is even enhanced in a dose-dependent manner, while in the case of wt *cagA*, an anti-proportional behavior is observed, which is also opposed to observations on transfected gastric cancer cell lines, including MKN45 (compare 4.1.1.2, second paragraph, and 4.2.4).

This completely opposite behavior in transduced MKN45 cells (see 3.2.1.2) with respect to *cagA*-$NT_{AA1-200}$ on the one hand and *cagA*-$CT_{AA201-1216}$ and wt *cagA* on the other hand should be questioned. Here, it might be that the experimental manipulations, not least the stable transduction performed preliminarily, have caused a fundamental disruption. Conceivably, this could be a switch in the TCF/LEF isoform expression (Tang et al., 2008), which would effectively intercede at the promoter level, or an actual pathway misdirection by means of differential gene expression (see 4.2.4). The conditions here could also have selected those cells with increased (canonical) Wnt/β-catenin signaling activity, as explained above (see 4.1). An accidental confusion of the firefly and *Renilla* luciferase values during the evaluation of the experiment can be considered excluded.

4.1.1.4 CagA (also) inhibits TCF/LEF transcriptional activity, and is partly antagonized by its N-terminal domain

In summary, considering the previous subchapters, there is an interaction between CagA and the general host cellular expression level (by means of constitutive *Renilla* luciferase expression): While the impact of wt CagA is more pronounced at higher host cellular Wnt/β-catenin signaling activity, high amounts of wt CagA are positively feeding back to cellular expression levels. Although observations revealed inadvertent technical shortcomings, they imply that (i) the impact of CagA basically seems to be dose-dependent and that (ii) its amino-terminal part around AA 200 (i.e., CagA-$NT_{AA1-200}$) also impinges on host cellular signal transduction, including Wnt/β-catenin signaling, which seems to be in opposition to wt and particularly to carboxy-terminal CagA (i.e., CagA-$CT_{AA201-1216}$). These findings are principally in line with the hypothesis of Pelz et al. (2011) (see 4, first paragraph) – although reversed at higher doses as well as by infection with wt *H. pylori*! The comprehensive discussion of observations, including transduction and infection experiments, concordantly indicates that, in general, wt CagA is capable of inhibiting (canonical) Wnt/β-catenin signaling activity in the host cell at medium to higher doses, while its amino-terminal domain around AA 200 counteracts this by causing an increment; this impact is reversed at lower doses (both accounting for unpolarized cells after 24 h of incubation).

4.1.2 Intracellular concentration of CagA

4.1.2.1 CM^W-mediated specific CagA degradation (in unpolarized cells)?

Whereas the anti-$CagA_{1-877}$ antibody did not show additional bands in the western blot from lysates of *cagA*-$NT_{AA1-200}$ transfected (polarized) 293T cells after 48 h of incubation (see Figure 6, A), lysates from *cagA*-$CT_{AA201-1216}$ and wt *cagA* (encoding for proteins of ~113 kDa and ~135 kDa, respectively) transfected 293T cells revealed further bands at roughly 75 and 90 kDa, respectively (see Figure 6, B). Similarly, supposing CagA has mostly been transferred via T4SS (see 4.1.2.2), the anti-$CagA_{1-877}$ antibody identified further bands at roughly 70, 100 and 110 kDa from lysates of wt CagA-proficient *H. pylori* strain PMSS1-infected AGS cells. In consideration of incubation times until lysis, and therefore the mostly disrupted polarization of 293T cells (see 1.2.4), these additional bands may point towards the intracellular breakdown of CagA, irrespective of the host cells' initial polarization status or mode of CagA insertion (T4SS vs. artificial). Although there is little published work in this respect and the mechanisms are not well understood, it is conceivable that the small CagA-$NT_{AA1-200}$ construct meets a different intracellular fate due to a lack of multimerization motifs (see 1.2.4, 2.4 and Figure 4). In AGS cells, Ishikawa et al. (2009) demonstrated that wt CagA is not

degraded by the 26S proteasome and that its half-life (of about 200 min) depends on PAR1 interaction at the CM^W motif, where, according to Tsugawa et al. (2012), Akt is a significant contributor in triggering autophagocytosis (in AGS cells). This fits well with the observation by Suzuki et al. (2009) that in CagA-proficient *H. pylori*-infected AGS cells, CagA's CM^W motifs target and presumably co-activate c-Met and therefore recruit PI3K/Akt (see 4.2.3).

Hypothesis Unpolarized cells: CM^W/PAR1 ⇢ c-Met/PI3K/Akt ⇡ ⇢ Autophagocytosis of CagA

4.1.2.2 CagA peak(s) upon very early infection?

Owing to the fact that wt *H. pylori*-infected unpolarized gastric cancer cell lines featured the hummingbird phenotype more frequently between 4 to 12 h p.i. and that it had almost completely regressed by 20 h p.i. (see Figure 8, A and B), it can be reasoned that (i) CagA seems to have access to fundamental cellular processes and that (ii), in line with El-Etr et al. (2004), the significance of CagA appears to change, which could be due to a shifting of the host cellular CagA concentration. It is unlikely to be a coincidence that over the same period, all gastric cancer cell lines co-cultured with the wt *H. pylori* strain PMSS1 showed an initial increment in firefly luciferase readouts (and thus in normalized TCF/LEF transcriptional activity level) between 4 and 12 h p.i. and then a certain consecutive decline (see Figure 7, A to C, upper small graph, right lateral).

It should be pointed out that although infected cell lines were not examined concerning successfully transferred CagA, this may nevertheless generally apply. Host cellular CagA concentrations in the context of a co-culture are subject to several conditions and therefore not easily derivable. Jimenez-Soto and Haas (2016) demonstrated that at 1 h p.i. (AGS cells, *H. pylori* strain P12, MOI 30), around 1.5% of the bacterial CagA pool was translocated to the host cells, and after 3 h it was roughly 7.5%. Since the transfer rate showed a linear progress, one could expect a transfer rate of roughly 30% after 12 h and almost 50% after 24 h of co-culture. One must take into account that at the outset of a co-culture, bacteria are still proliferating and that *cagA* expression depends on the actual bacterial growth phase. Thompson et al. (2003) determined an increment of the *cagA* expression rate by a factor of at least 2.6 at the transition from the log to the stationary *H. pylori* growth phase and that the latter subsequently evinces a doubling *cagA* expression time of initially a roughly 10 h. Not least due to the morphological changes from a motile long helical shape to rather less mobile rod-like shape after approximately one day of cultivation (Shimomura et al., 2004), one can assume that the transition from the log to the stationary growth phase occurred during the 24 h co-culture in the experiments in this work. This implicates a very effective CagA transfer causing an exponential increment of the host cells' cytosolic CagA amount during the very early stages of infection. As outlined in 4.1.2.1, unpolarized host cells in particular presumably shed wt CagA by means of autophagocytosis. Assuming a half-life of about 3 h in a co-culture of eukaryotic cells with CagA-proficient wt *H. pylori*, after 12 h only 6.25% and after 24 h only 0.4% of the original quantity of CagA are extant according to Ishikawa et al. (2009). Cautiously adding the T4SS-transferred CagA to host cells, the assumed doubling time of CagA production by *H. pylori* during co-culture (i.e., under terms of infection) and its mostly autophagocytosis-dependent much shorter half-life in host cells (that might need to initiate), would entail a relatively high host cellular CagA concentration at the very early stages of infection, which, in the longer term, might approach a steady state at a rather low concentration.

Despite the fact that the approach did not allow for the quantification of the effectively translocated CagA fraction, by comparing CagA amounts at 12 and 24 h p.i. in the western blot of AGS, MKN45 and 23132 cells (see Figure 9), it becomes obvious that the larger part of CagA was already substantially diminished one day after infection. Although investigating wt *cagA* in functional E-cadherin-featuring (polarized) MKN28 cells, a decline in its cellular amounts was observed by Murata-Kamiya et al. (2007) 24 h after initiating its expression (cf. Figure 3, A). In the absence of other explanations for the reduction of CagA in this context, be it a wash out of bacteria due to the repeated exchange of culture medium or its decay through unphysiological conditions, the difference in CagA amounts is very likely due to active depletion by host cell autophagocytosis. These observations are therefore indicative of (i) a large share of bacterial CagA being transferred to the host cells within 12 to 24 h of co-culture and (ii) a rather limited cytosolic half-life of T4SS-transferred CagA, entailing minute intracellular CagA concentrations in the longer term. CagA amounts at 12 h p.i., as determined from Figure 9 (A), might be a snapshot of an early CagA peak. This initial burst might have drastic transitory effects on the host cells, like an increased impact on (canonical) Wnt/β-catenin signaling activity and morphological changes.

4.1.3 Differential CagA domain membrane interaction

Since the polarization status of the host cells most likely alters CagA's signaling activity (see 4.2.3), it further appears to affect the interaction of N-terminal CagA with its target structures. In preliminary transfection experiments, when utilizing polarized MDCK cells, overexpressed *cagA*-$NT_{AA1-200}$ (pEGFP-C1 vector) showed a modest affinity for the plasma membrane by immunofluorescence imaging (see Figure 29 in the appendix), but also being granularly distributed in the cytoplasm and, in particular, concentrated close to the nucleus, presumably in the endoplasmic reticulum. More distinct and divergent results were obtained concerning the expression of *cagA*-$NT_{AA1-200}$ in unpolarized AGS and MKN45 cells (see 3.3 and below). On the contrary and independent of the polarization of the cells, in MDCK cells as well as in AGS and MKN45 cells, analogously applied *cagA*-$CT_{AA201-1216}$ indicated substantial membrane tethering, which is corresponding to the literature (Bagnoli et al., 2005, Higashi et al., 2005, Pelz et al., 2011). As with CagA-$CT_{AA201-1216}$, wt CagA was located at the plasma membrane of AGS and MKN45 cells (see Figures 17, 18, 19 and 20, lower two rows). The rather subordinate cytosolic localization of CagA-$CT_{AA201-1216}$ and wt CagA might be due to the saturation of membranous binding capacity resulting from overexpression.

Amino-terminal CagA (AA 1-877), which according to Pelz et al. (2011) could be further specified to its N-terminal AA 1-200, is attributed a pivotal role in attaching CagA's carboxy-terminal EPIYA motif (phosphorylation independently) to the membrane in transiently transfected polarized MDCK cells (even if both parts of *cagA* are expressed *in trans*), where CagA's C-terminal AA 550-1216 seem incapable of spontaneously doing this (Bagnoli et al., 2005). This is partly in line with Hayashi et al. (2012), delineating that the reach of roughly AA 450-600 can mediate membrane tethering in MDCK cells via a basic patch interacting with membranous phosphatidylserine. However, Higashi et al. (2005) investigated unpolarized AGS cells and demonstrated that CagA phosphorylation independently exhibits affinity to host cellular membrane if it features at least one EPIYA motif and an unspecified additional amino-terminal located part that seems to correlate to AA 587-868 (of CagA from *H. pylori* strain NCTC 11637). Here, the amino-terminal AA 1-612 do not attach to the cell membrane and are therefore diffusely spread throughout the cytoplasm.

Pelz et al. (2011) showed that 24 h after its expression was initiated, N-terminal CagA (AA 1-200; strain G27) co-localized with β-catenin around cell-cell junctions of transfected polarized MDCK cells, where β-catenin is bound to the plasma membrane by E-cadherin (Peifer et al., 1992, Oliveira et al., 2009). But this did not apply to CagA's AA 1-150 or AA 27-225. As mentioned introductory, tandem WW domains are located at this region (AA 120-152 and AA 204-236; see 1.2.4 and Figure 1). It seems conceivable that the colocalization of CagA's AA 1-200 with membrane bound β-catenin can be ascribed to at least one complete (singular) WW domain. Since AGS and MKN45 cells do not express functional E-cadherin (see 5.1.1.2), where β-catenin should thus not properly accumulate at the plasma membrane, the observation that CagA-$NT_{AA1-200}$ is freely distributed in the cytosol and nucleosol (see Figures 17, 18, 19 and 20, second row), is hardly surprising and in line with Higashi et al. (2005). Here, an (indirect) interaction between amino-terminal CagA and unbound (cytosolic) β-catenin seems possible. Regardless of localization, the interaction between N-terminal CagA and β-catenin could be mediated by RUNX (see 4.3.2), which are recognized by CagA's WW domains and interact directly with β-catenin (Tsang et al., 2010).

Hypothesis
Membrane interaction:

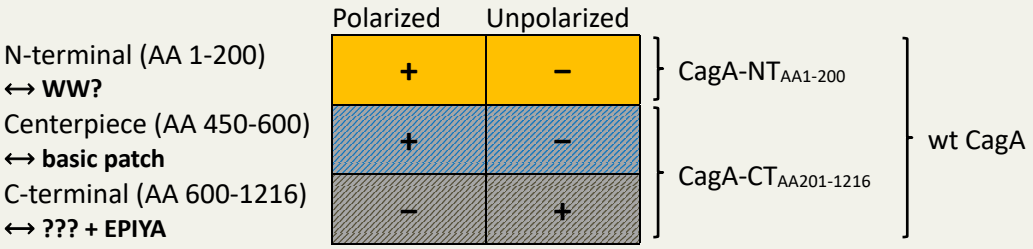

4.2 General objections and technical limitations

Within these experiments, an unexpected as well as contrary behavior with respect to CagA has been observed in several respects. In addition to the ambivalent effect on (canonical) Wnt/β-catenin signaling and on CMV-driven *Renilla* expression (see 4.1.1), ambiguities were also seen with respect to the cell lines used (in due consideration of the literature), as well as the means by which CagA was introduced into host cells. This chapter therefore addresses problematic aspects and technical limitations that result quite fundamentally from the conception and approach to achieving the objectives. The artificial transfer and expression of genes as well as characteristics of the cell lines used for this purpose are to be viewed in more detail. Ultimately, the methods applied may have been too drastic to provide a differentiated picture of the subtle nuances of CagA's impact on the host cells.

4.2.1 Lipofection of large nucleic acids and overexpression

In addition to the artificial way of introducing *cagA* (wt or constructs) into host cells by lipofection (i.e., transfection by liposomes through cationic lipids) and subsequent gene expression, the high molecular masses and high numbers of the molecules involved might (A) compromise the transfection outcome and furthermore (B) impair pivotal processes such as protein expression and signaling pathways. This could be due to the specific biochemistry of macromolecules like CagA-$CT_{AA201-1216}$ (~113 kDa) and wt CagA (~135 kDa).

(A) Although it has long been known that liposomes are capable of transferring DNA molecules successfully into eukaryotic cells (Felgner et al., 1987), the distinct steps and mechanisms that are elementary in directing foreign nucleic acids to the nucleus have not, to date, been fully elucidated and are thus susceptible to perturbations (Hoekstra et al., 2007, Pichon et al., 2010). Several obstacles are discussed in the course of lipofection-mediated DNA delivery. Once consigned to the cytosol after liberation from endosomes or liposomes, plasmids must find their way to the nucleus. In the context of molecular crowding, probably by high numbers of supplied plasmids as well as the high viscosity of eukaryotic cytosol, the cytoplasmic diffusion coefficient of plasmid DNA is inversely related to its molecule size (Lukacs et al., 2000). Thus, diffusion of the relatively large *cagA*-carrying plasmids (pcDNA4/TO wt *cagA* accounts for a 323 kDa molecule) through the cytosol appears to be rather languid, which, in addition, makes them prone to degradation by cytosolic nucleases (Lechardeur et al., 1999, Pollard et al., 2001). Even though cationic lipid/DNA complexes provide some protection from nucleases (Eastman et al., 1997), while apparently being mostly attached to the perinuclear region (Zabner et al., 1995), translocation into the nucleus does not occur immediately but notably at breakdown of the nuclear membrane during mitosis (Mortimer et al., 1999, Tseng et al., 1999). Among other reasons, such as degradation (see 4.1.2.1 and 4.1.2.2), this could be why transfection of *cagA*-$CT_{AA201-1216}$ or wt *cagA*, by comparison, shows less efficacy in terms of protein expression.

(B) In crowded or confining media, such as the cytosol of eukaryotic cells, large biomolecules with a high molecular mass show high effective concentrations depending on the actual concentration in a highly non-linear way. This signifies that increasing the former even further ultimately augments their chemical reactivity (Minton, 2001). This might pertain particularly to overexpressed EGFP-tagged CagA-$CT_{AA201-1216}$ (~140 kDa) and wt CagA (~162 kDa). Due to differences in excluded volumes, the kinetics of macromolecular reactions can be significantly altered (Minton, 2001), resulting in modified activity of DNA polymerases (Zimmerman and Harrison, 1987), altered protein folding processes (van den Berg et al., 1999, van den Berg et al., 2000) and affected protein shapes, hence compromising protein function and causing malfunction, respectively (Homouz et al., 2008). Thus, it cannot be excluded that *cagA*-$CT_{AA201-1216}$ or wt *cagA* might be improperly expressed and might not show true pathophysiological activity.

4.2.2 Aberrant host protein interaction through artificial CagA delivery

It was demonstrated that infection by wt *H. pylori* caused an altered gene expression of 92% of infection-activated eukaryotic host cell genes owing to the *cag*PAI (i.e., 610 of 670 genes). Of this, the expression of 79% (479) of genes was altered by CagA (El-Etr et al., 2004). This suggests that the expression of 21% (131) of genes was not altered by CagA, but rather other *cag*PAI-encoded (virulence) factors. These genes might therefore not be addressed by artificial CagA delivery, as this disregards T4SS and additional about 29 proteins encoded by the *cag*PAI (Tomb et al., 1997, Odenbreit, 2000). Hence, a considerable amount of highly conserved T4SS surface proteins and effector proteins (Fischer et al., 2001, Olbermann et al., 2010) relevant for CagA transfer and probably its activity in the host cell is disregarded. A finding by Wang et al. (2016) indicates that the host cellular stability of CagA depends on the *cag*PAI-encoded T4SS pilus component CagI. Furthermore, the pathophysiological instillation at the inner cell membrane via T4SS (Censini et al., 1996, Akopyants et al., 1998) requires direct contact of the pilus tip attached CagA with β1-integrine or phosphatidylserine at the

outer host cell membrane (Jiménez-Soto et al., 2009, Murata-Kamiya et al., 2010). Here, the T4SS pilus component CagL plays an important role in CagA translocation and its subsequent tyrosine phosphorylation (since mimicking fibronectin in various cellular functions, like the activation of β1-integrine and tyrosine kinases) (Kwok et al., 2007, Tegtmeyer et al., 2010, Conradi et al., 2012), finally causing induction of Erk/c-Myc. This is in line with findings from infection studies in AGS cells by Glowinski et al. (2014) that demonstrate distinct and divergent tyrosine phosphorylation events through T4SS/CagA by wt *H. pylori* strains or just T4SS in CagA-deficient isogenic mutants. Moreover, peptidoglycans are transferred via T4SS causing the activation of NF-κB via the IKK complex and Nod1 (Sokolova et al., 2014). Altogether, this ultimately hypothesizes a rather complex interplay and timing of CagA administration, which might not be accurately provided within the context of expression of plasmidic *cagA* by the host cells themselves. Consequently, the observed characteristics of TCF/LEF transcriptional activity levels might not reflect the true pathophysiologic behavior.

Concerning morphological changes and the interaction with certain pathways, there are reports that transfected *cagA* seems to diverge from T4SS-transferred CagA by *cag*PAI-positive *H. pylori*. Churin et al. (2003) did not show any motility changes due to *cagA* overexpression in AGS cells. A similar observation was made by other groups: Transiently *cagA*-transfected AGS cells showed cell scattering to a much lesser extent (7-25%) (Higashi et al., 2004) compared to those that were really infected by *cag*PAI-positive strains of *H. pylori* (70-80%) (Suzuki et al., 2005). Differences in host cell response regarding CagA delivery could be ascribed *inter alia* to interaction with divergent adapter proteins. No evidence was found for direct interaction between the SH2 adapter protein Grb2 and CagA that was artificially introduced (i.e., transfected) into AGS or COS7 cells, respectively (Churin et al., 2003, Tsutsumi et al., 2003), whereas infection experiments with *cag*PAI-positive *H. pylori* yielded such protein complexes in AGS cells (Mimuro et al., 2002), with Grb2 in particular representing the link towards activation of the MAPK/Erk (K-ras) pathway, thus causing the hummingbird phenotype morphological changes (see 1.2.4). The interaction of CagA with the Gab1 adapter protein, a key coordinator of cellular responses to c-Met (Birchmeier et al., 2003) and relevant for transcriptional activation of β-catenin/TCF/LEF and NF-κB (Suzuki et al., 2009), occurs if plasmidic *cagA* is transfected to AGS cells, but not if CagA is transferred into AGS cells via T4SS (Churin et al., 2003), where, according to Suzuki et al. (2009), the CagA CM^{W} motif directly interacts with c-Met (see 4.2.3).

4.2.3 Host cell polarization affects CagA's signaling activity

CagA's impact on host cellular signaling has been predominantly studied by means of immortalized human gastric adenocarcinoma-derived cell lines, which do not inevitably show a true physiological behavior. The fact that AGS cells in particular do not express functional E-cadherin (see 5.1.1.2.1) makes them more prone to evolve an invasive phenotype by infection (Oliveira et al., 2009) and appears to affect β-catenin turnover. This might also pertain to the other cell lines probed: Although it was shown that MKN45 cells strongly express E-cadherin, this might have a reduced membrane tethering potential since its key Ca^{2+}-binding motif seems to be impaired by conformational alterations due to a 4-amino acid deletion (Oda et al., 1994) (see 5.1.1.2.2). Klijn et al. (2015) demonstrated that the transcritptome of 23132 cells features a deleterious mutation in the *CDH1* gene, which is encoding E-cadherin (see 5.1.1.2.3).

Since AGS cells in particular do not show a polar organization, CagA-membrane interaction may be different from polarized host cells (Murata-Kamiya et al., 2010, Takahashi-Kanemitsu

et al., 2020). At infection of primordial unpolarized AGS cells with wt *H. pylori*, as has been demonstrated by Suzuki et al. (2009), CagA directly targets and presumably co-activates c-Met via CM^{W}, resulting in increased NF-κB signaling, but more importantly, an elevated cytosolic availability of β-catenin. Interestingly, infection-transferred CagA seems to build a complex with E-cadherin and c-Met at the membrane of AGS cells, having been stably transduced by functional E-cadherin. Here, on the contrary, a reduced c-Met phosphorylation was observed (Oliveira et al., 2009).

Although admittedly no direct correlation to (canonical) Wnt/β-catenin signaling can be inferred from this, the different polarization of AGS, MKN45 and 23132 cells on the one hand and 293T cells on the other hand could explain the divergent behavior regarding *cagA* up-titration (see Figure 11, olive bars, vs. Figure 15, C).

Hypothesis	Polarized cells:	[CagA]	⇢	c-Met ⇣	⇢	NF-κB ⇣, cytosolic β-catenin ?
	Unpolarized cells:	CM^{W}	⇢	c-Met ⇡	⇢	NF-κB ⇡, cytosolic β-catenin ⇡

4.2.4 Signaling misdirection because of differential gene expression (DGE) due to manipulations?

The literature includes several examples where pathway activity and gene expression indicate a rather unexpected (i.e., ambivalent) behavior. As (numerical) chromosome instability (CIN) is an essential feature of human cancer (Lengauer et al., 1998), it could be demonstrated that karyotypical heterogeneity increases the fitness of cultured cancer cells after several passages through genomic plasticity (Lukow et al., 2021). According to Ben-David et al. (2018), the clonal heterogeneity of cultured cancer cells is accompanied by differential gene expression (DGE), which is dependent on culture conditions and genetic manipulations; a median of 22% of the genome across 916 cell lines from the Cancer Cell Line Encyclopedia (CCLE) was estimated to be affected by subclonal events. Here, it was hypothesized that cultured cancer cell lines are basically neither clonal nor genetically stable, which causes variability relating to drug response. A potentially instable karyotype as well as subclonal events can thus be expected for all gastric cancer cell lines utilized in this work, as each evinces aneuploidy (see 2.3.1). Although not of cancerous provenance, this likewise pertains to 293T cells (Lilyestrom et al., 2006, Lin et al., 2014).

The transfer of foreign DNA appears to further increase the genetic instability (i.e., CIN) of the utilized cell lines and effectively entail DGE (Gao et al., 2007, Habermann et al., 2011). According to Bardwell (1989), foreign DNA can engender mutations of homologous host cellular chromatin and select subpopulations of recipient cells. Very interestingly, while only a relatively small amount of DGE was ascribed to recombinant DNA itself, Jacobsen et al. (2009) recognized off-target effects through both lipofection (particularly by Lipofectamine® 2000; see 2.7.2) and the empty vector backbone that were able to cause substantial DGE with respect to cellular metabolic processes and translation, which was analogous to a viral infection and intrinsic cellular immune responses. It could be demonstrated that replication stress (in terms of DNA damage response) or the stable transfection of 293 cells with an empty pcDNA3.1 vector can drive CIN (Burrell et al., 2013, Stepanenko and Dmitrenko, 2015). Ultimately, by causing DGE, the shift in karyotypic context and heterogeneity due to drug treatment also affects the activity of multiple signaling pathways (Stevens et al., 2014). Hence, it cannot be excluded that the latter also applied to

cell lines that were stably transfected with reporter plasmids some time (i.e., passages or mitoses, to be exact) before the actual experiments (see in particular 3.2.1.2), which would allow subclonal events or selection of specific clones.

In Addition, CagA as such seems to promote and presumably aim for CIN in host cells, aggravating the eventual manipulatory impact on genetic stability and making DGE even more likely. It could be demonstrated for polarized MKN28 cells (Guo et al., 2014) that CagA can cause (microtubule-based) spindle malformation by inhibiting PAR1 (Umeda et al., 2009), with increased mis-segregation of chromosomes due to a merotelic kinetochore orientation triggering CIN in stable, near-diploid cells (Thompson and Compton, 2008).

In conclusion, transferring *cagA* to cancer cell lines by employing (stable) transfection or transduction could have a sustained impact on the transcriptome (i.e., cause DGE). Concerning the experimental approaches in this work, the considerations described above reveal certain elements of uncertainty, as (i) cell lines potentially have instable karyotypes, according to which subclonal events and DGE must be considered, which is (ii) presumably aggravated due to (plain) manipulations such as (stable) transfection, transduction or infection, and (iii) hypothetically further potentiated through (the expression of) *cagA*, ultimately (iv) causing unpredictably altered, ambivalent signaling activity and therefore inconsistent results. This may provide an explanation why particularly MKN45 cells exhibited comparatively unusual behavior during transduction with *cagA* (see 3.2.1.2) that could not be observed regarding transfection (see 3.2.1.1).

4.3 Prospect: Ambivalence through interaction partners?

Assuming that observations are not exclusively attributable to an unfavorable conception and approach (see 4.1.1.1 and 4.2), this chapter will further elucidate the ambivalent impact of CagA on (canonical) Wnt/β-catenin signaling and hence evolve a possible prospect. This ambivalence may eventually also be due to specific (direct) interaction partners which have not yet been investigated in detail with respect to CagA, although this by no means excludes the aforementioned, of course. The control of the destruction complex (DC) is still elusive and it is presumed that CagA rather circumvents the complex coordination of (canonical) Wnt/β-catenin signaling by simply liberating β-catenin from membranous repositories (of primarily polarized host cells), assuming the DC is incapable of promptly degrading it (El-Etr et al., 2004, Suzuki et al., 2005, Murata-Kamiya et al., 2007, Kurashima et al., 2008). However, the conditions seem to be in fact more complex, as (i) altered (canonical) Wnt/β-catenin signaling activity is also reported from *a priori* unpolarized cell lines, basically not allowing for membranous β-catenin liberation due to a lack of functional E-cadherin (Franco et al., 2005, Suzuki et al., 2009), since (ii) CagA-competent wt *H. pylori*-infected unpolarized cell lines did not show considerable alterations of absolute cytosolic β-catenin amounts (see 3.1.3) and because (iii) if not affected by CagA itself, the activity of components of (canonical) Wnt/β-catenin signaling (viz. frizzled, dishevelled and particularly DC) would, on principle, unabatedly continue working (without coincidental inhibition by means of Wnt3a). Thus, additionally accruing cytosolic β-catenin would rapidly and effectively be degraded by the still active DC (Stamos and Weis, 2013). Furthermore, in the long term, concerning the promotion of carcinogenesis, a sustained impact on (canonical) Wnt/β-catenin signaling needs to be considered as a precondition. Therefore, rather than the transitory liberation of β-catenin from repositories such as the plasma membrane, more profound and potentially long-lasting alterations must be assumed.

Since the bustling CagA appears to be studded with functional domains that evidently (dose-dependently) interact with a variety of crucial signaling pathways, these interfaces appear to be substantial for impinging upon host cells. Type C EPIYA, for instance, directly activates TAK1 (TGFβ activated kinase 1) at the plasma membrane (host cell polarization independently), which is relevant for the activation of NF-κB signaling (Lamb et al., 2009, Lamb et al., 2013, Papadakos et al., 2013), as it is tightly cross-linked with (canonical) Wnt/β-catenin signaling (Deng et al., 2002, Deng et al., 2004, Kavitha et al., 2013, Ma and Hottiger, 2016). Apart from EPIYA and CM motifs, CagA features additional largely conserved functional domains in its amino-terminal part by means of the tandem WW domains (see 1.2.4), which proposes a tight interaction with further very effective factors. Yet it should be mentioned that Hayashi et al. (2012) doubt the functionality of CagA's WW domains due to inconclusive structural data (showing no short helix and disordered segment), although they investigated CagA from another *H. pylori* strain (26695), the primary structure of which differs from that of strain G27, which was studied in this work (and that of strain NTC 11637, see 1.2.4 or Tsang et al. (2010), respectively; strain 26695: WW1 domain starting at AA 125 rather than AA 120, K instead of N at position 133, corresponding to position 128). However, Ingham et al. (2005) identified a total of 148 binding partners of human WW domains that are at least related to transcription, RNA processing and cytoskeletal regulation. Accordingly, additional routes need to be taken into consideration regarding CagA's impact on Wnt/β-catenin signaling. For this, regulation of the DC, control of β-catenin nuclear import and the impact on the TCF/LEF activity level could provide auspicious perspectives.

4.3.1 WW/DDX3: Control of ß-catenin nuclear import and regulation of the destruction complex (DC)

The DEAD box (Asp-Glu-Ala-Asp) RNA helicase DDX3 (Park et al., 1998) interacts with abovementioned TAK1 (Sokolova et al., 2018) and thus potentially indirectly with type C EPIYA motifs at the C-terminal part of CagA. But more intriguingly, DDX3 features the PPxY motif and therefore is recognized by WW domains (Ingham et al., 2005), which suggests a direct interaction with N-terminal CagA. The impact of DDX3 on (canonical) Wnt/β-catenin signaling activity at least emanates from two characteristics that are virtually mutually exclusive: The control of the β-catenin nuclear import and the regulation of DC and therefore CagA destruction by means of CK1 isoforms. Bol et al. (2015) consider a direct involvement of DDX3 in β-catenin nuclear shuttling. According to Botlagunta et al. (2008), DDX3 relocates membranous β-catenin to the cytosol and nucleus, diminishes E-cadherin expression at a transcriptional level and can cause EMT in breast cancer cells. Moreover, for the medulloblastoma, Pugh et al. (2012) showed that the mutation of DDX3's helicase function (i.e., its RNA-binding domain) increases TCF transcriptional activity through ubiquitination-resistant β-catenin. It was demonstrated that DDX3 acts as both a tumor suppressor and tumor promoter in a tissue-specific way and that, by contrast, the inhibition of DDX3 negatively affects (canonical) Wnt/β-catenin signaling activity (Bol et al., 2015, Heerma van Voss, 2015). In line with this, according to Dolde et al. (2018), the inhibition of DDX3's helicase capability promotes its kinase activity that activates CK1 isoforms in a "moonlighting" way (Cruciat et al., 2013). CK1 isoforms are relevant for β-catenin destruction in two respects as CK1α is indispensable for β-catenin's priming phosphorylation at Ser45 (Liu et al., 2002, Sinnberg et al., 2010, Thorne et al., 2010) and CK1ε phosphorylates APC, which promotes β-catenin ubiquitination through an increased affinity for β-catenin (Rubinfeld et al., 2001, Ha et al., 2004).

In addition, DDX3 is relevant for antiviral innate immunity by activating several steps between RIG-I-like receptors (RLRs) and interferon beta (IFN-β) (Schroder, 2011, Oshiumi et al., 2016), and is therefore selectively targeted and attenuated by different viruses (Schroder et al., 2008, Wang et al., 2009). It is merely a matter of conjecture, however, with regard to a longer-term infection of the gastric mucosa, it is plausible that *H. pylori* might act in like manner and deploy CagA in order to affect DDX3 (i.e., its helicase function). But according to the logic of this project, nevertheless, simple premises are rather inappropriate as the aforementioned could also signify additional conceptional limitations (see 4.2): Cultured host cells might face lentiviral gene transfer or an unrecognized virus infection with a reduced DDX3 availability (Hempel et al., 2013, Heerma van Voss et al., 2017, Uphoff et al., 2019), which should then also apply to infection with *H. pylori* or exposure to CagA and further increase the uncertainty regarding impact on (canonical) Wnt/β-catenin signaling.

4.3.2 WW/RUNX: Direct interaction with ß-catenin/TCF

Runt-related transcription factors (RUNX) also show an ambivalent effect on (canonical) Wnt/β-catenin signaling and functionally overlap with DDX3 in several aspects. RUNX1 and RUNX3 likewise feature conserved PPxY motifs (Ito, 2004, Tsang et al., 2010) but were demonstrated to directly interact with CagA's WW domains (owing to specific recognition of their PPxY motifs, inducing CagA's proteasome-mediated degradation) (Tsang et al., 2010). Both RUNX1 and RUNX3 impact (canonical) Wnt/β-catenin transcriptional activity through the direct interaction with β-catenin/TCF, causing either an inhibition or activation of (canonical) Wnt/β-catenin signaling (Ito et al., 2008, Ito et al., 2011, Ju et al., 2014, Medina et al., 2016, Li et al., 2019, Sweeney et al., 2020). RUNX3's function in leukocytes seems essential concerning protection against pathogens and inflammation (Brenner et al., 2004, Cheroutre et al., 2011). The RUNX cluster is regulated by cell cycle and posttranslational modifications and, aside from the mandatory RUNX-cofactor CBFβ (core-binding factor subunit beta), a further cofactor is assumed (Ju et al., 2014).

Context-dependently, RUNXs can act as oncogenes (Ito et al., 2015), which was shown for RUNX3 in an *H. pylori*-mediated c-Src tyrosine phosphorylation-dependent way (Cinghu et al., 2012). Although Lotem et al. (2015) could clearly refute the "RUNX3 tumor suppressor paradigm", especially as it is typically not expressed in the gastric epithelium due to its markedly hypermethylated P1 promoter (Kurklu et al., 2015), the RUNX cluster seems to compensate for the reduced availability of particular members by up-regulation of others (Ito et al., 2015, Morita et al., 2017). As can be deduced from Figure 25, which shows relative RNA expression levels referred to the mean expression level of several HKG (see 5.1.2.3), the utilized gastric cancer cell lines (AGS, MKN45 and 23132) admittedly evince very minute to no expression of RUNX2 and RUNX3. In comparison, this is clearly overcome by RUNX1, most distinctly in AGS cells, while CBFβ is reliably expressed in each case, which is why the direct interaction between RUNX1 and N-terminal CagA seems plausible and must therefore be considered. This possibly affects (canonical) Wnt/β-catenin signaling.

4.3.3 EPIYA/TAK1/NLK: Noncanonical interaction with TCF

Owing to the above mentioned interaction between Type C EPIYA and TAK1 (see 4.3), the atypical MAP kinase NLK (Nemo-like kinase), as part of the noncanonical Wnt pathway, becomes activated, which directly inhibits TCF transcriptional activity downstream of β-catenin by means of TCF phosphorylation in a (polarized) 293 cell line-based pTOPflash

reporter gene assay (Ishitani et al., 1999, Ishitani et al., 2003). Thus, while entirely bypassing the canonical route, Type C EPIYA motifs exert a negative impact on the Wnt signaling activity of polarized cells (see 4.2.3) by using TAB2 (TAK1 binding protein 2) as the scaffolding protein, linking TAK1 and NLK (Li et al., 2010a). Interestingly, according to data from El-Etr et al. (2004), at early infection stages (8 h p.i.) of E-cadherin-competent (polarized) T84 cells with wt *H. pylori*, TAB2 intermittently becomes massively down-regulated, probably in order to compromise the EPIYA/TAK1/TAB2/NLK-induced inhibition of TCF activity.

4.4 Conclusions

In general, this project essentially suffered from three issues, which meant working was very much occupied by trouble shooting: (i) the difficult generation of *cagA* constructs, requiring elaborate cloning approaches (see 2.4), (ii) the context-dependent interference with the (constitutive) expression of *Renilla* luciferase (i.e., impairment of transfection control or expression reference), and (iii) the unpredictability (i.e., ambivalence) of TCF/LEF transcriptional responses to CagA, or more specifically, the unexpected observation of the inhibition of TCF/LEF transcriptional activity through wt CagA. As mentioned above (see 1.2.4), regarding the increment in (canonical) Wnt/β-catenin signaling activity levels, there is comprehensive evidence from studies, predominantly based on the transfection of recombinant DNA to human (gastric) cancer cell lines (El-Etr et al., 2004, Franco et al., 2005, Murata-Kamiya et al., 2007, Kurashima et al., 2008, Suzuki et al., 2009). However, the observed inhibition of TCF/LEF transcriptional activity in response to wt CagA that can be deduced from wt *H. pylori* infection experiments (see 3.1.1) as well as from transfection (see 3.2.1.1 and 3.2.2) or transduction (see 3.2.1.2) of *cagA*-expressing constructs of lentivirus necessitates a more detailed discussion.

In conclusion, the following can be stated:

Wt CagA is capable of reducing Wnt/β-catenin signaling activity through infection by *H. pylori*. In terms of transfection and transduction, the C-terminal 83% of CagA (AA 201-1216) behaves like wt CagA, whereas the N-terminal 17% of CagA (AA 1-200) differs in two respects concerning the host cell: (i) intracellular localization and (ii) dose-dependent impact on (canonical) Wnt/β-catenin signaling activity. While (i) CagA's N-terminal AA 1-200 distribute diffusely in the cytoplasm and nucleoplasm of functional E-cadherin-deficient host cells, CagA's C-terminal AA 201-1216 display affinity for the plasma membrane, comparable to wt CagA. In (ii) intermediate to higher concentrations in host cells, CagA's N-terminal AA 1-200 tend to increase TCF/LEF transcriptional activity. This is completely opposite to CagA's C-terminal AA 201-1216, which clearly cause its inhibition comparable to wt CagA and consistent with infection by CagA-proficient *H. pylori*. Furthermore, the higher the intrinsic (canonical) Wnt/β-catenin activity of the host cells, the more pronounced is the impact of CagA.

Comparison of the data with a comprehensive literature research also indicates that the polarization status of host cells predetermines CagA's scope of interaction. Moreover, the introduction of CagA by infection (i.e., T4SS-mediated) on the one hand, and transfection or transduction on the other, implies a divergent interaction between CagA and host cellular factors.

5 Appendix

5.1 Characterization of the cell lines

5.1.1 Mutation analysis

The comprehensive search for information on cell line-specific mutational data related to (canonical) Wnt/β-catenin signaling by means of a literature research is very time-consuming and rather dissatisfactory. Therefore, additional publicly available web-service databases for genomic studies were systematically scoured for relevant mutations in the cell lines used in this work, focusing on components that are crucial in (canonical) Wnt/β-catenin signaling, in particular targets of (canonical) Wnt/β-catenin signaling and certain other important gastric cancer related factors such as k-ras (*KRAS*), p53 (*TP53*) or E-cadherin (*CDH1*). Although some of them are typically not considered canonical, with respect to Wnt and frizzled proteins, all families were considered because most of them seem to be able to induce Wnt/β-catenin signaling in a context-dependent manner (MacDonald and He, 2012, Niehrs, 2012, Nusse and Clevers, 2017). While several databases address different cancer cell lines (namely AGS, MKN45, 23132 and NCI-N87 cells), obtaining mutational information on 293T cells has been more laborious (see below).

In general, and because this was most practical, mutation data were referred to the genome reference consortium human build 37 patch release 13 (GRCh37.p13). Whenever possible, mutation data were cross-checked with the web-services of the European Molecular Biology Laboratory (2021) genome browser (Ensembl), the Catalogue Of Somatic Mutations In Cancer (2021) (COSMIC), the National Center for Biotechnology Information (NCBI) concerning the Single Nucleotide Polymorphism Database (2020) (dbSNP) as well as the public archive of interpretations of clinically relevant variants (Landrum et al., 2014, Landrum et al., 2020) (ClinVar) and, furthermore, the Genome Aggregation Database (2018) (gnomAD). By this means, the findings were revised with regard to their relevance and potential adverse functional or clinical impact. The most common mutation-type was the single nucleotide variation (SNV) followed by short insertions or deletions (indels). Intronic localizations and synonymous (silent) substitutions have been disregarded. Therefore, relevant translocations were not obtained in all cancer cell lines investigated. For example, AGS cells show a duplication-like translocation in *TP53* (breakpoint 1 at 17:7582851+, breakpoint 2 at 17:7585042-) that is entirely intronic. In accordance with Lek et al. (2016) and Ghandi et al. (2019), an allelic frequency (AF) filter of 10^{-5} was applied to SNVs (AF predominantly attained from gnomAD v2.1.1) to exclude germline-like variants and emphasize potentially deleterious variants (which was causing no conflict with findings from the literature). Where corresponding records were accessible via web-services, prediction of the functional impact of non-synonymous (missense) substitutions was predominantly based on the composite and consequently superior measure REVEL, or at least on FATHMM or SIFT (see 5.1.1.1). Although it was not always commented on, frame shift mutations were basically considered to be deleterious. The mutation data were cross-checked with the literature concerning observations in gastric cancer in general as well as in the particular cell line (see Table 21, A to E, column “Literature / Comment”). For all cell lines, irrelevant mutation data were obtained regarding *WNT2*, *WNT2B*, *WNT3*, *WNT3B*, *WNT4*, *WNT5A*, *WNT6*, *WNT7A*, *WNT7B*, *WNT9A*, *WNT10A*, *LRP5*,

FZD3, *FZD4*, *DVL1*, *CSNK1A*, *CSNK1D*, *GSK3B*, *TCF4* (syn. *TCF7L2*), *TCF10*, *LEF1 (syn. TCF7L3)*, *TAK1* (syn. *MAP3K7*), *CCND1*, *RUNX1*, *RUNX2*, *RUNX3*, *CBFB*. This likewise pertains to *ACTB*, *GAPDH*, *MYC*, *IPO8*, and *PUM1* (see 5.1.2.3).

While Table 21 provides a detailed information, Figure 21 gives a condensed overview of the compiled mutation data, taking into account the observed or predicted pathogenicity. Although the gastric cancer cell line NCI-N87 was not used, at least in the experiments presented in this work, it is included as an internal reference (see 5.1.2.3).

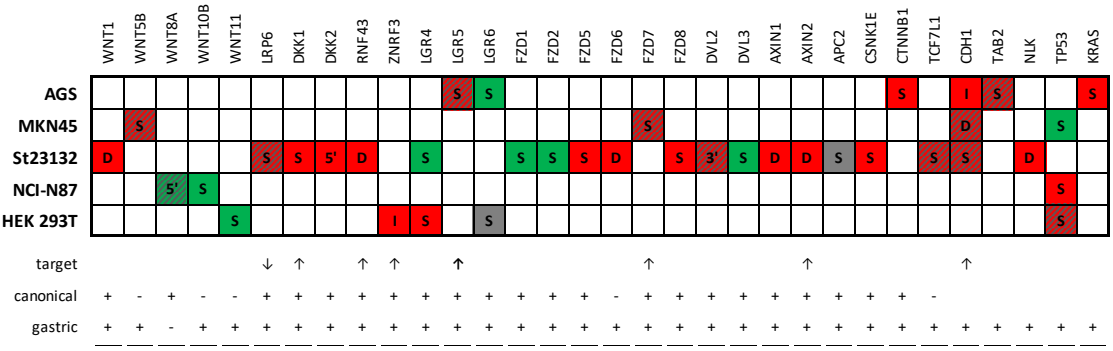

Figure 21: Compressed outline on cell lines mutational data.
AGS, MKN45, 23132, NCI-N87 and (HEK) 293T cell line-specific synopsis on mutated components crucial in Wnt/β-catenin signaling, targets of Wnt/β-catenin signaling and other important gastric cancer related factors, basically disregarding intronic localizations and synonymous (silent) substitutions; mutated genes are displayed in HGNC notation (*TCF7L1* is synonymous to *TCF3*); target of Wnt/β-catenin signaling (see 5.1.2.1), *bold up arrow*: up-regulation and positive feedback, *slender up arrow*: up-regulation and negative feedback, *down arrow*: down-regulation; canonical according to (Niehrs, 2012) and (MacDonald and He, 2012); gastric expression according to Evolutionary Bioinformatics group (2022) database (Bgee); *red boxes*: frame shift mutations or somatic SNV predicted deleterious (REVEL) with known AF, *red/grey hatched boxes*: somatic SNV predicted deleterious (REVEL) and AF higher than cut of (*FZD7* at MKN45) or somatic SNV predicted deleterious (just FATHMM) and AF unknown, *grey boxes*: somatic SNV with unknown prediction of functional impact and unknown AF, *green/grey hatched boxes*: somatic SNV predicted innocuous (just FATHMM) and known AF, *green boxes*: somatic SNV predicted innocuous (REVEL) with known AF; *D-tag*: deletion, *I-tag*: insertion, *S-tag*: SNV, *3'-tag*: SNV at 3'-UTR, *5'-tag*: SNV at 5'-UTR; abbreviations: AF = allelic frequency.

5.1.1.1 Predicting the functional impact of single nucleotide variations

REVEL (Rare Exome Variant Ensembl Learner): Prediction of the pathogenicity of missense variants by means of a composite of several individual tools (FATHMM, GERP, LRT, MutationAssessor, MutationTaster, MutPred, phastCons, phyloP, Poly-Phen, PROVEAN, SIFT, SiPhy and VEST); training was performed by comparing recently discovered rare neutral and pathogenic missense variants (while omitting those priorly used for training of individual tools), therefore showing best discriminating performance (Ioannidis et al., 2016).
Range 0-1, deleterious if > 0.5 (probability 75.4%; derived from Ensembl)

FATHMM (Functional Analysis Through Hidden Markov Models): Protein-related means for retrieving information on pathogenicity without background information on the protein; multiple sequence alignment by an iterative search procedure and species-specific so-called pathogenicity weights by comparison with the frequencies of functionally neutral and disease associated amino acids in conserved domains of the protein (Shihab et al., 2013).
Range 0-1, deleterious if ≥ 0.7 (derived from COSMIC)

SIFT (Sorting Intolerant From Tolerant): Estimating the probability of tolerance of an amino acid according to most tolerated amino acids at each position after alignment of related proteins in respect of the impact on the protein function (Ng and Henikoff, 2003).
Range 0-1, deleterious if < 0.05 (derived from Ensembl)

5.1.1.2 Gastric cancer cell lines

Mutation data on gastric cancer cell lines (AGS, MKN45, 23132 and NCI-N87) were primarily retrieved from the Cancer Cell Line Encyclopedia (2022) (CCLE) or, to be more precise, from the related Cancer Dependency Map (2021) (DepMap). This genomic studies database provides a cell line-specific tabulation of mutated genes and translocations. To this end, according to Ghandi et al. (2019), a variant calling pipeline and filtering of germline variants from sequencing data of whole exome sequencing, whole genome sequencing, RNA-seq data and other has been performed to identify mutations such as somatic SNVs and short indels; gene fusions have been analyzed from RNA-seq data. In consideration of Ben-David et al. (2018), the COSMIC cell lines project was used in an analogous manner, which combines data from full exome sequencing and molecular profiling of human cancer cell lines with COSMICs largely hand curated information on somatic mutations derived from the literature (Tate et al., 2019).

As mentioned above (see 5.1.1), no deleterious translocations (in terms of duplication- and deletion-like exonic mutations or frame shifts) were found in any of the gastric cancer cell lines investigated. If not already indicated by the CCLE results, somatic SNVs were cross-checked for reference SNPs (by dbSNP). There were some minor differences between the CCLE and COSMIC data, but on the whole the somatic SNV data were consistent and complementary.

5.1.1.2.1 AGS cells

AGS cells do not show many mutations at the genes that are predominantly crucial for (canonical) Wnt/β-catenin signaling (see Figure 21 and Table 21). In the first place, according to Caca et al. (1999), Asciutti et al. (2011) and Chang et al. (2016), the *CTNNB1* gene (β-catenin) has a pathologic somatic SNV at codon 34, which means activation of (canonical) Wnt/β-catenin signaling through constitutive TCF/LEF transcriptional activity, since mutated β-catenin is resistant to regulation by APC and GSK3β (Caca et al., 1999). The driver mutation of AGS cells is a missense substitution in the *KRAS* gene (k-ras), as described by Lee et al. (1995), Hotz et al. (2012) and Nemtsova et al. (2020). Comprehensibly, both SNVs show pathologic REVEL predictions. Caca et al. (1999) and Oliveira et al. (2009) state that a frameshift insertion at the *CDH1* gene entails dysfunctional E-cadherin expression. This is supported by the National Institutes of Health (NIH) based Clinical Genome Resource (2022) (ClinGen), as this results in a premature stop codon, causing a missing or truncated protein. According to CCLE and COSMIC, *LGR5* (Lgr5; leucine-rich repeat-containing G-protein coupled receptor 5) and *TAB2* (TGFβ activated kinase 1/MAP3K7 binding protein 2, syn. *MAP3K7IP2*) have a somatic SNV each, but in both cases, no reference SNP and no AF can be drawn from dbSNP or gnomAD. Their functional impact is predicted just by FATHMM, which proves to be deleterious. *LGR6* shows a somatic SNV with different ancestral allels at CCLE and COSMIC (c.2365G>C vs. c.2365G>T, the former is known to gnomAD and dpSNP). Since both cause an identical protein change (p.V789L), an innocuous REVEL prediction applies anyway.

SNV: *CTNNB1*, *LGR5*, *LGR6*, *TAB2, KRAS*
Other: *CDH1* (insertion)

5.1.1.2.2 MKN45 cells

Because the somatic SNV in *TP53* is predicted to be innocuous (see Figure 21 and Table 21), MKN45 cells express wild type p53 (Yokozaki, 2000, Mashima et al., 2005). However, homozygous deletion of the tumor suppressor gene *CDKN2A* (cyclin-dependent kinase inhibitor 2A) causes a depletion of the tumor suppressor p14ARF, which therefore does not stabilize the tumor suppressor p53 (Iida et al., 2000). Concerning *CDH1*, CCLE points to a deletion of 18 residues (GCTCTTCCAGGTATATCC) at 3' of Exon 6, the last eight residues of which are intronic, resulting in a splice donor variant and loss of four AAs (p.AlaLeuProGly275del). This is consistent with Oda et al. (1994), who describe a deletion of four amino acids between two key Ca^{2+}-binding motifs of the first cadherin domain, which presumably causes reduced cell-cell-adhesion. In accordance with both CCLE and COSMIC, *WNT5B* (Wnt 5B) features a somatic SNV, but neither a reference SNP (dbSNP) nor its AF (gnomAD) can be obtained, so prediction of its adverse functional effects is based solely on FATHMM. Although *FZD7* has a somatic SNV according to CCLE, its AF (4.03×10^{-4}) does not meet the cut-off criteria. However, because its functional impact is predicted deleterious (REVEL) and MKN45 cells show a strong expression of functional frizzled class receptor 7 (Flanagan et al., 2019), which is the predominant receptor for Wnt/β-catenin signaling in gastric cancer cells (Kirikoshi et al., 2001), this mutation is also included.

SNV: *WNT5B*, *FZD7, TP53*
Other: *CDH1* (deletion)

5.1.1.2.3 23132 cells

Due to microsatellite instability (MSI) (Ghandi et al., 2019), 23132 cells show several mutations at proteins involved in Wnt/β-catenin signaling (see Figure 21 and Table 21): *WNT1*, *FZD6*, *AXIN1* (axin-1), *AXIN2* (axin-related protein), *NLK* (Nemo-like kinase) and *RNF43* (ring finger protein 43). Concerning these short indels, the COSMIC genomic locations differ by 4 to 7 bp from those of CCLE despite identical reference transcripts. This is due to the short repetitive DNA sequences where deletions or insertions of single residues are referenced to either their 5' or 3' end. As recommended by den Dunnen et al. (2016), the most 3'-located position was considered here. *RNF43* shows another short deletion distant from a microsatellite, according to COSMIC. *FZD5*, *FZD8* and *DKK1* (dickkopf-related protein 1) show somatic SNVs, which REVEL predicts as deleterious. *LRP6* (low-density lipoprotein receptor-related protein 6) has a somatic SNV that FATHMM predicts as pathogenic; there are no records concerning its AF. According to CCLE, *DKK2* features an out of frame de novo start at 5'-UTR, which is predicted to be damaging. The somatic SNV at *CDH1* is localized in its extracellular part and causes an AA change in the so called "cadherin domain". In line with data from Klijn et al. (2015) (cf. supplementary data 3), FATHMM predicts it to be deleterious, but no records concerning its AF could be found. Somatic SNVs at *FZD1*, *FZD2*, *DVL3* (dishevelled segment polarity protein 3) and *LGR4* are predicted innocuous (REVEL). Two somatic SNVs at *DVL2* and *TCF3* (transcription factor 3, syn. *TCF7L1*), derived from COSMIC could not be comprehensively cross-checked, and therefore their deleterious functional impacts are predicted only according to FATHMM. In the case of *DVL2*, AF could not be obtained at all, presumably because it is located 3'-UTR, and in the case of *TCF3* (syn. *TCF7L1*), AF was only obtained from ExAC. The estimation of AF of a deleterious somatic SNV at *CSNK1E* (CK1ε, casein kinase 1ε) was obtained from TOPMed. *APC2* (adenomatous polyposis coli like) features two somatic SNVs according to CCLE, that have no

equivalents at COSMIC, dpSNP or gnomAD. Thus, there is no information about their AF nor any prediction about their functional impacts.

SNV: *LRP6*, *LGR4*, *DKK1*, *FZD1*, *FZD2*, *FZD5*, *FZD8*, *DVL2* (3'-UTR), *DVL3*, *CSNK1E*, APC2, *TCF3* (syn. *TCF7L1*), *CDH1*
Microsatellites: *WNT1* (deletion), *FZD6* (deletion), *RNF43* (deletion), *AXIN1* (deletion), *AXIN2* (deletion), *NLK* (deletion)
Other: *RNF43* (deletion), *DKK2* (out of frame de-novo-start at 5'-UTR)

5.1.1.2.4 NCI-N87 cells

As mentioned above (see 5.1.1), NCI-N87 cells were not used in the experiments presented in this work. However, since they are used to compare different cell lines (see 5.1.2), their relevant mutational data in respect of Wnt/β-catenin signaling will be briefly depicted. As shown in Figure 21 and Table 21, NCI-N87 have three somatic SNVs. The one located at the 5'-UTR of *WNT8A* as well as the one located at *WNT10B* are both predicted to be innocuous by FATHMM and REVEL. The third SNV, located at *TP53*, seems harmful according to REVEL. Note that WNT8A does not show gastric expression according to the database of the Evolutionary Bioinformatics group (2022) (Bgee).

SNV: *WNT8A*, *WNT10B*, *TP53*
Other: none

5.1.1.3 293T cells

293T call are neither of gastric origin nor cancer cells. Therefore, they are not taken account of in comprehensive cancer cell line databases like CCLE or COSMIC. Instead, mutational data on the 293T cell line were obtained from Lin et al. (2014) (cf. supplementary data 2) and from the related genomic study database HEK293 Multigenome Variation Viewer (2014), which is based on whole genome sequencing and provides a search tool for mutated genes. Since this web-service uses the NCBI36/hg18 reference genome, the coordinate mapping was translated to GRCh37.p13 using Ensembl (more precisely by BLAST against reference transcripts). As outlined above (see 5.1.1), mutation data were then cross-checked using Ensembl, COSMIC, dpSNP, ClinVar as well as gnomAD to get a prediction of the functional impact and clinical significance. Again, an AF filter of 10^{-5} for SNVs and indels was applied. According to Figure 21 and Table 21 somatic SNVs were obtained with comprehensive records for *WNT11* (innocuous) and *LGR4* (deleterious). *LGR6* shows an exonic SNV that causes a protein change for which there are no equivalents in other databases, hence no AF or prediction of its functional impact are available. *TP53* features a harmful missense substitution at the E4F1 interacting domain, which has a negative impact on DNA binding by p53 (Lin et al., 2014). This is supported by FATHMM prediction, but there are no reports concerning its AF. 293T cells show an insertion that causes a frameshift in *ZNRF3* (zinc and ring finger 3), which could not be cross-checked via COSMIC or Ensembl.

SNV: *WNT11*, *LGR4*, *LGR6*, *TP53*
Other: *ZNRF3* (insertion)

A: AGS

Gene		Protein	Mutation								COSMIC	dpSNP	gnomAD	Functional impact				ClinVar	Literature / Comment
HGNC	Enssembl		class	type	reference allel	ancestral allel	DNA change	prot. change	genomic coordinates	transcript	Genomic Mutation ID	reference SNP	AF (total)	REVEL	FATHMM	SIFT	DepMap / CCLE	clin. signif. (clinic)	
LGR5	ENSG00000139292	Leucine-rich repeat-containing G-protein coupled receptor 5	substitution - missense	SNV	A	C	c.1273A>C	p.Ile425Leu	12:71971769-71971769	ENST00000266674.5	COSV57003501	-	-	-	0.83				comment: exon 14 (ENSE00003660050);
LGR6	ENSG00000133067	Leucine-rich repeat-containing G-protein coupled receptor 6	substitution - missense	SNV	G	C	c.2365G>C	p.Val789Leu	1:202287796-202287796	ENST00000367278.3	-	rs199906695	3.19E-05	0.49	-	0		not reported	
			substitution - missense	SNV	G	T	c.2365G>T	p.Val789Leu	1:202287796-202287796	ENST00000367278.3	COSV55153065	-	-	-	0.97				comment: codon: V [GTG] > L [TTG];
CTNNB1	ENSG00000168036	β-catenin	substitution - missense	SNV	G	A	c.101G>A	p.Gly34Glu	3:41266104-41266104	ENST00000349496.5	COSV62688267	rs28931589	3.98E-06	0.59	0.98	0		(likely) pathogenic (adenocarcinoma of stomach and others)	
jhjhjhhjhhghgbbvbvbCDH1	ENSG00000039068	E-cadherin (cadherin 1)	insertion – frameshift	INS	_	C	c.1733dup	p.Gly579Argfs*9	16:68855925-68855926	ENST00000261769.5	COSV55729476	rs1555516821	-	-	-			pathogenic (hereditary diffuse gastric cancer)	cell line: Caca et al. (1999) & Oliveira et al. (2009): no functional E-cadherin expression; / gastric cancer: Becker et al. (1994), Guilford et al. (1998), Nemtsova et al. (2020); / comment: clinicalgenome.org: p.G579fs variant is predicted to result in a premature stop codon that leads to a truncated or absent protein, meets criteria to be classified as pathogenic (by curation expert panel);
TAB2	ENSG00000055208	TGF-beta activated kinase 1/MAP3K7 binding protein 2	substitution - missense	SNV	T	G	c.450T>G	p.Asn150Lys	6:149699501-149699501	ENST00000367456.1	COSV53851496	-	-	-	0.92				comment: exon 4 (ENSE00002151893);
KRAS	ENSG00000133703	k-ras	substitution - missense	SNV	C	T	c.35G>A	p.Gly12Asp	12:25398284-25398284	ENST00000256078.4	COSV55497369	rs121913529	4.01E-06	0.88	0.98	0	pathogenic (neoplasm of stomach and others)		cell line: Hotz et al. (2012): relevance unclear; / gastric cancer: Lee et al. (1995), Nemtsova et al. (2020);

B: MKN45

Gene		Protein	Mutation								COSMIC	dpSNP	gnomAD	Functional impact				ClinVar	Literature / Comment
HGNC	Enssembl		class	type	reference allel	ancestral allel	DNA change	prot. change	genomic coordinates	transcript	Genomic Mutation ID	reference SNP	AF (total)	REVEL	FATHMM	SIFT	DepMap / CCLE	clin. signif. (clinic)	lit. (cell line)
WNT5B	ENSG00000111186	Wnt 5B	substitution - missense	SNV	C	T	c.368C>T	p.Ala123Val	12:1748889-1748889	ENST00000397196.2	COSV60198062	-	-	-	0.97				comment: exon 4 (ENSE00000712187);
FZD7	ENSG00000155760	frizzled class receptor 7	substitution - missense	SNV	A	G	c.929A>G	p.Glu310Gly	2:202900299-202900299	ENST00000286201.1	COSV53808087	rs201306518	4.03E-04	0.55	0.98	1		not reported (none)	gastric cancer: Kirikoshi et al. (2001) up-regulation of FZD7 in human gastric cancer might play key roles in carcinogenesis through activation of the WNT/β-catenin signaling; Flanagan et al. (2019): strong expression of functional FZD7 in MKN45 cells;
CDH1	ENSG00000039068	E-cadherin (cadherin 1)	deletion - splice donor variant	DEL	GCTCTT CCAGGT ATATCC	_	c.1014_1023+8Cdel	p.AlaLeuProGly275del	16:68844235-68844252	ENST00000261769.5	COSV55729912	-	-	-	-		damaging		cell line: Oda et al. (1994) 4 amino acid deletion between two Ca^{2+} binding motifs of first cadherin domain, probably reduced cell-cell-adhesion; Yokozaki (2000): promotor mutation of E-cadherin; / gastric cancer: Becker et al. (1994), Guilford et al. (1998), Nemtsova et al. (2020); / comment: deletion 3' of exon 6 (ENSE00003478164) going over into intron (8 residues): 5'-Exon6-GCT.CTT.CCA.G|GT.ATA.TCC-Intron-3';
TP53	ENSG00000141510	p53	substitution - missense	SNV	C	T	c.328C>T	p.Arg110Cys	17:7579359-7579359	ENST00000269305.4	COSV52684761	rs587781371	1.99E-05	0.47	0.12	0.1		uncertain (Li-Fraumeni syndrome, hereditary cancer-predisposing syndrome)	cell line: Yokozaki (2000) & Mashima et al. (2005): wild type p53;

C: 23132

Gene		Protein	Mutation								COSMIC	dpSNP	gnomAD	Functional impact				ClinVar	Literature / Comment
HGNC	Enssembl		class	type	reference allel	ancestral allel	DNA change	prot. change	genomic coordinates	transcript	Genomic Mutation ID	reference SNP	AF (total)	REVEL	FATHMM	SIFT	DepMap / CCLE	clin. signif. (clinic)	
WNT1	ENSG00000125084	Wnt 1	deletion - frameshift	DEL	GGGGGGG	GGGGGG	c.506del	p.Gly169Alafs*30	12:49374354-49374354	ENST00000293549.3	COSV53295457	rs779969402	4.31E-06	-	-	-		not reported	gastric cancer: Mao et al. (2014);
LRP6	ENSG00000070018	low-density lipoprotein receptor-related protein 6	substitution - missense	SNV	G	C	c.1561G>C	p.Gly521Arg	12:12318214-12318214	ENST00000261349.4	COSV53797719	-	-	-	0.94	-			
DKK1	ENSG00000107984	dickkopf-related protein 1	substitution - missense	SNV	C	T	c.367C>T	p.Arg123Cys	10:54074806-54074806	ENST00000373970.3	COSV64760066	rs138015066	8.24E-06	0.59	0.87	0		not reported	gastric cancer: Katoh (2007);
DKK2	ENSG00000155011	dickkopf-related protein 2	de novo start - out of frame (5'-UTR)	SNV	A	?	-	-	4:107956984-107956984	ENST00000285311.3	-	-		-	-	-	damaging		
RNF43	ENSG00000108375	ring finger protein 43	deletion - frameshift	DEL	CCCCCC	CCCCC	c.1976del	p.Gly659Valfs*41	17:56435167-56435167	ENST00000584437.1	COSV68456684	rs755128667	4.00E-06	-	-	-	damaging	pathogenic	gastric cancer: Wang et al. (2014), Katoh and Katoh (2017);
			deletion - frameshift	DEL	A	_	c.1977del	p.Gly659Glyfs	17:56435160-56435160	ENST00000584437.1	COSV68456944	-	-	-	-	-			comment: exon 8 (ENSE00000820280); COSMIC says protein change p.S661Pfs*39, but not reasonable due to genomic localisation!;
LGR4	ENSG00000205213	leucine-rich repeat-containing G-protein coupled receptor 4	substitution - missense	SNV	C	T	c.2821C>T	p.Arg941Cys	11:27389449-27389449	ENST00000379214.4	COSV58725998	rs201095301	2.57E-05	0.36	0.99	0		not reported	
FZD1	ENSG00000157240	frizzled class receptor 1	substitution - missense	SNV	G	A	c.1700G>A	p.Arg567His	7:90895895-90895895	ENST00000287934.2	COSV55312350	rs984834944	3.99E-06	0.36	0.93	0.3		not reported	
FZD2	ENSG00000180340	frizzled class receptor 2	substitution - missense	SNV	C	T	c.500C>T	p.Ala167Val	17:42635556-42635556	ENST00000315323.3	COSV59530719	rs759427364	8.08E-06	0.15	-	0.4		not reported	
FZD5	ENSG00000163251	frizzled class receptor 5	substitution - missense	SNV	C	T	c.929C>T	p.Tyr310Met	2:208632535-208632535	ENST00000295417.3	COSV54945048	rs1197592175	4.13E-06	0.81	0.96	0		not reported	
FZD6	ENSG00000164930	frizzled class receptor 6	deletion - frameshift	DEL	TTTTT	TTTT	c.125del	p.Phe42Serfs*4	8:104312460-104312460	ENST00000358755.4	COSV62471707	-	-	-	-	-			
FZD8	ENSG00000177283	frizzled class receptor 8	substitution - missense	SNV	C	T	c.1691C>T	p.Tyr564Met	10:35928667-35928667	ENST00000374694.1	COSV65968667	rs373955864	1.11E-05	0.66	-	0		not reported	
DVL2	ENSG00000004975	dishevelled segment polarity protein 2	substitution - missense (3'-UTR)	SNV	C	T	c.*128C>T	-	17:7129056-7129056	ENST00000005340.5	COSV50040578	-	-	-	0.82	-			
DVL3	ENSG00000161202	dishevelled segment polarity protein 3	substitution - missense	SNV	G	A	c.1588G>A	p.Ala530Tyr	3:183887883-183887883	ENST00000313143.3	COSV53050965	rs1417240715	7.99E-06	0.11	-	0.6		not reported	
AXIN1	ENSG00000103126	axin	deletion - frameshift	DEL	CCCCCC	CCCCC	c.1523del	p.Gly508Valfs*197	16:347988-347988	ENST00000262320.3	COSV51982982	rs760961378	2.58E-05	-	-	-		not reported	gastric cancer: Kim et al. (2009), Mazzoni and Fearon (2014);
AXIN2	ENSG00000168646	axin-related protein	deletion - frameshift	DEL	CCCCCC	CCCCC	c.1799del	p.Gly600Alafs*24	17:63532591-63532591	ENST00000375702.5	COSV61055501	rs267606674	0.00E+00	-	-	-		pathogenic (colon carcinoma)	gastric cancer: Kim et al. (2009), Mazzoni and Fearon (2014);
APC2	ENSG00000115266	adenomatous polyposis coli like	substitution - missense	SNV	C	A	c.2714C>A	p.Pro335Tyr	19:1457038-1457038	ENST00000535453.1	-	-	-	-	-	-			comment: exon 8 (ENSE00000752922);
			substitution - missense	SNV	G	A	c.5814G>A	p.Ala1368Tyr	19:1467402-1467402	ENST00000535453.1	-	-	-	-	-	-			comment: exon 14 (ENSE00002266075);
CSNK1E	ENSG00000213923	Casein kinase 1ε	substitution - missense	SNV	G	A	c.61G>A	p.Gly21Arg	22:38710102-38710102	ENST00000405675.3	COSV63292578	rs990406832	*7.96E-06*	0.89	0.91	0		not reported	
TCF7L1	ENSG00000071564	TCF3 (lymphopoiesis)	substitution - missense	SNV	G	A	c.1676G>A	p.Arg559Gln	19:1615430-1615430	ENST00000262965.5	COSV53655282	-	*3.34E-05*	-	0.98	-			
CDH1	ENSG00000039068	E-cadherin (cadherin 1)	substitution - missense	SNV	G	A	c.1846G>A	p.Asp616Asn	16:68856038-68856038	ENST00000261769.5	COSV55745206	-	-	-	0.98	0			cell line: Klijn et al. (2015) (suppl. data 3): mutation in CDH1 - SIFT:deleterious(0), PolyPhen:probably damaging(0.983), Condel:deleterious(0.873); / gastric cancer: Becker et al. (1994), Guilford et al. (1998), Klijn et al. (2015), Nemtsova et al. (2020); / comment: localization: extracellular part, so called "cadherin domain"; exon 12 (ENSE00003463070);
NLK	ENSG00000087095	Nemo-linke kinase	deletion - frameshift	DEL	TTTTTTT	TTTTTT	c.576del	p.Phe192Leufs*30	17:26449746-26449746	ENST00000407008.3	COSV69407806	-	-	-	-	-			

D: NCI-N87

Gene		Protein	Mutation								COSMIC	dpSNP	gnomAD	Functional impact				ClinVar	Literature / Comment
HGNC	Enssembl		class	type	reference allel	ancestral allel	DNA change	prot. change	genomic coordinates	transcript	Genomic Mutation ID	reference SNP	AF (total)	REVEL	FATHMM	SIFT	DepMap / CCLE	clin. signif. (clinic)	
WNT8A	ENSG00000136997.17	Wnt 8A	substitution - missense (5'-UTR)	SNV	T	G	c.-79T>G	-	5:137419738-137419738	ENST00000506684.1	COSV64230793	rs1392479016	4.15E-06	-	0.37	-		not reported	
WNT10B	ENSG00000169884.14	Wnt 10B	substitution - missense	SNV	C	T	c.556C>T	p.Pro186Ser	12:49361884-49361884	ENST00000301061.4	COSV99975832	rs774197373	1.06E-05	0.11	0.3	0.8		not reported	
TP53	ENSG00000141510	p53	substitution - missense	SNV	G	A	c.743G>A	p.Arg248Gln	17:7577538-7577538	ENST00000269305.4	COSV52661580	rs11540652	1.19E-05	0.93	0.98	0		likely pathogenic (adenocarcinoma of the stomach)	gastric cancer: Chang et al. (2016);

E: 293T

Gene		Protein	Mutation								COSMIC	dpSNP	gnomAD	Functional impact				ClinVar	Literature / Comment
HGNC	Enssembl		class	type	reference allel	ancestral allel	DNA change	prot. change	genomic coordinates	transcript	Genomic Mutation ID	reference SNP	AF (total)	REVEL	FATHMM	SIFT	DepMap / CCLE	clin. signif. (clinic)	
WNT11	ENSG00000085741	Wnt 11	substitution - missense	SNV	G	A	c.409G>A	p.Gly137Ser	11:75905799-75905799	ENST00000322563.3	-	rs778521234	1.26E-05	0.25	-	0.7		not reported	
ZNRF3	ENSG00000183579	zinc and ring finger 3	insertion - frameshift	INS	_	G	c.1202insG	p.Asn342Glufs	22:29445195-29445195	ENST00000544604.2	-	-	-	-	-	-			gastric cancer: Katoh and Katoh (2017); / comment: exon 8 (ENSE00001308098);
LGR4	ENSG00000205213	Leucine-rich repeat-containing G-protein coupled receptor 4	substitution - missense	SNV	C	T	c.2219C>T	p.Ala740Val	11:27389979-27389979	ENST00000389858.4	-	rs556032916	3.98E-06	0.58	-	0		not reported	
LGR6	ENSG00000133067	Leucine-rich repeat-containing G-protein coupled receptor 6	substitution - missense	SNV	G	T	c.1545G>T	p.Glu515Asp	1:202287393-202287393	ENST00000439764.2	-	-	-	-	-	-			comment: exon 16 (ENSE00001611882);
TP53	ENSG00000141510	p53	substitution - missense	SNV	A	T	c.840A>T	p.Arg280Ser	17:7577098-7577098	ENST00000359597.4	COSV52801834	-	-	-	0.87	-		pathogenic (familial cancer of breast)	cell line: Lin et al. (2014) (suppl. Data 2): localized in the E4F1 interacting domain affecting DNA binding, in addition binding of SV40 LTag by p53;

Table 21: Detailed overview on cell lines' mutational data.
Mutated components crucial in Wnt/β-catenin signaling, targets of Wnt/β-catenin signaling or important gastric cancer related factors, basically disregarding intronic localizations and synonymous (silent) substitutions; [**A**] AGS, [**B**] MKN45, [**C**] 23132, [**D**] NCI-N87 and [**E**] 293T**;** genes are displayed in HGNC and Ensembl notation; type: SNV = single nucleotide variant, INS = insertion, DEL = deletion; DNA-change and protein-change according to HGVS; genomic coordinates according to GRCh37.p13; note that COSMIC Genomic Mutation ID (COSV123…) and/or dbSNP reference SNP (rs123…) are not always available; AF according to gnomAD exomes r2.1.1 (23132: in case *CSNK1E* and *TCF7L1* (syn. *TCF3*) according to TOPMed and ExAC, respectively); prediction of functional impact primarily by REVEL (obtained from Ensembl: *range 0-1, deleterious if > 0.5, probability 75.4%*), secondarily by FATHMM (obtained from COSMIC: *range 0-1, deleterious if ≥ 0.7*) and SIFT (obtained from Ensembl: *range 0-1, deleterious if < 0.05*).

5.1.2 Relative TCF/LEF transcriptional activity level of cell lines

The estimation of the (intrinsic) TCF/LEF activity of the respective cell lines allows to evaluate the impact of CagA on the Wnt pathway more precisely and furthermore to compare the cell lines with each other in this respect. In some studies, gastric cancer cell lines were compared for their TCF/LEF transcriptional activity level using a luciferase assay (Caca et al., 1999, Nojima et al., 2007, Asciutti et al., 2011). However, the relevance to the cell lines used in this work is rather limited because (i) none of the cited studies covered all cell lines investigated here at once and (ii) the approaches are methodically different, be it the way nucleic acids are introduced (i.e., transfection vs. transduction), the reporter plasmid used (i.e., pTOPflash/pFOPflash vs. pGL3-OT/pGL3-OF), the internal standard (i.e., *Renilla* luciferase vs. β-galactosidase) or the incubation time until lysis (i.e., 24 hours up to four days). In NCI-N87 cells, which have largely unimpaired core components of Wnt/β-catenin signaling (see 5.1.1.2.4), data of Nojima et al. (2007) show similar relative TCF/LEF transcriptional activity to MKN45 cells, which is considerably reduced in the case of AGS (0.044-fold) and KATOIII cells (0.018-fold). According to Caca et al. (1999), the TCF/LEF transcriptional activity of NCI-N87 cells (i.e., TOP/FOP mean fluorescent intensity) is only 0.14-fold that of AGS cells but exceeds that of SNU5 cells by more than 2-fold. Asciutti et al. (2011) report similar levels for NCI-N87, AGS and KATOIII cells, which, however, exceed SNU5 cell levels by more than 20-fold. Among the cell lines used in this work, it could therefore basically be deduced that AGS cells show a comparably strong and MKN45 cells a rather inferior TCF/LEF transcriptional activity level. In addition, there is no way to obtain an estimate of 23132 cells in which Wnt/β-catenin signaling seems to be affected by MSI and other mutations (see 5.1.1.2.3).

Lustig et al. (2002) reported a negative feedback loop of the (canonical) Wnt/β-catenin pathway through its target gene *AXIN2* in human tumors, particularly in cultured colorectal cancer cells. It was shown that it is possible to use the mRNA levels of Wnt/β-catenin target genes *AXIN2*, *NKD1* and *TCF7* (syn. *TCF1*) as specific biomarkers for activated Wnt/β-catenin signaling using real-time quantitative PCR related to the housekeeping gene *GAPDH* in the cultured colon cancer cell line SW620 (Yan et al., 2001) and 293T cells (Li et al., 2012). Accordingly, a culture of cell lines as a whole basically represents a steady state with respect to the activity of the signaling pathways (irrespective of any recent manipulation). Thus, a dynamic equilibrium is established in the diverse signaling pathways, not least due to feedback regulation by certain target genes. Or viewed the other way around, the expression level of target genes that generate feedback loops can be used to roughly estimate the signaling activity of a particular pathway, allowing comparison of different cultured cell lines. Since genomic study databases such as the DepMap portal provide cell line-specific gene expression levels, they are very useful for comparing cell lines in this regard. Therefore, the expression levels of Wnt/β-catenin signaling target genes that show feedback regulation by encoding for a component of the pathway (see 5.1.2.1) were related to the mean expression levels of selected housekeeping genes in a cell line-specific manner. Since the above studies on TCF/LEF transcriptional activity overall refer to NCI N87 cells, which have largely native Wnt/β-catenin signaling components (see 5.1.1.2.4), they were used as a reference, as were KATOIII and SNU5 cells, to provide a more conclusive picture.

5.1.2.1 Wnt/β-catenin signaling target genes encoding for pathway components

There are several components of (canonical) Wnt/β-catenin signaling that are themselves also target genes of (canonical) Wnt/β-catenin signaling and are regulated by it in a context-

dependent manner. With respect to the stomach, *LEF1* (lymphoid enhancer-binding factor 1, syn. *TCF7L3*) (Alok et al., 2017) and *LGR5* (Simon et al., 2012, Wang et al., 2018) are up-regulated by Wnt/β-catenin signaling and show positive feedback regulation. *AXIN2* (Alok et al., 2017), *NKD1* (Nkd1, naked cuticle 1) (Katoh, 2001, Alok et al., 2017) and *TCF7* (syn. *TCF1*) (Alok et al., 2017) are also up-regulated by Wnt/β-catenin signaling but show a negative feedback loop. Expression of the Wnt/β-catenin signaling inhibitors *RNF43* (Hao et al., 2012, Koo et al., 2012) and *ZNRF3* (Van der Flier et al., 2007, Hao et al., 2012) has been shown to be up-regulated, at least in the intestine. The human Wnt co-receptor *LRP6* (Khan et al., 2007, Li et al., 2010b) is down-regulated by Wnt/β-catenin signaling. Although it has been shown that the Wnt/β-catenin signaling target gene *DKK1* is up-regulated and to generates a negative feedback loop (Sato et al., 2010), it has not been considered due to its still controversial role in gastric cancer (Menezes et al., 2012), which has been shown to be a Wnt/β-catenin-independent (negative) prognostic factor for overall survival and disease-free survival if highly expressed (Gao et al., 2012, Lee et al., 2012a, Hong et al., 2018).

5.1.2.2 RNA-sequencing

By analyzing the entire transcriptome, RNA-sequencing (RNA-seq) permits assessment of the expression of specific genes. This requires the generation of complementary DNA (cDNA) by reverse transcription following selection and enrichment of messenger RNA (mRNA). After fragmentation and amplification, this cDNA library is subjected to high-throughput sequencing. The number of reads mapped to single loci or genes in the transcriptome assembly (read counts) quantifies the respective level of gene expression. The normalization of read counts basically comprises two steps: Due to different library sizes, comparison between experiments requires normalization for sequencing depth (i.e., coverage), which is done by referring to total number of reads per million. Since longer genes show more read counts, normalization based on gene length (reads per kilobase; RPK) is also performed. There is an ongoing debate about the normalization of quantification measures with respect to inter-sample comparison. Provided that identical sample preparation protocols were applied, that samples originated from the same tissue, and that total RNA amounts were similar, the normalized expression measure transcripts per million (TPM) allows comparison across samples (Wagner et al., 2012, Abrams et al., 2019, Zhao et al., 2020). But comparison across different samples by (common) quantification measures such as TPM is limited, especially in case of lowly expressed genes, and there is growing evidence for more appropriate measures, which, however, require not-differentially expressed genes (Dillies et al., 2013, Zhao et al., 2020, Zhao et al., 2021). Regarding TPM, the reads per kilobase (RPK), i.e., the read counts divided by the length of each gene in kilobases, are referred to the sum of all RPK values in a sample (that has been) divided by 10^6:

$$\text{TPM} = \text{RPK} \times 1/\sum(\text{RPK}) \times 10^6$$

$$\text{RPK} = (\text{total reads mapped to gene}) \times 10^3 / (\text{gene length [bp]})$$

The DepMap portal (see above) also provides bulk RNA-seq data on the gastric cancer cell lines AGS, MKN45, 23132 and NCI-N87. Here, alignment of RNA-seq reads was performed with a GTEx/TOPMed pipeline (GTEx Consortium, 2013) using a *Homo sapiens* reference genome (GRCh38). The expression measure of results is presented as $\log_2(\text{TPM}+1)$.

5.1.2.3 Comparison of the relative TCF/LEF transcriptional activity level of the cell lines

The expression measures obtained from the DepMap portal have been converted to plain TPM. Aside from the common housekeeping genes (HKG) *ACTB* (β-actin) and *GAPDH* (glyceraldehyde-3-phosphate dehydrogenase), according to Racz et al. (2021), the housekeeping genes *CNOT4* (CCR4-NOT transcription complex subunit 4), *HNRNPL* (heterogeneous nuclear ribonucleoprotein L), *IPO8* (importin 8), *PUM1* (pumilio RNA binding family member 1) and *SNW1* (SNW domain containing 1) were additionally used as internal standards, which show stable expression patterns in human cancer cell lines. As can be seen in Figure 22, the general expression levels (TPM) of the cell lines vary markedly for both housekeeping and Wnt/β-catenin signaling target genes, with the general expression level being most pronounced in AGS cells (see Figure 22, B, text box). In Addition, the expression levels of Wnt/β-catenin signaling target genes differ, in some cases substantially, from those of HKG, particularly highly expressed *ACTB* and *GAPDH*. Compared to all other cell lines investigated, KATOIII cells show considerable expression of *CTNNB1* (see Figure 22, C). Beside *CTNNB1* in AGS cells (see 5.1.1.2.1), there are some mutations of other HKGs: *CNOT4* shows an exonic frameshift by insertion of a single adenine at 23132 cells (COSV59654242, p.Gln84Tyrfs*5), *HNRNPL* shows a SNV at MKN45 cells (COSV55496396, rs764751159, p.Met567Val) and SNW1 shows a SNV at 23132 cells (COSV55054626, rs759186141, p.Ala85Val), both SNVs are predicted innocuous by REVEL. But the expression levels of these HKG in in the concerned cells do not differ.

For each cell line, the expression levels of target genes were normalized by the mean expression level of all HKG that were considered (*ACTB*, *CNOT4*, *GAPDH*, *HNRNPL*, *IPO8*, *PUM1*, and *SNW1*) and multiplied by 10^2 for convenience (see Figure 23). Relative Wnt/β-catenin signaling target gene expression levels indicate a comparatively high expression of Wnt/β-catenin signaling target genes in NCI-N87 (particularly *LEF1*, *AXIN2*, *NKD1*, *RNF43*) and their relatively strong expression in AGS cells (particularly *LGR5*, *AXIN2*, *RNF43*). KATOIII show a low mid-level relative expression of Wnt/β-catenin signaling target genes (see *AXIN2* and *RNF43*), 23132 and MKN45 indicate a considerably inferior expression levels, while SNU5 cells show almost inactive expression, by way of comparison. A clear reciprocal behavior of negatively controlled *LRP6* expression with respect to other target genes cannot be deduced.

While the expression of the target genes investigated could admittedly be driven by other pathways, the highly dissimilar relative expression of the Wnt/β-catenin signaling target genes suggests that there are also substantial differences in cellular Wnt/β-catenin signaling activity (with no significant deleterious mutations in the corresponding genes). Notably, *AXIN2* and *LGR5* are highly Wnt/β-catenin responsive target genes. Yan et al. (2001) demonstrated a strong correlation between the cytosolic amount of β-catenin and the expression level of *AXIN2* as well as *NKD1*, while Barker et al. (2010) depicted that the expression of *LGR5* in the stomach is highly up-regulated by increased activity of Wnt/β-catenin signaling. Consequently, the mean cell line-specific relative expression level of Wnt/β-catenin signaling target genes (excluding *LRP6*) gives a vague idea of the dimensions despite substantial measures of dispersion (SD): 11.11% (NCI-N87), 7.58% (AGS), 2.16% (KATOIII), 0.89% (23132), 0.68% (MKN45) and 0.17% (SNU5) (see Figures 23 and 24, small insert).

Consistent with the data of Caca et al. (1999), Nojima et al. (2007) and Asciutti et al. (2011) , AGS cells show a relatively strong Wnt/β-catenin signaling activity level among the cell lines

investigated, whereas SNU5 cells show the least activity. Unlike the other authors, but in line with Asciutti et al. (2011), NCI-N87 cells show the strongest mean relative Wnt/β-catenin signaling activity level. As mentioned earlier (see 5.1.1 and 5.1.1.2.4), NCI-N87 cells exhibit intact, i.e. native Wnt/β-catenin signaling components , and therefore their Wnt/β-catenin signaling levels can most likely be considered robust in the context of gastric cancer cell lines. The very low TCF/LEF signaling activity of NCI-N87 cells in the data of Caca et al. (1999) and Nojima et al. (2007) might be due to their limited transfectability (whereas Asciutti et al. (2011) transduced them with the reporter plasmid). In contrast to Nojima et al. (2007) and Asciutti et al. (2011), RNA-seq data for KATOIII cells show a comparatively low mean relative Wnt/β-catenin signaling activity level but a substantially stronger *CTNNB1* expression (see Figure 22, C), which is in agreement with data from Suriano et al. (2005) and may indicate an (false positive) impact on the expression of luciferase reporter plasmids and thus TCF/LEF transcriptional activity. Therefore, *CTNNB1* was excluded from calculation of mean HKG expression levels. The rather subordinate Wnt/β-catenin signaling level of the 23132 cells corresponds well the data from the mutational analysis (see 5.1.1.2.3), where, not least due to MSI, a considerable degradation of its signaling pathway components can be concluded (deleterious mutations at *AXIN2*, *DKK1*, *RNF43* and *LRP6*). MKN45 cells also show a comparatively weak mean relative Wnt/β-catenin signaling activity level, although the core components of signal transduction are largely unimpaired. As described above (see 5.1.2.1), pronounced expression of *DKK1* does not inevitably imply strong Wnt/β-catenin signaling activity. In the absence of a known cut-off value, *DKK1* was disregarded, potentially disfavoring MKN45 cells that show strong expression of *DKK1* (see Figure 22, E).

After normalization to NCI-N87 cells, the estimates for the mean expression levels of Wnt/β-catenin signaling target genes (excluding *LRP6*) are as follows: 0.68 (AGS), 0.19 (KATOIII), 0.08 (23132), 0.06 (MKN45) and 0.02 (SNU5) (see Figure 24).

A: NCI-N87

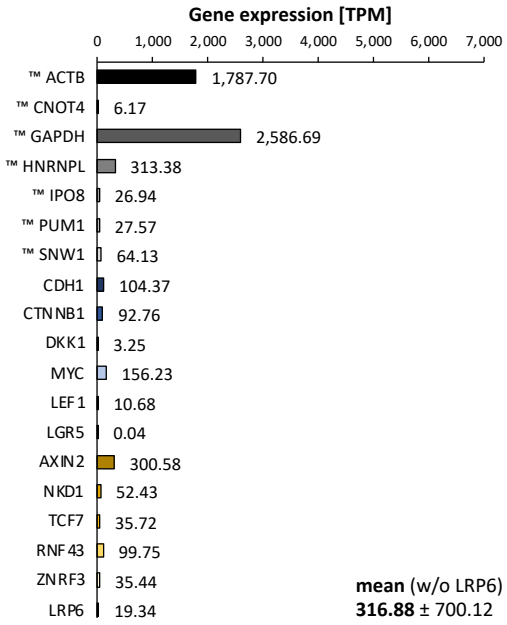

B: AGS

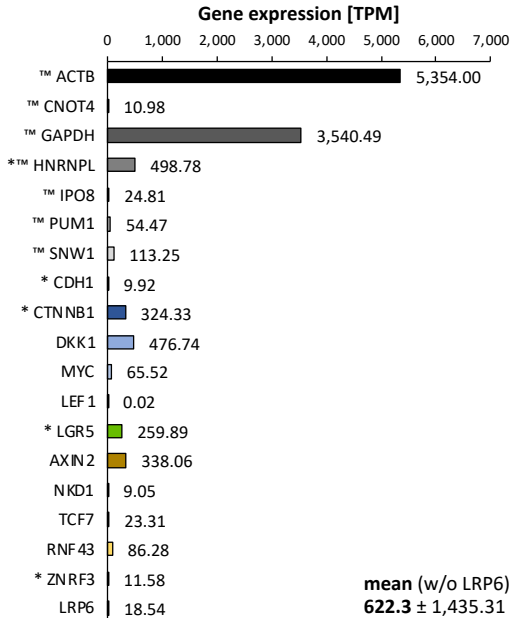

C: KATOIII

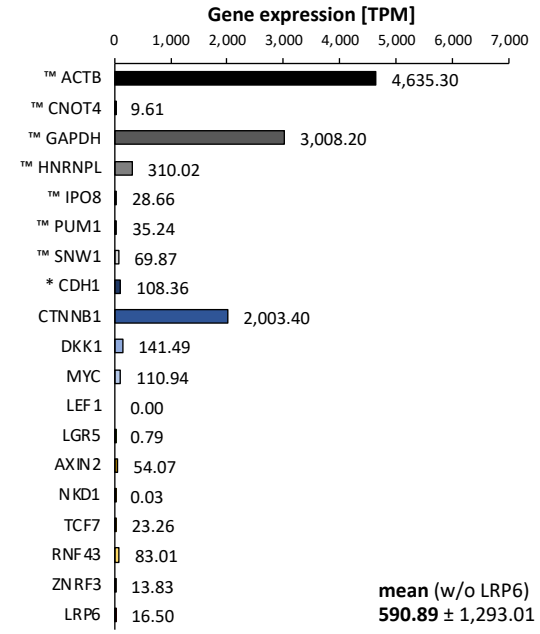

D: 23132

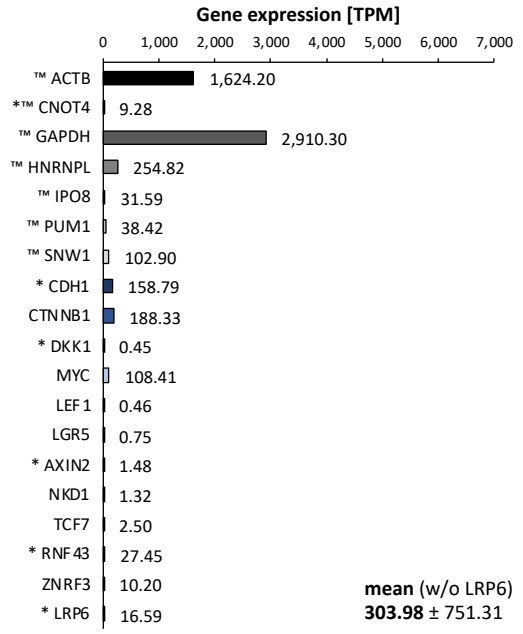

E: MKN45

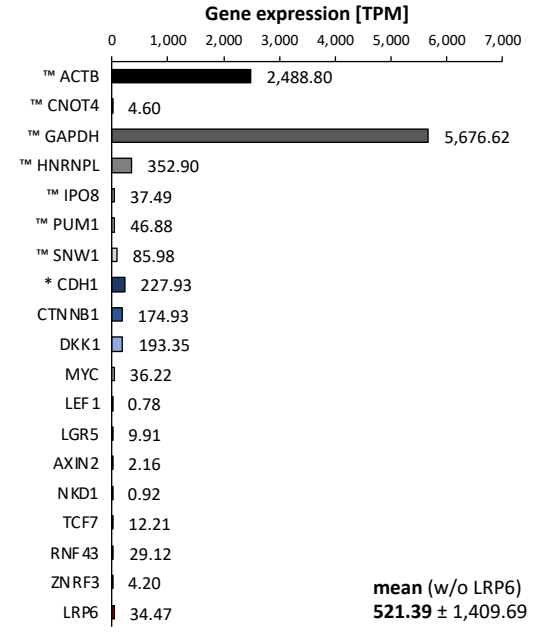

F: SNU5

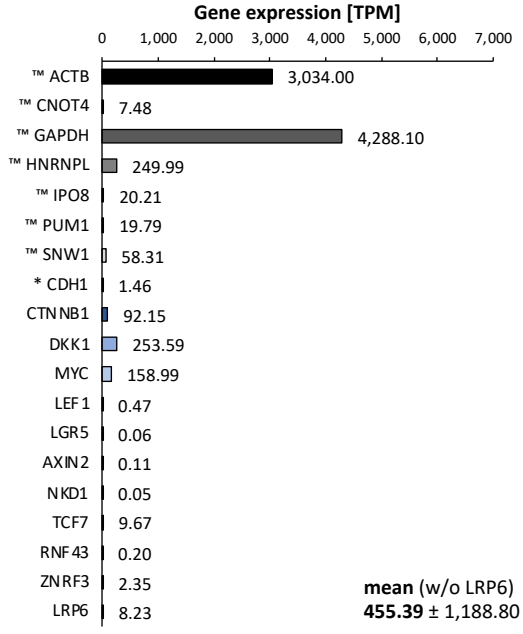

Figure 22: Evaluation of gene expression through RNA-seq [TPM].
Data obtained from Cancer Dependency Map (2021) genomic studies database as $\log_2$(TPM+1) were converted to TPM; genes displayed in HGNC notation; superscripts: trade-mark (™) = housekeeping gene (HKG) taken into account, asterisk (*) = deleterious mutation; [**A**] NCI-N87 cells, HKG 687.51 ± 1055.30; [**B**] AGS cells, HKG 1370.97 ± 2172.13; [**C**] KATOIII cells, HKG 1156.70 ± 1882.94; [**D**] 23132 cells, HKG 710.22 ± 1129.54; [**E**] MKN45 cells, HKG 1241.89 ± 2150.87; [**F**] SNU5 cells, HKG 1096.84 ± 1790.637 (mean TPM ± SD); *black/grey*: housekeeping genes (*ACTB*, *CNOT4*, *GAPDH*, *HNRNPL*, *IPO8*, *PUM1*, *SNW1*); *blue*: CTNNB1 and disregarded target genes (*CDH1*, *DKK1*, *MYC*); *green*: up-regulated positive feedback Wnt/β-catenin signaling target genes (*LEF1*, *LGR5*); *brown/yellow*: up-regulated negative feedback Wnt/β-catenin signaling target genes (*AXIN2*, *NKD1*, *TCF7* (*syn. TCF1*), *RNF43*, *ZNRF3*); *red*: down-regulated Wnt/β-catenin signaling target gene (*LRP6*); note that regulation of *RNF43*, *ZNRF3* and *LRP6* are not gastric cell-specific; text box: mean (± SD) of all investigated Cancer Dependency Map (2021) genes (except for *LRP6*).

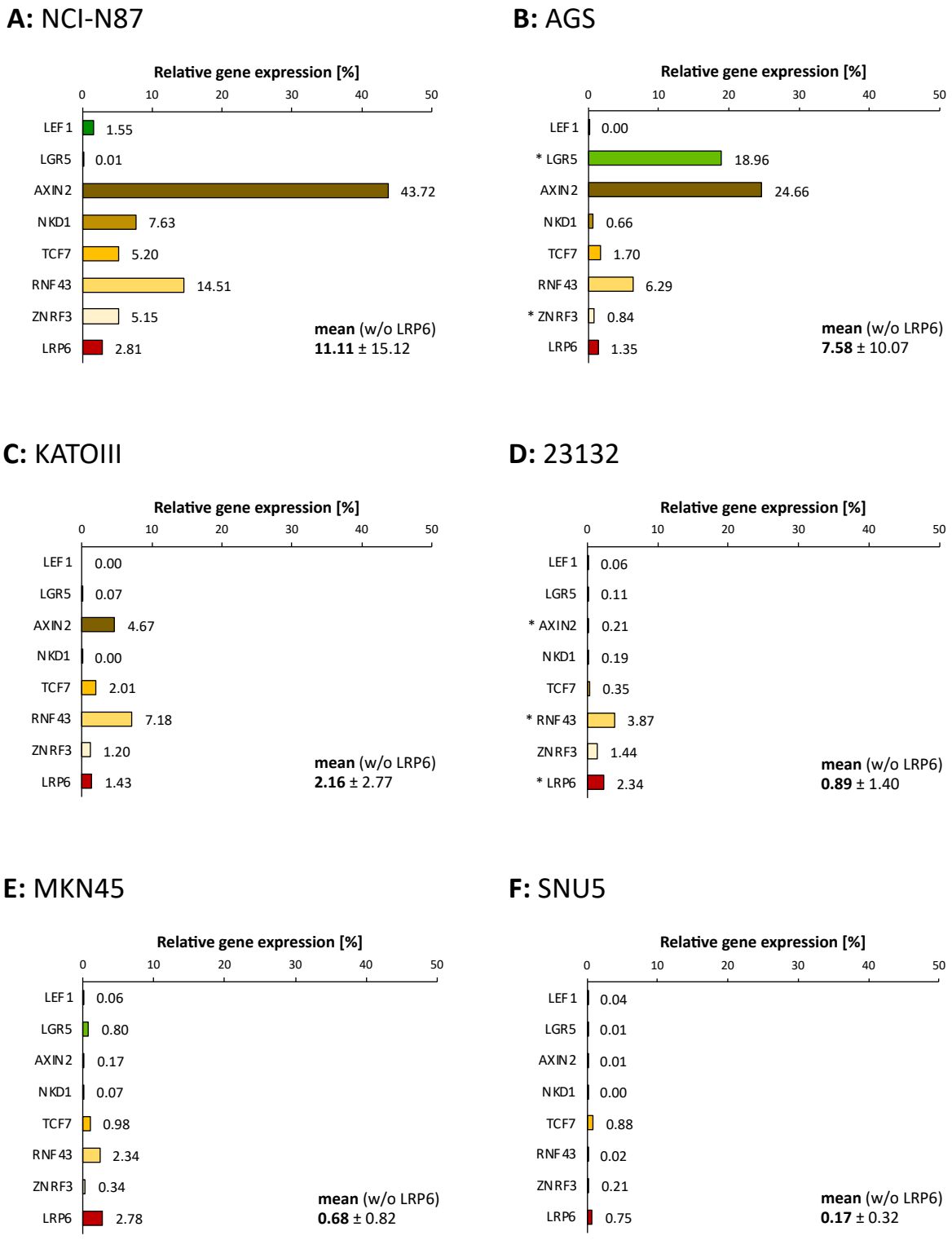

Figure 23: Relative cell line-specific Wnt/β-catenin target gene expression [%].
Gene expression data [TPM] (obtained from Cancer Dependency Map (2021) were cell line-specifically referred to mean TPM of HKG (*ACTB*, *CNOT4*, *GAPDH*, *HNRNPL*, *IPO8*, *MYC*, *PUM1*, *SNW1*) and multiplied by 10^2 (for convenience); genes displayed in HGNC notation; superscript: asterisk (*) = deleterious mutation; [**A**] NCI-N87 cells; [**B**] AGS cells; [**C**] KATOIII cells; [**D**] 23132 cells; [**E**] MKN45 cells; [**F**] SNU5 cells; *green*: up-regulated positive feedback Wnt/β-catenin signaling target genes (*LEF1*, *LGR5*); *brown/yellow*: up-regulated negative feedback Wnt/β-catenin signaling target genes (*AXIN2*, *NKD1*, *TCF7* (syn. *TCF1*), *RNF43*, *ZNRF3*); *red*: down-regulated Wnt/β-catenin signaling target gene (*LRP6*); note that regulation of *RNF43*, *ZNRF3* and *LRP6* are not gastric cell-specific; text box: relative mean (± SD) of all investigated target genes (except for *LRP6*).

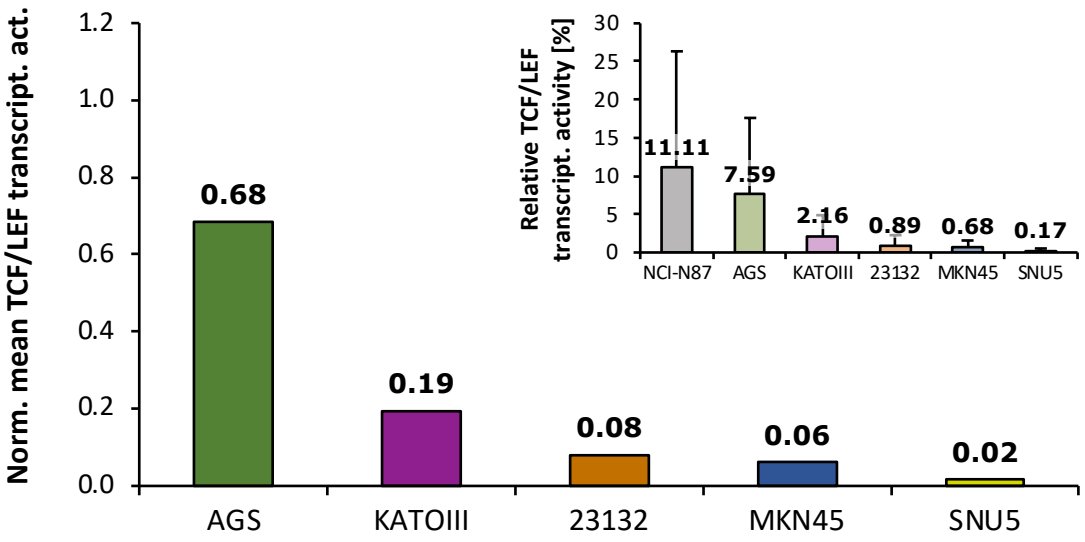

Figure 24: Mean relative Wnt/β-catenin target gene expression normalized to NCI-N87 cells.
Mean of relative cell line-specific Wnt/β-catenin target gene expression (*LEF1*, *LGR5*, *AXIN2*, *NKD1*, *TCF7* (syn. *TCF1*), *RNF43*, *ZNRF3,* excluding *LRP6*) normalized to NCI-N87 cell line; small insert: without normalization; NCI-N87 cells (*grey*): gastric cancer cell lines with unimpaired/robust Wnt/β-catenin signaling (mean relative 11.11% ± 15.12), AGS cells (*green*): strong signaling activity (mean relative 7.59% ± 10.07), KATOIII (*purple*): low mid-level (mean relative 2.16 ± 2.77), 23132 (*orange*): subordinate (0.89 ± 1.40), MKN45 (*blue*): weak (mean relative 0.68% ± 0.82), SNU5 (*yellow*) almost inactive (mean relative 0.17% ± 0.32); marked SD due to very distinct relative gene expression levels.

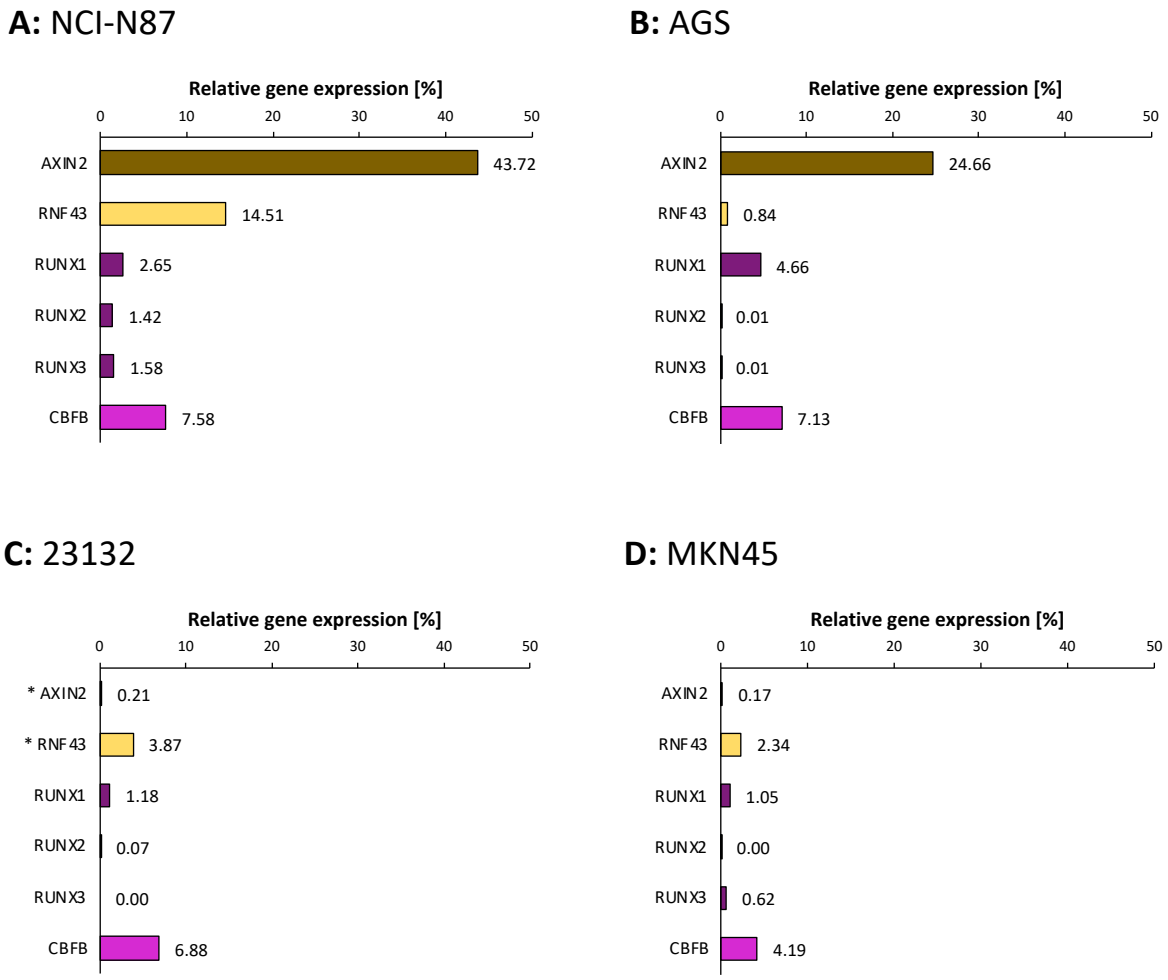

Figure 25: Relative cell line-specific gene expression of RUNX cluster [%].
Gene expression data [TPM] (obtained from Cancer Dependency Map (2021) were cell line-specifically referred to mean TPM of housekeeping genes (*ACTB*, *CNOT4*, *GAPDH*, *HNRNPL*, *IPO8*, *MYC*, *PUM1*, *SNW1*) and multiplied by 10^2 (for convenience); genes displayed in HGNC notation; superscript: asterisk (*) = deleterious mutation; [**A**] NCI-N87 cells; [**B**] AGS cells; [**C**] 23132 cells; [**D**] MKN45 cells; *brown* and *yellow*: *AXIN2* and *RNF43*, respectively (for comparison); *purple*: RUNX1, RUNX2, RUNX3; *lighter purple*: CBFB.

5.2 Cloning primers

5.2.1 pEGFP-*cagA* constructs: Restriction digestion (following TOPO® TA cloning)

Forward primers

PstI-*cagA*1-21-fwd (wt & 1-200) [L: 29 bp; GC: 41%; T_m: 63.9 °C]

```
5'-CTGCAGTAGTGACTAACGAAACCATTAAC-3'-->
   PstI    cagA 1-21
```

PstI-*cagA*601-620-fwd (201-1216) [L: 28 bp; GC: 60.71%; T_m: 71.98 °C]

```
5'-CTGCAGTAGGGCCTACTGGTGGGGATTG-3'-->
   PstI    cagA 601-620
```

Reverse primers

*cagA*580-600-SmaI-rev (1-200) [L: 30 bp; GC: 43%; T_m: 65.4 °C]

```
5'-CCCGGGTTATCCATTTTTTCTGCTTCTTG-3'-->
   SmaI     cagA 600-580
```

*cagA*3629-3648-SmaI-rev (wt & 201-1216) [L: 29 bp; GC: 48%; T_m: 66.7 °C]

```
5'-CCCGGGTTAGCAAGATTTTTGGAAACCAC-3'-->
   SmaI     cagA 3648-3629
```

***cagA* wt:** PstI-*cagA*1-21-fwd + *cagA*3629-3648-SmaI-rev

```
   PstI    cagA 1-21
5'-CTGCAGTAGTGACTAACGAAACCATTAAC-->>--GTGGTTTCCAAAAATCTTGCTAACCCGGG-3'
3'-GACGTCATCACTGATTGCTTTGGTAATTG--<<--CACCAAAGGTTTTTAGAACGATTGGGCCC-5'
                                   cagA 3629-3648        SmaI
          |_____________________________________________|
          cagA wt (AA 1-1216)
```

***cagA*-NT$_{AA1-200}$:** PstI-*cagA*1-21-fwd + *cagA*580-600-SmaI-rev

```
   PstI    cagA 1-21
5'-CTGCAGTAGTGACTAACGAAACCATTAAC-->>--CAAGAAGCAGAAAAAAATGGATAACCCGGG-3'
3'-GACGTCATCACTGATTGCTTTGGTAATTG--<<--GTTCTTCGTCTTTTTTTACCTATTGGGCCC-5'
                                   cagA 580-600          SmaI
          |_____________________________________________|
          cagA-NT (AA 1-200)
```

***cagA*-CT$_{AA201-1216}$:** PstI-*cagA*601-620-fwd + *cagA*3629-3648-SmaI-rev

```
   PstI    cagA 601-620
5'-CTGCAGTAGGGCCTACTGGTGGGGATTG-->>--GTGGTTTCCAAAAATCTTGCTAACCCGGG-3'
3'-GACGTCATCCCGGATGACCACCCCTAAC--<<--CACCAAAGGTTTTTAGAACGATTGGGCCC-5'
                                   cagA 3629-3648        SmaI
          |_____________________________________________|
          cagA-CT (AA 201-1216)
```

Figure 26: pEGFP-*cagA* cloning primers and concept.
Forward (fwd) and reverse (rev) primers to define *cagA* wt and its constructs (*cagA*-NT$_{AA1-200}$ and *cagA*-CT$_{AA201-1216}$) for introduction into (the multiple cloning site downstream of *EGFP* gene of) pEGFP-C1 vector (via TOPO® TA cloning and restriction digestion); reading frames as alternating normal/bold nucleotide triplets; since the PstI restriction site is shifted downstream by one nucleic acid, just two nucleotides between the PstI restriction sites and *cagA* at the forward primer (to keep *cagA* constructs in frame with the *EGFP* gene, stop codons downstream of SmaI in all reading frames); *teal*: *cagA*; *pink*: PstI restriction site; *blue*: SmaI restriction site; *orange*: spacer to keep cagA in frame; *hatched*: synthesized complementary strand; abbreviations: L = length, GC = guanine-cytosine content, T_m = melting temperature.

5.2.2 pcDNA4/TO-*cagA* constructs: Isothermal assembly

Vector (pcDNA4/TO)

Forward primers

pcDNA4-post-wo-fwd (wo 3'-FLAG, all) [L: 32 bp; GC: 62.5%; T_m: 70 °C]

```
5'-TCTGCAGATATCCAGCACAGTGGCGGCCGCTC-3'-->
   Vector
```

pcDNA4-post-3'-FLAG-fwd (3'-FLAG, all ASAS#) [L: 56 bp; GC: 46.43%; T_m: 72 °C]

```
5'-GCCTCGGCCTCGGATTATAAAGATGATGATGATAAGTCTGCAGATATCCAGCACAG-3'-->
   ASAS#       FLAG 1-24                Vector
```

Reverse primers

pcDNA4-pre-wo-rev (wo 5'-FLAG, all) [L: 41 bp; GC: 53.66%; T_m: 71 °C]

```
5'-CATGGTGGCCTTAAGTTTAAACGCTAGAGTCCGGAGGCTGG-3'-->
   Kozak    Vector
```

pcDNA4-pre-5'-FLAG-rev (5'-FLAG, all) [L: 68 bp; GC: 39.71%; T_m: 71 °C]

```
5'-TGATGCTGATGCCTTATCATCATCATCTTTATAATCCATGGTGGCCTTAAGTTTAAACGCTAGAGTCC-3'-->
   ASAS        FLAG 24-1               Kozak    Vector
```

Insert (*cagA*)

Forward primers

pcDNA4-pre-wo-*cagA*1-20-fwd (wo 5'-FLAG, wt & 1-200) [L: 50 bp; GC: 40%; T_m: 68 °C]

```
5'-ACTCTAGCGTTTAAACTTAAGGCCACCATGGTGACTAACGAAACCATTAA-3'-->
   Vector               Kozak    cagA 1-20
```

pcDNA4-pre-wo-*cagA*601-619-fwd (wo 5'-FLAG, 201-1216) [L: 49 bp; GC: 51.02%; T_m: 72 °C]

```
5'-ACTCTAGCGTTTAAACTTAAGGCCACCATGGGCCTACTGGTGGGGATT-3'-->
   Vector               Kozak    cagA 601-619
```

5'-FLAG-*cagA*1-22-fwd (5'-FLAG, wt & 1-200) [L: 52 bp; GC: 38.46%; T_m: 68 °C]

```
5'-AAAGATGATGATGATAAGGCATCAGCATCAGTGACTAACGAAACCATTAACC-3'-->
   FLAG 7-24         ASAS        cagA 1-22
```

5'-FLAG-*cagA*601-620-fwd (5'-FLAG, 201-1216) [L: 50 bp; GC: 48%; T_m: 71 °C]

```
5'-AAAGATGATGATGATAAGGCATCAGCATCAGGGCCTACTGGTGGGGATTG-3'-->
   FLAG 7-24         ASAS        cagA 601-620
```

Reverse primers

pcDNA4-post-wo-*cagA*581-600-rev (wo 3'-FLAG, 1-200) [L: 50 bp; GC: 50%; T_m: 72 °C]

```
5'-GCGGCCGCCACTGTGCTGGATATCTGCAGATCCATTTTTTCTGCTTCTT-3'-->
   Vector                        cagA 600-581
```

pcDNA4-post-wo-*cagA*3629-3648-rev (wo 3'-FLAG, wt & 201-1216) [L: 46 bp; GC: 50% T_m: 71 °C]

```
5'-CCGCCACTGTGCTGGATATCTGCAGAGCAAGATTTTTGGAAACCAC-3'-->
   Vector                    cagA 3648-3629
```

*cagA*578-600-3'-FLAG-rev (3'-FLAG, 1-200) [L: 51 bp; GC: 45.1%; T_m: 70 °C]

```
5'-CATCATCTTTATAATCCGAGGCCGAGGCTCCATTTTTTCTGCTTCTTGCC-3'-->
   FLAG 16-1       ASAS#       cagA 600-578
```

*cagA*3628-3648-3’-FLAG-rev (3’-FLAG, wt & 201-1216) [L: 49 bp; GC: 46.94%; T_m: 70 °C]

```
5’-CATCATCTTTATAATCCGAGGCCGAGGCGCAAGATTTTTGGAAACCACC-3’-->
   FLAG 16-1        ASAS#        cagA 3648-3628
```

Isothermal assembly

wo *cagA* wt:

Vector: pcDNA4-post-wo-fwd + pcDNA4-pre-wo-rev
Insert: pcDNA4-pre-wo-*cagA*1-20-fwd + pcDNA4-post-wo-*cagA*3629-3648-rev

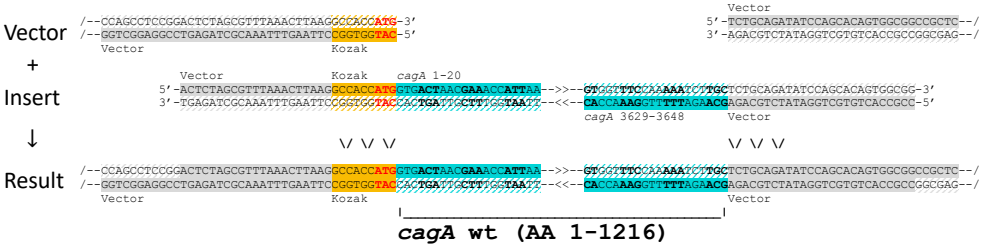

wo *cagA*-NT$_{AA1-200}$:

Vector: pcDNA4-post-wo-fwd + pcDNA4-pre-wo-rev
Insert: pcDNA4-pre-wo-*cagA*1-20-fwd + pcDNA4-post-wo-*cagA*581-600-rev

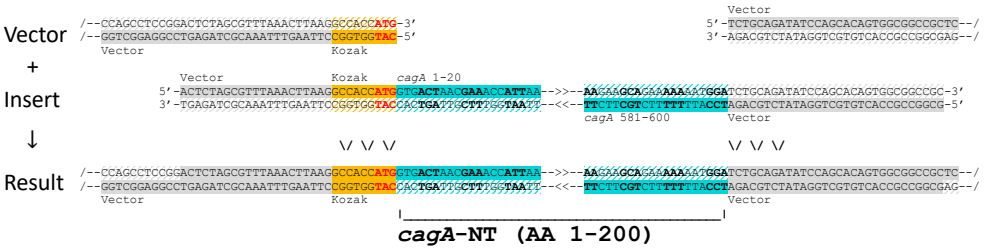

wo *cagA*-CT$_{AA201-1216}$:

Vector: pcDNA4-post-wo-fwd + pcDNA4-pre-wo-rev
Insert: pcDNA4-pre-wo-*cagA*601-619-fwd + pcDNA4-post-wo-*cagA*3629-3648-rev

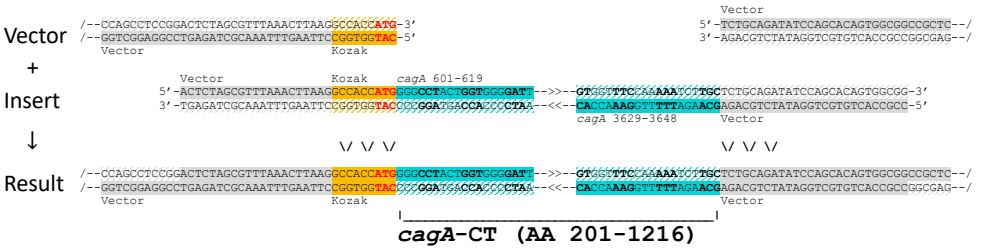

5’-FLAG *cagA* wt (N-terminal):

Vector: pcDNA4-post-wo-fwd + pcDNA4-pre-5’-FLAG-rev
Insert: 5’-FLAG-*cagA*1-22-fwd + pcDNA4-post-wo-*cagA*3629-3648-rev

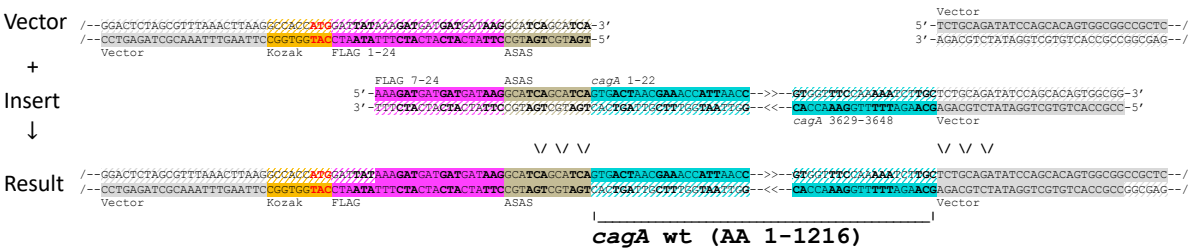

5’-FLAG *cagA*-NT$_{AA1-200}$ (N-terminal):

Vector: pcDNA4-post-wo-fwd + pcDNA4-pre-5’-FLAG-rev
Insert: 5’-FLAG-*cagA*1-22-fwd + pcDNA4-post-wo-*cagA*581-600-rev

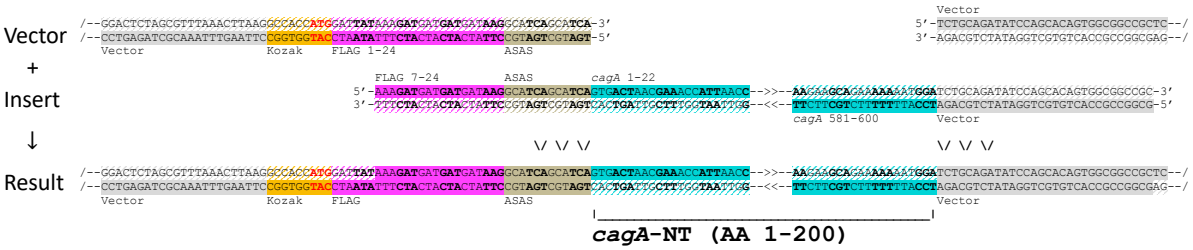

5’-FLAG *cagA*-CT$_{AA201-1216}$ (N-terminal):

Vector: pcDNA4-post-wo-fwd + pcDNA4-pre-5’-FLAG-rev
Insert: 5’-FLAG-*cagA*601-620-fwd + pcDNA4-post-wo-*cagA*3629-3648-rev

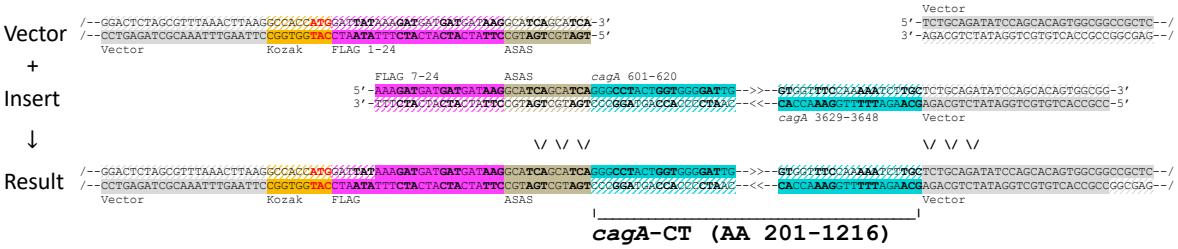

cagA wt 3’-FLAG (C-terminal):

Vector: pcDNA4-post-3’-FLAG-fwd + pcDNA4-pre-wo-rev
Insert: pcDNA4-pre-wo-*cagA*1-20-fwd + *cagA*3628-3648-3’-FLAG-rev

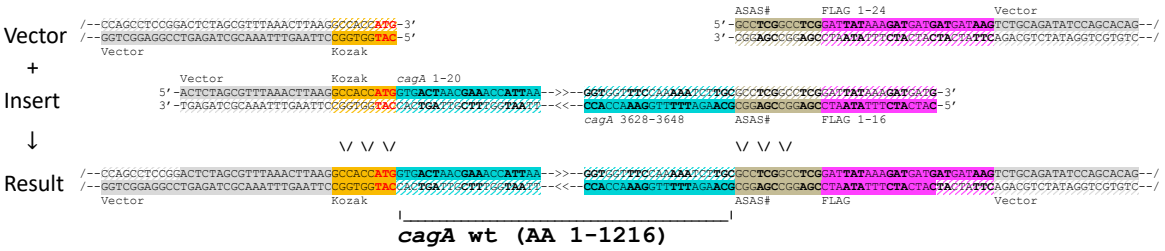

cagA-NT$_{AA1-200}$ 3’-FLAG (C-terminal):

Vector: pcDNA4-post-3’-FLAG-fwd + pcDNA4-pre-wo-rev
Insert: pcDNA4-pre-wo-*cagA*1-20-fwd + *cagA*578-600-3’-FLAG-rev

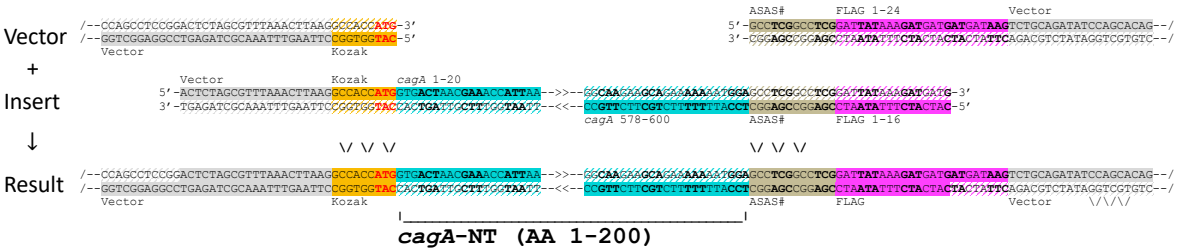

cagA-CT$_{AA201-1216}$ 3'-FLAG (C-terminal):

Vector: pcDNA4-post-3'-FLAG-fwd + pcDNA4-pre-wo-rev
Insert: pcDNA4-pre-wo-*cagA*601-619-fwd + *cagA*3628-3648-3'-FLAG-rev

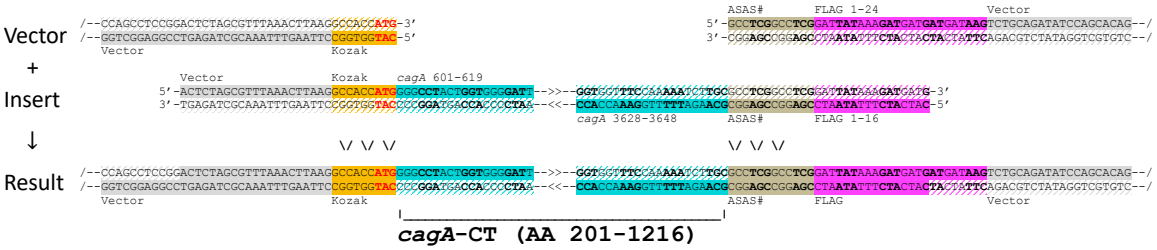

Figure 27: pcDNA4/TO-*cagA* cloning primers and concept.
Forward (fwd) and reverse (rev) primers to define *cagA* wt and its constructs (*cagA*-NT$_{AA1-200}$ and *cagA*-CT$_{AA201-1216}$) for introduction into pcDNA4/TO vector (behind the CMV2 promoter at the multiple cloning site followed by bGH terminator, via isothermal assembly); reading frames as alternating normal/bold nucleotide triplets; *teal*: cagA; *orange*: Kozak sequence (with start codon highlighted red); *brown*: short linker (ASAS); *pink*: FLAG-tag; *grey*: vector (pcDNA4/TO multi cloning site); *hatched*: synthesized complementary strand; abbreviations: L = length, GC = guanine-cytosine content, T_m = melting temperature.

5.2.3 pLenti-*cagA* constructs: Gateway® recombinational cloning

Forward primers

attB1-*cagA*1-22-fwd (wt & 1-200) [L: 53 bp; GC: 41.51%; T_m: 69.232 °C]

```
5′-GGGGACAAGTTTGTACAAAAAAGCAGGCTTAGTGACTAACGAAACCATTAACC-3′-->
      attB1                          cagA 1-22
```

attB1-*cagA*601-619-fwd (201-1216) [L: 50 bp; GC: 50%; T_m: 71.952 °C]

```
5′-GGGGACAAGTTTGTACAAAAAAGCAGGCTTAGGGCCTACTGGTGGGGATT-3′-->
      attB1                          cagA 601-619
```

Reverse primers

*cagA*578-600-attB2-rev (1-200) [L: 53 bp; GC: 45.28%; T_m: 70.779 °C]

```
5′-GGGGACCACTTTGTACAAGAAAGCTGGGTATCCATTTTTTCTGCTTCTTGCC-3′-->
      attB2                          cagA 600-578
```

*cagA*3628-3648-attB2-rev (wt & 201-1216) [L: 51 bp; GC: 47.06%; T_m: ,71.01 °C]

```
5′-GGGGACCACTTTGTACAAGAAAGCTGGGTAGCAAGATTTTTGGAAACCACC-3′-->
      attB2                          cagA 3648-3628
```

***cagA* wt:** attB1-*cagA*1-22-fwd + *cagA*3628-3648-attB2-rev

```
        attB1                    cagA 1-22
5′-GGGGACAAGTTTGTACAAAAAAGCAGGCTTAGTGACTAACGAAACCATTAACC-->>--GGTGGTTTCCAAAATCTTGCTACCCAGCTTTCTTGTACAAAGTGGTCCCC-3′
3′-CCCCTGTTCAAACATGTTTTTTCGTCCGAATCACTGATTGCTTTGGTAATTGG--<<--CCACCAAAGGTTTTTAGAACGATGGGTCGAAAGAACATGTTTCACCAGGGG-5′
                                                cagA 3628-3548        attB2
                                  |_____________________________________|
                                  cagA wt (AA 1-1216)
```

***cagA*-NT$_{AA1-200}$:** attB1-*cagA*1-22-fwd + *cagA*578-600-attB2-rev

```
        attB1                    cagA 1-22
5′-GGGGACAAGTTTGTACAAAAAAGCAGGCTTAGTGACTAACGAAACCATTAACC-->>--GGCAAGAAGCAGAAAAAATGGATACCCAGCTTTCTTGTACAAAGTGGTCCCC-3′
3′-CCCCTGTTCAAACATGTTTTTTCGTCCGAATCACTGATTGCTTTGGTAATTGG--<<--CCGTTCTTCGTCTTTTTTACCTATGGGTCGAAAGAACATGTTTCACCAGGGG-5′
                                                cagA 578-600          attB2
                                  |_____________________________________|
                                  cagA-NT (AA 1-200)
```

***cagA*-CT$_{AA201-1216}$:** attB1-*cagA*601-619-fwd + *cagA*3628-3648-attB2-rev

```
        attB1                    cagA 601-619
5′-GGGGACAAGTTTGTACAAAAAAGCAGGCTTAGGGCCTACTGGTGGGGATT-->>--GGTGGTTTCCAAAATCTTGCTACCCAGCTTTCTTGTACAAAGTGGTCCCC-3′
3′-CCCCTGTTCAAACATGTTTTTTCGTCCGAATCCCGGATGACCACCCCTAA--<<--CCACCAAAGGTTTTTAGAACGATGGGTCGAAAGAACATGTTTCACCAGGGG-5′
                                                cagA 3628-3648        attB2
                                  |_____________________________________|
                                  cagA-CT (AA 201-1216)
```

Figure 28: pLenti-*cagA* cloning primers and concept.
Forward (fwd) and reverse (rev) primers to define *cagA* wt and its constructs (*cagA*-NT$_{AA1-200}$ and *cagA*-CT$_{AA201-1216}$) for introduction into pLenti CMV Puro DEST vector (via BP und LR recombination reactions); reading frames as alternating normal/bold nucleotide triplets; to keep *cagA* constructs in frame with attB1 (and therefore the destination vector), two additional nucleotides have been introduced at the forward and one at the reverse primer; *teal*: *cagA*; *brown*: attB1 and attB2 sites; *grey*: recommended sites (according to manufacturer's protocol); *orange*: spacer to keep cagA in frame; *hatched*: synthesized complementary strand; abbreviations: L = length, GC = guanine-cytosine content, T_m = melting temperature.

5.3 Additional figures

5.3.1 MDCK cells: Intracellular localization of CagA-NT$_{AA1-200}$ and CagA-CT$_{AA201-1216}$

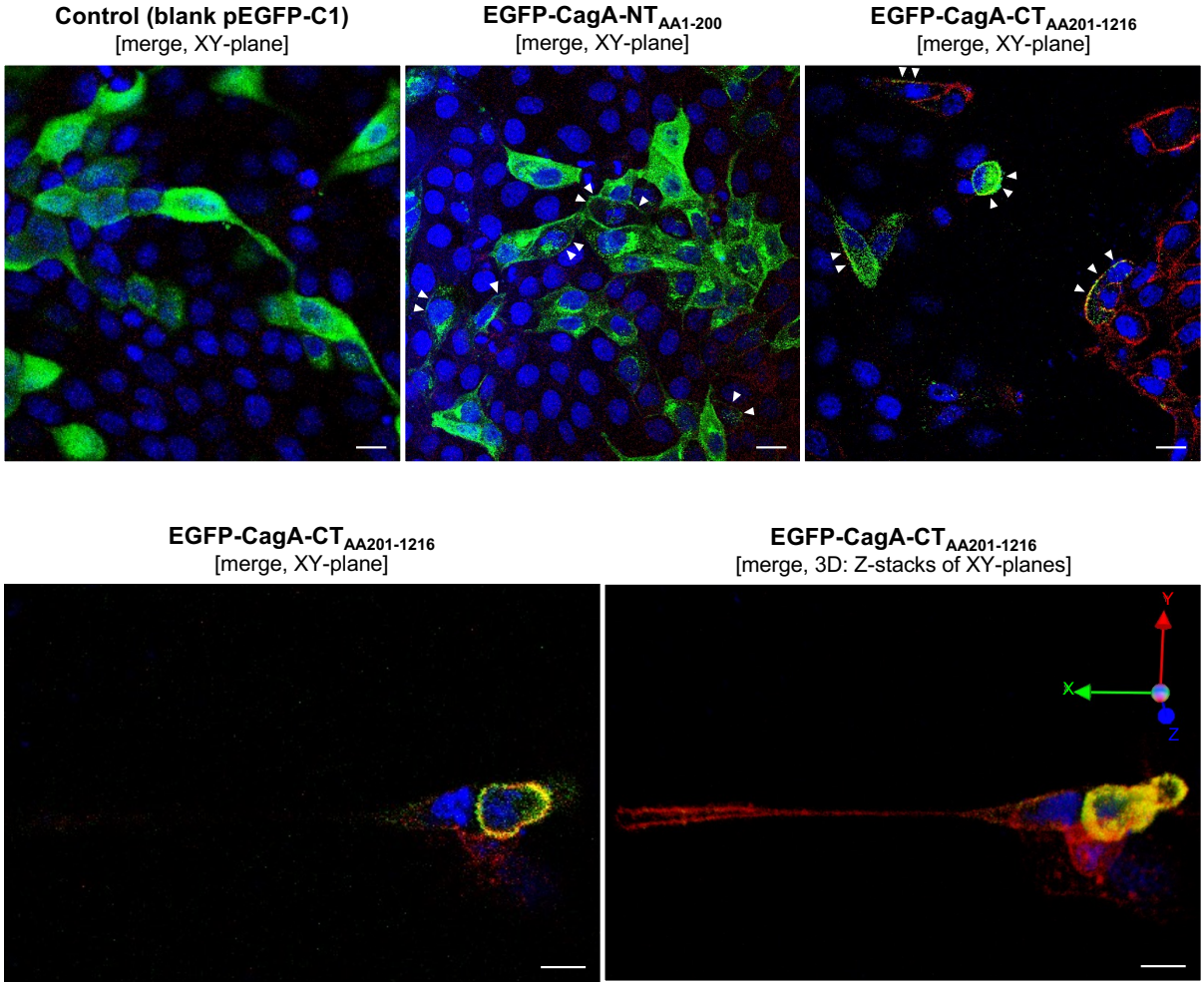

Figure 29: Spatial intracellular distribution of N-terminal EGFP-tagged CagA-NT$_{AA1-200}$ and CagA-CT$_{AA201-1216}$ in (transfected) MDCK cells.
Transient transfection of MDCK cells by means of pEGPF-C1 *cagA* constructs (confluency about 80%, Lipofectamine LTX & PLUS, 500 ng DNA/well, 24-well-plate, 24 h of incubation); confocal laser scanning microscopy: x-y planes and three-dimensional (3D) reconstruction (successive z-stacks of x-y planes), white scale bar: 20 µm; controls: transfection with blank pEGFP-C1; *cyan green*: EGFP (1st anti-body: mouse anti-GFP, 2nd anti-body: goat anti-mouse-IgG Alexa Fluor 488); *blue*: nucleus (DAPI); *red*: F-actin (i.e., plasma membrane, Phalloidin 594); *white arrowheads* (⊳) indicate accumulation at plasma membrane; in these preliminary experiments (with admittedly suboptimal image quality), channels have already been merged; blank vector pEGFP-C1 shows homogenous distribution throughout cytoplasm; EGFP-CagA-NT$_{AA1-200}$ displays affinity for the region of the plasma membrane at lower intracellular concentrations (taking into account the pseudopodia) in addition to strong accumulation in the perinuclear region (presumably rough endoplasmic reticulum) and the fine-granular distribution in the cytoplasm; the expression (i.e., intracellular concentration) of EGFP-CagA-CT$_{AA201-1216}$ was considerably lower, localizing mainly in the F-actin region, as indicated by superimposition (yellow), particularly in the 3D reconstruction; note that EGFP-CagA-NT$_{AA1-200}$ could definitely be verified by western blotting, whereas EGFP-CagA-CT$_{AA201-1216}$ could induce the hummingbird phenotype, but, at best, only the faintest traces of it could be detected in the western blot.

6 Literature

ABERLE, H., BAUER, A., STAPPERT, J., KISPERT, A. & KEMLER, R. 1997. Beta-Catenin Is a Target for the Ubiquitin Proteasome Pathway. *Embo J.,* 16**,** 3797-3804.

ABRAMS, Z. B., JOHNSON, T. S., HUANG, K., PAYNE, P. R. O. & COOMBES, K. 2019. A protocol to evaluate RNA sequencing normalization methods. *BMC Bioinformatics,* 20**,** 679.

AGUILERA, O., FRAGA, M. F., BALLESTAR, E., PAZ, M. F., HERRANZ, M., ESPADA, J., GARCIA, J. M., MUNOZ, A., ESTELLER, M. & GONZALEZ-SANCHO, J. M. 2006. Epigenetic inactivation of the Wnt antagonist DICKKOPF-1 (DKK-1) gene in human colorectal cancer. *Oncogene,* 25**,** 4116-21.

AKOPYANTS, N. S., CLIFTON, S. W., KERSULYTE, D., CRABTREE, J. E., YOUREE, B. E., REECE, C. A., BUKANOV, N. O., DRAZEK, E. S., ROE, B. A. & BERG, D. E. 1998. Analyses of the cag pathogenicity island of Helicobacter pylori. *Molecular Microbiology,* 28**,** 37-53.

ALM, R. A., LING, L. S., MOIR, D. T., KING, B. L., BROWN, E. D., DOIG, P. C., SMITH, D. R., NOONAN, B., GUILD, B. C., DEJONGE, B. L., CARMEL, G., TUMMINO, P. J., CARUSO, A., URIA-NICKELSEN, M., MILLS, D. M., IVES, C., GIBSON, R., MERBERG, D., MILLS, S. D., JIANG, Q., TAYLOR, D. E., VOVIS, G. F. & TRUST, T. J. 1999. Genomic-sequence comparison of two unrelated isolates of the human gastric pathogen Helicobacter pylori. *Nature,* 397**,** 176-80.

ALOK, A., LEI, Z., JAGANNATHAN, N. S., KAUR, S., HARMSTON, N., ROZEN, S. G., TUCKER-KELLOGG, L. & VIRSHUP, D. M. 2017. Wnt proteins synergize to activate beta-catenin signaling. *J Cell Sci,* 130**,** 1532-1544.

AMIEVA, M. R., VOGELMANN, R., COVACCI, A., TOMPKINS, L. S., NELSON, W. J. & FALKOW, S. 2003. Disruption of the epithelial apical-junctional complex by Helicobacter pylori CagA. *Science (New York, N.Y.),* 300**,** 1430-4.

ARAKI, Y., OKAMURA, S., HUSSAIN, S. P., NAGASHIMA, M., HE, P., SHISEKI, M., MIURA, K. & HARRIS, C. C. 2003. Regulation of Cyclooxygenase-2 Expression by the Wnt and Ras Pathways. *Cancer Res.,* 63**,** 728-734.

ARCE, L., YOKOYAMA, N. N. & WATERMAN, M. L. 2006. Diversity of LEF/TCF action in development and disease. *Oncogene,* 25**,** 7492-7504.

ARGENT, R. H., THOMAS, R. J., LETLEY, D. P., RITTIG, M. G., HARDIE, K. R. & ATHERTON, J. C. 2008. Functional association between the Helicobacter pylori virulence factors VacA and CagA. *Journal of medical microbiology,* 57**,** 145-50.

ASCIUTTI, S., AKIRI, G., GRUMOLATO, L., VIJAYAKUMAR, S. & AARONSON, S. A. 2011. Diverse mechanisms of Wnt activation and effects of pathway inhibition on proliferation of human gastric carcinoma cells. *Oncogene,* 30**,** 956-66.

BACKERT, S. & MEYER, T. F. 2006. Type IV secretion systems and their effectors in bacterial pathogenesis. *Current opinion in microbiology,* 9**,** 207-17.

BACKERT, S., SCHWARZ, T., MIEHLKE, S., KIRSCH, C., SOMMER, C., KWOK, T., GERHARD, M., GOEBEL, U. B., LEHN, N., KOENIG, W. & MEYER, T. F. 2004. Functional Analysis of the cag Pathogenicity Island in Helicobacter pylori Isolates from Patients with Gastritis, Peptic Ulcer, and Gastric Cancer. *Infection and Immunity,* 72**,** 1043-1056.

BACKERT, S. & TEGTMEYER, N. 2017. Type IV Secretion and Signal Transduction of Helicobacter pylori CagA through Interactions with Host Cell Receptors. *Toxins (Basel),* 9.

BACKERT, S., TEGTMEYER, N. & SELBACH, M. 2010. The versatility of helicobacter pylori caga effector protein functions: The master key hypothesis. *Helicobacter,* 15**,** 163-176.

BACKERT, S., ZISKA, E., BRINKMANN, V., ZIMNY-ARNDT, U., FAUCONNIER, A., JUNGBLUT, P. R., NAUMANN, M. & MEYER, T. F. 2000. Translocation of the Helicobacter pylori CagA protein in gastric epithelial cells by a type IV secretion apparatus. *Cell Microbiol,* 2**,** 155-64.

BAGNOLI, F., BUTI, L., TOMPKINS, L., COVACCI, A. & AMIEVA, M. R. 2005. Helicobacter pylori CagA induces a transition from polarized to invasive phenotypes in MDCK cells. *Proc Natl Acad Sci U S A,* 102**,** 16339-44.

BALTRUS, D. A., AMIEVA, M. R., COVACCI, A., LOWE, T. M., MERRELL, D. S., OTTEMANN, K. M., STEIN, M., SALAMA, N. R. & GUILLEMIN, K. 2009. The complete genome sequence of Helicobacter pylori strain G27. *Journal of Bacteriology,* 91**,** 447-448.

BARDWELL, L. 1989. The mutagenic and carcinogenic effects of gene transfer. *Mutagenesis,* 4**,** 245-53.

BARKER, N., HUCH, M., KUJALA, P., VAN DE WETERING, M., SNIPPERT, H. J., VAN ES, J. H., SATO, T., STANGE, D. E., BEGTHEL, H., VAN DEN BORN, M., DANENBERG, E., VAN DEN BRINK, S., KORVING, J., ABO, A., PETERS, P. J., WRIGHT, N., POULSOM, R. & CLEVERS, H. 2010. Lgr5(+ve) stem cells drive self-renewal in the stomach and build long-lived gastric units in vitro. *Cell Stem Cell,* 6**,** 25-36.

BASTOS, J., PELETEIRO, B., PINTO, H., MARINHO, A., GUIMARÃES, J. T., RAMOS, E., LA VECCHIA, C., BARROS, H. & LUNET, N. 2013. Prevalence, incidence and risk factors for Helicobacter pylori infection in a cohort of Portuguese adolescents (EpiTeen). *Digestive and liver disease : official journal of the Italian Society of Gastroenterology and the Italian Association for the Study of the Liver,* 45**,** 290-5.

BECKER, K. F., ATKINSON, M. J., REICH, U., BECKER, I., NEKARDA, H., SIEWERT, J. R. & HOFLER, H. 1994. E-cadherin gene mutations provide clues to diffuse type gastric carcinomas. *Cancer Res,* 54**,** 3845-52.

BEHRE, G., SMITH, L. T. & TENEN, D. G. 1999. Use of a promoterless Renilla luciferase vector as an internal control plasmid for transient co-transfection assays of Ras-mediated transcription activation. *Biotechniques,* 26**,** 24-6, 28.

BEHRENS, J., VON KRIES, J. P., KÜHL, M., BRUHN, L., WEDLICH, D., GROSSCHEDL, R. & BIRCHMEIER, W. 1996. Functional interaction of beta-catenin with the transcription factor LEF-1. *Nature,* 382**,** 638-42.

BEN-DAVID, U., SIRANOSIAN, B., HA, G., TANG, H., OREN, Y., HINOHARA, K., STRATHDEE, C. A., DEMPSTER, J., LYONS, N. J., BURNS, R., NAG, A., KUGENER, G., CIMINI, B., TSVETKOV, P., MARUVKA, Y. E., O'ROURKE, R., GARRITY, A., TUBELLI, A. A., BANDOPADHAYAY, P., TSHERNIAK, A., VAZQUEZ, F., WONG, B., BIRGER, C., GHANDI, M., THORNER, A. R., BITTKER, J. A., MEYERSON, M., GETZ, G., BEROUKHIM, R. & GOLUB, T. R. 2018. Genetic and transcriptional evolution alters cancer cell line drug response. *Nature,* 560**,** 325-330.

BERK, A. J. 2005. Recent lessons in gene expression, cell cycle control, and cell biology from adenovirus. *Oncogene,* 24**,** 7673-85.

BERTAUX-SKEIRIK, N., FENG, R., SCHUMACHER, M. A., LI, J., MAHE, M. M., ENGEVIK, A. C., JAVIER, J. E., PEEK, R. M., OTTEMANN, K., ORIAN-ROUSSEAU, V., BOIVIN, G. P., HELMRATH, M. A. & ZAVROS, Y. 2015. CD44 Plays a Functional Role in Helicobacter pylori-induced Epithelial Cell Proliferation. *PLoS Pathogens,* 11**,** 1-24.

BHANOT, P., BRINK, M., SAMOS, C. H., HSIEH, J. C., WANG, Y., MACKE, J. P., ANDREW, D., NATHANS, J. & NUSSE, R. 1996. A new member of the frizzled family from Drosophila functions as a Wingless receptor. *Nature,* 382**,** 225-30.

BIRCHMEIER, C., BIRCHMEIER, W., GHERARDI, E. & VANDE WOUDE, G. F. 2003. Met, metastasis, motility and more. *Nat Rev Mol Cell Biol,* 4**,** 915-25.

BLANCHARD, T. G. & NEDRUD, J. G. 2012. Laboratory maintenance of Helicobacter species. *Curr Protoc Microbiol,* Chapter 8**,** Unit8B 1.

BOL, G. M., VESUNA, F., XIE, M., ZENG, J., AZIZ, K., GANDHI, N., LEVINE, A., IRVING, A., KORZ, D., TANTRAVEDI, S., HEERMA VAN VOSS, M. R., GABRIELSON, K., BORDT, E. A., POLSTER, B. M., COPE, L., VAN DER GROEP, P., KONDASKAR, A., RUDEK, M. A., HOSMANE, R. S., VAN DER WALL, E., VAN DIEST, P. J., TRAN, P. T. & RAMAN, V. 2015. Targeting DDX3 with a small molecule inhibitor for lung cancer therapy. *EMBO Mol Med,* 7**,** 648-69.

BORGGREFE, T., LAUTH, M., ZWIJSEN, A., HUYLEBROECK, D., OSWALD, F. & GIAIMO, B. D. 2016. The Notch intracellular domain integrates signals from Wnt, Hedgehog, TGFβ/BMP and hypoxia pathways. *Biochimica et Biophysica Acta - Molecular Cell Research,* 1863**,** 303-313.

BOTLAGUNTA, M., VESUNA, F., MIRONCHIK, Y., RAMAN, A., LISOK, A., WINNARD, P., JR., MUKADAM, S., VAN DIEST, P., CHEN, J. H., FARABAUGH, P., PATEL, A. H. & RAMAN, V. 2008. Oncogenic role of DDX3 in breast cancer biogenesis. *Oncogene,* 27**,** 3912-22.

BRABLETZ, T., JUNG, A., DAG, S., HLUBEK, F. & KIRCHNER, T. 1999. β-Catenin Regulates the Expression of the Matrix Metalloproteinase-7 in Human Colorectal Cancer. *The American journal of pathology,* 155**,** 1033-1038.

BRANDT, S., KWOK, T., HARTIG, R., KÖNIG, W. & BACKERT, S. 2005. NF-kappaB activation and potentiation of proinflammatory responses by the Helicobacter pylori CagA protein. *Proceedings of the National Academy of Sciences of the United States of America,* 102**,** 9300-5.

BRENNER, O., LEVANON, D., NEGREANU, V., GOLUBKOV, O., FAINARU, O., WOOLF, E. & GRONER, Y. 2004. Loss of Runx3 function in leukocytes is associated with spontaneously developed colitis and gastric mucosal hyperplasia. *Proc Natl Acad Sci U S A,* 101**,** 16016-21.

BRONTE-TINKEW, D. M., TEREBIZNIK, M., FRANCO, A., ANG, M., AHN, D., MIMURO, H., SASAKAWA, C., ROPELESKI, M. J., PEEK, R. M., JR. & JONES, N. L. 2009. Helicobacter pylori cytotoxin-associated gene A activates the signal transducer and activator of transcription 3 pathway in vitro and in vivo. *Cancer Res,* 69**,** 632-9.

BURRELL, R. A., MCCLELLAND, S. E., ENDESFELDER, D., GROTH, P., WELLER, M. C., SHAIKH, N., DOMINGO, E., KANU, N., DEWHURST, S. M., GRONROOS, E., CHEW, S. K., ROWAN, A. J., SCHENK, A., SHEFFER, M., HOWELL, M., KSCHISCHO, M., BEHRENS, A., HELLEDAY, T., BARTEK, J., TOMLINSON, I. P. & SWANTON, C. 2013. Replication stress links structural and numerical cancer chromosomal instability. *Nature,* 494**,** 492-496.

CACA, K., KOLLIGS, F. T., JI, X., HAYES, M., QIAN, J., YAHANDA, A., RIMM, D. L., COSTA, J. & FEARON, E. R. 1999. Beta- and gamma-catenin mutations, but not E-cadherin inactivation, underlie T-cell factor/lymphoid enhancer factor transcriptional deregulation in gastric and pancreatic cancer. *Cell Growth & Differentiation,* 10**,** 369–376.

CAMPEAU, E. 2016. *www.ericcampeau.com* [Online]. Eric Campeau. Available: http://www.ericcampeau.com/manuals.html [Accessed].

CAMPEAU, E., RUHL, V. E., RODIER, F., SMITH, C. L., RAHMBERG, B. L., FUSS, J. O., CAMPISI, J., YASWEN, P., COOPER, P. K. & KAUFMAN, P. D. 2009. A Versatile Viral System for Expression and Depletion of Proteins in Mammalian Cells. *PLoS ONE,* 4**,** e6529-e6529.

CANCER CELL LINE ENCYCLOPEDIA. 2022. *CCLE* [Online]. Broad Institute, Cambridge, Massachusetts, United States. Available: https://sites.broadinstitute.org/ccle/ [Accessed 2021].

CANCER DEPENDENCY MAP. 2021. *DepMap portal (Expression 22Q1 Public)* [Online]. Broad Institute, Cambridge, Massachusetts, United States. Available: https://depmap.org/portal/ [Accessed 2021].

CASTELLONE, M. D., TERAMOTO, H., WILLIAMS, B. O., DRUEY, K. M. & GUTKIND, J. S. 2005. Prostaglandin E2 promotes colon cancer cell growth through a Gs-axin-beta-catenin signaling axis. *Science (New York, N.Y.),* 310**,** 1504-10.

CATALOGUE OF SOMATIC MUTATIONS IN CANCER. 2021. *COSMIC (v95, released 24-NOV-21)* [Online]. Wellcome Sanger Institute, Hinxton, United Kingdom. Available: https://cancer.sanger.ac.uk/cosmic, https://cancer.sanger.ac.uk/cell_lines/ [Accessed 2021].

CELLI, J. P., TURNER, B. S., AFDHAL, N. H., KEATES, S., GHIRAN, I., KELLY, C. P., EWOLDT, R. H., MCKINLEY, G. H., SO, P., ERRAMILLI, S. & BANSIL, R. 2009. Helicobacter pylori moves through mucus by reducing mucin viscoelasticity. *Proceedings of the National Academy of Sciences of the United States of America,* 106**,** 14321-6.

CENSINI, S., LANGE, C., XIANG, Z., CRABTREE, J. E., GHIARA, P., BORODOVSKY, M., RAPPUOLI, R. & COVACCI, A. 1996. cag, a pathogenicity island of Helicobacter pylori, encodes type I-specific and disease-associated virulence factors. *Proceedings of the National Academy of Sciences of the United States of America,* 93**,** 14648-53.

CHALFIE, M., TU, Y., EUSKIRCHEN, G., WARD, W. W. & PRASHER, D. C. 1994. Green fluorescent protein as a marker for gene expression. *Science (New York, N.Y.),* 263**,** 802-805.

CHANG, M. T., ASTHANA, S., GAO, S. P., LEE, B. H., CHAPMAN, J. S., KANDOTH, C., GAO, J., SOCCI, N. D., SOLIT, D. B., OLSHEN, A. B., SCHULTZ, N. & TAYLOR, B. S. 2016. Identifying recurrent mutations in cancer reveals widespread lineage diversity and mutational specificity. *Nat Biotechnol,* 34**,** 155-63.

CHEN, W., TEN BERGE, D., BROWN, J., AHN, S., HU, L. A., MILLER, W. E., CARON, M. G., BARAK, L. S., NUSSE, R. & LEFKOWITZ, R. J. 2003. Dishevelled 2 recruits beta-arrestin 2 to mediate Wnt5A-stimulated endocytosis of Frizzled 4. *Science (New York, N.Y.),* 301**,** 1391-4.

CHEROUTRE, H., LAMBOLEZ, F. & MUCIDA, D. 2011. The light and dark sides of intestinal intraepithelial lymphocytes. *Nat Rev Immunol,* 11**,** 445-56.

CHURIN, Y., AL-GHOUL, L., KEPP, O., MEYER, T. F., BIRCHMEIER, W. & NAUMANN, M. 2003. Helicobacter pylori CagA protein targets the c-Met receptor and enhances the motogenic response. *J Cell Biol,* 161**,** 249-55.

CINGHU, S., GOH, Y. M., OH, B. C., LEE, Y. S., LEE, O. J., DEVARAJ, H. & BAE, S. C. 2012. Phosphorylation of the gastric tumor suppressor RUNX3 following H. pylori infection results in its localization to the cytoplasm. *J Cell Physiol,* 227**,** 1071-80.

CLEMENTS, W. M., WANG, J., SARNAIK, A., KIM, O. J., MACDONALD, J., FENOGLIO-PREISER, C., GRODEN, J. & LOWY, A. M. 2002. β-Catenin Mutation Is a Frequent Cause of Wnt Pathway Activation in Gastric Cancer. *Cancer Research,* 62**,** 3503-3506.

CLEVERS, H. 2006. Wnt/β-Catenin Signaling in Development and Disease. *Cell,* 127**,** 469-480.

CLEVERS, H. & NUSSE, R. 2012. Wnt/β-Catenin Signaling and Disease. *Cell,* 149**,** 1192-1205.

CLINICAL GENOME RESOURCE. 2022. *ClinGen* [Online]. National Institutes of Health (NIH), Bethesda, Maryland, United States. Available: https://clinicalgenome.org/ [Accessed 2022].

CONRADI, J., TEGTMEYER, N., WOŹNA, M., WISSBROCK, M., MICHALEK, C., GAGELL, C., COVER, T. L., FRANK, R., SEWALD, N. & BACKERT, S. 2012. An RGD helper sequence in CagL of Helicobacter pylori assists in interactions with integrins and injection of CagA. *Frontiers in cellular and infection microbiology,* 2**,** 70-70.

COOKE, C. L., HUFF, J. L. & SOLNICK, J. V. 2005. The role of genome diversity and immune evasion in persistent infection with Helicobacter pylori. *FEMS immunology and medical microbiology,* 45**,** 11-23.

CORMACK, B. P., VALDIVIA, R. H. & FALKOW, S. 1996. FACS-optimized mutants of the green fluorescent protein (GFP). *Gene,* 173**,** 33-8.

CORREA, P. 1988. A Human Model of Gastric Carcinogenesis. *Cancer Research,* 48**,** 3554-3560.

COVACCI, A., CENSINI, S., BUGNOLI, M., PETRACCA, R., BURRONI, D., MACCHIA, G., MASSONE, A., PAPINI, E., XIANG, Z. & FIGURA, N. 1993. Molecular characterization of the 128-kDa immunodominant antigen of Helicobacter pylori associated with cytotoxicity and duodenal ulcer. *Proceedings of the National Academy of Sciences,* 90**,** 5791-5795.

COVACCI, A., TELFORD, J. L., DEL GIUDICE, G., PARSONNET, J. & RAPPUOLI, R. 1999. Helicobacter pylori virulence and genetic geography. *Science (New York, N.Y.),* 284**,** 1328-1333.

COVER, T. L. & BLANKE, S. R. 2005. Helicobacter pylori VacA, a paradigm for toxin multifunctionality. *Nature reviews. Microbiology,* 3**,** 320-32.

CRABTREE, J. E., KERSULYTE, D., LI, S. D., LINDLEY, I. J. & BERG, D. E. 1999. Modulation of Helicobacter pylori induced interleukin-8 synthesis in gastric epithelial cells mediated by cag PAI encoded VirD4 homologue. *J Clin Pathol,* 52**,** 653-657.

CRUCIAT, C. M., DOLDE, C., DE GROOT, R. E., OHKAWARA, B., REINHARD, C., KORSWAGEN, H. C. & NIEHRS, C. 2013. RNA helicase DDX3 is a regulatory subunit of casein kinase 1 in Wnt-beta-catenin signaling. *Science,* 339**,** 1436-41.

DANIELS, D. L. & WEIS, W. I. 2005. Beta-catenin directly displaces Groucho/TLE repressors from Tcf/Lef in Wnt-mediated transcription activation. *Nature structural & molecular biology,* 12**,** 364-71.

DE BERNARD, M., ARICO, B., PAPINI, E., RIZZUTO, R., GRANDI, G., RAPPUOLI, R. & MONTECUCCO, C. 1997. Helicobacter pylori toxin VacA induces vacuole formation by acting in the cell cytosol. *Molecular microbiology,* 26**,** 665-74.

DEMEREC, M., ADELBERG, E. A., CLARK, A. J. & HARTMAN, P. E. 1966. A proposal for a uniform nomenclature in bacterial genetics. *Genetics,* 54**,** 61-76.

DEN DUNNEN, J. T., DALGLEISH, R., MAGLOTT, D. R., HART, R. K., GREENBLATT, M. S., MCGOWAN-JORDAN, J., ROUX, A. F., SMITH, T., ANTONARAKIS, S. E. & TASCHNER, P. E. 2016. HGVS Recommendations for the Description of Sequence Variants: 2016 Update. *Hum Mutat,* 37**,** 564-9.

DEN HOLLANDER, W. J., HOLSTER, I. L., DEN HOED, C. M., VAN DEURZEN, F., VAN VUUREN, A. J., JADDOE, V. W., HOFMAN, A., PEREZ PEREZ, G. I., BLASER, M. J., MOLL, H. A. & KUIPERS, E. J. 2013. Ethnicity is a strong predictor for Helicobacter pylori infection in

young women in a multi-ethnic European city. *Journal of gastroenterology and hepatology,* 28**,** 1705-11.

DENG, J., MILLER, S. A., WANG, H.-Y., XIA, W., WEN, Y., ZHOU, B. P., LI, Y., LIN, S.-Y. & HUNG, M.-C. 2002. β-catenin interacts with and inhibits NF-κB in human colon and breast cancer. *Cancer Cell,* 2**,** 323-334.

DENG, J., XIA, W., MILLER, S. A., WEN, Y., WANG, H. Y. & HUNG, M. C. 2004. Crossregulation of NF-kappaB by the APC/GSK-3beta/beta-catenin pathway. *Mol Carcinog,* 39**,** 139-46.

DILLIES, M. A., RAU, A., AUBERT, J., HENNEQUET-ANTIER, C., JEANMOUGIN, M., SERVANT, N., KEIME, C., MAROT, G., CASTEL, D., ESTELLE, J., GUERNEC, G., JAGLA, B., JOUNEAU, L., LALOE, D., LE GALL, C., SCHAEFFER, B., LE CROM, S., GUEDJ, M., JAFFREZIC, F. & FRENCH STATOMIQUE, C. 2013. A comprehensive evaluation of normalization methods for Illumina high-throughput RNA sequencing data analysis. *Brief Bioinform,* 14**,** 671-83.

DOLDE, C., BISCHOF, J., GRUTER, S., MONTADA, A., HALEKOTTE, J., PEIFER, C., KALBACHER, H., BAUMANN, U., KNIPPSCHILD, U. & SUTER, B. 2018. A CK1 FRET biosensor reveals that DDX3X is an essential activator of CK1epsilon. *J Cell Sci,* 131.

DUBRIDGE, R. B., TANG, P., HSIA, H. C., LEONG, P.-M., MILLER, J. H. & CALOS, M. P. 1987. Analysis of Mutation in Human Cells by Using an Epstein-Barr Virus Shuttle System. *MOLECULAR AND CELLULAR BIOLOGY,* 7**,** 379-387.

DUVAL, A., IACOPETTA, B., RANZANI, G. N., LOTHE, R. A., THOMAS, G. & HAMELIN, R. 1999. Variable mutation frequencies in coding repeats of TCF-4 and other target genes in colon, gastric and endometrial carcinoma showing microsatellite instability. *Oncogene,* 18**,** 6806-9.

EASTMAN, S. J., SIEGEL, C., TOUSIGNANT, J., SMITH, A. E., CHENG, S. H. & SCHEULE, R. K. 1997. Biophysical characterization of cationic lipid: DNA complexes. *Biochimica et biophysica acta,* 1325**,** 41-62.

EBERT, M. P., FEI, G., KAHMANN, S., MULLER, O., YU, J., SUNG, J. J. & MALFERTHEINER, P. 2002. Increased beta-catenin mRNA levels and mutational alterations of the APC and beta-catenin gene are present in intestinal-type gastric cancer. *Carcinogenesis,* 23**,** 87-91.

EL-ETR, S. H., MUELLER, A., TOMPKINS, L. S., FALKOW, S. & MERRELL, D. S. 2004. Phosphorylation-independent effects of CagA during interaction between Helicobacter pylori and T84 polarized monolayers. *The Journal of infectious diseases,* 190**,** 1516-23.

ERNST, P. B. & GOLD, B. D. 2000. The disease spectrum of Helicobacter pylori: the immunopathogenesis of gastroduodenal ulcer and gastric cancer. *Annual review of microbiology,* 54**,** 615-40.

EUROPEAN MOLECULAR BIOLOGY LABORATORY. 2021. *Ensembl (release 105 - Dec 2021)* [Online]. European Bioinformatics Institute (EBI), European Molecular Biology Laboratory (EMBL). Available: https://www.ensembl.org [Accessed 2021].

EVERHART, J. E. 2000. Recent developments in the epidemiology of Helicobacter pylori. *Gastroenterology clinics of North America,* 29**,** 559-78.

EVOLUTIONARY BIOINFORMATICS GROUP. 2022. *Bgee (Version 14.2)* [Online]. Swiss Institute of Bioinformatics, University of Lausanne, Lausanne, Switzerland. Available: https://bgee.org [Accessed 2022].

FALUSH, D., STEPHENS, M. & PRITCHARD, J. K. 2003. Inference of population structure using multilocus genotype data: linked loci and correlated allele frequencies. *Genetics,* 164**,** 1567-87.

FANG, Z., XIONG, Y., LI, J., LIU, L., ZHANG, W., ZHANG, C. & WAN, J. 2012. APC gene deletions in gastric adenocarcinomas in a Chinese population: a correlation with tumour progression. *Clin Transl Oncol,* 14**,** 60-5.

FASSAN, M., SIMBOLO, M., BRIA, E., MAFFICINI, A., PILOTTO, S., CAPELLI, P., BENCIVENGA, M., PECORI, S., LUCHINI, C., NEVES, D., TURRI, G., VICENTINI, C., MONTAGNA, L., TOMEZZOLI, A., TORTORA, G., CHILOSI, M., DE MANZONI, G. & SCARPA, A. 2014. High-throughput mutation profiling identifies novel molecular dysregulation in high-grade intraepithelial neoplasia and early gastric cancers. *Gastric Cancer,* 17**,** 442-9.

FELGNER, P. L., GADEK, T. R., HOLM, M., ROMAN, R., CHAN, H. W., WENZ, M., NORTHROP, J. P., RINGOLD, G. M. & DANIELSEN, M. 1987. Lipofection: a highly efficient, lipid-mediated DNA-transfection procedure. *Proceedings of the National Academy of Sciences,* 84**,** 7413-7417.

FISCHER, W., PULS, J., BUHRDORF, R., GEBERT, B., ODENBREIT, S. & HAAS, R. 2001. Systematic mutagenesis of the Helicobacter pylori cag pathogenicity island: essential genes for CagA translocation in host cells and induction of interleukin-8. *Mol Microbiol,* 42**,** 1337-48.

FLANAGAN, D. J., BARKER, N., COSTANZO, N. S. D., MASON, E. A., GURNEY, A., MENIEL, V. S., KOUSHYAR, S., AUSTIN, C. R., ERNST, M., PEARSON, H. B., BOUSSIOUTAS, A., CLEVERS, H., PHESSE, T. J. & VINCAN, E. 2019. Frizzled-7 Is Required for Wnt Signaling in Gastric Tumors with and Without Apc Mutations. *Cancer Res,* 79**,** 970-981.

FRANCO, A. T., ISRAEL, D. A., WASHINGTON, M. K., KRISHNA, U., FOX, J. G., ROGERS, A. B., NEISH, A. S., COLLIER-HYAMS, L., PEREZ-PEREZ, G. I., HATAKEYAMA, M., WHITEHEAD, R., GAUS, K., O'BRIEN, D. P., ROMERO-GALLO, J. & PEEK, R. M., JR. 2005. Activation of beta-catenin by carcinogenic Helicobacter pylori. *Proc Natl Acad Sci U S A,* 102**,** 10646-51.

FUKASE, K., KATO, M., KIKUCHI, S., INOUE, K., UEMURA, N., OKAMOTO, S., TERAO, S., AMAGAI, K., HAYASHI, S., ASAKA, M. & JAPAN GAST STUDY, G. 2008. Effect of eradication of Helicobacter pylori on incidence of metachronous gastric carcinoma

after endoscopic resection of early gastric cancer: an open-label, randomised controlled trial. *Lancet,* 372**,** 392-7.

GAO, C., FURGE, K., KOEMAN, J., DYKEMA, K., SU, Y., CUTLER, M. L., WERTS, A., HAAK, P. & VANDE WOUDE, G. F. 2007. Chromosome instability, chromosome transcriptome, and clonal evolution of tumor cell populations. *Proc Natl Acad Sci U S A,* 104**,** 8995-9000.

GAO, C., XIE, R., REN, C. & YANG, X. 2012. Dickkopf-1 expression is a novel prognostic marker for gastric cancer. *J Biomed Biotechnol,* 2012**,** 804592.

GENOME AGGREGATION DATABASE. 2018. *gnomAD (v2.1.1 variant)* [Online]. Broad Institute, Cambridge, Massachusetts, United States. Available: https://gnomad.broadinstitute.org [Accessed 2022].

GERHARD, M., LEHN, N., NEUMAYER, N., BORÉN, T., RAD, R., SCHEPP, W., MIEHLKE, S., CLASSEN, M. & PRINZ, C. 1999. Clinical relevance of the Helicobacter pylori gene for blood-group antigen-binding adhesin. *Proceedings of the National Academy of Sciences of the United States of America,* 96**,** 12778-12783.

GHANDI, M., HUANG, F. W., JANE-VALBUENA, J., KRYUKOV, G. V., LO, C. C., MCDONALD, E. R., 3RD, BARRETINA, J., GELFAND, E. T., BIELSKI, C. M., LI, H., HU, K., ANDREEV-DRAKHLIN, A. Y., KIM, J., HESS, J. M., HAAS, B. J., AGUET, F., WEIR, B. A., ROTHBERG, M. V., PAOLELLA, B. R., LAWRENCE, M. S., AKBANI, R., LU, Y., TIV, H. L., GOKHALE, P. C., DE WECK, A., MANSOUR, A. A., OH, C., SHIH, J., HADI, K., ROSEN, Y., BISTLINE, J., VENKATESAN, K., REDDY, A., SONKIN, D., LIU, M., LEHAR, J., KORN, J. M., PORTER, D. A., JONES, M. D., GOLJI, J., CAPONIGRO, G., TAYLOR, J. E., DUNNING, C. M., CREECH, A. L., WARREN, A. C., MCFARLAND, J. M., ZAMANIGHOMI, M., KAUFFMANN, A., STRANSKY, N., IMIELINSKI, M., MARUVKA, Y. E., CHERNIACK, A. D., TSHERNIAK, A., VAZQUEZ, F., JAFFE, J. D., LANE, A. A., WEINSTOCK, D. M., JOHANNESSEN, C. M., MORRISSEY, M. P., STEGMEIER, F., SCHLEGEL, R., HAHN, W. C., GETZ, G., MILLS, G. B., BOEHM, J. S., GOLUB, T. R., GARRAWAY, L. A. & SELLERS, W. R. 2019. Next-generation characterization of the Cancer Cell Line Encyclopedia. *Nature,* 569**,** 503-508.

GIBSON, D. G. 2011. Enzymatic assembly of overlapping DNA fragments. *Methods in Enzymology,* 498**,** 349-361.

GIBSON, D. G., YOUNG, L., CHUANG, R.-Y., VENTER, J. C., HUTCHISON, C. A. & SMITH, H. O. 2009. Enzymatic assembly of DNA molecules up to several hundred kilobases. *Nature methods,* 6**,** 343-5.

GLOWINSKI, F., HOLLAND, C., THIEDE, B., JUNGBLUT, P. R. & MEYER, T. F. 2014. Analysis of T4SS-induced signaling by H. pylori using quantitative phosphoproteomics. *Front Microbiol,* 5**,** 356.

GO, M., KAPUR, V., GRAHAM, D. & MUSSER, J. 1996. Population genetic analysis of Helicobacter pylori by multilocus enzyme electrophoresis: extensive allelic diversity and recombinational population structure. *Journal of bacteriology,* 178**,** 3934-8.

GOENTORO, L. & KIRSCHNER, M. W. 2009. Evidence that Fold-Change, and Not Absolute Level, of ??-Catenin Dictates Wnt Signaling. *Molecular Cell,* 36**,** 872-884.

GONG, Y., BOURHIS, E., CHIU, C., STAWICKI, S., DEALMEIDA, V. I., LIU, B. Y., PHAMLUONG, K., CAO, T. C., CARANO, R. A. D., ERNST, J. A., SOLLOWAY, M., RUBINFELD, B., HANNOUSH, R. N., WU, Y., POLAKIS, P. & COSTA, M. 2010. Wnt isoform-specific interactions with coreceptor specify inhibition or potentiation of signaling by LRP6 antibodies. *PloS one,* 5**,** e12682-e12682.

GRAHAM, D. Y. 2015. Helicobacter pylori Update: Gastric Cancer, Reliable Therapy, and Possible Benefits. *Gastroenterology,* 148**,** 719-731.e3.

GRAHAM, F. L., SMILEY, J., RUSSELL, W. C. & NAIRN, R. 1977. Characteristics of a human cell line transformed by DNA from human adenovirus type 5. *J Gen Virol,* 36**,** 59-74.

GTEX CONSORTIUM 2013. The Genotype-Tissue Expression (GTEx) project. *Nat Genet,* 45**,** 580-5.

GUILFORD, P., HOPKINS, J., HARRAWAY, J., MCLEOD, M., MCLEOD, N., HARAWIRA, P., TAITE, H., SCOULAR, R., MILLER, A. & REEVE, A. E. 1998. E-cadherin germline mutations in familial gastric cancer. *Nature,* 392**,** 402-5.

GUO, Z., NEILSON, L. J., ZHONG, H., MURRAY, P. S., ZANIVAN, S. & ZAIDEL-BAR, R. 2014. E-cadherin interactome complexity and robustness resolved by quantitative proteomics. *Sci Signal,* 7**,** rs7.

HA, N. C., TONOZUKA, T., STAMOS, J. L., CHOI, H. J. & WEIS, W. I. 2004. Mechanism of phosphorylation-dependent binding of APC to beta-catenin and its role in beta-catenin degradation. *Mol Cell,* 15**,** 511-21.

HABERMANN, J. K., BUNDGEN, N. K., GEMOLL, T., HAUTANIEMI, S., LUNDGREN, C., WANGSA, D., DOERING, J., BRUCH, H. P., NORDSTROEM, B., ROBLICK, U. J., JORNVALL, H., AUER, G. & RIED, T. 2011. Genomic instability influences the transcriptome and proteome in endometrial cancer subtypes. *Mol Cancer,* 10**,** 132.

HADJIHANNAS, M. V., BRUCKNER, M. & BEHRENS, J. 2010. Conductin/axin2 and Wnt signalling regulates centrosome cohesion. *EMBO Rep,* 11**,** 317-24.

HAO, H. X., XIE, Y., ZHANG, Y., CHARLAT, O., OSTER, E., AVELLO, M., LEI, H., MICKANIN, C., LIU, D., RUFFNER, H., MAO, X., MA, Q., ZAMPONI, R., BOUWMEESTER, T., FINAN, P. M., KIRSCHNER, M. W., PORTER, J. A., SERLUCA, F. C. & CONG, F. 2012. ZNRF3 promotes Wnt receptor turnover in an R-spondin-sensitive manner. *Nature,* 485**,** 195-200.

HART, M. J., DE LOS SANTOS, R., ALBERT, I. N., RUBINFELD, B. & POLAKIS, P. 1998. Downregulation of β-catenin by human Axin and its association with the APC tumor suppressor, β-catenin and GSK3β. *Current Biology,* 8**,** 573-581.

HARTLEY, J. L., TEMPLE, G. F. & BRASCH, M. A. 2000. DNA cloning using in vitro site-specific recombination. *Genome research,* 10**,** 1788-95.

HATAKEYAMA, M. 2004. Oncogenic mechanisms of the Helicobacter pylori CagA protein. *Nature reviews. Cancer,* 4**,** 688-94.

HAUSER, C. A., WESTWICK, J. K. & QUILLIAM, L. A. 1995. Ras-mediated transcription activation: analysis by transient cotransfection assays. *Methods Enzymol,* 255**,** 412-26.

HAYASHI, T., SENDA, M., MOROHASHI, H., HIGASHI, H., HORIO, M., KASHIBA, Y., NAGASE, L., SASAYA, D., SHIMIZU, T., VENUGOPALAN, N., KUMETA, H., NODA, N. N., INAGAKI, F., SENDA, T. & HATAKEYAMA, M. 2012. Tertiary structure-function analysis reveals the pathogenic signaling potentiation mechanism of Helicobacter pylori oncogenic effector CagA. *Cell host & microbe,* 12**,** 20-33.

HE, T. C., SPARKS, A. B., RAGO, C., HERMEKING, H., ZAWEL, L., DA COSTA, L. T., MORIN, P. J., VOGELSTEIN, B. & KINZLER, K. W. 1998. Identification of c-MYC as a target of the APC pathway. *Science (New York, N.Y.),* 281**,** 1509-12.

HEDGEPETH, C. M., CONRAD, L. J., ZHANG, J., HUANG, H. C., LEE, V. M. & KLEIN, P. S. 1997. Activation of the Wnt signaling pathway: a molecular mechanism for lithium action. *Dev Biol,* 185**,** 82-91.

HEERMA VAN VOSS, M. R., VAN DIEST, P. J. & RAMAN, V. 2017. Targeting RNA helicases in cancer: The translation trap. *Biochim Biophys Acta Rev Cancer,* 1868**,** 510-520.

HEERMA VAN VOSS, M. R. V. F. R., V. 2015. Identification of the DEAD box RNA helicase DDX3 as a therapeutic target in colorectal cancer. *Oncotarget,* 6**,** 28312-28326.

HEK293 MULTIGENOME VARIATION VIEWER. 2014. *Version 1* [Online]. Vlaams Instituut voor Biotechnologie (VIB), Belgium. Available: http://www.hek293genome.org/v1/ [Accessed 2021].

HEMPEL, H. A., BURNS, K. H., DE MARZO, A. M. & SFANOS, K. S. 2013. Infection of Xenotransplanted Human Cell Lines by Murine Retroviruses: A Lesson Brought Back to Light by XMRV. *Front Oncol,* 3**,** 156.

HENDRIKS, B. & REICHMANN, E. 2002. Wnt signaling: a complex issue. *Biological research,* 35**,** 277-86.

HERBST, A., JURINOVIC, V., KREBS, S., THIEME, S. E., BLUM, H., GOKE, B. & KOLLIGS, F. T. 2014. Comprehensive analysis of beta-catenin target genes in colorectal carcinoma cell lines with deregulated Wnt/beta-catenin signaling. *BMC Genomics,* 15**,** 74.

HIGASHI, H., NAKAYA, A., TSUTSUMI, R., YOKOYAMA, K., FUJII, Y., ISHIKAWA, S., HIGUCHI, M., TAKAHASHI, A., KURASHIMA, Y., TEISHIKATA, Y., TANAKA, S., AZUMA, T. & HATAKEYAMA, M. 2004. Helicobacter pylori CagA Induces Ras-independent Morphogenetic Response through SHP-2 Recruitment and Activation. *Journal of Biological Chemistry,* 279**,** 17205-17216.

HIGASHI, H., TSUTSUMI, R., FUJITA, A., YAMAZAKI, S., ASAKA, M., AZUMA, T. & HATAKEYAMA, M. 2002a. Biological activity of the Helicobacter pylori virulence factor CagA is determined by variation in the tyrosine phosphorylation sites. *Proceedings of the National Academy of Sciences of the United States of America,* 99**,** 14428-33.

HIGASHI, H., TSUTSUMI, R., MUTO, S., SUGIYAMA, T., AZUMA, T., ASAKA, M. & HATAKEYAMA, M. 2002b. SHP-2 tyrosine phosphatase as an intracellular target of Helicobacter pylori CagA protein. *Science (New York, N.Y.),* 295**,** 683-6.

HIGASHI, H., YOKOYAMA, K., FUJII, Y., REN, S., YUASA, H., SAADAT, I., MURATA-KAMIYA, N., AZUMA, T. & HATAKEYAMA, M. 2005. EPIYA Motif Is a Membrane-targeting Signal of Helicobacter pylori Virulence Factor CagA in Mammalian Cells. *Journal of Biological Chemistry,* 280**,** 23130-23137.

HIRATA, Y., MAEDA, S., MITSUNO, Y., TATEISHI, K., YANAI, A., AKANUMA, M., YOSHIDA, H., KAWABE, T., SHIRATORI, Y. & OMATA, M. 2002. Helicobacter pylori CagA protein activates serum response element-driven transcription independently of tyrosine phosphorylation. *Gastroenterology,* 123**,** 1962-71.

HOEKSTRA, D., REJMAN, J., WASUNGU, L., SHI, F. & ZUHORN, I. 2007. Gene delivery by cationic lipids: in and out of an endosome. *Biochemical Society transactions,* 35**,** 68-71.

HOLBROOK, J. D., PARKER, J. S., GALLAGHER, K. T., HALSEY, W. S., HUGHES, A. M., WEIGMAN, V. J., LEBOWITZ, P. F. & KUMAR, R. 2011. Deep sequencing of gastric carcinoma reveals somatic mutations relevant to personalized medicine. *J Transl Med,* 9**,** 119.

HOMOUZ, D., PERHAM, M., SAMIOTAKIS, A., CHEUNG, M. S. & WITTUNG-STAFSHEDE, P. 2008. Crowded, cell-like environment induces shape changes in aspherical protein. *Proceedings of the National Academy of Sciences of the United States of America,* 105**,** 11754-9.

HONG, S. A., YOO, S. H., LEE, H. H., SUN, S., WON, H. S., KIM, O. & KO, Y. H. 2018. Prognostic value of Dickkopf-1 and ss-catenin expression in advanced gastric cancer. *BMC Cancer,* 18**,** 506.

HOPP, T. P., PRICKETT, K. S., PRICE, V. L., LIBBY, R. T., MARCH, C. J., PAT CERRETTI, D., URDAL, D. L. & CONLON, P. J. 1988. A Short Polypeptide Marker Sequence Useful for Recombinant Protein Identification and Purification. *Bio/Technology,* 6**,** 1204-1210.

HOTZ, B., KEILHOLZ, U., FUSI, A., BUHR, H. J. & HOTZ, H. G. 2012. In vitro and in vivo antitumor activity of cetuximab in human gastric cancer cell lines in relation to epidermal growth factor receptor (EGFR) expression and mutational phenotype. *Gastric Cancer,* 15**,** 252-64.

HUGO GENE NOMENCLATURE COMMITTEE. 2021. *HGNC* [Online]. European Bioinformatics Institute (EBI), European Molecular Biology Laboratory (EMBL). Available: www.genenames.org [Accessed 2022].

IIDA, S., AKIYAMA, Y., NAKAJIMA, T., ICHIKAWA, W., NIHEI, Z., SUGIHARA, K. & YUASA, Y. 2000. Alterations and hypermethylation of thep14ARF gene in gastric cancer. *International Journal of Cancer,* 87**,** 654-658.

IKEDA, S., KISHIDA, S., YAMAMOTO, H., MURAI, H., KOYAMA, S. & KIKUCHI, A. 1998. Axin, a negative regulator of the Wnt signaling pathway, forms a complex with GSK-3β and β-

catenin and promotes GSK-3β-dependent phosphorylation of β-catenin. *EMBO Journal,* 17**,** 1371-1384.

INGHAM, R. J., COLWILL, K., HOWARD, C., DETTWILER, S., LIM, C. S., YU, J., HERSI, K., RAAIJMAKERS, J., GISH, G., MBAMALU, G., TAYLOR, L., YEUNG, B., VASSILOVSKI, G., AMIN, M., CHEN, F., MATSKOVA, L., WINBERG, G., ERNBERG, I., LINDING, R., O'DONNELL, P., STAROSTINE, A., KELLER, W., METALNIKOV, P., STARK, C. & PAWSON, T. 2005. WW domains provide a platform for the assembly of multiprotein networks. *Mol Cell Biol,* 25**,** 7092-106.

IOANNIDIS, N. M., ROTHSTEIN, J. H., PEJAVER, V., MIDDHA, S., MCDONNELL, S. K., BAHETI, S., MUSOLF, A., LI, Q., HOLZINGER, E., KARYADI, D., CANNON-ALBRIGHT, L. A., TEERLINK, C. C., STANFORD, J. L., ISAACS, W. B., XU, J., COONEY, K. A., LANGE, E. M., SCHLEUTKER, J., CARPTEN, J. D., POWELL, I. J., CUSSENOT, O., CANCEL-TASSIN, G., GILES, G. G., MACINNIS, R. J., MAIER, C., HSIEH, C. L., WIKLUND, F., CATALONA, W. J., FOULKES, W. D., MANDAL, D., EELES, R. A., KOTE-JARAI, Z., BUSTAMANTE, C. D., SCHAID, D. J., HASTIE, T., OSTRANDER, E. A., BAILEY-WILSON, J. E., RADIVOJAC, P., THIBODEAU, S. N., WHITTEMORE, A. S. & SIEH, W. 2016. REVEL: An Ensemble Method for Predicting the Pathogenicity of Rare Missense Variants. *Am J Hum Genet,* 99**,** 877-885.

ISHIKAWA, S., OHTA, T. & HATAKEYAMA, M. 2009. Stability of Helicobacter pylori CagA oncoprotein in human gastric epithelial cells. *FEBS Lett,* 583**,** 2414-8.

ISHIMOTO, T., OSHIMA, H., OSHIMA, M., KAI, K., TORII, R., MASUKO, T., BABA, H., SAYA, H. & NAGANO, O. 2010. CD44+ slow-cycling tumor cell expansion is triggered by cooperative actions of Wnt and prostaglandin E2 in gastric tumorigenesis. *Cancer Science,* 101**,** 673-678.

ISHITANI, T., KISHIDA, S., HYODO-MIURA, J., UENO, N., YASUDA, J., WATERMAN, M., SHIBUYA, H., MOON, R. T., NINOMIYA-TSUJI, J. & MATSUMOTO, K. 2003. The TAK1-NLK mitogen-activated protein kinase cascade functions in the Wnt-5a/Ca(2+) pathway to antagonize Wnt/beta-catenin signaling. *Mol Cell Biol,* 23**,** 131-9.

ISHITANI, T., NINOMIYA-TSUJI, J., NAGAI, S., NISHITA, M., MENEGHINI, M., BARKER, N., WATERMAN, M., BOWERMAN, B., CLEVERS, H., SHIBUYA, H. & MATSUMOTO, K. 1999. The TAK1-NLK-MAPK-related pathway antagonizes signalling between beta-catenin and transcription factor TCF. *Nature,* 399**,** 798-802.

ISRAEL, D. A., SALAMA, N., KRISHNA, U., RIEGER, U. M., ATHERTON, J. C., FALKOW, S. & PEEK, R. M. 2001. Helicobacter pylori genetic diversity within the gastric niche of a single human host. *Proceedings of the National Academy of Sciences of the United States of America,* 98**,** 14625-14630.

ITO, K., CHUANG, L. S., ITO, T., CHANG, T. L., FUKAMACHI, H., SALTO-TELLEZ, M. & ITO, Y. 2011. Loss of Runx3 is a key event in inducing precancerous state of the stomach. *Gastroenterology,* 140**,** 1536-46 e8.

ITO, K., LIM, A. C., SALTO-TELLEZ, M., MOTODA, L., OSATO, M., CHUANG, L. S., LEE, C. W., VOON, D. C., KOO, J. K., WANG, H., FUKAMACHI, H. & ITO, Y. 2008. RUNX3 attenuates beta-catenin/T cell factors in intestinal tumorigenesis. *Cancer Cell,* 14**,** 226-37.

ITO, Y. 2004. Oncogenic potential of the RUNX gene family: 'overview'. *Oncogene,* 23**,** 4198-208.

ITO, Y., BAE, S. C. & CHUANG, L. S. 2015. The RUNX family: developmental regulators in cancer. *Nat Rev Cancer,* 15**,** 81-95.

JACOBSEN, L., CALVIN, S. & LOBENHOFER, E. 2009. Transcriptional effects of transfection: the potential for misinterpretation of gene expression data generated from transiently transfected cells. *Biotechniques,* 47**,** 617-24.

JIMENEZ-SOTO, L. F. & HAAS, R. 2016. The CagA toxin of Helicobacter pylori: abundant production but relatively low amount translocated. *Sci Rep,* 6**,** 23227.

JIMÉNEZ-SOTO, L. F., KUTTER, S., SEWALD, X., ERTL, C., WEISS, E., KAPP, U., ROHDE, M., PIRCH, T., JUNG, K., RETTA, S. F., TERRADOT, L., FISCHER, W. & HAAS, R. 2009. Helicobacter pylori type IV secretion apparatus exploits beta1 integrin in a novel RGD-independent manner. *PLoS pathogens,* 5**,** e1000684-e1000684.

JU, X., ISHIKAWA, T. O., NAKA, K., ITO, K., ITO, Y. & OSHIMA, M. 2014. Context-dependent activation of Wnt signaling by tumor suppressor RUNX3 in gastric cancer cells. *Cancer Sci,* 105**,** 418-24.

KAPLAN-TÜRKÖZ, B., JIMÉNEZ-SOTO, L. F., DIAN, C., ERTL, C., REMAUT, H., LOUCHE, A., TOSI, T., HAAS, R. & TERRADOT, L. 2012. Structural insights into Helicobacter pylori oncoprotein CagA interaction with β1 integrin. *Proceedings of the National Academy of Sciences of the United States of America,* 109**,** 14640-5.

KATOH, M. 2001. Molecular cloning, gene structure, and expression analyses of NKD1 and NKD2. *Int J Oncol,* 19**,** 963-9.

KATOH, M. 2007. Networking of WNT, FGF, Notch, BMP, and Hedgehog signaling pathways during carcinogenesis. *Stem cell reviews,* 3**,** 30-8.

KATOH, M. & KATOH, M. 2017. Molecular genetics and targeted therapy of WNT-related human diseases (Review). *Int J Mol Med,* 40**,** 587-606.

KATZEN, F. 2007. Gateway® recombinational cloning: a biological operating system. *Expert Opinion on Drug Discovery*.

KAVITHA, K., KOWSHIK, J., KISHORE, T. K., BABA, A. B. & NAGINI, S. 2013. Astaxanthin inhibits NF-kappaB and Wnt/beta-catenin signaling pathways via inactivation of Erk/MAPK and PI3K/Akt to induce intrinsic apoptosis in a hamster model of oral cancer. *Biochim Biophys Acta,* 1830**,** 4433-44.

KESTLER, H. A. & KÜHL, M. 2008. From individual Wnt pathways towards a Wnt signalling network. *Philosophical transactions of the Royal Society of London. Series B, Biological sciences,* 363**,** 1333-47.

KHAN, Z., VIJAYAKUMAR, S., DE LA TORRE, T. V., ROTOLO, S. & BAFICO, A. 2007. Analysis of endogenous LRP6 function reveals a novel feedback mechanism by which Wnt negatively regulates its receptor. *Molecular and cellular biology,* 27**,** 7291-7301.

KIM, M. S., KIM, S. S., AHN, C. H., YOO, N. J. & LEE, S. H. 2009. Frameshift mutations of Wnt pathway genes AXIN2 and TCF7L2 in gastric carcinomas with high microsatellite instability. *Human pathology,* 40**,** 58-64.

KIRIKOSHI, H., SEKIHARA, H. & KATOH, M. 2001. Up-regulation of Frizzled-7 (FZD7) in human gastric cancer. *Int J Oncol,* 19**,** 111-5.

KLIJN, C., DURINCK, S., STAWISKI, E. W., HAVERTY, P. M., JIANG, Z., LIU, H., DEGENHARDT, J., MAYBA, O., GNAD, F., LIU, J., PAU, G., REEDER, J., CAO, Y., MUKHYALA, K., SELVARAJ, S. K., YU, M., ZYNDA, G. J., BRAUER, M. J., WU, T. D., GENTLEMAN, R. C., MANNING, G., YAUCH, R. L., BOURGON, R., STOKOE, D., MODRUSAN, Z., NEVE, R. M., DE SAUVAGE, F. J., SETTLEMAN, J., SESHAGIRI, S. & ZHANG, Z. 2015. A comprehensive transcriptional portrait of human cancer cell lines. *Nat Biotechnol,* 33**,** 306-12.

KOO, B. K., SPIT, M., JORDENS, I., LOW, T. Y., STANGE, D. E., VAN DE WETERING, M., VAN ES, J. H., MOHAMMED, S., HECK, A. J., MAURICE, M. M. & CLEVERS, H. 2012. Tumour suppressor RNF43 is a stem-cell E3 ligase that induces endocytosis of Wnt receptors. *Nature,* 488**,** 665-9.

KORINEK, V., BARKER, N., MORIN, P. J., VAN WICHEN, D., DE WEGER, R., KINZLER, K. W., VOGELSTEIN, B. & CLEVERS, H. 1997. Constitutive transcriptional activation by a beta-catenin-Tcf complex in APC-/- colon carcinoma. *Science,* 275**,** 1784-7.

KOZAK, M. 1987. An analysis of 5'-noncoding sequences from 699 vertebrate messenger RNAs. *Nucleic acids research,* 15**,** 8125-48.

KRAFT, C., STACK, A., JOSENHANS, C., NIEHUS, E., DIETRICH, G., CORREA, P., FOX, J. G., FALUSH, D. & SUERBAUM, S. 2006. Genomic changes during chronic Helicobacter pylori infection. *Journal of bacteriology,* 188**,** 249-54.

KURASHIMA, Y., MURATA-KAMIYA, N., KIKUCHI, K., HIGASHI, H., AZUMA, T., KONDO, S. & HATAKEYAMA, M. 2008. Deregulation of β-catenin signal by Helicobacter pylori CagA requires the CagA-multimerization sequence. *International Journal of Cancer,* 122**,** 823-831.

KURKLU, B., WHITEHEAD, R. H., ONG, E. K., MINAMOTO, T., FOX, J. G., MANN, J. R., JUDD, L. M., GIRAUD, A. S. & MENHENIOTT, T. R. 2015. Lineage-specific RUNX3 hypomethylation marks the preneoplastic immune component of gastric cancer. *Oncogene,* 34**,** 2856-66.

KWOK, T., ZABLER, D., URMAN, S., ROHDE, M., HARTIG, R., WESSLER, S., MISSELWITZ, R., BERGER, J., SEWALD, N., KÖNIG, W. & BACKERT, S. 2007. Helicobacter exploits integrin for type IV secretion and kinase activation. *Nature,* 449**,** 862-6.

KYRILLOS, A., ARORA, G., MURRAY, B. & ROSENWALD, A. G. 2016. The Presence of Phage Orthologous Genes in Helicobacter pylori Correlates with the Presence of the Virulence Factors CagA and VacA. *Helicobacter,* 21**,** 226-233.

LAMB, A., CHEN, J., BLANKE, S. R. & CHEN, L. F. 2013. Helicobacter pylori activates NF-kappaB by inducing Ubc13-mediated ubiquitination of lysine 158 of TAK1. *J Cell Biochem,* 114**,** 2284-92.

LAMB, A., YANG, X. D., TSANG, Y. H., LI, J. D., HIGASHI, H., HATAKEYAMA, M., PEEK, R. M., BLANKE, S. R. & CHEN, L. F. 2009. Helicobacter pylori CagA activates NF-kappaB by targeting TAK1 for TRAF6-mediated Lys 63 ubiquitination. *EMBO Rep,* 10**,** 1242-9.

LANDRUM, M. J., CHITIPIRALLA, S., BROWN, G. R., CHEN, C., GU, B., HART, J., HOFFMAN, D., JANG, W., KAUR, K., LIU, C., LYOSHIN, V., MADDIPATLA, Z., MAITI, R., MITCHELL, J., O'LEARY, N., RILEY, G. R., SHI, W., ZHOU, G., SCHNEIDER, V., MAGLOTT, D., HOLMES, J. B. & KATTMAN, B. L. 2020. ClinVar: improvements to accessing data. *Nucleic Acids Res,* 48**,** D835-D844.

LANDRUM, M. J., LEE, J. M., RILEY, G. R., JANG, W., RUBINSTEIN, W. S., CHURCH, D. M. & MAGLOTT, D. R. 2014. ClinVar: public archive of relationships among sequence variation and human phenotype. *Nucleic Acids Res,* 42**,** D980-5.

LECHARDEUR, D., SOHN, K. J., HAARDT, M., JOSHI, P. B., MONCK, M., GRAHAM, R. W., BEATTY, B., SQUIRE, J., O'BRODOVICH, H. & LUKACS, G. L. 1999. Metabolic instability of plasmid DNA in the cytosol: a potential barrier to gene transfer. *Gene therapy,* 6**,** 482-97.

LEE, A., O'ROURKE, J., DE UNGRIA, M. C., ROBERTSON, B., DASKALOPOULOS, G. & DIXON, M. F. 1997. A standardized mouse model of Helicobacter pylori infection: Introducing the Sydney strain. *Gastroenterology,* 112**,** 1386-1397.

LEE, H. S., LEE, H. E., PARK, D. J., KIM, H. H., KIM, W. H. & PARK, K. U. 2012a. Clinical significance of serum and tissue Dickkopf-1 levels in patients with gastric cancer. *Clin Chim Acta,* 413**,** 1753-60.

LEE, I. O., KIM, J. H., CHOI, Y. J., PILLINGER, M. H., KIM, S. Y., BLASER, M. J. & LEE, Y. C. 2010. Helicobacter pylori CagA phosphorylation status determines the gp130-activated SHP2/ERK and JAK/STAT signal transduction pathways in gastric epithelial cells. *J Biol Chem,* 285**,** 16042-50.

LEE, J., VAN HUMMELEN, P., GO, C., PALESCANDOLO, E., JANG, J., PARK, H. Y., KANG, S. Y., PARK, J. O., KANG, W. K., MACCONAILL, L. & KIM, K. M. 2012b. High-throughput mutation profiling identifies frequent somatic mutations in advanced gastric adenocarcinoma. *PLoS One,* 7**,** e38892.

LEE, K. H., LEE, J. S., SUH, C., KIM, S. W., KIM, S. B., LEE, J. H., LEE, M. S., PARK, M. Y., SUN, H. S. & KIM, S. H. 1995. Clinicopathologic significance of the K-ras gene codon 12 point mutation in stomach cancer. An analysis of 140 cases. *Cancer,* 75**,** 2794-801.

LEHOURS, P., VALE, F. F., BJURSELL, M. K., MELEFORS, O., ADVANI, R., GLAVAS, S., GUEGUENIAT, J., GONTIER, E., LACOMME, S., ALVES MATOS, A., MENARD, A., MEGRAUD, F., ENGSTRAND, L. & ANDERSSON, A. F. 2011. Genome sequencing reveals a phage in Helicobacter pylori. *mBio,* 2.

LEK, M., KARCZEWSKI, K. J., MINIKEL, E. V., SAMOCHA, K. E., BANKS, E., FENNELL, T., O'DONNELL-LURIA, A. H., WARE, J. S., HILL, A. J., CUMMINGS, B. B., TUKIAINEN, T., BIRNBAUM, D. P., KOSMICKI, J. A., DUNCAN, L. E., ESTRADA, K., ZHAO, F., ZOU, J., PIERCE-HOFFMAN, E., BERGHOUT, J., COOPER, D. N., DEFLAUX, N., DEPRISTO, M., DO, R., FLANNICK, J., FROMER, M., GAUTHIER, L., GOLDSTEIN, J., GUPTA, N., HOWRIGAN, D., KIEZUN, A., KURKI, M. I., MOONSHINE, A. L., NATARAJAN, P., OROZCO, L., PELOSO, G. M., POPLIN, R., RIVAS, M. A., RUANO-RUBIO, V., ROSE, S. A., RUDERFER, D. M., SHAKIR, K., STENSON, P. D., STEVENS, C., THOMAS, B. P., TIAO, G., TUSIE-LUNA, M. T., WEISBURD, B., WON, H. H., YU, D., ALTSHULER, D. M., ARDISSINO, D., BOEHNKE, M., DANESH, J., DONNELLY, S., ELOSUA, R., FLOREZ, J. C., GABRIEL, S. B., GETZ, G., GLATT, S. J., HULTMAN, C. M., KATHIRESAN, S., LAAKSO, M., MCCARROLL, S., MCCARTHY, M. I., MCGOVERN, D., MCPHERSON, R., NEALE, B. M., PALOTIE, A., PURCELL, S. M., SALEHEEN, D., SCHARF, J. M., SKLAR, P., SULLIVAN, P. F., TUOMILEHTO, J., TSUANG, M. T., WATKINS, H. C., WILSON, J. G., DALY, M. J., MACARTHUR, D. G. & EXOME AGGREGATION, C. 2016. Analysis of protein-coding genetic variation in 60,706 humans. *Nature,* 536**,** 285-91.

LENGAUER, C., KINZLER, K. W. & VOGELSTEIN, B. 1998. Genetic instabilities in human cancers. *Nature,* 396**,** 643-9.

LI, M., WANG, H., HUANG, T., WANG, J., DING, Y., LI, Z., ZHANG, J. & LI, L. 2010a. TAB2 scaffolds TAK1 and NLK in repressing canonical Wnt signaling. *J Biol Chem,* 285**,** 13397-404.

LI, Q., LAI, Q., HE, C., FANG, Y., YAN, Q., ZHANG, Y., WANG, X., GU, C., WANG, Y., YE, L., HAN, L., LIN, X., CHEN, J., CAI, J., LI, A. & LIU, S. 2019. RUNX1 promotes tumour metastasis by activating the Wnt/beta-catenin signalling pathway and EMT in colorectal cancer. *J Exp Clin Cancer Res,* 38**,** 334.

LI, V. S., NG, S. S., BOERSEMA, P. J., LOW, T. Y., KARTHAUS, W. R., GERLACH, J. P., MOHAMMED, S., HECK, A. J., MAURICE, M. M., MAHMOUDI, T. & CLEVERS, H. 2012. Wnt signaling through inhibition of beta-catenin degradation in an intact Axin1 complex. *Cell,* 149**,** 1245-56.

LI, Y., LU, W., KING, T. D., LIU, C. C., BIJUR, G. N. & BU, G. 2010b. Dkk1 stabilizes Wnt co-receptor LRP6: implication for Wnt ligand-induced LRP6 down-regulation. *PLoS One,* 5**,** e11014.

LILYESTROM, W., KLEIN, M. G., ZHANG, R., JOACHIMIAK, A. & CHEN, X. S. 2006. Crystal structure of SV40 large T-antigen bound to p53: interplay between a viral oncoprotein and a cellular tumor suppressor. *Genes Dev,* 20**,** 2373-82.

LIM, S. H., KWON, J.-W., KIM, N., KIM, G. H., KANG, J. M., PARK, M. J., YIM, J. Y., KIM, H. U., BAIK, G. H., SEO, G. S., SHIN, J. E., JOO, Y.-E., KIM, J. S. & JUNG, H. C. 2013. Prevalence

and risk factors of Helicobacter pylori infection in Korea: nationwide multicenter study over 13 years. *BMC gastroenterology,* 13**,** 104-104.

LIN, Y. C., BOONE, M., MEURIS, L., LEMMENS, I., VAN ROY, N., SOETE, A., REUMERS, J., MOISSE, M., PLAISANCE, S., DRMANAC, R., CHEN, J., SPELEMAN, F., LAMBRECHTS, D., VAN DE PEER, Y., TAVERNIER, J. & CALLEWAERT, N. 2014. Genome dynamics of the human embryonic kidney 293 lineage in response to cell biology manipulations. *Nat Commun,* 5**,** 4767.

LIU, C., LI, Y., SEMENOV, M., HAN, C., BAEG, G.-H., TAN, Y., ZHANG, Z., LIN, X. & HE, X. 2002. Control of β-Catenin Phosphorylation/Degradation by a Dual-Kinase Mechanism. *Cell,* 108**,** 837-847.

LIU, H., FERGUSSON, M. M., CASTILHO, R. M., LIU, J., CAO, L., CHEN, J., MALIDE, D., ROVIRA, II, SCHIMEL, D., KUO, C. J., GUTKIND, J. S., HWANG, P. M. & FINKEL, T. 2007. Augmented Wnt signaling in a mammalian model of accelerated aging. *Science,* 317**,** 803-6.

LOGAN, C. Y. & NUSSE, R. 2004. The Wnt signaling pathway in development and disease. *Annual Review of Cell and Developmental Biology,* 20**,** 781-810.

LOGAN, R. P. H. 1994. Helicobacter pylori and gastric cancer. *The Lancet,* 344**,** 1078-1079.

LOTEM, J., LEVANON, D., NEGREANU, V., BAUER, O., HANTISTEANU, S., DICKEN, J. & GRONER, Y. 2015. Runx3 at the interface of immunity, inflammation and cancer. *Biochim Biophys Acta,* 1855**,** 131-43.

LUKACS, G. L., HAGGIE, P., SEKSEK, O., LECHARDEUR, D., FREEDMAN, N. & VERKMAN, A. S. 2000. Size-dependent DNA mobility in cytoplasm and nucleus. *Journal of Biological Chemistry,* 275**,** 1625-1629.

LUKOW, D. A., SAUSVILLE, E. L., SURI, P., CHUNDURI, N. K., WIELAND, A., LEU, J., SMITH, J. C., GIRISH, V., KUMAR, A. A., KENDALL, J., WANG, Z., STORCHOVA, Z. & SHELTZER, J. M. 2021. Chromosomal instability accelerates the evolution of resistance to anti-cancer therapies. *Dev Cell,* 56**,** 2427-2439 e4.

LUSTIG, B., JERCHOW, B., SACHS, M., WEILER, S., PIETSCH, T., KARSTEN, U., VAN DE WETERING, M., CLEVERS, H., SCHLAG, P. M., BIRCHMEIER, W. & BEHRENS, J. 2002. Negative feedback loop of Wnt signaling through upregulation of conductin/axin2 in colorectal and liver tumors. *Mol Cell Biol,* 22**,** 1184-93.

MA, B. & HOTTIGER, M. O. 2016. Crosstalk between Wnt/β-Catenin and NF-κB Signaling Pathway during Inflammation. *Frontiers in Immunology,* 7.

MACDONALD, B. T. & HE, X. 2012. Frizzled and LRP5/6 receptors for Wnt/beta-catenin signaling. *Cold Spring Harb Perspect Biol,* 4.

MAJOR, M. B., CAMP, N. D., BERNDT, J. D., YI, X., GOLDENBERG, S. J., HUBBERT, C., BIECHELE, T. L., GINGRAS, A.-C., ZHENG, N., MACCOSS, M. J., ANGERS, S. & MOON, R. T. 2007.

Wilms tumor suppressor WTX negatively regulates WNT/beta-catenin signaling. *Science (New York, N.Y.),* 316**,** 1043-6.

MANN, B., GELOS, M., SIEDOW, A., HANSKI, M. L., GRATCHEV, A., ILYAS, M., BODMER, W. F., MOYER, M. P., RIECKEN, E. O., BUHR, H. J. & HANSKI, C. 1999. Target genes of beta-catenin-T cell-factor/lymphoid-enhancer-factor signaling in human colorectal carcinomas. *Proceedings of the National Academy of Sciences of the United States of America,* 96**,** 1603-1608.

MAO, J., FAN, S., MA, W., FAN, P., WANG, B., ZHANG, J., WANG, H., TANG, B., ZHANG, Q., YU, X., WANG, L., SONG, B. & LI, L. 2014. Roles of Wnt/beta-catenin signaling in the gastric cancer stem cells proliferation and salinomycin treatment. *Cell Death Dis,* 5**,** e1039.

MARSHALL, B. J. & WARREN, J. R. 1984. Unidentified curved bacilli in the stomach of patients with gastritis and peptic ulceration. *Lancet,* 1**,** 1311-5.

MASHIMA, T., OH-HARA, T., SATO, S., MOCHIZUKI, M., SUGIMOTO, Y., YAMAZAKI, K., HAMADA, J., TADA, M., MORIUCHI, T., ISHIKAWA, Y., KATO, Y., TOMODA, H., YAMORI, T. & TSURUO, T. 2005. p53-defective tumors with a functional apoptosome-mediated pathway: a new therapeutic target. *J Natl Cancer Inst,* 97**,** 765-77.

MAZZONI, S. M. & FEARON, E. R. 2014. AXIN1 and AXIN2 variants in gastrointestinal cancers. *Cancer Lett,* 355**,** 1-8.

MBOM, B. C., NELSON, W. J. & BARTH, A. 2013. beta-catenin at the centrosome: discrete pools of beta-catenin communicate during mitosis and may co-ordinate centrosome functions and cell cycle progression. *Bioessays,* 35**,** 804-9.

MEDINA, M. A., UGARTE, G. D., VARGAS, M. F., AVILA, M. E., NECUNIR, D., ELORZA, A. A., GUTIERREZ, S. E. & DE FERRARI, G. V. 2016. Alternative RUNX1 Promoter Regulation by Wnt/beta-Catenin Signaling in Leukemia Cells and Human Hematopoietic Progenitors. *J Cell Physiol,* 231**,** 1460-7.

MENEZES, M. E., DEVINE, D. J., SHEVDE, L. A. & SAMANT, R. S. 2012. Dickkopf1: a tumor suppressor or metastasis promoter? *Int J Cancer,* 130**,** 1477-83.

MIEHLKE, S., HACKELSBERGER, A., MEINING, A., VON ARNIM, U., MULLER, P., OCHSENKUHN, T., LEHN, N., MALFERTHEINER, P., STOLTE, M. & BAYERDORFFER, E. 1997. Histological diagnosis of Helicobacter pylori gastritis is predictive of a high risk of gastric carcinoma. *Int J Cancer,* 73**,** 837-839.

MIMURO, H., SUZUKI, T., TANAKA, J., ASAHI, M., HAAS, R. & SASAKAWA, C. 2002. Grb2 Is a Key Mediator of Helicobacter pylori CagA Protein Activities. *Molecular Cell,* 10**,** 745-755.

MINTON, A. P. 2001. The Influence of Macromolecular Crowding and Macromolecular Confinement on Biochemical Reactions in Physiological Media. *Journal of Biological Chemistry,* 276**,** 10577-10580.

MIYAZAWA, K., IWAYA, K., KURODA, M., HARADA, M., SERIZAWA, H., KOYANAGI, Y., SATO, Y., MIZOKAMI, Y., MATSUOKA, T. & MUKAI, K. 2000. Nuclear accumulation of beta-catenin in intestinal-type gastric carcinoma: correlation with early tumor invasion. *Virchows Arch,* 437**,** 508-13.

MOHI, M. G. & NEEL, B. G. 2007. The role of Shp2 (PTPN11) in cancer. *Current opinion in genetics & development,* 17**,** 23-30.

MOLENAAR, M., VAN DE WETERING, M., OOSTERWEGEL, M., PETERSON-MADURO, J., GODSAVE, S., KORINEK, V., ROOSE, J., DESTRÉE, O. & CLEVERS, H. 1996. XTcf-3 Transcription Factor Mediates β-Catenin-Induced Axis Formation in Xenopus Embryos. *Cell,* 86**,** 391-399.

MORITA, K., SUZUKI, K., MAEDA, S., MATSUO, A., MITSUDA, Y., TOKUSHIGE, C., KASHIWAZAKI, G., TANIGUCHI, J., MAEDA, R., NOURA, M., HIRATA, M., KATAOKA, T., YANO, A., YAMADA, Y., KIYOSE, H., TOKUMASU, M., MATSUO, H., TANAKA, S., OKUNO, Y., MUTO, M., NAKA, K., ITO, K., KITAMURA, T., KANEDA, Y., LIU, P. P., BANDO, T., ADACHI, S., SUGIYAMA, H. & KAMIKUBO, Y. 2017. Genetic regulation of the RUNX transcription factor family has antitumor effects. *J Clin Invest,* 127**,** 2815-2828.

MORTIMER, I., TAM, P., MACLACHLAN, I., GRAHAM, R. W., SARAVOLAC, E. G. & JOSHI, P. B. 1999. Cationic lipid-mediated transfection of cells in culture requires mitotic activity. *Gene therapy,* 6**,** 403-11.

MURATA-KAMIYA, N., KIKUCHI, K., HAYASHI, T., HIGASHI, H. & HATAKEYAMA, M. 2010. Helicobacter pylori exploits host membrane phosphatidylserine for delivery, localization, and pathophysiological action of the CagA oncoprotein. *Cell host & microbe,* 7**,** 399-411.

MURATA-KAMIYA, N., KURASHIMA, Y., TEISHIKATA, Y., YAMAHASHI, Y., SAITO, Y., HIGASHI, H., ABURATANI, H., AKIYAMA, T., PEEK, R. M., AZUMA, T. & HATAKEYAMA, M. 2007. Helicobacter pylori CagA interacts with E-cadherin and deregulates the β-catenin signal that promotes intestinal transdifferentiation in gastric epithelial cells. *Oncogene,* 26**,** 4617-4626.

NAGARAJAN, N., BERTRAND, D., HILLMER, A. M., ZANG, Z. J., YAO, F., JACQUES, P. E., TEO, A. S., CUTCUTACHE, I., ZHANG, Z., LEE, W. H., SIA, Y. Y., GAO, S., ARIYARATNE, P. N., HO, A., WOO, X. Y., VEERAVALI, L., ONG, C. K., DENG, N., DESAI, K. V., KHOR, C. C., HIBBERD, M. L., SHAHAB, A., RAO, J., WU, M., TEH, M., ZHU, F., CHIN, S. Y., PANG, B., SO, J. B., BOURQUE, G., SOONG, R., SUNG, W. K., TEAN TEH, B., ROZEN, S., RUAN, X., YEOH, K. G., TAN, P. B. & RUAN, Y. 2012. Whole-genome reconstruction and mutational signatures in gastric cancer. *Genome Biol,* 13**,** R115.

NAGASE, L., HAYASHI, T., SENDA, T. & HATAKEYAMA, M. 2015. Dramatic increase in SHP2 binding activity of Helicobacter pylori Western CagA by EPIYA-C duplication: its implications in gastric carcinogenesis. *Scientific reports,* 5**,** 15749-15749.

NEMTSOVA, M. V., KALINKIN, A. I., KUZNETSOVA, E. B., BURE, I. V., ALEKSEEVA, E. A., BYKOV, II, KHOROBRYKH, T. V., MIKHAYLENKO, D. S., TANAS, A. S., KUTSEV, S. I., ZALETAEV, D. V. & STRELNIKOV, V. V. 2020. Clinical relevance of somatic mutations in main driver

genes detected in gastric cancer patients by next-generation DNA sequencing. *Sci Rep,* 10**,** 504.

NESIC, D., MILLER, M. C., QUINKERT, Z. T., STEIN, M., CHAIT, B. T. & STEBBINS, C. E. 2010. Helicobacter pylori CagA inhibits PAR1-MARK family kinases by mimicking host substrates. *Nat Struct Mol Biol,* 17**,** 130-2.

NG, P. C. & HENIKOFF, S. 2003. SIFT: Predicting amino acid changes that affect protein function. *Nucleic Acids Res,* 31**,** 3812-4.

NGUYEN, L. V., VANNER, R., DIRKS, P. & EAVES, C. J. 2012. Cancer stem cells: an evolving concept. *Nat Rev Cancer,* 12**,** 133-43.

NIEHRS, C. 2012. The complex world of WNT receptor signalling. *Nat Rev Mol Cell Biol,* 13**,** 767-79.

NIEHRS, C. & ACEBRON, S. P. 2012. Mitotic and mitogenic Wnt signalling. *EMBO J,* 31**,** 2705-13.

NISHIKAWA, H., HAYASHI, T., ARISAKA, F., SENDA, T. & HATAKEYAMA, M. 2016. Impact of structural polymorphism for the Helicobacter pylori CagA oncoprotein on binding to polarity-regulating kinase PAR1b. *Sci Rep,* 6**,** 30031.

NOJIMA, M., SUZUKI, H., TOYOTA, M., WATANABE, Y., MARUYAMA, R., SASAKI, S., SASAKI, Y., MITA, H., NISHIKAWA, N., YAMAGUCHI, K., HIRATA, K., ITOH, F., TOKINO, T., MORI, M., IMAI, K. & SHINOMURA, Y. 2007. Frequent epigenetic inactivation of SFRP genes and constitutive activation of Wnt signaling in gastric cancer. *Oncogene,* 26**,** 4699-713.

NUSSE, R. 2016. *RE: The Wnt Homepage.*

NUSSE, R. & CLEVERS, H. 2017. Wnt/beta-Catenin Signaling, Disease, and Emerging Therapeutic Modalities. *Cell,* 169**,** 985-999.

ODA, T., KANAI, Y., OYAMA, T., YOSHIURA, K., SHIMOYAMA, Y., BIRCHMEIER, W., SUGIMURA, T. & HIROHASHI, S. 1994. E-cadherin gene mutations in human gastric carcinoma cell lines. *Proc Natl Acad Sci U S A,* 91**,** 1858-62.

ODENBREIT, S. 2000. Translocation of Helicobacter pylori CagA into Gastric Epithelial Cells by Type IV Secretion. *Science,* 287**,** 1497-1500.

OGASAWARA, N., TSUKAMOTO, T., MIZOSHITA, T., INADA, K., CAO, X., TAKENAKA, Y., JOH, T. & TATEMATSU, M. 2006. Mutations and nuclear accumulation of beta-catenin correlate with intestinal phenotypic expression in human gastric cancer. *Histopathology,* 49**,** 612-21.

OHNISHI, N., YUASA, H., TANAKA, S., SAWA, H., MIURA, M., MATSUI, A., HIGASHI, H., MUSASHI, M., IWABUCHI, K., SUZUKI, M., YAMADA, G., AZUMA, T. & HATAKEYAMA, M. 2008. Transgenic expression of Helicobacter pylori CagA induces gastrointestinal and hematopoietic neoplasms in mouse. *Proceedings of the National Academy of Sciences of the United States of America,* 105**,** 1003-8.

OLBERMANN, P., JOSENHANS, C., MOODLEY, Y., UHR, M., STAMER, C., VAUTERIN, M., SUERBAUM, S., ACHTMAN, M. & LINZ, B. 2010. A global overview of the genetic and functional diversity in the Helicobacter pylori cag pathogenicity island. *PLoS Genet,* 6**,** e1001069.

OLIVEIRA, M. J., COSTA, A. M., COSTA, A. C., FERREIRA, R. M., SAMPAIO, P., MACHADO, J. C., SERUCA, R., MAREEL, M. & FIGUEIREDO, C. 2009. CagA associates with c-Met, E-cadherin, and p120-catenin in a multiproteic complex that suppresses Helicobacter pylori-induced cell-invasive phenotype. *The Journal of infectious diseases,* 200**,** 745-55.

OOI, C. H., IVANOVA, T., WU, J., LEE, M., TAN, I. B., TAO, J., WARD, L., KOO, J. H., GOPALAKRISHNAN, V., ZHU, Y., CHENG, L. L., LEE, J., RHA, S. Y., CHUNG, H. C., GANESAN, K., SO, J., SOO, K. C., LIM, D., CHAN, W. H., WONG, W. K., BOWTELL, D., YEOH, K. G., GRABSCH, H., BOUSSIOUTAS, A. & TAN, P. 2009. Oncogenic pathway combinations predict clinical prognosis in gastric cancer. *PLoS Genet,* 5**,** e1000676.

OSHIUMI, H., KOUWAKI, T. & SEYA, T. 2016. Accessory Factors of Cytoplasmic Viral RNA Sensors Required for Antiviral Innate Immune Response. *Frontiers in Immunology,* 7.

PAN, K. F., FORMICHELLA, L., ZHANG, L., ZHANG, Y., MA, J. L., LI, Z. X., LIU, C., WANG, Y. M., GOETTNER, G., ULM, K., CLASSEN, M., YOU, W. C. & GERHARD, M. 2014. Helicobacter pylori antibody responses and evolution of precancerous gastric lesions in a Chinese population. *International Journal of Cancer,* 134**,** 2118-2125.

PAPADAKOS, K. S., SOUGLERI, I. S., MENTIS, A. F., HATZILOUKAS, E. & SGOURAS, D. N. 2013. Presence of terminal EPIYA phosphorylation motifs in Helicobacter pylori CagA contributes to IL-8 secretion, irrespective of the number of repeats. *PLoS One,* 8**,** e56291.

PAPINI, E., DE BERNARD, M., MILIA, E., BUGNOLI, M., ZERIAL, M., RAPPUOLI, R. & MONTECUCCO, C. 1994. Cellular vacuoles induced by Helicobacter pylori originate from late endosomal compartments. *Proceedings of the National Academy of Sciences of the United States of America,* 91**,** 9720-4.

PARK, S. H., LEE, S. G., KIM, Y. & SONG, K. 1998. Assignment of a human putative RNA helicase gene, DDX3, to human X chromosome bands p11.3-->p11.23. *Cytogenet Cell Genet,* 81**,** 178-9.

PARK, W. S., OH, R. R., PARK, J. Y., LEE, S. H., SHIN, M. S., KIM, Y. S., KIM, S. Y., LEE, H. K., KIM, P. J., OH, S. T., YOO, N. J. & LEE, J. Y. 1999. Frequent somatic mutations of the beta-catenin gene in intestinal-type gastric cancer. *Cancer Res,* 59**,** 4257-60.

PARSONNET, J., FRIEDMAN, G. D., VANDERSTEEN, D. P., CHANG, Y., VOGELMAN, J. H., ORENTREICH, N. & SIBLEY, R. K. 1991. Helicobacter pylori infection and the risk of gastric carcinoma. *The New England journal of medicine,* 325**,** 1127-31.

PEEK, R. M. & BLASER, M. J. 2002. Helicobacter Pylori and Gastrointestinal Tract Adenocarcinomas. *Nature Reviews Cancer,* 2**,** 28-37.

PEIFER, M., MCCREA, P. D., GREEN, K. J., WIESCHAUS, E. & GUMBINER, B. M. 1992. The vertebrate adhesive junction proteins beta-catenin and plakoglobin and the Drosophila segment polarity gene armadillo form a multigene family with similar properties. *Journal of cell biology,* 118**,** 681-691.

PELETEIRO, B., BASTOS, A., FERRO, A. & LUNET, N. 2014. Prevalence of Helicobacter pylori infection worldwide: A systematic review of studies with national coverage. *Digestive Diseases and Sciences,* 59**,** 1698-1709.

PELZ, C., STEININGER, S., WEISS, C., COSCIA, F. & VOGELMANN, R. 2011. A novel inhibitory domain of Helicobacter pylori protein CagA reduces CagA effects on host cell biology. *The Journal of biological chemistry,* 286**,** 8999-9008.

PICHON, C., BILLIET, L. & MIDOUX, P. 2010. Chemical vectors for gene delivery: uptake and intracellular trafficking. *Current opinion in biotechnology,* 21**,** 640-5.

PINSON, K. I., BRENNAN, J., MONKLEY, S., AVERY, B. J. & SKARNES, W. C. 2000. An LDL-receptor-related protein mediates Wnt signalling in mice. *Nature,* 407**,** 535-8.

PLUMMER, M., FRANCESCHI, S., VIGNAT, J., FORMAN, D. & DE MARTEL, C. 2015. Global burden of gastric cancer attributable to Helicobacter pylori. *Int J Cancer,* 136**,** 487-90.

POLLARD, H., TOUMANIANTZ, G., AMOS, J. L., AVET-LOISEAU, H., GUIHARD, G., BEHR, J. P. & ESCANDE, D. 2001. Ca2+-sensitive cytosolic nucleases prevent efficient delivery to the nucleus of injected plasmids. *The journal of gene medicine,* 3**,** 153-64.

PUGH, T. J., WEERARATNE, S. D., ARCHER, T. C., POMERANZ KRUMMEL, D. A., AUCLAIR, D., BOCHICCHIO, J., CARNEIRO, M. O., CARTER, S. L., CIBULSKIS, K., ERLICH, R. L., GREULICH, H., LAWRENCE, M. S., LENNON, N. J., MCKENNA, A., MELDRIM, J., RAMOS, A. H., ROSS, M. G., RUSS, C., SHEFLER, E., SIVACHENKO, A., SOGOLOFF, B., STOJANOV, P., TAMAYO, P., MESIROV, J. P., AMANI, V., TEIDER, N., SENGUPTA, S., FRANCOIS, J. P., NORTHCOTT, P. A., TAYLOR, M. D., YU, F., CRABTREE, G. R., KAUTZMAN, A. G., GABRIEL, S. B., GETZ, G., JAGER, N., JONES, D. T., LICHTER, P., PFISTER, S. M., ROBERTS, T. M., MEYERSON, M., POMEROY, S. L. & CHO, Y. J. 2012. Medulloblastoma exome sequencing uncovers subtype-specific somatic mutations. *Nature,* 488**,** 106-10.

RACZ, G. A., NAGY, N., TOVARI, J., APATI, A. & VERTESSY, B. G. 2021. Identification of new reference genes with stable expression patterns for gene expression studies using human cancer and normal cell lines. *Sci Rep,* 11**,** 19459.

REN, S., HIGASHI, H., LU, H., AZUMA, T. & HATAKEYAMA, M. 2006. Structural basis and functional consequence of Helicobacter pylori CagA multimerization in cells. *J Biol Chem,* 281**,** 32344-52.

RHYU, M. G., PARK, W. S., JUNG, Y. J., CHOI, S. W. & MELTZER, S. J. 1994. Allelic deletions of MCC/APC and p53 are frequent late events in human gastric carcinogenesis. *Gastroenterology,* 106**,** 1584-8.

RUBINFELD, B., TICE, D. A. & POLAKIS, P. 2001. Axin-dependent phosphorylation of the adenomatous polyposis coli protein mediated by casein kinase 1epsilon. *J Biol Chem,* 276**,** 39037-45.

SAADAT, I., HIGASHI, H., OBUSE, C., UMEDA, M., MURATA-KAMIYA, N., SAITO, Y., LU, H., OHNISHI, N., AZUMA, T., SUZUKI, A., OHNO, S. & HATAKEYAMA, M. 2007. Helicobacter pylori CagA targets PAR1/MARK kinase to disrupt epithelial cell polarity. *Nature,* 447**,** 330-333.

SALAMA, N. R., HARTUNG, M. L. & MULLER, A. 2013. Life in the human stomach: persistence strategies of the bacterial pathogen Helicobacter pylori. *Nat Rev Microbiol,* 11**,** 385-99.

SALMON, P. & TRONO, D. 2001. *Current Protocols in Human Genetics,* Hoboken, NJ, USA, John Wiley & Sons, Inc.

SATO, N., YAMABUKI, T., TAKANO, A., KOINUMA, J., ARAGAKI, M., MASUDA, K., ISHIKAWA, N., KOHNO, N., ITO, H., MIYAMOTO, M., NAKAYAMA, H., MIYAGI, Y., TSUCHIYA, E., KONDO, S., NAKAMURA, Y. & DAIGO, Y. 2010. Wnt inhibitor Dickkopf-1 as a target for passive cancer immunotherapy. *Cancer Res,* 70**,** 5326-36.

SATO, T., VAN ES, J. H., SNIPPERT, H. J., STANGE, D. E., VRIES, R. G., VAN DEN BORN, M., BARKER, N., SHROYER, N. F., VAN DE WETERING, M. & CLEVERS, H. 2011. Paneth cells constitute the niche for Lgr5 stem cells in intestinal crypts. *Nature,* 469**,** 415-8.

SCHRODER, M. 2011. Viruses and the human DEAD-box helicase DDX3: inhibition or exploitation? *Biochem Soc Trans,* 39**,** 679-83.

SCHRODER, M., BARAN, M. & BOWIE, A. G. 2008. Viral targeting of DEAD box protein 3 reveals its role in TBK1/IKKepsilon-mediated IRF activation. *EMBO J,* 27**,** 2147-57.

SEGAL, E. D., CHA, J., LO, J., FALKOW, S. & TOMPKINS, L. S. 1999. Altered states: involvement of phosphorylated CagA in the induction of host cellular growth changes by Helicobacter pylori. *Proceedings of the National Academy of Sciences of the United States of America,* 96**,** 14559-64.

SELBACH, M., MOESE, S., HAUCK, C. R., MEYER, T. F. & BACKERT, S. 2002. Src is the kinase of the Helicobacter pylori CagA protein in vitro and in vivo. *The Journal of biological chemistry,* 277**,** 6775-8.

SELBACH, M., PAUL, F. E., BRANDT, S., GUYE, P., DAUMKE, O., BACKERT, S., DEHIO, C. & MANN, M. 2009. Host Cell Interactome of Tyrosine-Phosphorylated Bacterial Proteins. *Cell Host and Microbe,* 5**,** 397-403.

SHAW, G., MORSE, S., ARARAT, M. & GRAHAM, F. L. 2002. Preferential transformation of human neuronal cells by human adenoviruses and the origin of HEK 293 cells. *Faseb j,* 16**,** 869-71.

SHIHAB, H. A., GOUGH, J., COOPER, D. N., STENSON, P. D., BARKER, G. L., EDWARDS, K. J., DAY, I. N. & GAUNT, T. R. 2013. Predicting the functional, molecular, and phenotypic

consequences of amino acid substitutions using hidden Markov models. *Hum Mutat,* 34**,** 57-65.

SHIMOMURA, H., HAYASHI, S., YOKOTA, K., OGUMA, K. & HIRAI, Y. 2004. Alteration in the composition of cholesteryl glucosides and other lipids in Helicobacter pylori undergoing morphological change from spiral to coccoid form. *FEMS Microbiol Lett,* 237**,** 407-13.

SHTUTMAN, M., ZHURINSKY, J., SIMCHA, I., ALBANESE, C., D'AMICO, M., PESTELL, R. & BEN-ZE'EV, A. 1999. The cyclin D1 gene is a target of the beta-catenin/LEF-1 pathway. *Proc Natl Acad Sci U S A,* 96**,** 5522-7.

SIMON, E., PETKE, D., BOGER, C., BEHRENS, H. M., WARNEKE, V., EBERT, M. & ROCKEN, C. 2012. The spatial distribution of LGR5+ cells correlates with gastric cancer progression. *PLoS One,* 7**,** e35486.

SINGLE NUCLEOTIDE POLYMORPHISM DATABASE. 2020. *dbSNP* [Online]. National Center for Biotechnology Information (NCBI), Bethesda, Maryland, United States. Available: https://www.ncbi.nlm.nih.gov/snp/ [Accessed 2021].

SINNBERG, T., MENZEL, M., KAESLER, S., BIEDERMANN, T., SAUER, B., NAHNSEN, S., SCHWARZ, M., GARBE, C. & SCHITTEK, B. 2010. Suppression of casein kinase 1alpha in melanoma cells induces a switch in beta-catenin signaling to promote metastasis. *Cancer Res,* 70**,** 6999-7009.

SOKOLOVA, O., KAHNE, T., BRYAN, K. & NAUMANN, M. 2018. Interactome analysis of transforming growth factor-beta-activated kinase 1 in Helicobacter pylori-infected cells revealed novel regulators tripartite motif 28 and CDC37. *Oncotarget,* 9**,** 14366-14381.

SOKOLOVA, O., MAUBACH, G. & NAUMANN, M. 2014. MEKK3 and TAK1 synergize to activate IKK complex in Helicobacter pylori infection. *Biochim Biophys Acta,* 1843**,** 715-24.

SONG, J. H., KIM, S. G., JUNG, S.-A., LEE, M. K., JUNG, H. C. & SONG, I. S. 2010. The interleukin-8-251 AA genotype is associated with angiogenesis in gastric carcinogenesis in Helicobacter pylori-infected Koreans. *Cytokine,* 51**,** 158-65.

STAMBOLIC, V., RUEL, L. & WOODGETT, J. R. 1996. Lithium inhibits glycogen synthase kinase-3 activity and mimics wingless signalling in intact cells. *Curr Biol,* 6**,** 1664-8.

STAMOS, J. L. & WEIS, W. I. 2013. The beta-catenin destruction complex. *Cold Spring Harb Perspect Biol,* 5**,** a007898.

STEIN, M., BAGNOLI, F., HALENBECK, R., RAPPUOLI, R., FANTL, W. J. & COVACCI, A. 2002. c-Src/Lyn kinases activate Helicobacter pylori CagA through tyrosine phosphorylation of the EPIYA motifs. *Molecular Microbiology,* 43**,** 971-980.

STEPANENKO, A. A. & DMITRENKO, V. V. 2015. HEK293 in cell biology and cancer research: phenotype, karyotype, tumorigenicity, and stress-induced genome-phenotype evolution. *Gene,* 569**,** 182-90.

STEPANENKO, A. A., VASSETZKY, Y. S. & KAVSAN, V. M. 2013. Antagonistic functional duality of cancer genes. *Gene,* 529**,** 199-207.

STEVENS, J. B., LIU, G., ABDALLAH, B. Y., HORNE, S. D., YE, K. J., BREMER, S. W., YE, C. J., KRAWETZ, S. A. & HENG, H. H. 2014. Unstable genomes elevate transcriptome dynamics. *Int J Cancer,* 134**,** 2074-87.

STINGL, K. & DE REUSE, H. 2005. Staying alive overdosed: how does Helicobacter pylori control urease activity? *International journal of medical microbiology : IJMM,* 295**,** 307-15.

STOLZ, A., NEUFELD, K., ERTYCH, N. & BASTIANS, H. 2015. Wnt-mediated protein stabilization ensures proper mitotic microtubule assembly and chromosome segregation. *EMBO reports,* 16**,** 490-9.

SUDOL, M., CHEN, H. I., BOUGERET, C., EINBOND, A. & BORK, P. 1995. Characterization of a novel protein-binding module - the WW domain. *FEBS Letters,* 369**,** 67-71.

SUDOL, M. & HUNTER, T. 2000. NeW wrinkles for an old domain. *Cell,* 103**,** 1001-4.

SURIANO, G., VRCELJ, N., SENZ, J., FERREIRA, P., MASOUDI, H., COX, K., NABAIS, S., LOPES, C., MACHADO, J. C., SERUCA, R., CARNEIRO, F. & HUNTSMAN, D. G. 2005. beta-catenin (CTNNB1) gene amplification: a new mechanism of protein overexpression in cancer. *Genes Chromosomes Cancer,* 42**,** 238-46.

SUZUKI, M., MIMURO, H., KIGA, K., FUKUMATSU, M., ISHIJIMA, N., MORIKAWA, H., NAGAI, S., KOYASU, S., GILMAN, R. H., KERSULYTE, D., BERG, D. E. & SASAKAWA, C. 2009. Helicobacter pylori CagA Phosphorylation-Independent Function in Epithelial Proliferation and Inflammation. *Cell Host & Microbe,* 5**,** 23-34.

SUZUKI, M., MIMURO, H., SUZUKI, T., PARK, M., YAMAMOTO, T. & SASAKAWA, C. 2005. Interaction of CagA with Crk plays an important role in Helicobacter pylori-induced loss of gastric epithelial cell adhesion. *The Journal of experimental medicine,* 202**,** 1235-47.

SWEENEY, K., CAMERON, E. R. & BLYTH, K. 2020. Complex Interplay between the RUNX Transcription Factors and Wnt/beta-Catenin Pathway in Cancer: A Tango in the Night. *Mol Cells,* 43**,** 188-197.

TAKAHASHI-KANEMITSU, A., KNIGHT, C. T. & HATAKEYAMA, M. 2020. Molecular anatomy and pathogenic actions of Helicobacter pylori CagA that underpin gastric carcinogenesis. *Cell Mol Immunol,* 17**,** 50-63.

TAKAISHI, S., OKUMURA, T., TU, S., WANG, S. S. W., SHIBATA, W., VIGNESHWARAN, R. G. S. A. K., SHIMADA, Y. & WANG, T. C. 2009. Identification of Gastric Cancer Stem Cells Using the Cell Surface Marker CD44. *Stem Cells,* 27**,** 1006-1020.

TAKEBE, N., HARRIS, P. J., WARREN, R. Q. & IVY, S. P. 2011. Targeting cancer stem cells by inhibiting Wnt, Notch, and Hedgehog pathways. *Nature reviews. Clinical oncology,* 8**,** 97-106.

TALBOT, L. J., BHATTACHARYA, S. D. & KUO, P. C. 2012. Epithelial-mesenchymal transition, the tumor microenvironment, and metastatic behavior of epithelial malignancies. *Int J Biochem Mol Biol,* 3**,** 117-36.

TAMAI, K., ZENG, X., LIU, C., ZHANG, X., HARADA, Y., CHANG, Z. & HE, X. 2004. A Mechanism for Wnt Coreceptor Activation. *Molecular Cell,* 13**,** 149-156.

TAMMER, I., BRANDT, S., HARTIG, R., KÖNIG, W. & BACKERT, S. 2007. Activation of Abl by Helicobacter pylori: a novel kinase for CagA and crucial mediator of host cell scattering. *Gastroenterology,* 132**,** 1309-19.

TANG, W., DODGE, M., GUNDAPANENI, D., MICHNOFF, C., ROTH, M. & LUM, L. 2008. A genome-wide RNAi screen for Wnt/beta-catenin pathway components identifies unexpected roles for TCF transcription factors in cancer. *Proc Natl Acad Sci U S A,* 105**,** 9697-702.

TATE, J. G., BAMFORD, S., JUBB, H. C., SONDKA, Z., BEARE, D. M., BINDAL, N., BOUTSELAKIS, H., COLE, C. G., CREATORE, C., DAWSON, E., FISH, P., HARSHA, B., HATHAWAY, C., JUPE, S. C., KOK, C. Y., NOBLE, K., PONTING, L., RAMSHAW, C. C., RYE, C. E., SPEEDY, H. E., STEFANCSIK, R., THOMPSON, S. L., WANG, S., WARD, S., CAMPBELL, P. J. & FORBES, S. A. 2019. COSMIC: the Catalogue Of Somatic Mutations In Cancer. *Nucleic Acids Res,* 47**,** D941-D947.

TEGTMEYER, N., HARTIG, R., DELAHAY, R. M., ROHDE, M., BRANDT, S., CONRADI, J., TAKAHASHI, S., SMOLKA, A. J., SEWALD, N. & BACKERT, S. 2010. A small fibronectin-mimicking protein from bacteria induces cell spreading and focal adhesion formation. *J Biol Chem,* 285**,** 23515-26.

TEGTMEYER, N., ZABLER, D., SCHMIDT, D., HARTIG, R., BRANDT, S. & BACKERT, S. 2009. Importance of EGF receptor, HER2/Neu and Erk1/2 kinase signalling for host cell elongation and scattering induced by the Helicobacter pylori CagA protein: antagonistic effects of the vacuolating cytotoxin VacA. *Cellular microbiology,* 11**,** 488-505.

TETSU, O. & MCCORMICK, F. 1999. Beta-catenin regulates expression of cyclin D1 in colon carcinoma cells. *Nature,* 398**,** 422-6.

THOMPSON, L. J., MERRELL, D. S., NEILAN, B. A., MITCHELL, H., LEE, A. & FALKOW, S. 2003. Gene Expression Profiling of Helicobacter pylori Reveals a Growth-Phase-Dependent Switch in Virulence Gene Expression. *Infection and Immunity,* 71**,** 2643-2655.

THOMPSON, S. L. & COMPTON, D. A. 2008. Examining the link between chromosomal instability and aneuploidy in human cells. *J Cell Biol,* 180**,** 665-72.

THORNE, C. A., HANSON, A. J., SCHNEIDER, J., TAHINCI, E., ORTON, D., CSELENYI, C. S., JERNIGAN, K. K., MEYERS, K. C., HANG, B. I., WATERSON, A. G., KIM, K., MELANCON, B., GHIDU, V. P., SULIKOWSKI, G. A., LAFLEUR, B., SALIC, A., LEE, L. A., MILLER, D. M., 3RD & LEE, E. 2010. Small-molecule inhibition of Wnt signaling through activation of casein kinase 1alpha. *Nat Chem Biol,* 6**,** 829-36.

TOLLER, I. M., NEELSEN, K. J., STEGER, M., HARTUNG, M. L., HOTTIGER, M. O., STUCKI, M., KALALI, B., GERHARD, M., SARTORI, A. A., LOPES, M. & MÜLLER, A. 2011. Carcinogenic bacterial pathogen Helicobacter pylori triggers DNA double-strand breaks and a DNA damage response in its host cells. *Proceedings of the National Academy of Sciences of the United States of America,* 108**,** 14944-9.

TOMB, J. F., WHITE, O., KERLAVAGE, A. R., CLAYTON, R. A., SUTTON, G. G., FLEISCHMANN, R. D., KETCHUM, K. A., KLENK, H. P., GILL, S., DOUGHERTY, B. A., NELSON, K., QUACKENBUSH, J., ZHOU, L., KIRKNESS, E. F., PETERSON, S., LOFTUS, B., RICHARDSON, D., DODSON, R., KHALAK, H. G., GLODEK, A., MCKENNEY, K., FITZEGERALD, L. M., LEE, N., ADAMS, M. D., HICKEY, E. K., BERG, D. E., GOCAYNE, J. D., UTTERBACK, T. R., PETERSON, J. D., KELLEY, J. M., COTTON, M. D., WEIDMAN, J. M., FUJII, C., BOWMAN, C., WATTHEY, L., WALLIN, E., HAYES, W. S., BORODOVSKY, M., KARP, P. D., SMITH, H. O., FRASER, C. M. & VENTER, J. C. 1997. The complete genome sequence of the gastric pathogen Helicobacter pylori. *Nature,* 388**,** 539-47.

TSANG, Y. H., LAMB, A., ROMERO-GALLO, J., HUANG, B., ITO, K., PEEK, R. M., JR., ITO, Y. & CHEN, L. F. 2010. Helicobacter pylori CagA targets gastric tumor suppressor RUNX3 for proteasome-mediated degradation. *Oncogene,* 29**,** 5643-50.

TSENG, W.-C., HASELTON, F. R. & GIORGIO, T. D. 1999. Mitosis enhances transgene expression of plasmid delivered by cationic liposomes. *Biochimica et Biophysica Acta (BBA) - Gene Structure and Expression,* 1445**,** 53-64.

TSUGAWA, H., SUZUKI, H., SAYA, H., HATAKEYAMA, M., HIRAYAMA, T., HIRATA, K., NAGANO, O., MATSUZAKI, J. & HIBI, T. 2012. Reactive oxygen species-induced autophagic degradation of Helicobacter pylori CagA is specifically suppressed in cancer stem-like cells. *Cell Host Microbe,* 12**,** 764-77.

TSUTSUMI, R., HIGASHI, H., HIGUCHI, M., OKADA, M. & HATAKEYAMA, M. 2003. Attenuation of Helicobacter pylori CagA·SHP-2 signaling by interaction between CagA and C-terminal Src kinase. *Journal of Biological Chemistry,* 278**,** 3664-3670.

TUMMURU, M. K., COVER, T. L. & BLASER, M. J. 1993. Cloning and expression of a high-molecular-mass major antigen of Helicobacter pylori: evidence of linkage to cytotoxin production. *Infect. Immun.,* 61**,** 1799-1809.

UEMURA, N., OKAMOTO, S., YAMAMOTO, S., MATSUMURA, N., YAMAGUCHI, S., YAMAKIDO, M., TANIYAMA, K., SASAKI, N. & SCHLEMPER, R. J. 2001. Helicobacter pylori infection and the development of gastric cancer. *N Engl J Med,* 345**,** 784-9.

UMEDA, M., MURATA-KAMIYA, N., SAITO, Y., OHBA, Y., TAKAHASHI, M. & HATAKEYAMA, M. 2009. Helicobacter pylori CagA causes mitotic impairment and induces chromosomal instability. *J Biol Chem,* 284**,** 22166-22172.

UPADHYAY, G., GOESSLING, W., NORTH, T. E., XAVIER, R., ZON, L. I. & YAJNIK, V. 2008. Molecular association between beta-catenin degradation complex and Rac guanine exchange factor DOCK4 is essential for Wnt/beta-catenin signaling. *Oncogene,* 27**,** 5845-55.

UPHOFF, C. C., POMMERENKE, C., DENKMANN, S. A. & DREXLER, H. G. 2019. Screening human cell lines for viral infections applying RNA-Seq data analysis. *PLoS One,* 14**,** e0210404.

VAN AMERONGEN, R. & NUSSE, R. 2009. Towards an integrated view of Wnt signaling in development. *Development (Cambridge, England),* 136**,** 3205-3214.

VAN DE WETERING, M., CASTROP, J., KORINEK, V. & CLEVERS, H. 1996. Extensive alternative splicing and dual promoter usage generate Tcf-1 protein isoforms with differential transcription control properties. *Mol Cell Biol,* 16**,** 745-52.

VAN DEN BERG, B., ELLIS, R. J. & DOBSON, C. M. 1999. Effects of macromolecular crowding on protein folding and agregation. *EMBO J,* 18**,** 6927-6933.

VAN DEN BERG, B., WAIN, R., DOBSON, C. M. & ELLIS, R. J. 2000. Macromolecular crowding perturbs protein refolding kinetics: implications for folding inside the cell. *EMBO J,* 19**,** 3870-5.

VAN DER FLIER, L. G., SABATES-BELLVER, J., OVING, I., HAEGEBARTH, A., DE PALO, M., ANTI, M., VAN GIJN, M. E., SUIJKERBUIJK, S., VAN DE WETERING, M., MARRA, G. & CLEVERS, H. 2007. The Intestinal Wnt/TCF Signature. *Gastroenterology,* 132**,** 628-32.

VIALA, J., CHAPUT, C., BONECA, I. G., CARDONA, A., GIRARDIN, S. E., MORAN, A. P., ATHMAN, R., MÉMET, S., HUERRE, M. R., COYLE, A. J., DISTEFANO, P. S., SANSONETTI, P. J., LABIGNE, A., BERTIN, J., PHILPOTT, D. J. & FERRERO, R. L. 2004. Nod1 responds to peptidoglycan delivered by the Helicobacter pylori cag pathogenicity island. *Nature immunology,* 5**,** 1166-74.

VLAD, A., RÖHRS, S., KLEIN-HITPASS, L. & MÜLLER, O. 2008. The first five years of the Wnt targetome. *Cellular signalling,* 20**,** 795-802.

VOGELMANN, R. & AMIEVA, M. R. 2007. The role of bacterial pathogens in cancer. *Current opinion in microbiology,* 10**,** 76-81.

WAGNER, A. D., UNVERZAGT, S., GROTHE, W., KLEBER, G., GROTHEY, A., HAERTING, J. & FLEIG, W. E. 2010. Chemotherapy for advanced gastric cancer. *The Cochrane database of systematic reviews***,** CD004064-CD004064.

WAGNER, G. P., KIN, K. & LYNCH, V. J. 2012. Measurement of mRNA abundance using RNA-seq data: RPKM measure is inconsistent among samples. *Theory in Biosciences,* 131**,** 281-285.

WANG, H., KIM, S. & RYU, W. S. 2009. DDX3 DEAD-Box RNA helicase inhibits hepatitis B virus reverse transcription by incorporation into nucleocapsids. *J Virol,* 83**,** 5815-24.

WANG, H., YAO, Y., NI, B., SHEN, Y., WANG, X., SHEN, H. & SHAO, S. 2016. Helicobacter pylori CagI is associated with the stability of CagA. *Microbial Pathogenesis,* 99**,** 130-134.

WANG, K., KAN, J., YUEN, S. T., SHI, S. T., CHU, K. M., LAW, S., CHAN, T. L., KAN, Z., CHAN, A. S., TSUI, W. Y., LEE, S. P., HO, S. L., CHAN, A. K., CHENG, G. H., ROBERTS, P. C., REJTO, P. A., GIBSON, N. W., POCALYKO, D. J., MAO, M., XU, J. & LEUNG, S. Y. 2011. Exome

sequencing identifies frequent mutation of ARID1A in molecular subtypes of gastric cancer. *Nat Genet,* 43**,** 1219-23.

WANG, K., YUEN, S. T., XU, J., LEE, S. P., YAN, H. H., SHI, S. T., SIU, H. C., DENG, S., CHU, K. M., LAW, S., CHAN, K. H., CHAN, A. S., TSUI, W. Y., HO, S. L., CHAN, A. K., MAN, J. L., FOGLIZZO, V., NG, M. K., CHAN, A. S., CHING, Y. P., CHENG, G. H., XIE, T., FERNANDEZ, J., LI, V. S., CLEVERS, H., REJTO, P. A., MAO, M. & LEUNG, S. Y. 2014. Whole-genome sequencing and comprehensive molecular profiling identify new driver mutations in gastric cancer. *Nat Genet,* 46**,** 573-82.

WANG, X., WANG, X., LIU, Y., DONG, Y., WANG, Y., KASSAB, M. A., FAN, W., YU, X. & WU, C. 2018. LGR5 regulates gastric adenocarcinoma cell proliferation and invasion via activating Wnt signaling pathway. *Oncogenesis,* 7**,** 57.

WAUGH, D. J. J. & WILSON, C. 2008. The interleukin-8 pathway in cancer. *Clinical cancer research : an official journal of the American Association for Cancer Research,* 14**,** 6735-41.

WHITE, B. D., CHIEN, A. J. & DAWSON, D. W. 2012. Dysregulation of Wnt/β-catenin signaling in gastrointestinal cancers. *Gastroenterology,* 142**,** 219-232.

WILLERT, K., BROWN, J. D., DANENBERG, E., DUNCAN, A. W., WEISSMAN, I. L., REYA, T., YATES, J. R. & NUSSE, R. 2003. Wnt proteins are lipid-modified and can act as stem cell growth factors. *Nature,* 423**,** 448-452.

WILLERT, K. & NUSSE, R. 2012. Wnt Proteins. *Cold Spring Harb Perspect Biol.,* 4.

WIRTH, T., WANG, X., LINZ, B., NOVICK, R. P., LUM, J. K., BLASER, M., MORELLI, G., FALUSH, D. & ACHTMAN, M. 2004. Distinguishing human ethnic groups by means of sequences from Helicobacter pylori: lessons from Ladakh. *Proceedings of the National Academy of Sciences of the United States of America,* 101**,** 4746-51.

WOO, D. K., KIM, H. S., LEE, H. S., KANG, Y. H., YANG, H. K. & KIM, W. H. 2001. Altered expression and mutation of beta-catenin gene in gastric carcinomas and cell lines. *Int J Cancer,* 95**,** 108-113.

WROBLEWSKI, L. E., PIAZUELO, M. B., CHATURVEDI, R., SCHUMACHER, M., AIHARA, E., FENG, R., NOTO, J. M., DELGADO, A., ISRAEL, D. A., ZAVROS, Y., MONTROSE, M. H., SHROYER, N., CORREA, P., WILSON, K. T. & PEEK, R. M. 2015. Helicobacter pylori targets cancer-associated apical-junctional constituents in gastroids and gastric epithelial cells. *Gut,* 64**,** 720-730.

YAN, D., WIESMANN, M., ROHAN, M., CHAN, V., JEFFERSON, A. B., GUO, L., SAKAMOTO, D., CAOTHIEN, R. H., FULLER, J. H., REINHARD, C., GARCIA, P. D., RANDAZZO, F. M., ESCOBEDO, J., FANTL, W. J. & WILLIAMS, L. T. 2001. Elevated expression of axin2 and hnkd mRNA provides evidence that Wnt/beta -catenin signaling is activated in human colon tumors. *Proc Natl Acad Sci U S A,* 98**,** 14973-8.

YOKOZAKI, H. 2000. Molecular characteristics of eight gastric cancer cell lines established in Japan. *Pathol Int,* 50**,** 767-77.

ZABNER, J., FASBENDER, A. J., MONINGER, T., POELLINGER, K. A. & WELSH, M. J. 1995. Cellular and Molecular Barriers to Gene Transfer by a Cationic Lipid. *Journal of Biological Chemistry,* 270**,** 18997-19007.

ZANG, Z. J., CUTCUTACHE, I., POON, S. L., ZHANG, S. L., MCPHERSON, J. R., TAO, J., RAJASEGARAN, V., HENG, H. L., DENG, N., GAN, A., LIM, K. H., ONG, C. K., HUANG, D., CHIN, S. Y., TAN, I. B., NG, C. C., YU, W., WU, Y., LEE, M., WU, J., POH, D., WAN, W. K., RHA, S. Y., SO, J., SALTO-TELLEZ, M., YEOH, K. G., WONG, W. K., ZHU, Y. J., FUTREAL, P. A., PANG, B., RUAN, Y., HILLMER, A. M., BERTRAND, D., NAGARAJAN, N., ROZEN, S., TEH, B. T. & TAN, P. 2012. Exome sequencing of gastric adenocarcinoma identifies recurrent somatic mutations in cell adhesion and chromatin remodeling genes. *Nat Genet,* 44**,** 570-4.

ZENG, X., TAMAI, K., DOBLE, B., LI, S., HUANG, H., HABAS, R., OKAMURA, H., WOODGETT, J. & HE, X. 2005. A dual-kinase mechanism for Wnt co-receptor phosphorylation and activation. *Nature,* 438**,** 873-7.

ZHAO, S., YE, Z. & STANTON, R. 2020. Misuse of RPKM or TPM normalization when comparing across samples and sequencing protocols. *RNA,* 26**,** 903-909.

ZHAO, Y., LI, M. C., KONATE, M. M., CHEN, L., DAS, B., KARLOVICH, C., WILLIAMS, P. M., EVRARD, Y. A., DOROSHOW, J. H. & MCSHANE, L. M. 2021. TPM, FPKM, or Normalized Counts? A Comparative Study of Quantification Measures for the Analysis of RNA-seq Data from the NCI Patient-Derived Models Repository. *J Transl Med,* 19**,** 269.

ZIMMERMAN, S. B. & HARRISON, B. 1987. Macromolecular crowding increases binding of DNA polymerase to DNA: an adaptive effect. *Proceedings of the National Academy of Sciences of the United States of America,* 84**,** 1871-1875.

ZUFFEREY, R., NAGY, D., MANDEL, R. J., NALDINI, L. & TRONO, D. 1997. Multiply attenuated lentiviral vector achieves efficient gene delivery in vivo. *Nature biotechnology,* 15**,** 871-5.

7 List of figures

8 Danksagung

Als ich seinerzeit anfing, mich mit dieser Thematik auseinanderzusetzen, war ich fasziniert von der Tatsache, dass es einen Zusammenhang zwischen einer Infektion und einer malignen Erkrankung geben kann. Getragen von naturwissenschaftlichem Elan habe ich mich sämtlichen Unwägbarkeiten zum Trotz in diese Arbeit vertieft – diese Worte bezeugen, dass es mir schließlich möglich war, wenn auch deutlich später als beabsichtigt, meine Einblicke und Gedanken in einer verständlichen Form zum Ausdruck zu bringen. Vollkommen unstrittig ließ sich dies nur durch teils sehr umfangreiche und wohlwollende Unterstützung realisieren, in erster Linie fachlicher Art, nicht zuletzt jedoch auch in emotionaler Hinsicht.

Mein besonderer Dank gilt allervorderst Herrn Prof. Dr. Markus Gerhard, meinem Doktorvater. Neben der exzellenten fachlichen Betreuung möchte ich mich insbesondere auch für die kritischen Anmerkungen und das konstruktive Feedback in aller Form bedanken. Dies ging sehr deutlich über das Maß des Erwartbaren hinaus, ohne seinen Einsatz hätte diese Arbeit nicht abgeschlossen werden können.

Bedanken möchte ich mich auch recht herzlich bei Herrn PD Dr. Roger Vogelmann, der mich bis zu seinem Wechsel nach Mannheim in hohem Maße förderte und mir sehr half, mit der Thematik und Methodik vertraut zu werden. Ebenso bei Frau PD Dr. Raquel Mejias Luque, für ihre ausgezeichnete fachliche und praktische Hilfestellung.

Auch Frau Dr. Sylvia Steininger, Frau Dr. Anke Loregger und Frau Dr. Martina Grandl möchte ich für ihre großartige und geduldige Unterstützung und Zusammenarbeit danken.

Schlussendlich gilt mein aufrichtiger Dank auch meiner Familie, die mich durch sämtliche Phasen dieser Arbeit begleitet und mir stets die erforderliche Motivation zugesprochen hat.

München, 22.08.2024

Martin Kullik